

---

# **Analysis of the subcellular behavior of *Arabidopsis thaliana* LysM-proteins and their role in plant innate immunity**

Dissertation

zur Erlangung des mathematisch-naturwissenschaftlichen Doktorgrades

"Doctor rerum naturalium"

der Georg-August-Universität Göttingen

im Promotionsprogramm „Biologie“

der Georg-August University School of Science (GAUSS)

vorgelegt von

**Jan Erwig**

aus Hildesheim

Göttingen, 2016

---

---

## Betreuungsausschuss

- 1. Betreuer: Prof. Dr. Volker Lipka**  
Zellbiologie der Pflanze,  
Albrecht-von-Haller Institut für Pflanzenwissenschaften
- 2. Betreuer: Prof. Dr. Ivo Feußner**  
Biochemie der Pflanze,  
Albrecht-von-Haller Institut für Pflanzenwissenschaften
- Anleiter: Dr. Elena K. Petutschnig**  
Zellbiologie der Pflanze,  
Albrecht-von-Haller Institut für Pflanzenwissenschaften

## Mitglieder der Prüfungskommission

- Referent: Prof. Dr. Volker Lipka**  
Zellbiologie der Pflanze,  
Albrecht-von-Haller Institut für Pflanzenwissenschaften
- Korreferent: Prof. Dr. Ivo Feußner**  
Biochemie der Pflanze,  
Albrecht-von-Haller Institut für Pflanzenwissenschaften

## Weitere Mitglieder der Prüfungskommission

**Prof. Dr. Christiane Gatz**  
Molekularbiologie und Physiologie der Pflanze,  
Albrecht-von-Haller Institut für Pflanzenwissenschaften

**Prof. Dr. Andrea Polle**  
Forstbotanik und Baumphysiologie,  
Fakultät für Forstwissenschaften und Waldökologie

**PD Dr. Thomas Teichmann**  
Zellbiologie der Pflanze,  
Albrecht-von-Haller Institut für Pflanzenwissenschaften

**Dr. Martin Fulda**  
Biochemie der Pflanze,  
Albrecht-von-Haller Institut für Pflanzenwissenschaften

---

---

**Promovierenden-Erklärung  
der Georg-August-Universität Göttingen**

Die Gelegenheit zum vorliegenden Promotionsvorhaben ist mir nicht kommerziell vermittelt worden. Insbesondere habe ich keine Organisation eingeschaltet, die gegen Entgelt Betreuerinnen und Betreuer für die Anfertigung von Dissertationen sucht oder die mir obliegenden Pflichten hinsichtlich der Prüfungsleistungen für mich ganz oder teilweise erledigt.

Hilfe Dritter wurde bis jetzt und wird auch künftig nur in wissenschaftlich vertretbarem und prüfungsrechtlich zulässigem Ausmaß in Anspruch genommen. Insbesondere werden alle Teile der Dissertation selbst angefertigt; unzulässige fremde Hilfe habe ich dazu weder unentgeltlich noch entgeltlich entgegengenommen und werde dies auch zukünftig so halten.

Die Ordnung zur Sicherung der guten wissenschaftlichen Praxis an der Universität Göttingen wurde von mir beachtet.

Eine entsprechende Promotion wurde an keiner anderen Hochschule im In- oder Ausland beantragt; die eingereichte Dissertation oder Teile von ihr wurden nicht für ein anderes Promotionsvorhaben verwendet.

Mir ist bekannt, dass unrichtige Angaben die Zulassung zur Promotion ausschließen bzw. später zum Verfahrensabbruch oder zur Rücknahme des erlangten Grades führen.

Jan Erwig

Göttingen, den 07. März 2016

---



*Für meine Familie*



---

## Abstract

Health and survival of all higher eukaryotic organisms depend on efficient pathogen detection and rapid activation of defense mechanisms. Plants detect potential pathogens by recognizing conserved microbial molecules, so-called microbe- or pathogen-associated molecular patterns (MAMPs/PAMPs), via pattern recognition receptors (PRRs). Recognition of MAMPs/PAMPs initiates defense signaling which leads to the establishment of plant innate immunity. The fungal polysaccharide chitin is perceived through lysin motif receptor-like kinases (LysM-RLKs) and receptor-like proteins (LysM-RLPs) which are thought to form receptor complexes for signal transduction.

This study focuses on the analysis of *Arabidopsis* CERK1, a LysM-RLK essential for the perception of chitin, and the LysM-RLKs LYK5 and LYK4, which contribute to chitin signaling. *lyk5* and *lyk5 lyk4* double mutant plants were impaired in chitin-induced CERK1 phosphorylation but not MAPK activation. To quantify the effect of LYK5 and LYK4 disruption on immune responses chitin-induced marker gene expression was tested. *lyk5* and *lyk5 lyk4* plants showed moderately but significantly reduced expression of *WRKY30*, *WRKY33* and *WRKY53* upon chitin stress. To investigate ligand-induced spatial dynamics, the subcellular behavior of CERK1 and LYK5 in response to chitin was tested. Both LysM-RLKs localized to the plasma membrane and showed constitutive endomembrane trafficking, but only LYK5 underwent clear chitin-induced relocalization into mobile intracellular vesicles. Inhibitor approaches, co-localization studies and quantitative confocal microscopy demonstrated that chitin perception transiently induces the internalization of LYK5 into endocytic compartments that traffic along the cytoskeleton. *In vitro* phosphorylation assays revealed that LYK5 and LYK4 are substrates of CERK1 phosphorylation. CERK1-dependent and chitin-specific LYK5 phosphorylation was detected *in planta*. Interestingly, plants that lack CERK1 or express an enzymatically inactive CERK1 variant did not exhibit chitin-induced endocytosis of LYK5. Together, these results suggest that chitin-induced phosphorylation of LYK5 by CERK1 triggers LYK5 endocytosis.

LYM2, a LysM-RLP with chitin binding activity, represents another putative component of the *Arabidopsis* chitin recognition complex. However, *lym2* mutants show no defects in canonical chitin signaling. Confocal laser scanning microscopy showed plasma membrane localization of LYM2. Upon chitin elicitation LYM2 specifically relocalizes into plasmodesmata (PD) in a CERK1-independent manner. Surprisingly, *lyk5 lyk4 lym2* triple mutant plants were not viable, potentially suggesting an involvement of these proteins in plant developmental processes. The

results of this work contribute to a better understanding of the role of LYK5, LYK4 and LYM2 in CERK1-mediated chitin signaling and shed light on their subcellular behavior.

## Zusammenfassung

Die Gesundheit und das Überleben aller höheren eukaryotischen Organismen hängen von einer effizienten Pathogenerkennung und einer schnellen Aktivierung von Abwehrmechanismen ab. Pflanzen erkennen potenzielle Pathogene durch die Wahrnehmung von konservierten mikrobiellen Molekülen, sogenannte Mikroben- oder Pathogenassoziierte Molekulare Muster (MAMPs/PAMPs\*), über Muster-Erkennungs-Rezeptoren (PRRs\*). Die Erkennung von MAMPs/PAMPs initiiert Abwehrsignale die zu der Aktivierung der pflanzlichen Immunabwehr führen. Das pilzliche Polysaccharid Chitin wird durch Lysin Motiv rezeptorartige Kinasen (LysM-RLKs) oder rezeptorartige Proteine (LysM-RLPs) erkannt, von denen man ausgeht, dass sie zusammen in einem Rezeptorkomplex agieren.

Diese Studie ist auf die Analyse von *Arabidopsis* CERK1, einer LysM-RLK essentiell für die Chitinerkennung, und den LysM-RLKs LYK5 und LYK4, welche an dem Chitinsignalweg mitwirken, fokussiert. *lyk5* und *lyk5 lyk4* Doppelmutanten waren in der chitin-induzierten Phosphorylierung von CERK1 beeinträchtigt, allerdings nicht in der Aktivierung von MAPKs. Um den Effekt von einem Verlust von LYK5 und LYK4 zu quantifizieren wurde die Expression von chitin-induzierten Markergenen getestet. *lyk5* und *lyk5 lyk4* Pflanzen zeigten eine moderate aber signifikant reduzierte Expression von *WRKY30*, *WRKY33* und *WRKY53* nach Chitinstress. Um die ligandeninduzierte räumliche Dynamik zu untersuchen, wurde das subzelluläre Verhalten von CERK1 und LYK5 als Antwort auf Chitingabe getestet. Beide LysM-RLKs wurden in der Plasmamembran lokalisiert und zeigten einen konstitutiven Endomembrantransport, aber nur LYK5 relokalierte auf Chitin hin in mobile intrazelluläre Vesikel. Inhibitorexperimente, Kollokalisierung und quantitative konfokale Mikroskopie zeigten, dass die Erkennung von Chitin eine vorübergehende Internalisierung von LYK5 in endozytotische Kompartimente induziert, die entlang des Zytoskeletts transportiert werden. *In vitro* Phosphorylierungsanalysen offenbarten, dass LYK5 und LYK4 Substrate der CERK1-Phosphorylierung sind. CERK1-abhängige und chitin-spezifische Phosphorylierung von LYK5 wurde auch *in planta* gefunden. Interessanterweise zeigten auch Pflanzen die kein oder ein enzymatisch inaktives CERK1-protein produzierten keine chitin-induzierte Endozytose von LYK5. Zusammengefasst deuten die Resultate darauf hin, dass die chitin-induzierte Phosphorylierung von LYK5 durch CERK1 die Endozytose von LYK5 auslöst.

LYM2, ein LysM-RLP mit hoher Chitinbindung, repräsentiert einen weiteren möglichen Bestandteil des Proteinkomplexes zu der Chitinerkennung in *Arabidopsis*. Jedoch zeigten *lym2* Mutanten keine Beeinträchtigung in der kanonischen Chitinantwort. Konfokale Laser scanning

Mikroskopie zeigte, dass LYM2 an der Plasmamembran lokalisiert ist. Nach Zugabe von Chitin relokalisiert LYM2 spezifisch und unabhängig von CERK1 in Plasmodesmata. Überraschenderweise waren *lyk5 lyk4 lym2* Dreifachmutanten nicht lebensfähig, was eine mögliche Beteiligung in der pflanzlichen Entwicklung suggeriert. Die Ergebnisse dieser Arbeit tragen zu einem besseren Verständnis der Rolle von LYK5, LYK4 und LYM2 in dem CERK1-vermittelten Chitinsignalweg bei und ermöglichen Einblicke auf deren subzelluläres Verhalten.

---

\* Für sämtliche Abkürzungen werden im Folgenden die gängigen englischen Abkürzungen verwendet (siehe hierfür auch: Seite V, Abbreviations).

## List of abbreviations

$\alpha$	anti
$\lambda$ -PPase	Lambda phosphatase
$\Phi$	Phi, a bulky and hydrophobic amino acid
6xHis	hexa-histidine
$^{\circ}\text{C}$	degree Celsius
::	fused to
$\mu\text{g}$	microgram
$\mu\text{l}$	microliter
$\mu\text{m}$	micrometer
$\mu\text{M}$	micromolar
aa	aminoacids
ADP	Adenosindiphosphat
Amp	Ampicillin
AP	adaptor protein complex or alkaline phosphatase
APS	ammonium persulfate
ARF	ADP ribosylation factor
ARG	autoradiograph
<i>At</i>	<i>Arabidopsis thaliana</i>
ATP	Adenosintriphosphat
<i>A. tumefaciens</i>	<i>Agrobacterium tumefaciens</i>
Avr	avirulence
BAK1/SERK3	BRI1-ASSOCIATED KINASE 1/SOMATIC EMBRYOGENESIS RECEPTOR KINASE 3
bp	base pair
BDM	2,3-butanedione monoxime
BFA	Brefeldin A
BiFC	Bimolecular Fluorescence Complementation
BIK1	BOTRYTIS-INDUCED KINASE 1
BKI1	BRI1-KINASE INHIBITOR 1
BL	Brassinolid
BR	Brassinosteroid
BRI1	BRASSINOSTEROID INSENSITIVE 1
BSA	Bovine serum albumin
CBB	Coomassie Brilliant Blue

CCV	clathrin-coated vesicle
cDNA	complementary DNA
CEBiP	CHITIN ELICITOR BINDING PROTEIN
CERK1	CHITIN ELICITOR RECEPTOR LIKE KINASE
CHC	clathrin heavy chain
CIE	clathrin-independent endocytosis
CLC	clathrin light chain
CLR1	CERK1-INTERACTING LYSM-RLK-LIKE RLCK1
CLSM	Confocal laser scanning microscopy
cm	centimeter
cM	centi Morgan
CME	Clathrin-mediated endocytosis
Col-0	Columbia-0
Co-IP	co-immunoprecipitation
ConcA	Concanamycin A
COP	coat protein complex
CPD	chitin pull-down
d	day(s)
DAMP	damage-associated molecular pattern
ddH <sub>2</sub> O	double-distilled water
DMSO	Dimethylsulfoxid
DNA	Deoxyribonucleic acid
dNTP	deoxyribonucleotidetriphosphosphate
DTT	Dithiothreitol
<i>E. coli</i>	<i>Escherichia coli</i>
e.g.	exempli gratia
EDTA	Ethylenediaminetetraacetic acid
EE	early endosomes
EFR	elongation factor thermo unstable receptor
EF-Tu	elongation factor thermo unstable
EGFR	epidermal growth factor receptor
EHD2	EH-DOMAIN CONTAINING 2
EIX	ethylene-inducing xylanase
ER	endoplasmic reticulum
ESCRT	ENDOSOMAL SORTING COMPLEX REQUIRED FOR TRANSPORT
ETI	effector-triggered immunity

ETS	effector-triggered susceptibility
FLS2	FLAGELLIN SENSING 2
FM	Fei Mao
FRET	Förster resonance energy transfer
g	gram or gravitation
GABI	Genomanalyse im biologischen System Pflanze
GAP	GTPase-activating protein
gDNA	genomic DNA
GDP	guaninediphosphate
GEF	Guanine nucleotide exchange factor
Gent	Gentamycin
GFP	Green fluorescent protein
GlcNAc	N-acetyl-D-glucosamine
GNL1	GNOM-LIKE1
GPI-anchor	glycosylphosphatidylinositol-anchor
G protein	GTPase
GSH	reduced glutathione
GSL	GLUCAN SYNTHASE-LIKE/CALLOSE SYNTHASE
GST	glutathione-S-transferase
GTP	guaninetriphosphosphate
h	hour(s)
HEPES	4-(2-hydroxyethyl)-1-piperazineethanesulfonic acid
het	heterozygous
hom	homozygous
HR	hypersensitive response
Hyg	Hygromycin
Hz	Hertz
i.e.	id est
ID	intracellular domain
IMAC	immobilized metal affinity chromatography
IPTG	isopropylthio- $\beta$ -D-galactoside
ITC	isothermal titration calorimetry
Kan	kanamycin
kB	kilo base(s)



---

K <sub>d</sub>	dissociation constant
kDa	kilo Dalton
l	liter
LB	left border primer or Luria-Bertani
LE	late endosome
<i>Lj</i>	<i>Lotus japonicus</i>
LOF	loss of function
LRR-RLK	leucine-rich repeat receptor-like kinase
LRRs	leucine rich repeats
LT16b	LOW-TEMPERATURE INDUCED 6b
LYK	LysM receptor-like kinase
LYM	LysM-containing receptor-like proteins
LysM	lysine motif
MAMP	microbe associated molecular pattern
MAPK	mitogen-activated protein kinase
MCS	multiple cloning site
min	minute(s)
ml	milliliter
mM	Millimolar
mm	Millimeter
MS	Murashige-Skoog
<i>Mt</i>	<i>Medicago truncatula</i>
MurNAc	<i>N</i> -acetylmuramic acid
MVB	multivesicular body
myc	myc- factors
NADPH	Nicotinamidadeninucleotidphosphat
NASC	Nottingham Arabidopsis Stock Centre
NFP	NOD FACTOR PERCEPTION
NFR	NOD FACTOR RECEPTOR
NFs	Nod-factors
NLR	nucleotide-binding leucine-rich repeat
nm	nanometer
nM	nanomolar
OA	okadaic acid

---

OD <sub>600</sub>	optical density at a wavelength of 600 nm
Os	<i>Oryza sativa</i>
<i>p</i>	promoter
PAMP	pathogen associated molecular pattern
PBS	phosphate buffered saline
PCR	Polymerase Chain Reaction
PD	plasmodesma(ta)
PDLP	PD-Located Protein
PEPR1	PEP receptor
Peps	plant elicitor peptides
PGN	Peptidoglycan
PIC	protease inhibitor cocktail
PI3Ks	phosphoinosite 3 kinases
PIN-proteins	PIN-FORMED protein
PM	plasma membrane
p-MAPK	phosphorylated MAPK
PMSF	phenylmethanesulfonylfluoride or phenylmethylsulfonyl fluoride
PIPES	Piperazine-N,N'-bis(2-ethanesulfonic acid)
PPT	phosphinotricin
PRR	pattern recognition receptor
PTI	PAMP-triggered immunity
PVDF	polyvinylidene fluoride
R-	resistance
RFP	Red fluorescent protein
Rif	rifampicin
RLCK	receptor-like cytoplasmic kinase
RLK	receptor-like kinase
RLP	receptor-like protein
RNA	ribonucleic acid
ROS	reactive oxygen species
rpm	rounds per minute
RT	room temperature
RTK	receptor tyrosine kinase
(q)RT-PCR	(quantitative) reverse transcriptase PCR
s	second(s)

SA	Salicylic acid
SAIL	Syngenta Arabidopsis Insertion Library
<i>S. cerevisiae</i>	<i>Saccharomyces cerevisiae</i>
SD	Standard Deviation
SDS	Sodium dodecyl sulfate
SDS-PAGE	Sodium dodecyl sulfate polyacrylamide gel electrophoresis
SEL	size exclusion limit
SERK4/BKK1	SOMATIC-EMBRYOGENESIS RECEPTOR-LIKE KINASE4/BAK1-LIKE1
SOBIR1	SUPPRESSOR OF BIR1-1
SP	Signal peptide
TAE	Tris-acetic acid EDTA
TAIR	The Arabidopsis Information Resource
TBS-T	Tris buffered saline - Tween-20
T-DNA	transfer-DNA
TE	Total protein extracts
TEMED	Tetramethylethylenediamine
Tet	tetracyclin
TGN	trans-golgi network
TIR	Toll-Interleukin-1 receptor
$T_m$	melting temperature
TM	transmembrane domain
TMV	tobacco mosaic virus
TTSS	type III secretion system
UBQ	Ubiquitine
VA-TIRFM	variable angle total internal reflection fluorescence microscopy
v/v	volume per volume
V-ATPases	vacuolar type H <sup>+</sup> - ATPases
w/o	without
w/v	Weight per volume
Wm	Wortmannin
WRKY	Transcription factor with WRKY amino acid sequence at the N-terminus
WT	wild type

## Table of contents

<b>Abstract</b> .....	<b>I</b>
<b>Zusammenfassung</b> .....	<b>III</b>
<b>List of abbreviations</b> .....	<b>V</b>
<b>Table of contents</b> .....	<b>XI</b>
<b>1 Introduction</b> .....	<b>1</b>
<b>1.1 The plant immune system</b> .....	<b>1</b>
<b>1.2 MAMP recognition via pattern recognition receptors</b> .....	<b>4</b>
1.2.1 LRR-RLK complexes and the recognition of peptide MAMPs .....	5
1.2.2 LysM-RLK complexes and the recognition of carbohydrate MAMPs.....	6
1.2.2.1 Chitin perception .....	7
1.2.2.2 Nod-factor perception .....	12
1.2.2.3 Peptidoglycan perception.....	13
<b>1.3 Receptor endocytosis in plants</b> .....	<b>14</b>
1.3.1 Endocytosis of the LRR-RLK FLS2.....	17
1.3.2 Endocytosis of the LRR-RLK BRI1 .....	19
1.3.3 Endocytosis of the LRR-RLPs <i>LeEIX2</i> and <i>Cf4</i> .....	20
<b>1.4 Regulation of plant endocytosis</b> .....	<b>21</b>
1.4.1 Protein phosphorylation and ubiquitination .....	21
1.4.2 Small G proteins.....	22
<b>1.5 Plasmodesmata</b> .....	<b>24</b>
1.5.1 The function of plasmodesmata in plant innate immunity .....	27
<b>1.6 Thesis aims</b> .....	<b>28</b>
<b>2 Materials and Methods</b> .....	<b>30</b>
<b>2.1 Materials</b> .....	<b>30</b>
2.1.1 Plants.....	30
2.1.1.1 <i>Arabidopsis thaliana</i> .....	30
2.1.2 Bacterial strains.....	33
2.1.2.1 <i>Escherichia coli</i> .....	33

---

2.1.2.2 <i>Agrobacterium tumefaciens</i> .....	33
2.1.3 Yeast strain for cloning and transformation.....	33
2.1.3.1 <i>Saccharomyces cerevisiae</i> .....	33
2.1.4 Vectors .....	33
2.1.5 Oligonucleotides.....	35
2.1.6 Enzymes.....	39
2.1.6.1 Restriction endonucleases .....	39
2.1.6.2 Polymerases and nucleic acid modifying enzymes .....	39
2.1.7 Chemicals.....	39
2.1.7.1 Antibiotics.....	39
2.1.7.2 Media .....	40
2.1.7.3 Inhibitors.....	42
2.1.7.4 Antibodies .....	42
2.1.7.5 Buffers and solutions .....	43
<b>2.2 Methods.....</b>	<b>50</b>
2.2.1 Methods for working with plants and plant material .....	50
2.2.1.1 Surface sterilization of <i>Arabidopsis</i> seeds .....	50
2.2.1.1.1 Sterilization using chlorine .....	50
2.2.1.1.2 Sterilization using ethanol.....	50
2.2.1.2 Plant growth conditions for tissue culture .....	50
2.2.1.3 Plant growth conditions for cultivation on soil .....	50
2.2.1.4 Crossing <i>Arabidopsis thaliana</i> .....	51
2.2.1.5 <i>Agrobacterium</i> -mediated stable transformation of <i>Arabidopsis</i> .....	51
2.2.1.6 Selection of stably transformed <i>Arabidopsis</i> plants.....	52
2.2.1.6.1 Basta <sup>®</sup> selection on soil .....	52
2.2.1.6.2 <i>In vitro</i> selection of <i>Arabidopsis</i> transformants.....	52
2.2.1.7 Treatment of <i>Arabidopsis thaliana</i> leaves with elicitors and inhibitors .....	52
2.2.2 Methods for working with bacteria.....	53
2.2.2.1 Cultivation of bacteria .....	53
2.2.2.2 Preparation of chemically competent <i>E.coli</i> cells.....	53
2.2.2.3 Preparation of electro-competent <i>A. tumefaciens</i> cells .....	54
2.2.2.4 Transformation of chemically competent <i>E.coli</i> cells .....	54
2.2.2.5 Transformation of electro-competent <i>A. tumefaciens</i> cells.....	54
2.2.2.6 Storage of bacterial cultures .....	54
2.2.3 Methods for working with <i>Saccharomyces cerevisiae</i> .....	55

---

2.2.3.1 Cultivation and storage of <i>S. cerevisiae</i> .....	55
2.2.3.2 Preparation of chemically competent <i>S. cerevisiae</i> cells.....	55
2.2.3.3 Transformation of chemically competent <i>S. cerevisiae</i> cells .....	55
2.2.4 Molecular biological methods.....	55
2.2.4.1 Isolation of genomic DNA (gDNA) from <i>Arabidopsis thaliana</i> .....	55
2.2.4.2 Isolation of plasmid DNA from <i>E.coli</i> .....	56
2.2.4.3 Polymerase chain reaction (PCR).....	56
2.2.4.3.1 Standard PCR and colony PCR .....	56
2.2.4.3.2 PCR for generation of DNA fragments used for cloning.....	57
2.2.4.4 DNA agarose gel electrophoresis .....	57
2.2.4.5 Purification of DNA fragments.....	58
2.2.4.6 Photometric measurement of DNA and RNA concentration.....	58
2.2.4.7 Cloning via homologous recombination in <i>S. cerevisiae</i> .....	58
2.2.4.8 Isolation of plasmid DNA from <i>S. cerevisiae</i> .....	59
2.2.4.9 Restriction enzyme digestion of DNA .....	59
2.2.4.10 Dephosphorylation of plasmid DNA .....	59
2.2.4.11 Ligation of DNA fragments.....	59
2.2.4.12 Sequencing of DNA .....	60
2.2.4.13 Preparation of RNA from plants .....	60
2.2.4.14 Synthesis of cDNA (complementary DNA) .....	60
2.2.4.15 Semi-quantitative RT-PCR.....	60
2.2.4.16 Quantitative reverse transcription PCR (qRT-PCR) .....	60
2.2.5 Biochemical methods .....	62
2.2.5.1 Protein extraction and purification from plants.....	62
2.2.5.1.1 Total protein extraction .....	62
2.2.5.1.2 Protein pull-down from total protein extracts .....	62
2.2.5.2 Lambda Protein Phosphatase (λPPase) treatment .....	62
2.2.5.3 Expression of 6xHis- and GST-fusion proteins in <i>E. coli</i> .....	63
2.2.5.4 Extraction and purification of 6xHis- and GST-tagged proteins from <i>E. coli</i> .....	63
2.2.5.5 Protein concentration measurement via the Bradford assay .....	64
2.2.5.6 SDS-polyacrylamide gel electrophoresis (SDS-PAGE).....	64
2.2.5.7 <i>In vitro</i> kinase assay .....	66
2.2.5.8 Immunoblot analysis (Western blot).....	67
2.2.5.9 Coomassie staining of SDS-PAGE gels and PVDF membranes .....	68
2.2.5.10 Drying of Coomassie stained SDS-PAGE gels.....	68

---

2.2.6 Confocal laser scanning microscopy (CLSM) and endosome quantification .....	68
2.2.6.1 Confocal laser scanning microscopy (CLSM) .....	68
2.2.6.2 Endosome quantification .....	69
2.2.7 Statistical analysis .....	70
<b>3 Results .....</b>	<b>71</b>
<b>3.1 Analysis of the subcellular behavior of CERK1 .....</b>	<b>71</b>
3.1.1 The CERK1-GFP fusion protein is functional .....	71
3.1.2 Confocal microscopy suggests that chitin treatment does not alter the subcellular localization of CERK1-GFP .....	73
3.1.3 CERK1-GFP positive vesicles accumulate after co-treatment with ConcA and chitin .....	74
3.1.4 CERK1-GFP undergoes constitutive endomembrane trafficking .....	76
<b>3.2 Analysis of LYK5 and LYK4 T-DNA insertion lines .....</b>	<b>77</b>
3.2.1 Isolation of <i>lyk5-2</i> and <i>lyk4-2</i> T-DNA insertion lines and <i>lyk5-2 lyk4-2</i> double mutants .....	77
3.2.2 <i>lyk5-2</i> and <i>lyk5-2 lyk4-1</i> plants show reduced chitin-induced phosphorylation of CERK1 but MAPK activation is normal .....	78
3.2.3 <i>lyk5-2</i> and <i>lyk5-2 lyk4-2</i> mutants show moderately decreased chitin-induced gene expression .....	80
<b>3.3 Analysis of the subcellular behavior of LYK5 and LYK4 .....</b>	<b>83</b>
3.3.1 LYK5-mCitrine and LYK4-mCitrine fusion proteins are functional .....	83
3.3.2 Chitin induces transient, CERK1-dependent formation of LYK5-mCitrine positive vesicles....	85
3.3.3 LYK4-mCitrine is weakly expressed in leaves and may show chitin-induced vesicle formation .....	87
3.3.4 LYK5-mCitrine internalization is chitin specific .....	89
3.3.5 LYK5-mCitrine is specifically internalized from the plasma membrane .....	90
3.3.6 LYK5-mCitrine co-localizes with LE/MVB markers ARA6 and Rha1 but not with recycling endosomes .....	92
3.3.7 Chitin-induced endocytosis of LYK5-mCitrine is BFA-insensitive. ....	95
3.3.8 LYK5-mCitrine endocytosis is affected by inhibitors of endomembrane trafficking, the cytoskeleton and protein phosphorylation. ....	97
<b>3.4 LYK5-mCitrine and CERK1 phosphorylation studies .....</b>	<b>100</b>
3.4.1 Chitin-induced and CERK1-dependent phosphorylation of LYK5-mCitrine .....	100
3.4.2 LYK4-mCitrine may show chitin-induced and CERK1-dependent phosphorylation .....	102
3.4.3 CERK1 directly phosphorylates LYK5 and LYK4 <i>in vitro</i> .....	103
3.4.4 CERK1-dependent phosphorylation of LYK5-mCitrine is required for its endocytosis .....	105
<b>3.5 Analysis of LYM T-DNA insertion lines .....</b>	<b>108</b>

---

3.5.1 Isolation of <i>lym1-1</i> , <i>lym2-1</i> and <i>lym3-1</i> T-DNA insertion lines and <i>lym1-1 lym2-1 lym3-1</i> triple mutant.....	108
3.5.2 <i>LYM</i> single and triple mutants are not impaired in CERK1 chitin binding and phosphorylation .....	109
<b>3.6 Analysis of LYM2 subcellular localization.....</b>	<b>110</b>
3.6.1 Chitin induces CERK1-independent mCitrine-LYM2 re-localization at the PM.....	110
3.6.2 Chitin triggers mCitrine-LYM2 accumulation at PD.....	113
<b>3.7 Generation and identification of <i>lyk5-2 lyk4-2 lym2-1</i> triple mutant plants .....</b>	<b>115</b>
<b>4 Discussion .....</b>	<b>120</b>
<b>4.1 The role of LYK5 and LYK4 in chitin perception and signaling .....</b>	<b>120</b>
<b>4.2 The subcellular behavior of CERK1, LYK5, and LYK4 .....</b>	<b>124</b>
4.2.1 CERK1-GFP may show chitin-dependent endosomal localization .....	124
4.2.2 LYK5 undergoes chitin-induced endocytosis .....	125
4.2.3 CERK1 and LYK5 constitutively traffic in a BFA-sensitive manner .....	128
<b>4.3 Phosphorylation of LYK5 by CERK1 is a prerequisite for LYK5 endocytosis.....</b>	<b>129</b>
<b>4.4 Chitin receptor complex formation in <i>Arabidopsis</i> .....</b>	<b>133</b>
<b>4.5 LYM proteins are not involved in CERK1-dependent chitin signaling .....</b>	<b>135</b>
4.5.1 LYM2 re-localizes at PD after chitin stimulus.....	136
<b>4.6 Generation and identification of a <i>lyk5-2 lyk4-2 lym2-1</i> triple mutant .....</b>	<b>137</b>
4.6.1 LYK5, LYK4, and LYM2 may play a role in embryogenesis and fertility .....	138
<b>4.7 Conclusion.....</b>	<b>140</b>
<b>4.8 Outlook.....</b>	<b>141</b>
<b>5 References.....</b>	<b>143</b>
<b>6 Supplemental material .....</b>	<b>168</b>
<b>List of figures .....</b>	<b>178</b>
<b>List of tables .....</b>	<b>181</b>
<b>List of supplemental figures .....</b>	<b>182</b>
<b>Danksagung.....</b>	<b>183</b>
<b>Lebenslauf .....</b>	<b>186</b>



---

# 1 Introduction

Plants are constantly interacting with their environment. They are exposed to abiotic stresses like unfavorable light and soil conditions and harmful organisms such as herbivores and pathogenic microbes (de Wit, 2007). Microbial plant pathogens are bacteria, fungi, oomycetes, or viruses and may exhibit a variety of different infection strategies and lifestyles (Dodds and Rathjen, 2010). To defend themselves against potential invaders, plants - like all higher eukaryotic organisms - depend on their efficient detection and subsequent rapid activation of cellular defense responses (Jones and Dangl, 2006; Nürnberger and Kemmerling, 2006). Since plants lack an adaptive immune system, they rely on innate immunity. The plant immune system consists of different layers of defense that have been shaped by a co-evolutional arms race of plants and their pathogens (Postel and Kemmerling, 2009). As a result, plants are resistant against the majority of pathogens and susceptible to only a small number of adapted microbes (Jones and Dangl, 2006).

## 1.1 The plant immune system

Plants protect themselves against pathogens through a variety of passive and active defense mechanisms. Physical barriers that fend off pathogens are for example the epidermal cuticle, epicuticular waxes and the rigid plant cell wall. Additionally, pre-formed low molecular weight secondary metabolites with antimicrobial activity known as phytoanticipins (Osbourn *et al.*, 2011) or anti-microbial enzymes may restrict pathogen proliferation (Heath, 2000; Carvalho Ade and Gomes, 2011). Many microbes fail to overcome these preformed barriers but some pathogens are able to penetrate the leaf or root surface through exertion of pressure and/or enzymatic degradation or enter their host through wounds and natural openings like stomata (Chisholm *et al.*, 2006). Pathogens that passed the cell wall reach the plasma membrane (PM) and encounter the two-layered active defense mechanisms of the plant immune system (Jones and Dangl, 2006). The first layer of this defense system is based on sensing characteristic molecular signatures known as microbe- or pathogen-associated molecular patterns (MAMPs or PAMPs) and damage-associated molecular patterns (DAMPs) via cell-surface located pattern recognition receptors (PRRs) (Figure 1). MAMPs/PAMPs are highly conserved molecular structures that are characteristic of a whole class of microbes but absent from the host. They are molecules that are indispensable for the pathogen and cannot be easily lost or modified. DAMPs are host-derived molecules that are generated in the plant upon pathogen attack or other forms of cell damage. Typical DAMPs are constituent parts of the plant that are released upon pathogen attack (Chisholm *et al.*, 2006; Boller and Felix, 2009; Boller and He, 2009;

Postel and Kemmerling, 2009). Chemically, most MAMPs and DAMPs are either proteins/peptides or carbohydrates. Recognition of these molecules by their corresponding PRRs activates innate immune responses leading to PAMP-triggered immunity (PTI) (Figure 1, 1) which confers resistance to most pathogens (Boller and Felix, 2009; Monaghan and Zipfel, 2012). Interestingly, the responses to most MAMPs/DAMPs are largely overlapping, suggesting that plants perceive MAMPs and DAMPs from various pathogens via specialized receptors and then utilize a conserved, common downstream pathway to mediate disease resistance (Wan *et al.*, 2008b).

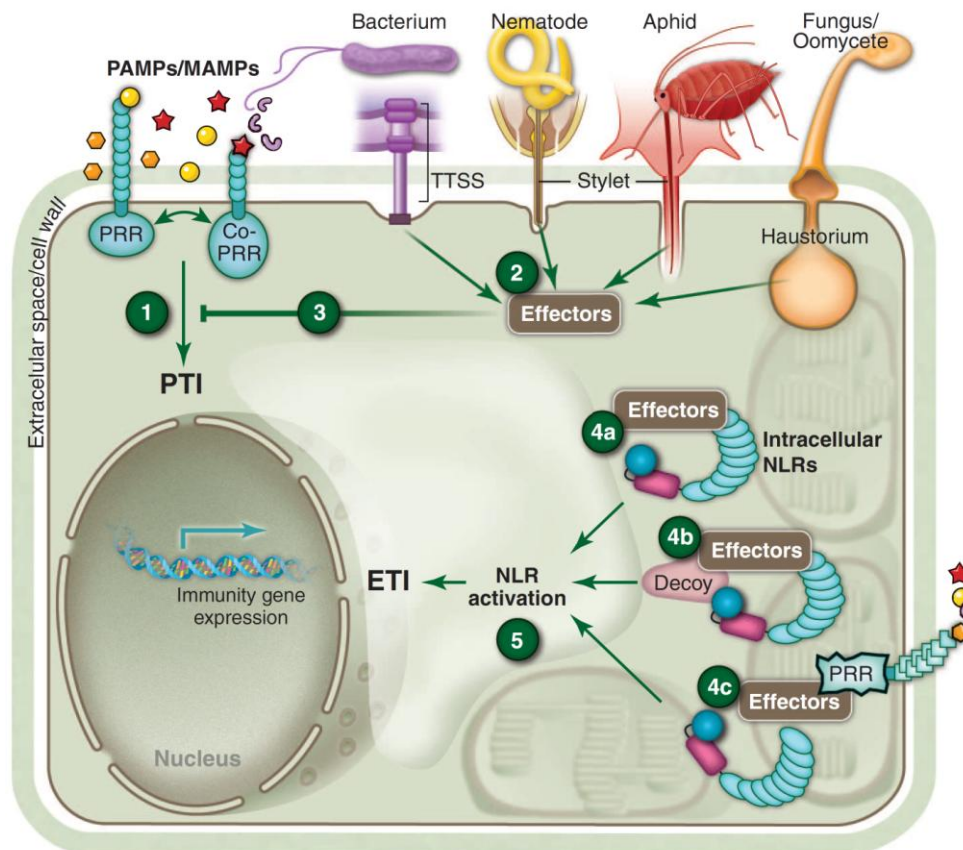


**Figure 1: Schematic representation of the plant immune system.**

Microbe- or pathogen-associated molecular patterns (MAMPs/PAMPs) are recognized by cognate pattern recognition receptors (PRRs) at the PM. **(1)** Perception of MAMPs/PAMPs initiates the PAMP-triggered immunity (PTI). As a consequence pathogens have evolved effector proteins which can be delivered into the host cell **(2)** and compromise (PTI) **(3)** which is referred to as effector-triggered susceptibility (ETS). Plants in turn, have evolved intracellular nucleotide-binding leucine-rich repeat (NLR) type resistance (R) proteins to recognize the effectors. NLRs can recognize effectors either directly **(4a)** or indirectly by **(4b)** guarding decoy proteins that mimic host effector targets, or **(4c)** sensing alterations made to host effector targets. **(5)** Recognition of effectors by NLRs leads to effector-triggered immunity (ETI). Figure adapted from Dangl *et al.* (2013).

In general, elicitation of PRRs by MAMPs/DAMPs induces a range of defense responses in plants, typically including early responses like the generation of reactive oxygen species (ROS) via PM-bound NADPH oxidases, alkalinisation of the apoplast, calcium influx into the cytosol and protein phosphorylation including the activation of mitogen-activated protein kinases (MAPKs) (Boller and Felix, 2009). Later responses are induced expression of defense-related genes, for example members of the *WRKY* class of transcription factors (Zipfel *et al.*, 2004) and callose deposition at the cell wall (Bittel and Robatzek, 2007; Boller and Felix, 2009). Together, this leads to resistance of members of an entire plant species against all isolates of a specific pathogen, a phenomenon called non-host resistance (Thordal-Christensen, 2003; Nürnberger and Lipka, 2005). Non-host resistance is the most common and durable type of plant resistance. However, some highly specialized pathogens are able to suppress this first layer of defense by deploying effector molecules (Figure 1, 2) that render the host susceptible. Suppression of PTI by effectors has been termed effector-triggered susceptibility (ETS) (Jones and Dangl, 2006; Chatterjee *et al.*, 2013) (Figure 1, 3). Effector molecules are secreted by pathogens into the apoplastic space or transferred directly into the plant cell. To do so, pathogens evolved specific mechanisms. Pathogenic bacteria, e.g. the gram-negative bacterium *Pseudomonas syringae*, can directly inject effector molecules into the plant cell via a needle like structure formed by the type III secretion system (TTSS) (Figure 1). *P. syringae* that are defective in components of the TTSS are not able to counteract the activated defense responses (Alfano and Collmer, 1997; Badel *et al.*, 2003; Jin *et al.*, 2003). Pathogenic fungi or oomycetes use specialized organs, so-called haustoria, to invaginate the PM, take up nutrients and secrete effector molecules (O'Connell and Panstruga, 2006; De Wit *et al.*, 2009). Since fungal and oomycete pathogens lack a TTSS, microbe-independent effector entry has been discussed lately (Tyler *et al.*, 2013). However, the exact mechanisms how their effectors enter the host is not clear.

Pathogen effectors may suppress PTI at various levels. They may prevent recognition of the pathogen by sequestering MAMPs or by targeting PRRs (de Jonge *et al.*, 2010; Mentlak *et al.*, 2012). They may also interfere with downstream signaling (Zhang *et al.*, 2007) or later events during PTI, such as vesicle transport (Nomura *et al.*, 2006; Kang *et al.*, 2014). To counteract ETS, plants evolved resistance (R) proteins that recognize effector molecules and establish a second layer of defense known as effector-triggered immunity (ETI) (Jones and Dangl, 2006) (Figure 1, 5). Recognition of effectors by R-proteins can be direct or indirect. Direct recognition is based on physical binding of the effector molecule to the R-protein (Figure 1, 4a). However, there are relatively few examples for this. Indirect recognition has been observed more frequently. In this case, R-proteins monitor a host protein and trigger defense responses when

this protein is modified by the action of an effector. Two models have been proposed for indirect recognition: the guard model, in which the R-protein surveils a component of the PTI machinery that is targeted by effectors (Figure 1, **4c**), and the decoy model (Figure 1, **4b**), where the R-protein monitors a host protein that mimics an effector target, but does not play a role in PTI itself (Dodds and Rathjen, 2010; Dangl *et al.*, 2013). Typically, plant R-proteins contain a nucleotide binding pocket (NB-ARC-domain) and C-terminal leucine rich repeats (LRRs) and thus are structurally related to the animal (NOD)-like immune receptors (Ausubel, 2005). NB-LRRs R-proteins are further distinguished by the presence of a variable N-terminal domain into CC (coiled coil)-NB-LRRs and TIR (Toll-Interleukin-1 receptor)-NB-LRRs (Dangl and Jones, 2001; Elmore *et al.*, 2011). Effector recognition by R-proteins results in rapid and strong activation of defense responses which are often associated with programmed cell death. This type of cell death restricts growth of biotrophic pathogens and is referred to as hypersensitive response (HR) (Jones and Dangl, 2006). Effectors that are recognized by R-proteins lead to an incompatible interaction between the pathogen and the host and are therefore termed avirulence (Avr) factors. The resistance that effector recognition confers is typically race-specific, i.e. limited to the interaction of certain pathogen strains with certain host accessions (Chisholm *et al.*, 2006; Jones and Dangl, 2006).

The classification of plant immune responses into PTI and ETI (Jones and Dangl, 2006) is useful to illustrate the evolutionary mechanisms in plant immunity. However, in recent years an increasing number of reports describe immune receptors and pathways that do not strictly fit into one of the two classes. Therefore, a revised model has been proposed that views immune responses as a continuum between PTI and ETI (Thomma *et al.*, 2011; Böhm *et al.*, 2014).

## 1.2 MAMP recognition via pattern recognition receptors

To perceive MAMPs, plants possess PM-located PRRs that are either receptor-like kinases (RLKs) or receptor-like proteins (RLPs) (Monaghan and Zipfel, 2012). Both types of receptors contain an extracellular ligand-binding domain, which may contain different functional motifs, depending on the MAMP perceived. In addition, RLKs possess a transmembrane (TM) domain and a cytoplasmic protein kinase domain. RLPs lack that intracellular part and are attached to the PM either via a TM domain or a C-terminal GPI-anchor (Monaghan and Zipfel, 2012; Macho and Zipfel, 2014). Since RLPs do not contain signaling domains, they most likely function in conjunction with RLKs to initiate signal transduction. In recent years it has become apparent that, like in animal systems, plant receptor kinases also form complexes via homo- and/or heterooligomerization for ligand recognition and activation of downstream signaling (Macho and

Zipfel, 2014). A number of studies identified receptor-like cytoplasmic kinases (RLCKs) as a part of signaling complexes at the PM. RLCKs lack an extracellular domain but share homology to RLKs in the kinase domain (Shiu and Bleecker, 2001).

### 1.2.1 LRR-RLK complexes and the recognition of peptide MAMPs

Proteins or peptide MAMPs are typically perceived by PRRs that harbor LRRs in their extracellular domain. A prominent example is the LRR-RLK FLAGELLIN SENSING 2 (FLS2) (Gomez-Gomez and Boller, 2000), which perceives the conserved bacterial flagellin in diverse plant species such as *Arabidopsis*, tobacco and rice (Zipfel *et al.*, 2004; Takai *et al.*, 2008; Boller and Felix, 2009). A 22 amino acid epitope of flagellin, flg22, is sufficient for recognition by FLS2 (Gomez-Gomez and Boller, 2000; Chinchilla *et al.*, 2006). flg22 perception initiates typical MAMP responses like the production of ROS, phosphorylation of MAPKs and transcriptional changes (Monaghan and Zipfel, 2012). Consequently, FLS2-deficient plants show enhanced susceptibility to adapted and non-adapted bacterial pathogens (Zipfel *et al.*, 2004; Li *et al.*, 2005; Hann and Rathjen, 2007). Similarly, bacteria with altered flg22 can evade plant defense responses and render plants more susceptible (Boller and Felix, 2009).

Another prominent PRR is the ELONGATION FACTOR THERMO UNSTABLE RECEPTOR (EFR), which is a LRR-RLK similar to FLS2 (Shiu and Bleecker, 2003). EFR binds elf18, an 18 amino acid peptide corresponding to the acetylated N-terminus of bacterial elongation factor Tu (EF-Tu) (Zipfel *et al.*, 2006; Boller and Felix, 2009). *efr* mutants are more susceptible to infection with *Agrobacterium tumefaciens*, resulting in higher transformation rates (Zipfel *et al.*, 2006).

In contrast to the exogenous elicitors, endogenous peptidic DAMPs have been identified to trigger PTI. Several plant elicitor peptides (Peps) have been identified together with their cognate LRR-RLKs, the PEP RECEPTORS (PEPRs) (Bartels and Boller, 2015). A well-studied example is Pep1 that is derived from its precursor protein PROPEP1 and is perceived by PEPR1 and PEPR2 (Yamaguchi *et al.*, 2006; Krol *et al.*, 2010; Yamaguchi *et al.*, 2010). Pep recognition leads to defense responses in *Arabidopsis* and maize such as Ca<sup>2+</sup> spiking, enhanced resistance against pathogen infection and defense against herbivores (Huffaker and Ryan, 2007; Qi *et al.*, 2010; Huffaker *et al.*, 2013). A critical component of many LRR-RLK complexes is the kinase active co-receptor BRI1-ASSOCIATED KINASE1/SOMATIC EMBRYOGENESIS RECEPTOR KINASE 3 (BAK1/SERK3). BAK1 is a LRR-RLK with a short ectodomain (Shiu and Bleecker, 2003) and was initially identified as positive regulator of the brassinosteroid receptor BRI1 (Li *et al.*, 2002; Nam and Li, 2002; Wang *et al.*, 2008; Sun *et al.*, 2013a). BAK1 and a close homolog, SERK4/BKK1, have also been identified as signaling

partners of the MAMP receptors FLS2 (Chinchilla *et al.*, 2007; Schulze *et al.*, 2010; Sun *et al.*, 2013b), EFR (Roux *et al.*, 2011) as well as PEPR1/2 (Postel *et al.*, 2010). Consequently, *bak1* mutants show reduced responses to BR as well as MAMPs/Peps (Chinchilla *et al.*, 2007; Roux *et al.*, 2011). Upon ligand binding, BAK1 rapidly heterodimerizes with its partner LRR-RLK, which leads to transphosphorylation of the intracellular domains and subsequent activation of downstream signaling components (Chinchilla *et al.*, 2007; Heese *et al.*, 2007; Schulze *et al.*, 2010). The transphosphorylation events involve the RLCK BIK1 (BOTRYTIS-INDUCED KINASE 1) which is subsequently released from the receptor complex (Lu *et al.*, 2010; Zhang *et al.*, 2010; Liu *et al.*, 2013).

In recent years, a number of LRR-RLPs have been identified as immune receptors. Several have been reported to require a LRR-RLK, SOBIR1 (SUPPRESSOR OF BIR1-1), for their function in immune responses (Gao *et al.*, 2009; Liebrand *et al.*, 2013; Zhang *et al.*, 2013). SOBIR1 resembles BAK1 in that it has a short extracellular domain. Thus it has been proposed that SOBIR1 acts as an adaptor for RLP-type PRRs and that SOBIR1-RLP dimers are functionally equivalent to LRR-RLKs (Gust and Felix, 2014). Indeed, numerous LRR-RLPs were shown to require BAK1 as a co-receptor (Gust and Felix, 2014; Postma *et al.*, 2015). Relevant for this work are the LRR-RLPs Cf4 and *LeEIX2* because they have been studied concerning receptor endocytosis (see section 1.3.3). The tomato LRR-RLP Cf4 recognizes the *Cladosporium fulvum* effector Avr4 and initiates immune responses resulting in a hypersensitive response (Thomas *et al.*, 1997). In agreement with the proposed receptor model, Cf4 constitutively interacts with SOBIR1 (Liebrand *et al.*, 2013) and associates with BAK1 (Postma *et al.*, 2015) after elicitation with its ligand, Avr4 (Thomas *et al.*, 1997). *LeEIX2*, another LRR-RLP from tomato bind the fungal elicitor ethylene-inducing xylanase (EIX) together with its co-receptor *LeEIX1*. However, only *LeEIX2* mediates the EIX-induced hypersensitive response (Ron and Avni, 2004) and was shown to interact with SOBIR1 (Liebrand *et al.*, 2013) but not BAK1 (Bar *et al.*, 2010). In contrast, *LeEIX1* interacts with BAK1 and has been reported to function as an EIX decoy receptor that attenuates *LeEIX2* signaling (Bar *et al.*, 2010).

### 1.2.2 LysM-RLK complexes and the recognition of carbohydrate MAMPs

The lysin motif (LysM) exists in prokaryotes as well as eukaryotes and is known to bind *N*-acetylglucosamine (GlcNAc) containing poly- or oligosaccharides. In bacteria, it is frequently found in lysins that bind the bacterial cell wall polymer peptidoglycan (Buist *et al.*, 2008). In plants, LysM domains are present in RLKs and RLPs that function in plant defense or symbiosis pathways. The GlcNAc-containing ligands they bind are the fungal cell wall component chitin

and chitooligosaccharides (Ryan, 1987; Buist *et al.*, 2008) as well as bacterial peptidoglycan (Gust *et al.*, 2007; Gust *et al.*, 2012). Lipochitooligosaccharides, modified chitin oligomers which rhizobia and mycorrhizal fungi secrete to establish symbiosis are also perceived by LysM-receptors (Antolin-Llovera *et al.*, 2012). In contrast to signaling pathways, mediated by LRR-RLKs or RLPs, immune responses that depend on LysM domain proteins are BAK1-independent (Shan *et al.*, 2008; Gimenez-Ibanez *et al.*, 2009b; Schulze *et al.*, 2010).

### 1.2.2.1 Chitin perception

The fungal cell wall component chitin is a polymer of  $\beta$ -1,4-linked *N*-acetyl-D-glucosamine (GlcNAc) (Muzzarelli, 1977) and is not found in plants. It has long been recognized that polymeric and oligomeric chitin, as well as its partially deacetylated form chitosan, induce typical MAMP-associated defense responses in plants (Felix *et al.*, 1998; Boller and Felix, 2009)

In rice (*Oryza sativa*), the PM-located LysM-protein OsCEBiP (CHITIN ELICITOR BINDING PROTEIN) is the main chitin receptor (Kaku *et al.*, 2006; Hayafune *et al.*, 2014). Rice plants lacking OsCEBiP showed drastically impaired chitin-induced defense responses and are more sensitive to fungal pathogens (Kaku *et al.*, 2006; Kishimoto *et al.*, 2010; Kouzai *et al.*, 2014b). OsCEBiP directly binds chitin oligomers. Two OsCEBiP molecules bind to one chitin octamer, leading to dimerization of OsCEBiP (Hayafune *et al.*, 2014). Hayafune and colleagues showed that only chitin oligomers with *N*-acetyl groups on either side of the molecule are able to induce receptor dimerization and defense responses. This led to a model of “sandwich type” dimerization, where the two OsCEBiP molecules bind on either face of the chitin oligomer (Figure 2). Since OsCEBiP lacks a kinase domain, it must cooperate with (co-) receptors to transduce the signal into the cell and activate defense. Recently, it has been shown that OsCEBiP interacts with the LysM-RLK OsCERK1 (CHITIN ELICITOR RECEPTOR-LIKE KINASE 1) and forms heterooligomers in response to chitin treatment (Figure 2) (Shimizu *et al.*, 2010). The OsCERK1 protein has no chitin binding activity by itself, although the extracellular part of the protein harbors LysM domains (Shinya *et al.*, 2012). Silencing of OsCERK1, similar to OsCEBiP, results in decreased chitin-induced defense responses and increased susceptibility to fungal pathogens (Shimizu *et al.*, 2010; Kouzai *et al.*, 2014a). Based on these data a model has been proposed, where dimerization of OsCEBiP recruits two OsCERK1 molecules that also dimerize and initiate signal transduction (Hayafune *et al.*, 2014; Shinya *et al.*, 2015) (Figure 2). The receptor complex also contains the RLCK OsRLCK185. OsRLCK185 interacts with OsCERK1 at the PM and is phosphorylated by OsCERK1 upon chitin perception.



Phosphorylated OsRLCK185 then dissociates from the complex in order to activate further downstream responses (Yamaguchi *et al.*, 2013).

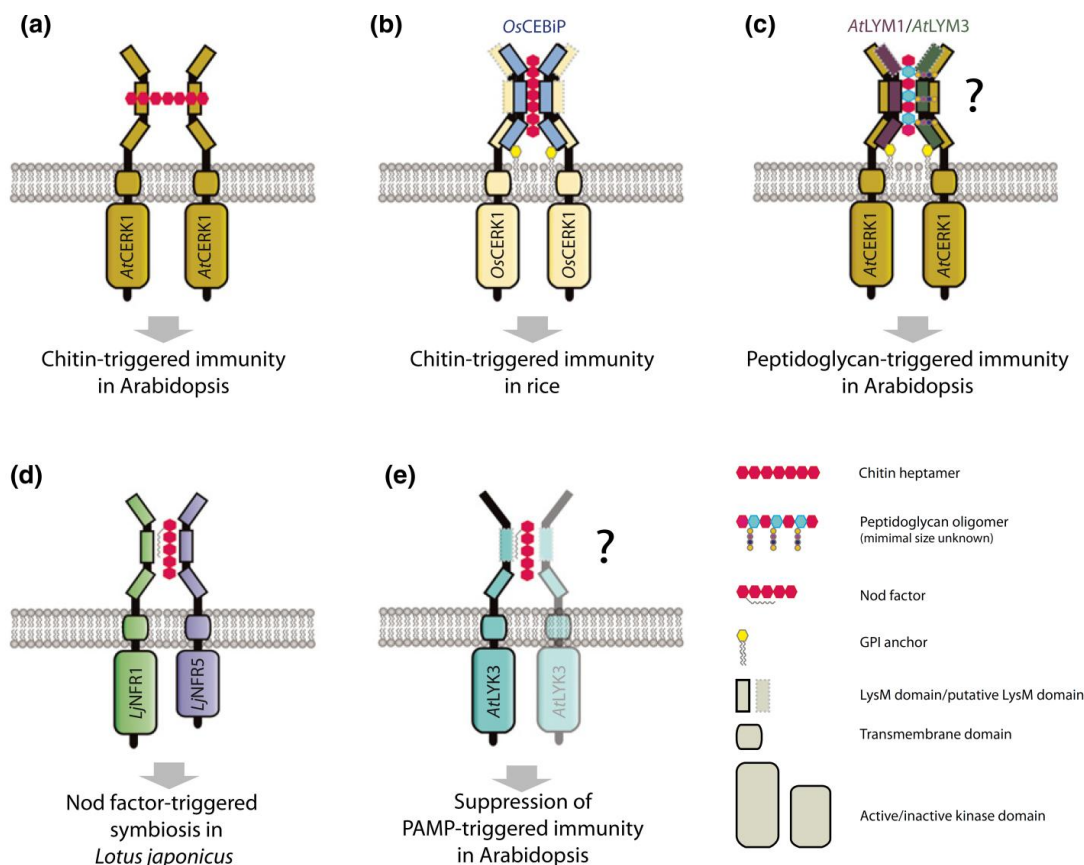


**Figure 2: Model for LysM-RLK and LysM-RLP receptor complex formation upon perception of N-acetylglucosamine (GlcNAc)-containing ligands in Arabidopsis, rice and Lotus japonicus.**

The recognition of GlcNAc-containing ligands initiates defense responses or symbiosis signaling. **(a)** Upon binding of chitin or chitin oligomers with a minimum length of seven GlcNAc units with its central LysM, AtCERK1 homodimerizes. This leads to downstream signaling and activation of chitin-induced defense responses. Chitin binding in rice (*Oryza sativa*) requires two types of LysM-proteins. **(b)** Two OsCEBiP molecules bind one chitin oligomer with their central LysMs leading to homodimerization. In order to transmit the signal into the cell OsCERK1 associates with the formed homodimer. **(c)** Two OsCEBiP homologs in *Arabidopsis*, AtLYM1 and AtLYM3 have PGN binding activity and require AtCERK1 for downstream signaling. AtLYM1 and AtLYM3 bind to PGN which leads to signaling events that require AtCERK1 for signal transduction. A model is suggested that resembles the chitin recognition in rice. AtLYM1 and AtLYM3 heterodimerizes and form a heterotetramer with two AtCERK1 proteins. **(d)** In *Lotus japonicus*, the LysM-RLKs NFR1 (NOD FACTOR RECEPTOR 1) and NFR5 (NOD FACTOR RECEPTOR 5) have been shown to function in a complex for perception of Nod factors (NFs). NFR1/5 bind NFs *in vitro* and have been shown to interact *in vivo*. **(e)** Interestingly, NFs and chitin tetramers are able to suppress PAMP-triggered defense responses. This suppression seems to be mediated by AtLYK3. However, the exact chitin binding mechanisms and complex formation are not fully understood. Adapted and modified from Antolin-Llovera *et al.* (2014a).

*Arabidopsis* contains also a homologue of OsCEBiP, which is named LYSM-CONTAINING RECEPTOR-LIKE PROTEIN2 (LYM2) as well as two related proteins, LYM1 and LYM3. All three LYM proteins are attached to the PM via a GPI-anchor (Borner *et al.*, 2003) (Figure S1). In contrast to LYM1 and LYM3 (Willmann *et al.*, 2011), LYM2 shows chitin binding affinity (Petutschnig *et al.*, 2010; Shinya *et al.*, 2012). Surprisingly, typical chitin induced defense reaction such as ROS generation or defense gene induction are affected neither in *lym2* single mutant plants nor *lym1 lym2 lym3* triple knock-out mutants (Shinya *et al.*, 2012; Wan *et al.*, 2012). These findings suggest that there are profound differences in the chitin perception mechanisms of *Arabidopsis* and rice. Recently it has been shown that *lym2* mutants are impaired in regulation of the plasmodesmal flux in response to chitin (Faulkner *et al.*, 2013).

Like in rice, the *Arabidopsis* PM-located (Petutschnig *et al.*, 2014) LysM-RLK CERK1/LysM-RLK1 was identified to be indispensable for chitin perception and also contributes to resistance against fungal pathogens (Miya *et al.*, 2007; Wan *et al.*, 2008a). In contrast to OsCERK1, the *Arabidopsis* CERK1 ectodomain directly binds polymeric chitin as well as chitin oligomers (Iizasa *et al.*, 2010; Petutschnig *et al.*, 2010; Liu *et al.*, 2012b). A  $K_d$  of 45  $\mu$ M was determined for binding of chitin octamer (Liu *et al.*, 2012b). The extracellular domain of CERK1 contains three LysMs (Miya *et al.*, 2007) and structural analyses revealed that the three LysM domains are tightly packed resulting in an overall globular structure (Liu *et al.*, 2012b). Crystallization in the presence of chitin identified that the chitin binding site is formed by two loops in the second LysM (Liu *et al.*, 2012b). One chitin binding site accommodates four GlcNAc moieties. Thus, chitin octamers and polymeric chitin allow simultaneous binding of two receptor molecules, resulting in CERK1 dimerization (Figure 2) (Liu *et al.*, 2012b) which is a prerequisite for transphosphorylation on the intracellular domains (Petutschnig *et al.*, 2010; Liu *et al.*, 2012b). This phosphorylation is essential for downstream signaling and can be visualized in immunoblots as a band shift of the CERK1 protein (Petutschnig *et al.*, 2010). Liu *et al.* (2012) report that chitin tetramers and pentamers can be bound by CERK1, but do not lead to CERK1 dimerization or phosphorylation. Overall, reports on the biological activity of chitooligosaccharides of different length are somewhat conflicting and further research will be required to determine the minimum effective degree of polymerization.

RLKs and RLPs typically form receptor complexes for signal transduction. Since CERK1 is not involved in LYM2-mediated PD regulation (Faulkner *et al.*, 2013) indicates that a second, “non-canonical” chitin response pathway exists that differs from the classical CERK1-dependent signal transduction cascade. Evidence for the significance of this CERK1-independent LYM2 function comes from two reports that demonstrate increased susceptibility to necrotrophic fungal

pathogens in *lym2* mutants (Faulkner *et al.*, 2013; Narusaka *et al.*, 2013). Thus, LYM2 seems to act independently of CERK1 and a CERK1-LYM2 complex formation is unlikely. *Arabidopsis* contains four LysM-RLKs in addition to CERK1 (Figure 3 and Figure S2). A proteomics approach identified two of them, LYK4 (LysM-RLK4) and LYK5 (LysM-RLK3), as chitin binding proteins (Petutschnig *et al.*, 2010). Therefore, they are good candidates for complex partners of CERK1.

The LYK5 (At2g33580) and LYK4 (At2g23770) proteins are encoded by single exon genes and are 664 aa (72.5 kDa) and 612 aa (66.6 kDa) in size (Lamesch *et al.*, 2012). Both proteins show a typical RLK domain organization with an N-terminal signal peptide followed by the extracellular domain, transmembrane domain and intracellular protein kinase domain. The prediction tool MyHits Motif scan (Pagni *et al.*, 2004) detects one LysM in the ectodomain of LYK5 and two in LYK4 (Figure 3 and Figure 10). However, an alignment (Figure 3) and homology modeling with other LysM-proteins (Cao *et al.*, 2014) suggests that there are three LysM-domains present in both proteins. The kinase domains of LYK5 and LYK4 lack conserved subdomains that are required for enzymatic activity and thus were predicted to be kinase dead. Indeed, kinase activity of LYK4 (Wan *et al.*, 2012) and LYK5 (Cao *et al.*, 2014) could not be detected in *in vitro* assays. T-DNA insertion lines of LYK4 and LYK5 were investigated in the initial studies on CERK1 (Miya *et al.*, 2007; Wan *et al.*, 2008a) and found to display normal chitin-induced ROS burst or defense gene expression. A later study characterized *lyk4-1*, a mutant with slightly impaired chitin-induced generation of ROS, calcium influx and resistance against bacterial and fungal pathogens (Wan *et al.*, 2012). Thus, a minor role in the general chitin defense signaling was attributed to LYK4 (Wan *et al.*, 2012). Studies regarding the role of LYK5 in chitin signaling are also contradictory. *lyk5-1*, a T-DNA mutant in the Landsberg (Ler) background was initially reported to show no alteration in chitin-triggered expression of *WRKY53* (Wan *et al.*, 2008a; Wan *et al.*, 2012) and *MAPK3* (Wan *et al.*, 2008a). Recently, the same group reported that LYK5 is crucial for chitin signaling (Cao *et al.*, 2014). Surprisingly, the authors found a subtle reduction in *WRKY33* expression upon chitin elicitation as well as reduced CERK1 phosphorylation and activation of MAPKs in the *lyk5-1* mutant. These chitin responses were more drastically and significantly reduced in a new T-DNA insertion line (*lyk5-2*) in the Col-0 background. The *lyk5-2* mutant additionally showed significantly reduced ROS burst, calcium influx and expression of other defense genes after chitin octamer treatment (Cao *et al.*, 2014). The differences between *lyk5-1* and *lyk5-2* mutant lines were speculated to be caused by the different ecotype backgrounds (Cao *et al.*, 2014). The reduction in typical defense responses in the *lyk5-2* mutant was not as severe as in *cerk1-2* mutants. However,

*lyk5-2 lyk4-1* double mutant plants, resembled *cerk1-2* with regards to chitin triggered ROS generation and MAPK activation (Cao *et al.*, 2014). This indicates functional redundancy between LYK4 and LYK5 in chitin signaling (Cao *et al.*, 2014). LYK5 was reported to form homodimers already without any stimulus and to rapidly associate with CERK1 after chitin treatment. This is required for chitin-triggered CERK1 phosphorylation (Cao *et al.*, 2014). Although LYK5 is kinase dead the kinase domain is important for complementing the *lyk5-2* phenotype, downstream signaling and the interaction with CERK1 (Cao *et al.*, 2014). In the study of Cao *et al.*, isothermal titration calorimetry (ITC) was performed with proteins heterologously expressed in *E. coli* and LYK5 was found to have a higher affinity for chitooctaose ( $K_d = 1.72 \mu\text{M}$ ) than CERK1 ( $K_d = 455 \mu\text{M}$ ). On this basis it was suggested that LYK5 acts as the primary chitin receptor in *Arabidopsis* (Cao *et al.*, 2014). However, some open questions remain. In contrast to CERK1 (Liu *et al.*, 2012b), LYK5 did not bind chitin tetramers (Cao *et al.*, 2014). Also, the reported  $K_d$ -value for CERK1 and chitin octamer in Cao *et al.* ( $455 \mu\text{M}$ ) was much higher than in a previous study ( $45 \mu\text{M}$ ) (Liu *et al.*, 2012b). In all instances, the chitin affinities of CERK1 and LYK5 were very low compared to ligand affinities of other LysM-RLKs (see below) (Broghammer *et al.*, 2012). Thus, the exact structure of the chitin recognition complex and the involved mechanisms are so far not clear.

Similar to the situation in rice, RLCKs are involved in chitin perception in *Arabidopsis*. The closest *Arabidopsis* homolog to OsRLCK185 is PBL27 (Shinya *et al.*, 2014). *pbl27* mutants are impaired in chitin-induced callose deposition, activation of MAPKs and showed enhanced sensitivity to fungal and bacterial pathogens. Moreover, PBL27 is a direct target of CERK1 phosphorylation (Shinya *et al.*, 2014). A recent study identified another *Arabidopsis* RLCK involved in chitin signaling, the CERK1-INTERACTING LYSM-RLK-LIKE RLCK1 (CLR1) (Ziegler, 2015). CLR1 shares high homology with LysM-RLKs in the kinase domain and is kinase defective. CERK1 phosphorylates CLR1 *in vitro* and *in vivo* and *clr1* mutants exhibit reduced chitin-induced ROS generation, MAPK activation and expression of defense genes. Furthermore, mutant plants were not impaired in resistance against fungal pathogens, but showed an enhanced sensitivity to *P. syringae* (Ziegler, 2015).

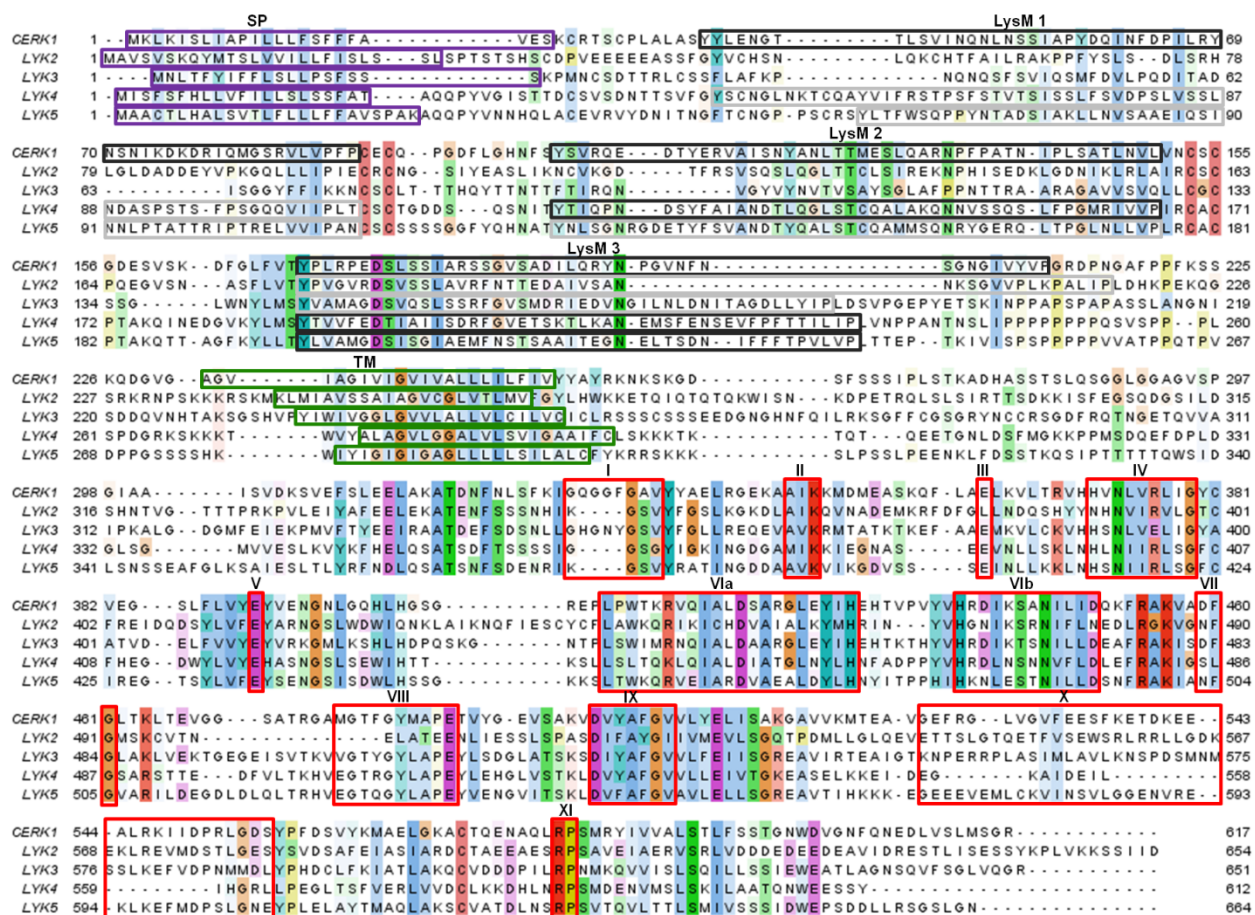


**Figure 3: Alignment of full length amino acid sequences of *Arabidopsis* LysM-RLKs (LYKs).**

Protein features: SP: Signal peptide predicted by SignalP 4.1 (<http://www.cbs.dtu.dk/services/SignalP>, Nielsen and Krogh (1998)); LysM: lysin motif (black predicted by MyHits (<http://myhits.isb-sib.ch>, Pagni *et al.* (2004)), light grey predicted by sequence comparison); TM: Transmembrane domain predicted using the TMHMM Server 2.0 (<http://www.cbs.dtu.dk/services/TMHMM>, Krogh *et al.* (2001)). Red boxes indicate kinase subdomains I – XI (Hanks *et al.* (1988); Hanks and Hunter (1995)). The alignment was generated with Genius 7.1.5 using the ClustalW algorithm (Kearse *et al.*, 2012) and colored in Jalview 2.9.0b2 (settings: ClustalX, conservation threshold of 30; Waterhouse *et al.* (2009)). Red: positively charged amino acids, purple: negatively charged amino acids, blue: amino acids with hydrophobic side chains, green: neutral amino acids.

### 1.2.2.2 Nod-factor perception

During the establishment of symbiosis, nitrogen-fixing rhizobial bacteria and arbuscular mycorrhizal fungi secrete modified lipochitooligosaccharides, so-called Nod-factors (NFs) or myc-factors (myc) which are recognized by LysM-RLKs (Maillet *et al.*, 2011; Antolin-Llovera *et al.*, 2014a). In plant–rhizobial symbioses, NFs are important for host nodule formation (Radutoiu *et al.*, 2003; Nakagawa *et al.*, 2011; Rey *et al.*, 2013). Host specificity is mainly determined by

NFs as the NFs of rhizobial species carry different chemical modifications (Limpens *et al.*, 2003; Oldroyd and Downie, 2008).

In *Lotus japonicus*, the kinase active LysM-RLKs NFR1 (NOD FACTOR RECEPTOR 1) and the inactive LysM-RLK NFR5 (NOD FACTOR RECEPTOR 5) have been shown to function in a complex for the perception of NFs (Figure 2) (Madsen *et al.*, 2003; Radutoiu *et al.*, 2003; Madsen *et al.*, 2011). NFR1 and NFR5 bind to Nod factor with high affinity.  $K_d$ -values of 4.9 nM and 10.1 nM were calculated for NFR1 and NFR5 (Broghammer *et al.*, 2012), respectively. Compared to the estimated chitooctase affinity of LYK5 ( $K_d= 1.72 \mu\text{M}$ ) and CERK1 ( $K_d= 455 \mu\text{M}$ ), Nod factor binding of NFR1 and NFR5 occurs instantaneously. *nfr1* and *nfr5* mutant plants are unable to establish a proper symbiotic relationship with rhizobia and consistent with a role in NF perception, the interaction is blocked at a very early stage (Radutoiu *et al.*, 2003). In *Medicago truncatula* the LysM-RLK NFP (NOD FACTOR PERCEPTION), is involved in the recognition of Nod factors together with the LysM-RLK LYK3 (Arrighi *et al.*, 2006; Smit *et al.*, 2007). Like *LjNFR5*, *MtNFP* has no kinase activity suggesting an interaction with an active kinase such as *MtLYK3* to transduce signals (Arrighi *et al.*, 2006; Smit *et al.*, 2007; Lohmann *et al.*, 2010; Madsen *et al.*, 2011). Mutant analyses suggest that *MtNFP* likely functions in NF perception and initial NF responses (Mulder *et al.*, 2006; Rey *et al.*, 2013), whereas *MtLYK3* is required for recognition of specific NF structures and thus the formation of compatible rhizobial infection (Limpens *et al.*, 2003; Smit *et al.*, 2007). Interestingly, a perception system for NFs has been reported for *Arabidopsis thaliana* (Liang *et al.*, 2013), although this model plant cannot establish symbiosis with rhizobia or mycorrhizal fungi. The *Arabidopsis* LysM-RLK LYK3, which does not bind to polymeric chitin (Petutschnig *et al.*, 2010; Cao *et al.*, 2014), is suggested to detect NFs (Figure 2) which leads to the suppression of PTI (Liang *et al.*, 2013). Interestingly, the closest LYK3 homolog in *Lotus japonicus* (EPR3) was recently shown to bind directly to bacterial exopolysaccharides (EPS) and distinguishes compatible and incompatible EPS (Kawaharada *et al.*, 2015). Thus, EPR3 plays a pivotal role in the establishment of legume-rhizobium symbiosis.

### 1.2.2.3 Peptidoglycan perception

Petidoglycan (PGN) is an essential component of the outer part of the bacterial cell wall. PGN consists of a linear glycan backbone composed of alternating  $\beta$ -(1,4)-linked GlcNAc and *N*-acetylmuramic acid (MurNAc) residues, which are cross-linked by peptide chains attached to the MurNAc moieties (Schleifer and Kandler, 1972). The PGN-backbone is highly conserved

throughout gram-negative and gram-positive bacteria and thus serves as a MAMP in plant-microbe interactions (Gust *et al.*, 2007).

Rice plants lacking functional OsCERK1 are not only impaired in the perception of chitin, but also in the activation of defense upon PGN application (Ao *et al.*, 2014). The OsCEBiP homologues OsLYP4 and OsLYP6 have been shown to bind to chitin and PGN and the respective mutants exhibited reduced chitin- and PGN-induced defense responses as well as decreased resistance against fungal and bacterial pathogens (Liu *et al.*, 2012a; Ao *et al.*, 2014; Kouzai *et al.*, 2014a). OsCERK1 was shown to interact with OsLYP4 and OsLYP6 upon PGN treatment, suggesting that these proteins form a PGN receptor complex (Ao *et al.*, 2014). Two RLCKs, OsRLCK185 (Yamaguchi *et al.*, 2013) and OsRLCK176 (Ao *et al.*, 2014) have been implicated as transducers of PGN signals in rice.

*Arabidopsis cerk1* mutants showed enhanced susceptibility to strains of the bacterial pathogen *Pseudomonas syringae* (Gimenez-Ibanez *et al.*, 2009a), suggesting a role of CERK1 in recognition of bacterial MAMPs. Recent work has revealed that two OsCEBiP homologs in *Arabidopsis*, LYM1 and LYM3 have PGN binding activity (Willmann *et al.*, 2011). *lym1* and *lym3* mutants are impaired in PGN perception and resistance to bacterial pathogens. These responses are dependent on CERK1, although CERK1 itself has no PGN binding affinity. Thus, a model has been proposed where LYM1 and LYM3 associate with CERK1 for PGN signal transduction (Figure 2) (Willmann *et al.*, 2011). Chitin and PGN signaling are mechanistically distinct in *Arabidopsis* since PGN triggers neither CERK1 dimerization nor phosphorylation (Petutschnig *et al.*, 2010; Liu *et al.*, 2012b).

### 1.3 Receptor endocytosis in plants

The uptake of substances from outside the cell by invagination of and subsequent budding from the PM is called endocytosis. Endocytosis is a conserved cellular mechanism in eukaryotic cells and is required for processes like metabolism and signal transduction and plays a role in plant development and defense (Murphy *et al.*, 2005; Otegui and Spitzer, 2008). In the case of plant defense against potential pathogens, the PRR must be present at the PM to successfully perceive its cognate ligand and consequently trigger immunity. Transportation of newly synthesized proteins to the PM and removal from the PM via secretory and endocytic vesicles are processes to regulate the subcellular localization and dynamics of receptors (Figure 4). Upon ligand perception the PM-resident receptor becomes activated. To regulate defense signaling the activated receptor is later removed from the PM via endocytosis. Protein endocytosis starts at the PM using either clathrin-coated or clathrin-independent endocytic

vesicles (Murphy *et al.*, 2005; Ben Khaled *et al.*, 2015). Endocytotic vesicles transport their cargo to the TGN/EE. After transport to the TGN/EE endosomal cargo is either recycled back to the PM or transferred into late endosomes (LEs) and multivesicular bodies (MVBs, Figure 4) (Scheuring *et al.*, 2011). There, cargo destined for degradation is sorted to intraluminal vesicles and later discharged into the vacuole by MVB fusion (Cai *et al.*, 2014). In plants only two distinct endosomal compartments have been identified via FM-staining, namely the TGN/EE and LEs/MVBs (Dettmer *et al.*, 2006; Reyes *et al.*, 2011).

Endocytosis of receptor kinases has first been described in the animal system and the mammalian RTK EPIDERMAL GROWTH FACTOR RECEPTOR (EGFR) is a well-studied example. After perception of its ligand, EGFR is rapidly endocytosed from the PM into endosomal compartments. From there, it is either recycled back to the PM, or shuttled to the lysosome for degradation (Waterman and Yarden, 2001). Endocytosis and endomembrane trafficking of receptors may serve a number of different purposes. It may reduce the number of activated receptors at the PM to attenuate signaling (Katzmann *et al.*, 2002; Irani and Russinova, 2009; Antolin-Llovera *et al.*, 2014a). Alternatively, endocytosis may promote signal transduction. As multiple receptor proteins are continuously present at the PM it is conceivable that the space for signaling is limited. Endocytic vesicles may provide an additional platform for signaling by allowing important components of downstream signaling cascades to make rapid contact with the receptor. Indeed, EGFR continues to signal from vesicles and important downstream components, such as MAPKs and scaffold proteins, are localized to endosomal compartments (Teis *et al.*, 2002). Receptor endocytosis followed by recycling may ensure appropriate receptor distribution throughout the PM and may contribute to cell polarity as it has been shown for PIN-proteins (Dhonukshe *et al.*, 2007).

In animals, yeast and plants, the primary endocytic route into the cell is via clathrin-coated vesicles (CCVs) (Kirchhausen, 2000; Geldner and Robatzek, 2008). CCVs are not only formed at the PM during endocytosis, but are also released from the TGN to mediate transport of cargo to MVB. Clathrin-mediated endocytosis (CME) is essential for all eukaryotic organisms (Dhonukshe *et al.*, 2007; Chen *et al.*, 2011) and represents the best characterized endocytic pathway. CME is initiated at the PM when binding of the designated cargo to adapter protein complexes (APs) results in the recruitment of the coat machinery. For the formation of the clathrin coat self-polymerizing clathrin proteins are assembled from the cytosol. The resulting clathrin cage consists of three clathrin heavy chains (CHCs) and three clathrin light chains (CLCs) that form triskelion-shaped subunits (Kirchhausen, 2009; Chen *et al.*, 2011).



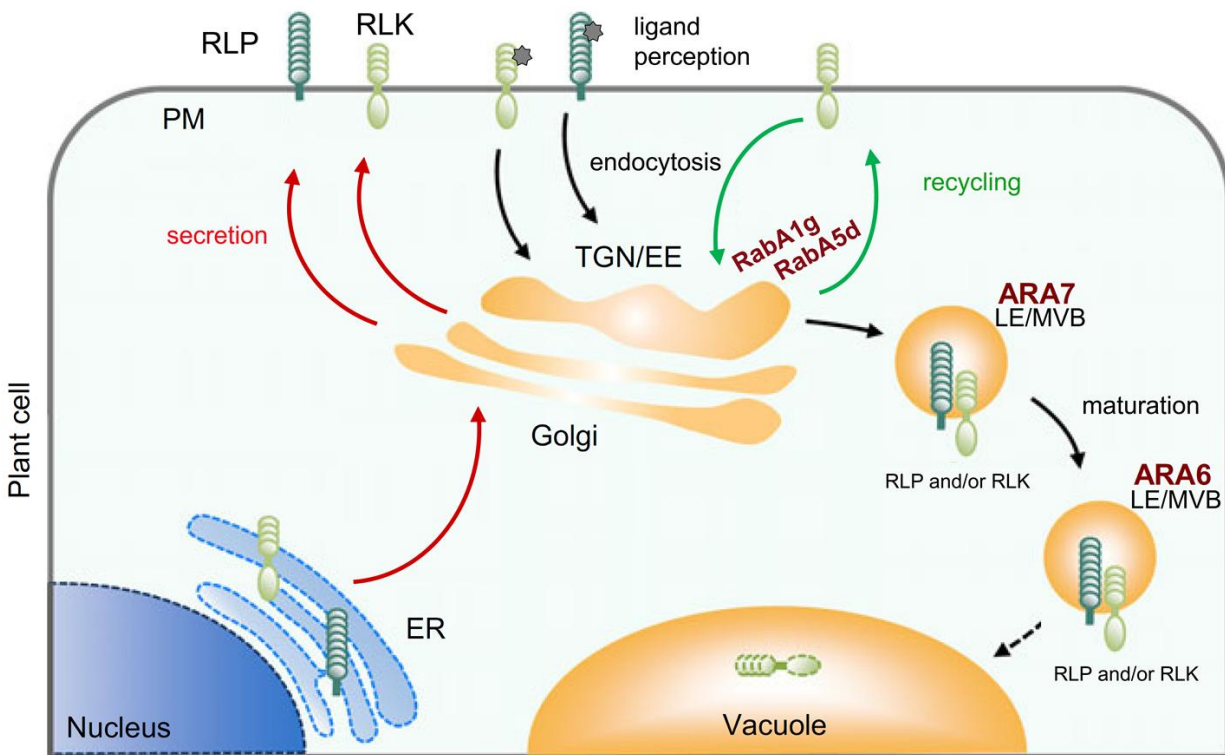


**Figure 4: Schematic representation of the endocytic pathway in plants**

After correct folding and maturation in the ER, newly synthesized RLPs and RLKs follow the secretory route via the Golgi stack for PM localization (red pathway) where they monitor the cell environment for potential pathogens. Some RLKs are known to constitutively recycle between the PM and the TGN (green pathway). This trafficking pathway is often mediated via RabA-members (e.g. RabA1g or RabA5d). Upon ligand perception, activated RLPs or RLKs enter the endocytic pathway via vesicle formation. These vesicles are targeted to the TGN/EE where the cargo is sorted into ARA7- and ARA6-positive compartments, namely different populations of LEs/MVBs. Finally, this late endosomal pathway directs the cargo to the vacuole for lytic degradation. Figure adapted and modified from Postma *et al.* (2016).

The formation of the clathrin cage and thereby maturation of CCVs requires APs, because clathrin proteins themselves cannot bind to the PM or specific cargos. Several different AP complexes are present in animals, but AP-2 is the main adaptor complex for clathrin-mediated endocytosis at the PM and the same appears to be the case in plants (Di Rubbo *et al.*, 2013; Kelly *et al.*, 2014). The AP-2 complex consists of multiple subunits and is crucial for recognition and selection of specific cargo via sorting motifs (Traub, 2009). In addition to the AP-2 complex, numerous other adapter proteins associate with CCVs in mammals and several of them have orthologs encoded in plant genomes (Barth and Holstein, 2004; Gadeyne *et al.*, 2014). These accessory proteins have different functions like linking the cargo or membrane lipids to the

maturing CCV, recruiting actin filaments or binding to dynamin which then performs scission of CCVs from the PM.

In addition to the already discussed CME, endocytic pathways exist in animal cells that do not involve clathrin (Mayor and Pagano, 2007). Research of the recent years indicates that plants also have mechanisms of clathrin-independent endocytosis (CIE) (Li *et al.*, 2012). Starting point of CIE are distinct microdomains within the PM which are enriched in sterols and sphingolipids and can be visualized with fluorescently labelled marker proteins such as, flotillins and remorins (Haney and Long, 2010; Lefebvre *et al.*, 2010). It is believed that upon specific stimuli, the cargo proteins form clusters in microdomains. The clustering then reduces the dynamics of the proteins. Subsequently, the proteins undergo membrane microdomain-associated endocytosis where the detailed steps are currently unknown.

Upon endocytosis, early endosomes (EEs) are the first endomembrane compartments that receive cargo from the PM. According to the current model of endomembrane trafficking, the TGN acts as an EE compartment in plants (Reyes *et al.*, 2011). Studies with different marker proteins suggest that the plant TGN may contain distinct sub-domains that may take on different specialized functions (Contento and Bassham, 2012; Drakakaki *et al.*, 2012). From the TGN/EE, cargo assigned for degradation traffics to the vacuole via LEs/MVBs (Figure 4) (Irani and Russinova, 2009; Ben Khaled *et al.*, 2015). There, cargo destined for degradation is sorted to intraluminal vesicles by the ENDOSOMAL SORTING COMPLEX REQUIRED FOR TRANSPORT (ESCRT) machinery and later discharged into the vacuole by MVB fusion (Cai *et al.*, 2014). Additionally, a pathway has been defined that enables the endocytosed material to travel back from the TGN to the PM (Figure 4) (Robinson *et al.*, 2008a), possibly via a specialized compartment, the recycling endosomes (Contento and Bassham, 2012). Once sorted into endosomal compartments, the protein follows a given route throughout the cell. The cytoskeleton plays a pivotal role in endomembrane trafficking (Geli and Riezman, 1996; Ayscough, 2000). Both the actin cytoskeleton and microtubules play distinct roles in CME (Kaksonen *et al.*, 2005; Merrifield *et al.*, 2005; Yarar *et al.*, 2005) and CIE (Li *et al.*, 2012). Not surprisingly, drugs affecting actin and microtubule stability inhibit endocytosis (Baluska *et al.*, 2002; Aniento and Robinson, 2005).

### 1.3.1 Endocytosis of the LRR-RLK FLS2

The first example of ligand-induced receptor endocytosis in plants was shown by Robatzek *et al.* in 2006. In transgenic plant lines, a functional FLS2-GFP fusion protein localized to the PM. Upon flg22 stimulus, FLS2-GFP accumulated in internal vesicles and co-staining with FM4-64

revealed that FLS2 is internalized into *bona fide* endosomes (Beck *et al.*, 2012). The localization of FLS2 is sensitive to the endomembrane trafficking inhibitor BFA in flg22-treated as well as untreated plants, which was interpreted as evidence for constitutive FLS2 recycling (Beck *et al.*, 2012). FLS2 is specifically internalized after challenge with flg22, since inactive flg22 variants did not trigger endocytosis (Robatzek *et al.*, 2006; Beck *et al.*, 2012). FLS2 endocytosis depends on the co-receptor BAK1 (Chinchilla *et al.*, 2007). When FLS2 is mutated in a highly conserved threonine residue within the kinase domain, flg22-triggered FLS2 endocytosis and downstream signaling is impaired (Robatzek *et al.*, 2006). Also, the application of the kinase inhibitor K252a inhibits FLS2 endocytosis similar to the absence of BAK1, suggesting an involvement of phosphorylation steps in the regulation of FLS2 endocytosis (Robatzek *et al.*, 2006; Chinchilla *et al.*, 2007). Internalization of FLS2-GFP becomes visible after approximately 20 min and longer incubation times result in almost complete loss of FLS2 signal at the PM (Robatzek *et al.*, 2006; Beck *et al.*, 2012). When flg22 was washed out, the FLS2 signal returned to the PM. This could be blocked by cycloheximide, indicating that the returning signal stemmed from newly synthesized FLS2. flg22 treatment also led to decreased FLS2 signals in Western blot experiments (Lu *et al.*, 2011; Smith *et al.*, 2014), suggesting degradation of the protein. In agreement with this idea, co-localization with defined endosomal markers demonstrated that flg22-activated FLS2 travels from the TGN/EE to LEs/MVBs (Beck *et al.*, 2012; Choi *et al.*, 2013). The co-localization studies were supported by extensive inhibitor analysis. The VHA inhibitor Concanamycin A (ConcA) which interferes with the TGN to LE/MVB trafficking significantly increased the numbers of FLS2-GFP vesicles after flg22 treatment (Beck *et al.*, 2012). Furthermore, treatment with Wortmannin (Wm), which affects internalization from the PM and leads to homotypic fusion of MVBs, decreased the amount of flg22-triggered FLS2-GFP vesicles and concurrently enlarged their size (Beck *et al.*, 2012). FLS2-positive endosome formation was affected in the presence of inhibitors of tubulin and actin polymerization, highlighting the role of the cytoskeleton in FLS2 trafficking (Robatzek *et al.*, 2006; Beck *et al.*, 2012). Recent research provided first insights into the molecular machinery required for FLS2 endocytosis and trafficking. Internalization of FLS2 is reduced in null mutants of the Dynamin-Related Protein 2B (DRP2B) (Smith *et al.*, 2014) which suggests that FLS2 endocytosis occurs - at least in part - via clathrin coated vesicles. This notion is backed up by the fact that treatment with Tyrphostin A23, an inhibitor of CME, reduces FLS2 endocytosis, but does not block it completely (Beck *et al.*, 2012). flg22-activated FLS2 is sorted into luminal vesicles of MVBs via the ESCRT machinery, presumably by direct interaction with the ESCRT-I subunit VPS37-1 (Spallek *et al.*, 2013). An Involvement of the ESCRT machinery suggests that ubiquitination is

the driving signal behind FLS2 endocytosis. Indeed, FLS2 is polyubiquitinated upon flg22 treatment by the E3 ligases PUB12/13 in a BAK1-dependent manner (Lu *et al.*, 2011). Ubiquitination and degradation of FLS2 can also be mediated by *Pseudomonas syringae* effector AvrPtoB, which acts as an E3 ubiquitin ligase and associates with FLS2 (Göhre *et al.*, 2008).

While the cell biology of FLS2 has been studied extensively, very little is known about the function of FLS2 endocytosis. *Arabidopsis* leaves that were treated with flg22 are unable to establish a second ROS burst or activate MAPKs after an additional round of flg22 application within 60 min. This correlates with degradation of FLS2. At later time points, FLS2 re-accumulates and plants are able to respond to flg22 again (Smith *et al.*, 2014). Based on these findings, it has been postulated that FLS2 degradation serves the purpose of flg22-desensitization to avoid overstimulation of the system and later enables accumulation of new, signaling-competent receptor at the PM (Smith *et al.*, 2014). However, inhibitors that block FLS2-endocytosis and thus FLS2 degradation were also shown to reduce flg22-induced defense responses (Serrano *et al.*, 2007; Smith *et al.*, 2014). Moreover, desensitization to flg22 also takes place after application of inhibitors blocking FLS2 endocytosis as well as in a *bak1* mutant background, where FLS2 endocytosis is drastically reduced (Smith *et al.*, 2014). These data suggest that in addition to FLS2 endocytosis, there are other factors regulating sensitivity to flg22.

### 1.3.2 Endocytosis of the LRR-RLK BRI1

Another well-studied *Arabidopsis* example for RLK trafficking is the brassinosteroid receptor BRI1. BRI1 encodes a LRR-RLK that is a critical component of the PM-resident BR-receptor complex in *Arabidopsis* (Lamesch *et al.*, 2012). The binding of the ligand induced rapid dimerization of BRI1 with its co-receptor BAK1 (Nam and Li, 2002). In the BRI1-BAK1 interaction, BAK1 amplifies brassinosteroid signaling by phosphorylating BRI1: upon brassinosteroid binding, BRI1 autophosphorylates itself and BAK1 gets activated by transphosphorylation (Wang *et al.*, 2008). The activated BAK1 in turn transphosphorylates BRI1, leading to an intensified signal and regulation of brassinosteroid-dependent plant development. BRI1-GFP localizes to the PM and intracellular mobile vesicles in root meristem cells irrespectively of brassinosteroid treatment (Irani *et al.*, 2012). BRI1-positive vesicles were found to co-localize with the endocytic marker FM4-64 which identified them as endosomes (Geldner *et al.*, 2007). Similar to FLS2, localization of BRI1 is BFA-sensitive, suggesting that it undergoes constitutive trafficking between the TGN and PM (Geldner *et al.*, 2007; Irani *et al.*, 2012).

Initially, it has been reported that BRI1 trafficking is not affected by BR-treatment (Geldner *et al.*, 2007) or the absence of the co-receptor BAK1 (Ruscinova *et al.*, 2004), suggesting that it is a process independent of BL signaling. However, BFA treatment stimulated the BL pathway, which led to the hypothesis that signaling occurs in endosomes (Geldner *et al.*, 2007). Later work showed that inhibition of BRI1 endocytosis leads to enhanced brassinosteroid signaling (Geldner *et al.*, 2007; Irani *et al.*, 2012; Di Rubbo *et al.*, 2013) and elegant study with a fluorescently labelled brassinosteroid revealed that this is caused by retention of the active BRI1-brassinosteroid complexes at the PM (Irani *et al.*, 2012). Recently, the relationship between BL signaling and BRI1 endocytosis was investigated in more detail using specific inhibitors and high resolution techniques such as variable angle total internal reflection fluorescence microscopy (VA-TIRFM) (Wang *et al.*, 2015). BRI1 is endocytosed via AP-2 dependent clathrin-coated vesicles (Di Rubbo *et al.*, 2013). Accordingly, Wang *et al.* (2015) found that BFA-sensitivity of BRI1 localization was reduced when plants were treated with Tyrphostin A23. Similar results were observed when BRI1-GFP was expressed in CHC mutant plants (Wang *et al.*, 2015). These results confirm clathrin-mediated endocytosis of BRI1. However, neither TyrA23, nor mutations in CHCs totally blocked the internalization, indicating a clathrin-independent endocytosis pathway for BRI1. Co-localization studies with microdomain marker proteins revealed that BR-induced association of BRI1 with microdomains (Wang *et al.*, 2015). Pharmacological studies suggested that clathrin-mediated endocytosis of BRI1 downregulates BR signaling, while the microdomain-associated endocytosis pathway promotes it (Wang *et al.*, 2015). Transient expression assays in cowpea protoplasts showed that BRI1 and BAK1 interact and both proteins are endocytosed, but their localization in endosomes is only partially overlapping (Ruscinova *et al.*, 2004). Internalization of BRI1 is triggered by ubiquitination, which is largely independent of the BL ligand, but depends on BRI1 kinase activity and its co-receptor BAK1 (Martins *et al.*, 2015).

### 1.3.3 Endocytosis of the LRR-RLPs *LeEIX2* and *Cf4*

Similar to FLS2, the tomato LRR-RLPs *LeEIX2* and *Cf4* undergo ligand-induced endocytosis (Ron and Avni, 2004; Bar and Avni, 2009b; a; Postma *et al.*, 2015). *LeEIX2* was shown to be rapidly and transiently internalized into endosomes upon EIX treatment (Bar and Avni, 2009a). Endocytosis of *LeEIX2* is likely mediated by clathrin-coated vesicles, because it is reduced by application of the dynamin inhibitor Dynasore (Shinya *et al.*, 2012). Moreover, the cytoplasmic tail of *LeEIX2* contains a YXX $\Phi$  signature (Ron and Avni, 2004), which is a binding motif for AP adapter complexes (Geldner and Robatzek, 2008). Mutation of YXX $\Phi$  blocks *LeEIX2*

endocytosis, corroborating a role for CCVs in *LeEIX2* internalization (Bar and Avni, 2009a). Additionally, microdomain-mediated endocytosis pathways may exist for *LeEIX2*, since recent research suggests that *LeEIX2* internalization is sterol-dependent (Sharfman *et al.*, 2014). Several lines of evidence indicate that *LeEIX2* signals from endosomes. Blocking endocytosis of *LeEIX2* with pharmacological inhibitors, by mutating its YXX $\Phi$  motif or by overexpressing EH-DOMAIN CONTAINING 2 (EHD2), a *LeEIX2*-interacting protein that negatively regulates its endocytosis, also suppresses *LeEIX2*-mediated HR (Ron and Avni, 2004). Heterodimerization of *LeEIX2* with the related receptor *LeEIX1* suppresses *LeEIX2* endocytosis. This also leads to attenuation of EIX signaling (Bar *et al.*, 2010), further supporting the hypothesis that *LeEIX2* signaling occurs in endosomes.

Previous studies in *N. benthamiana* showed Cf4 interacting with SOBIR1 at the PM and both proteins undergo endocytosis. SOBIR1 constitutively localizes to endosomes whereas Cf4 is specifically internalized upon ligand stimulus in a BAK1-dependent manner (Postma *et al.*, 2015).

## 1.4 Regulation of plant endocytosis

Endocytosis involves uptake of cargo from outside the cell, invagination and budding of the PM as well as trafficking between different endosomal compartments. Selection of cargo and the continuous movement and fusion of membranes requires tightly regulated processes and dysregulation of these important cellular events leads to severe defects (Jelinkova *et al.*, 2010).

### 1.4.1 Protein phosphorylation and ubiquitination

One mechanism that regulates endocytosis is protein phosphorylation. In animals, receptor tyrosine kinases are the biggest receptor kinase family and their endocytosis is coupled to phosphorylation on tyrosine residues (Goh and Sorkin, 2013). In contrast, plant RLKs belong to the monophyletic group of Ser/Thr kinases (Shiu and Bleecker, 2003; Shiu *et al.*, 2004). However, recent research shows that several plant RLKs also have Tyr kinase activity, thus Tyr phosphorylation might be a regulatory mechanism in plant RLKs as well (Betz *et al.*, 1992; Oh *et al.*, 2009; Macho *et al.*, 2015). Upon ligand perception most enzymatically active plant RLKs autophosphorylate (Battey *et al.*, 1999). The resulting phosphorylated residues represent possible scaffolds for recruitment of accessory proteins and complex partners. This involves homo- or heterooligomerization of RLKs and subsequent transphosphorylation reactions, similar to animal receptor kinases (Wang *et al.*, 2005; Wang *et al.*, 2008; Karlova *et al.*, 2009). The *Arabidopsis* LRR-RLKs BRI1 and FLS2 interact with BAK1 which acts as a positive regulator in their signaling pathways (Nam and Li, 2002; Chinchilla *et al.*, 2007; Heese *et al.*, 2007). The role

of BAK1 in BRI1 internalization has not been investigated, but the interaction of FLS2 with BAK1 is known to be crucial for FLS2 endocytosis (Chinchilla *et al.*, 2007; Beck *et al.*, 2012). Transphosphorylation by BAK1 might be required for FLS2 endocytosis, since Robatzek *et al.* (2006) showed that a mutation in a potential phosphorylation motif of FLS2 prevents its internalization. However, direct evidence for receptor phosphorylation as a prerequisite for receptor endocytosis is still missing.

In animals, ligand- triggered phosphorylation of several growth factor receptor family members recruits E3 ubiquitin ligases leading to receptor ubiquitination and subsequent CME (Mosesson *et al.*, 2003; Mukherjee *et al.*, 2006; Goh and Sorkin, 2013). In particular, the endocytic pathway has been extensively studied for the RTK EGFR. It signals through GRB2, which binds to phosphotyrosine residues of EGFR and recruits an E3 ubiquitin ligase that ubiquitinates EGFR (Jiang *et al.*, 2003). EGFR then binds via ubiquitin-interacting motifs of EPSIN1 to AP2, clathrin and phospholipids. RNAi-mediated knockdown of EPSIN1 perturbs EGFR endocytosis, suggesting a link between ubiquitination of EGFR and endocytosis (Kazazic *et al.*, 2009). The type of ubiquitination determines the fate of the protein. Proteins can be monoubiquitinated or coupled to polyubiquitin chains with different linkage patterns. K48- and- K11 linked polyubiquitin chains target soluble proteins for degradation via the 26S proteasome (Jacobson *et al.*, 2009; Matsumoto *et al.*, 2012). In contrast, mono- or multimonoubiquitination (Barberon *et al.*, 2011) and K63-polyubiquitination (Martins *et al.*, 2015) play a role in protein endocytosis, membrane trafficking and endosomal sorting (Raiborg and Stenmark, 2009; MacGurn *et al.*, 2012). The role of ubiquitination during the early stages of endocytosis is relatively poorly understood (Haglund and Dikic, 2012). At later stages, sorting of ubiquitinated proteins occurs in MVBs and is controlled via the ESCRT machinery. The plant ESCRT consists of three major ESCRT sub-complexes (ESCRT-I to – III). It is required for formation of interluminal vesicles in endosomes resulting in the formation of MVBs and also mediates recognition of ubiquitinated cargo proteins (Raiborg and Stenmark, 2009; Shields and Piper, 2011; Cai *et al.*, 2014). Although ubiquitination is the predominant mechanism to target proteins for sorting by the ESCRT, there are several examples which require other signals. In these cases, the recognition of the MVB cargo proteins is mediated by sorting motifs (Geldner and Robatzek, 2008).

#### **1.4.2 Small G proteins**

Vesicle trafficking is mediated by small GTPases (G proteins) of the Ras superfamily. Small G proteins regulate various cellular processes by switching between a GTP-bound (“on”) and a

GDP-bound (“off”) state. Guanine nucleotide exchange factors (GEFs) activate the GTPase by increasing the GDP-to-GTP exchange rate, whereas GTPase-activating proteins (GAPs) achieve the opposite effect by enhancing their intrinsic GTPase activity (Molendijk *et al.*, 2004). The Ras superfamily is classified into five groups (Ras, Roh, Ran, Rab and Arf) (Rojas *et al.*, 2012), of which four (all but Ras) exist in plants (Molendijk *et al.*, 2004). Members of two classes, Arf (ADP ribosylation factor) and Rab, play important roles in vesicle trafficking. ARFs can be further subdivided into Sar, Arf and Arl GTPases. Sar members are required for trafficking of coat protein complex II (COPII) vesicles from the endoplasmic reticulum (ER) to the Golgi. The Arf subgroup regulates COPI-dependent retrograde transport in the Golgi as well as budding of CCVs at the TGN and the PM (Molendijk *et al.*, 2004). There are eight ARF-GEFs in *Arabidopsis*, where five of which are BFA-sensitive according to their amino acid sequence (Geldner *et al.*, 2003). The secretory pathway of *Arabidopsis* PM traffic is comparatively insensitive to BFA treatment whereas endosomal recycling of endocytosed PM proteins is rather sensitive (Geldner *et al.*, 2003; Richter *et al.*, 2007; Teh and Moore, 2007). GNOM and GNL2 participate in the endosomal recycling pathways from the TGN to the PM (Geldner *et al.*, 2003; Richter *et al.*, 2012). In contrast, the BFA insensitivity of the secretory pathway depends on GNOM-LIKE1 (GNL1), which mediates COPI-vesicle formation in retrograde Golgi-ER traffic (Richter *et al.*, 2007; Teh and Moore, 2007). Out of the other five ARF-GEFs only BIG5 has been intensively studied. BIG5 localizes to the TGN/EE and is distinct from GNOM or GNOM-LIKE2 (GNL2). It is suggested to control the cargo transit between EE and RE of recycling PM proteins. However, BIG5 function is not affected by BFA (Nomura *et al.*, 2006; Tanaka *et al.*, 2009). Similarly, analysis of its amino acid sequence suggests that BIG3 is not a target of BFA but its function is not fully solved. A recent report showed that BIG1-4 play a crucial role in post-Golgi traffic and are jointly involved in cytokinesis (Richter *et al.*, 2014). However, this function then includes BFA-sensitive as well as BFA-insensitive secretory and endocytotic pathways (Richter *et al.*, 2014).

Rab GTPases are present at various different endomembrane compartments and shuttle between the cytosol and membranes. They regulate the vesicle trafficking, vesicle formation, and govern the directionality of vesicle transport processes (Ebine *et al.*, 2011). Rab proteins determine the fusion partners, define the lipid composition of the membranes, affect vesicle motility and modulate vesicular transport through interactions with cytoskeletal components (Woollard and Moore, 2008). The Rab class of small GTPases includes 57 proteins in *Arabidopsis* which are subdivided into eight groups (RabA to RabH) (Rutherford and Moore,



2002; Vernoud *et al.*, 2003). The RabA and RabF classes will be discussed below, because they typically localize to endosomes (Vernoud *et al.*, 2003).

RabA is an expanded group with 27 members (Rutherford and Moore, 2002). RabAs play a role in many processes including pollen tube (Szumlanski and Nielsen, 2009) and root tip growth (Preuss *et al.*, 2004; Szumlanski and Nielsen, 2009; Ovecka *et al.*, 2010) as well as regulating the trafficking between the TGN and PM (Feraru *et al.*, 2012; Asaoka *et al.*, 2013). Based on their homology to yeast and mammalian Rabs, RabAs are generally predicted to localize to the TGN and post-golgi-vesicles and are thought to play roles in TGN to PM trafficking (Vernoud *et al.*, 2003; Qi and Zheng, 2013). TGN/endosome localization has been experimentally demonstrated for several *Arabidopsis* members including RabA1g (Geldner *et al.*, 2009; Ganguly *et al.*, 2014; Lei *et al.*, 2014) and RabA5d (Geldner *et al.*, 2009; Drdova *et al.*, 2013). RabA1g and RabA5d have been suggested as markers for recycling endosomes, based on the strong BFA sensitivity of their localization (Geldner *et al.*, 2009). RabF is a much smaller group with three members in *Arabidopsis*, i.e. ARA6/RabF1 (Ueda *et al.*, 2001), Rha1/RabF2a (Sohn *et al.*, 2003; Lee *et al.*, 2004) and ARA7/ RabF2b (Lee *et al.*, 2004). All three RabFs have been shown to localize to LEs/MVBs (Kotzer *et al.*, 2004; Lee *et al.*, 2004; Haas *et al.*, 2007) but the localization pattern of ARA6/RabF1 does not completely overlap with that of RabF2a/b. (Ueda *et al.*, 2004). Similarly, all three RabFs are activated by the same GEF VSP9a, but the interaction of RabF1 with VSP9a is mechanistically different from RabF2a/b (Goh *et al.*, 2007). Functional differences between RabF1 and RabF2a/b were also revealed by analysis of the respective knock-out mutants (Ebine *et al.*, 2011). Rha1/RabF2a and ARA7/RabF2b were found to be involved in trafficking between MVBs and vacuoles (Sohn *et al.*, 2003), while ARA6 has been implicated in the mediation of direct transport from endosomes to the plasma membrane (Ebine *et al.*, 2011).

## 1.5 Plasmodesmata

All multi-cellular organisms require effective intercellular communication to coordinate cellular processes. In plants, cell-to-cell contact is restricted by the presence of a rigid cell wall. Nevertheless, cells are connected via plasmodesmata (PD), membrane-lined, cell wall channels that provide cytoplasmic continuity and form a tightly regulated system that allows exchange of molecules between neighboring cells. (Lee and Lu, 2011; Maule *et al.*, 2011; Burch-Smith and Zambryski, 2012). In general, PD are lined with PM and a tube of the ER, the so-called desmotubule, that is tightly coiled by reticulons, runs across the pore (Figure 5). Callose, a plant specific polysaccharide consisting of  $\beta$ -1,3 linked glucose, may be deposited in the neck regions

of the tunnel to restrict the PD-flux (Maule *et al.*, 2011; Burch-Smith and Zambryski, 2012; Maule *et al.*, 2012). The cytoplasmic sleeve, the space between PM and desmotubule is filled with cytoskeletal proteins that are important for the PD structure and form and modulate the size exclusion limit (SEL) for transport through the PD (Christensen *et al.*, 2009; Chen *et al.*, 2010). In addition to the cytoplasmic sleeve, the membrane of the desmotubule as well as its lumen serve as trafficking pathways (Guenoune-Gelbart *et al.*, 2008; Barton *et al.*, 2011). Recent analyses of PD-enriched cell wall fractions suggest that PD-associated membranes have distinct features. The studies revealed the presence of proteins like remorins (Raffaele *et al.*, 2009), tetraspanins (Salmon and Bayer, 2012), RLKs and GPI-anchored proteins (Fernandez-Calvino *et al.*, 2011) in PD. Interestingly, PD membranes are enrichment in sterols and sphingolipids with very long chain saturated fatty acids (Grison *et al.*, 2015). This lipid profile is reminiscent of detergent-insoluble PM microdomains which have been found to typically harbor RLKs and GPI-anchored proteins (Thomas *et al.*, 2008; Raffaele *et al.*, 2009; Simpson *et al.*, 2009) (Figure 5). The microdomain-like nature of PD membranes may be important for its function, such as in sorting and recruiting associated proteins.

The structure of the PM allows small uncharged molecules to diffuse through. Various proteins, including ion channels, protein pumps and carrier proteins help large or charged molecules pass through the cell membrane. Transport through PD is presumed to be passive but there is evidence that they facilitate the active transposition of so called non-cell autonomous proteins (NCAPs) acting in developmental processes (Haywood *et al.*, 2002). Moreover, developmental control includes hormone signaling, transcription factor and sRNA/mRNA trafficking between cells and tissues (Zambryski and Crawford, 2000).

PD are involved in several processes one of which is the regulation of plant growth and development. They also may help to determine a program of cell differentiation, such as sealing off root and stem epidermal cells from the rest of the plant (Zambryski and Crawford, 2000; Burch-Smith *et al.*, 2011; Burch-Smith and Zambryski, 2012). Moreover, by regulating their diameter PD play an important role to establish and maintain physiological gradients between cells. The translocation of molecules is limited by the SEL (Xu and Jackson, 2010; Xu *et al.*, 2012). Molecules smaller than the SEL of plasmodesmata are able to move freely through the cytoplasmic channel of plasmodesmata by simple diffusion. The SEL can be modified due to environmental changes such as cytoplasmic calcium levels or in response to changes in turgor pressure between cells (Burch-Smith *et al.*, 2011; Burch-Smith and Zambryski, 2012). The signaling processes are tightly regulated by limiting the active and passive transport through

PD. Interestingly, also auxin could be linked to locally down regulated symplastic permeability by inducing callose deposition at PD (Han *et al.*, 2014). Recent research identified PD-resident proteins involved in callose homeostasis that are associated with the regulation of the PD-flux in both developmental and disease-related contexts (Guseman *et al.*, 2010; Vaten *et al.*, 2011; Maule *et al.*, 2012).

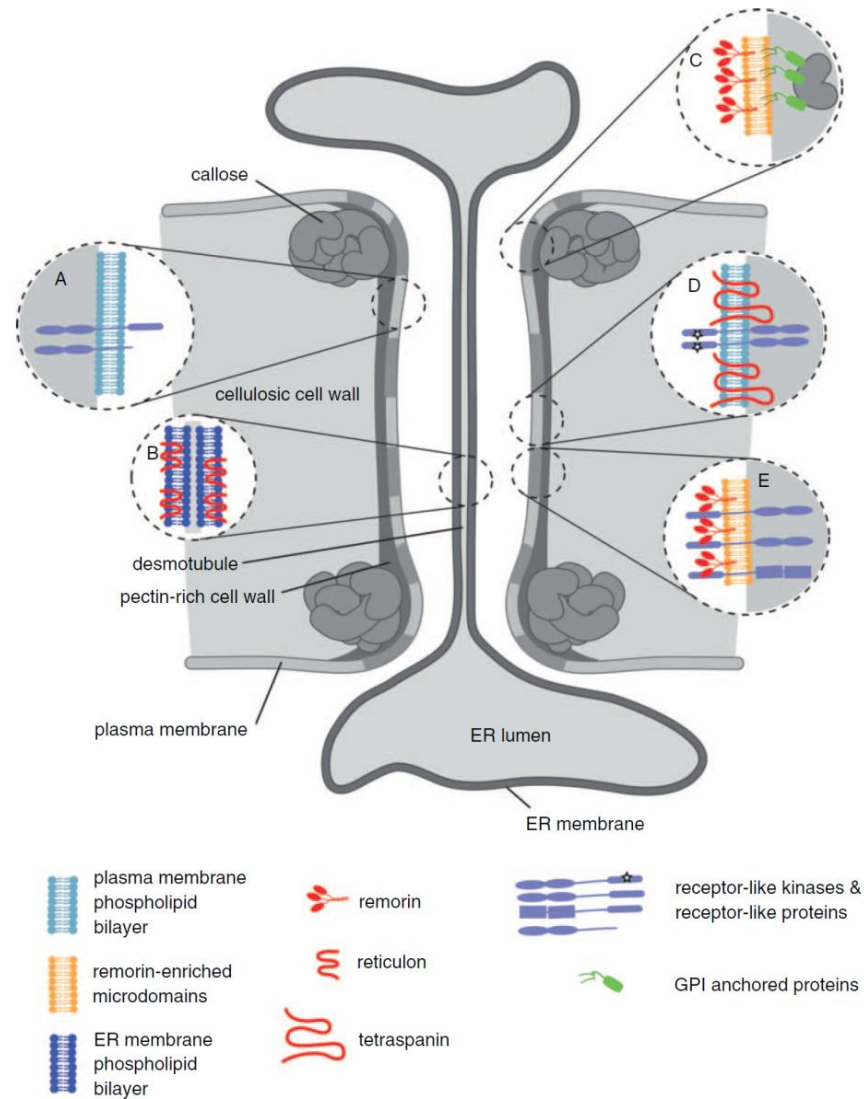


**Figure 5: Simplified model of a plasmodesma.**

The illustration shows the structural domains of the PD pore. The cellulosic or pectin rich cell wall, the PM and the desmotubule are depicted. Different membrane domains are found at PD **(A)** the PM, **(B)** the desmotubule coiled by reticulons, **(C)** remorin enriched microdomains with GPI-anchored proteins or **(E)** receptor-like proteins and **(D)** tetraspanin-enriched microdomains that provide a platform for receptor function. Figure adapted from Maule *et al.* (2011).

### 1.5.1 The function of plasmodesmata in plant innate immunity

A number of pathogens move through plasmodesmata to colonize plant tissues. For example, most plant viruses use their movement proteins to modify PD and spread from cell to cell (Ueki and Citovsky, 2011; Tilsner *et al.*, 2013). Other pathogens like the hemibiotrophic fungus *Magnaporthe oryzae*, exploit these structures by growing through PD to infect the neighboring cells (Kankanala *et al.*, 2007). Strategies to recognize and remodel PD by pathogens allow rapid entry into neighboring cells by keeping the PM intact and thereby prevent plant defense. Therefore PD are ideal locations for structural components of plants innate immunity. Indeed, PD are membrane domains rich in receptor proteins (Fernandez-Calvino *et al.*, 2011). Guarding the PD tunnel with several types of receptor proteins is a plant strategy to counteract pathogens using PD as a route of cell-to-cell movement. *Arabidopsis* contains eight PD-located Proteins (PDLPs), a family of PD-specific RLPs with cysteine-rich ectodomains (Thomas *et al.*, 2008; Lee *et al.*, 2011). Overexpression of PDLP5 causes callose deposition at PD and consequently decreased PD transport. It also causes over-accumulation of SA and an associated cell death phenotype. Moreover PDLP5 overexpression restricts proliferation of *Pseudomonas syringae* and tobacco mosaic virus (TMV), presumably reduced PD connectivity and increased SA levels (Lee *et al.*, 2011). The chitin-binding LysM-RLP LYM2 was also found in a proteomic study on PD proteins (Fernandez-Calvino *et al.*, 2011). Analysis of plants expressing mCitrine-LYM2 fusion proteins indicated that LYM2 is distributed throughout the PM, but shows areas of higher accumulation at PD (Faulkner *et al.*, 2013). Chitin treatment leads to a reduction in PD connectivity in wild type *Arabidopsis* plants. Interestingly, *lym2* mutants were no longer able to restrict transport through PD upon chitin treatment, whereas this response was normal in *cerk1-2*. These results suggest a CERK1-independent role of LYM2 in PD regulation, which is also important for resistance to fungal pathogens (Faulkner *et al.*, 2013). The fact that the PD-located proteins PDLP5 and LYM2 confer resistance to plant pathogens emphasize the crucial role of PD in plant defense (Lee and Lu, 2011).

## 1.6 Thesis aims

In order to detect potential pathogens, plants perceive the fungal polysaccharide chitin via lysin motif receptor-like kinases/proteins (LysM-RLKs/ RLPs). CERK1 is a chitin binding LysM-RLK that dimerizes and autophosphorylates upon chitin perception and mediates downstream chitin signaling (Petutschnig *et al.*, 2010; Liu *et al.*, 2012b). Since the related LysM-RLKs LYK5 and LYK4 as well as the LysM-RLP LYM2 were identified in a chitin pull-down experiment (Petutschnig *et al.*, 2010) they potentially act together with CERK1 in a chitin recognition complex. A function for LYK4 (Wan *et al.*, 2012) and LYK5 (Cao *et al.*, 2014) in chitin triggered defense has been recently demonstrated. However, these findings are contradictory to initial studies where LYK5 and LYK4 were reported to have no role in chitin signaling (Miya *et al.*, 2007; Wan *et al.*, 2008a). Thus, one of the aims of the study is to re-evaluate LYK4 and LYK5 function in chitin signaling by analyzing CERK1 phosphorylation, MAPK activation and defense gene expression in *lyk5* and *lyk4* single mutants and, to rule out functional redundancy, also in a *lyk5 lyk4* double mutant.

Receptor kinases typically reside at the PM and their subcellular localization is dynamically regulated by endomembrane trafficking (Irani and Russinova, 2009; Ben Khaled *et al.*, 2015). Ligand-induced endocytosis has been shown for the PRRs FLS2 (Robatzek *et al.*, 2006), *LeEIX2* (Bar and Avni, 2009a) and Cf4 (Postma *et al.*, 2015). To investigate the ligand-induced spatial dynamics of chitin receptor components, the subcellular localization of CERK1, LYK4 and LYK5 will be analyzed using functional fluorescently-tagged proteins stably expressed in the *Arabidopsis thaliana* Col-0 ecotype and the *cerk1-2* mutant. In order to further characterize trafficking pathways and components involved in the intracellular dynamics of CERK1, LYK4 and LYK5, pharmacological inhibitor studies and co-expression with endosomal marker lines will be carried out.

LYK5 and LYK4 are predicted to be catalytically inactive since they lack conserved kinase subdomains. CERK1, in contrast, harbors an active kinase domain (Miya *et al.*, 2007; Petutschnig *et al.*, 2010). To experimentally examine LYK5 and LYK4 kinase activities and to investigate if LYK5 and LYK4 are substrates for phosphorylation by CERK1, auto- and transphosphorylation assays will be performed *in vitro* with heterologously expressed intracellular domains of CERK1, LYK5 and LYK4. To investigate the phosphorylation of LYK5 and LYK4 by CERK1 *in planta*, transgenic plants expressing tagged LYK5 or LYK4 proteins in Col-0 and *cerk1-2* will be biochemically analyzed. Additionally, plants expressing tagged LYKs and a kinase defective version of CERK1 will be investigated.

LYM2 is a candidate for a CERK1 interaction partner but appears to play no significant role in the canonical chitin response (Shinya *et al.*, 2012). To investigate this in more detail, immunoblot experiments will be performed to visualize CERK1 protein abundance and chitin induced CERK1 phosphorylation in mutants of LYM2 and its homologs. Previously, LYM2 was shown to regulate PD-flux in a chitin-dependent manner (Faulkner *et al.*, 2013). To test for a potential PD-association of LYM2, *Arabidopsis* plants expressing mCitrine-tagged LYM2 will be generated and used to assess the subcellular behavior and chitin-induced dynamics of LYM2. Finally, the project aim includes the generation of a *lyk5 lyk4 lym2* triple knock out plant to further characterize the function of these proteins in chitin signaling and developmental processes.

## 2 Materials and Methods

### 2.1 Materials

#### 2.1.1 Plants

##### 2.1.1.1 *Arabidopsis thaliana*

The *Arabidopsis* (L.) Heynh. accession Columbia-0 (Col-0) was used as wild type line (J. Dangel, University of North Carolina, USA). T-DNA insertion lines from the SALK collection (Alonso *et al.*, 2003) and the SAIL collection (Sessions *et al.*, 2002) were ordered from the Nottingham Arabidopsis Stock Center (NASC) (Scholl *et al.*, 2000). T-DNA insertion lines from the GABI collection were obtained from GABI-KAT (Kleinboelting *et al.*, 2012). Information on T-DNA mutants used in this study are given in Table 1. Transgenic lines generated and/or used in this work are listed in Table 2

**Table 1: *Arabidopsis thaliana* T-DNA mutant lines used in this work.**

Allele	AGI locus	Accession	T-DNA	Reference/ Source
<b>Single mutants</b>				
<i>cerk1-2</i>	At3g21630	Col-0	GABI_096F09	Miya <i>et al.</i> , 2007
<i>lyk4-2</i>	At2g23770	Col-0	GABI_897A10	This work
<i>lyk5-2</i>	At2g33580	Col-0	SALK_131911C	Cao <i>et al.</i> , 2014
<i>lym1-1</i>	At1g21880	Col-0	GABI_419G07	Willmann <i>et al.</i> , 2011; Shinya <i>et al.</i> , 2012
<i>lym2-1</i>	At2g12170	Col-0 <i>qrt</i>	SAIL_343_B03	Shinya <i>et al.</i> , 2012
<i>lym3-1</i>	At1g88630	Col-0	SALK_111212	Willmann <i>et al.</i> , 2011; Shinya <i>et al.</i> , 2012
<b>Double and higher order mutants containing <i>lyk</i> or <i>lym</i> alleles</b>				
<i>lyk5-2 lyk4-2</i>		Col-0		This work
<i>lym1-1 lym2-1 lym3-1</i>		Col-0		Shinya <i>et al.</i> , 2012
<i>lyk5-2 lyk4-2 lym2-1</i> (het/ het/ hom)		Col-0		This work

Table 2: Transgenic *Arabidopsis thaliana* lines used in this work.

Transgene	Background	Vector	Selection marker	Reference
<b>Single transgenic lines</b>				
CERK1-GFP	<i>cerk1-2</i>	<i>pAM-MCS-NotI-pCERK1::CERK1-GFP</i>	Kan <sup>R</sup>	Petutschnig <i>et al.</i> , 2014
LYK5-mCitrine	Col-0	<i>pGreenII-0229-JE-pLYK5::LYK5-mCitrine</i>	Basta <sup>®R</sup>	This work
LYK5-mCitrine	<i>cerk1-2</i>	<i>pGreenII-0229-JE-pLYK5::LYK5-mCitrine</i>	Basta <sup>®R</sup>	This work
LYK5-mCitrine	<i>lyk5-2 lyk4-2</i>	<i>pGreenII-0229-JE-pLYK5::LYK5-mCitrine</i>	Basta <sup>®R</sup>	This work
LYK4-mCitrine	Col-0	<i>pGreenII-0229-JE-pLYK4::LYK4-mCitrine</i>	Basta <sup>®R</sup>	This work
LYK4-mCitrine	<i>cerk1-2</i>	<i>pGreenII-0229-JE-pLYK4::LYK4-mCitrine</i>	Basta <sup>®R</sup>	This work
LYK4-mCitrine	<i>lyk5-2 lyk4-2</i>	<i>pGreenII-0229-JE-pLYK4::LYK4-mCitrine</i>	Basta <sup>®R</sup>	This work
mCitrine-LYM2	Col-0	<i>pGreenII-0229-JE-pLYM2::mCitrine-LYM2</i>	Basta <sup>®R</sup>	This work
mCitrine-LYM2	<i>cerk1-2</i>	<i>pGreenII-0229-JE-pLYM2::mCitrine-LYM2</i>	Basta <sup>®R</sup>	This work
FLS2-GFP	Col-0	<i>pCAMBIA2300-pFLS2::FLS2-GFP</i>	Kan <sup>R</sup>	Göhre <i>et al.</i> , 2008
LTI6b-mKate2	Col-0	<i>pGreen0178-p35S::LTI6b-mKate2</i>	Hyg <sup>R</sup>	H. Ghareeb, unpublished
ARA6-RFP	Col-0	<i>pGJ2185-p35S::ARA6-RFP</i>	Basta <sup>®R</sup>	U. Lipka, unpublished
mCherry-Rha1	Col-0	<i>pNIGEL17-pUBQ10::mCherry-Rha1</i>	Hyg <sup>R</sup>	Geldner <i>et al.</i> , 2009



mCherry-RabA1g	Col-0	<i>pNIGEL17- pUBQ10::mCherry-RabA1g</i>	Hyg <sup>R</sup>	Geldner <i>et al.</i> , 2009
mCherry-RabA5d	Col-0	<i>pNIGEL17- pUBQ10::mCherry-RabA5d</i>	Hyg <sup>R</sup>	Geldner <i>et al.</i> , 2009
CERK1-WT	<i>cerk1-2</i>	<i>pAM-MCS-NotI- pCERK1::CERK1-WT</i>	Kan <sup>R</sup>	Petutschnig <i>et al.</i> , 2010
CERK1-LOF	<i>cerk1-2</i>	<i>pAM-MCS-NotI- pCERK1::CERK1-LOF</i>	Kan <sup>R</sup>	Petutschnig <i>et al.</i> , 2010
<b>Double transgenic lines</b>				
LYK5-mCitrine LTI6b-mKate2	Col-0		Basta <sup>®R</sup> , Hyg <sup>R</sup>	This work
mCitrine-LYM2 LTI6b-mKate2	Col-0		Basta <sup>®R</sup> , Hyg <sup>R</sup>	This work
LYK5-mCitrine ARA6-RFP	Col-0		Basta <sup>®R</sup>	This work
LYK5-mCitrine mCherry-Rha1	Col-0		Basta <sup>®R</sup> , Hyg <sup>R</sup>	This work
LYK5-mCitrine mCherry-RabA1g	Col-0		Basta <sup>®R</sup> , Hyg <sup>R</sup>	This work
LYK5-mCitrine mCherry-RabA5d	Col-0		Basta <sup>®R</sup> , Hyg <sup>R</sup>	This work
LYK5-mCitrine CERK1-WT	<i>cerk1-2</i>		Basta <sup>®R</sup> , Kan <sup>R</sup>	This work
LYK5-mCitrine CERK1-LOF	<i>cerk1-2</i>		Basta <sup>®R</sup> , Kan <sup>R</sup>	This work

## 2.1.2 Bacterial strains

### 2.1.2.1 *Escherichia coli*

#### *Escherichia coli* TOP 10

For cloning approaches chemically competent *Escherichia coli* (*E. coli*) TOP10 cells (Invitrogen, Carlsbad, USA) [ $F^-$  *mcrA*  $\Delta$ (*mrr* *hsd* *RMS^-* *mcrBC*)  $\Phi$ 80/*lacZ* $\Delta$ M15  $\Delta$ *lacX74* *recA1* *ara* $\Delta$ 139  $\Delta$ (*ara-leu*) 7697 *galJ* *galK* *rpsL* (Str<sup>R</sup>) *endA1* *nupG*] were used.

#### *Escherichia coli* ArcticExpress<sup>®</sup>

For protein expression chemically competent *E. coli* ArcticExpress<sup>®</sup> cells (Agilent Technologies, Santa Clara, USA) [*E. coli* B  $F^-$  *ompT* *hsdS*( $r_B^- m_B^-$ ) *dcm*<sup>+</sup> *Tet* *gal* *endA* *Hte* [*cpn10* *cpn60* *Gent*<sup>r</sup>]] were used.

### 2.1.2.2 *Agrobacterium tumefaciens*

The *A. tumefaciens* strain GV3101 (Koncz and Schell, 1986) was used for stable transformation of *A. thaliana* plants. Two different strains were used that either carry the helper plasmid pMP90RK, which confers resistance to kanamycin (Koncz and Schell, 1986) or pSoup, which confers resistance to tetracyclin (Hellens *et al.*, 2000).

## 2.1.3 Yeast strain for cloning and transformation

### 2.1.3.1 *Saccharomyces cerevisiae*

For homologous recombination of DNA fragments, chemically competent *S. cerevisiae* S288C-derived haploid BY4741 (*MATa* *his3* $\Delta$ 1 *leu2* $\Delta$ 0 *met15* $\Delta$ 0 *ura3* $\Delta$ 0) (Brachmann *et al.*, 1998) cells were used

## 2.1.4 Vectors

The following table lists vectors used or generated during this work, as well as their description and antibiotic resistance.

Table 3: Vectors used or generated in this study.

Name	Description	Selectionmarker yeast, <i>bacteria</i> , plant	Reference/ Source
<i>pRS426</i>	Vector for cloning via homologous recombination in yeast	<u>Ura3</u> , Amp <sup>R</sup>	Sikorski and Hieter, 1989; Christianson <i>et al.</i> , 1992
<i>pAM-MCS-35S</i>	Binary vector for <i>A. tumefaciens</i> -mediated transformation of plants and subsequent expression from the <i>p35S</i>	Amp <sup>R</sup> , Kan <sup>R</sup>	Lipka <i>et al.</i> , 2005
<i>pGreenII-0229</i>	Binary vector for <i>A. tumefaciens</i> -mediated transformation of plants	Kan <sup>R</sup> , Basta <sup>®R</sup>	Hellens <i>et al.</i> , 2000
<i>pGreenII-0229-JE</i>	Binary vector for <i>A. tumefaciens</i> -mediated transformation of plants equipped with the expression cassette of <i>pAM-MCS-35S</i>	Kan <sup>R</sup> , Basta <sup>®R</sup>	This work
<i>pGreenII-0229-JE-pLYK5::LYK5-mCitrine</i>	Binary vector for <i>A. tumefaciens</i> -mediated transformation of plants and expression of the <i>LYK5</i> gDNA with a C-terminal mCitrine-tag under control of <i>pLYK5</i> .	Kan <sup>R</sup> , Basta <sup>®R</sup>	This work
<i>pGreenII-0229-JE-pLYK4::LYK4-mCitrine</i>	Binary vector for <i>A. tumefaciens</i> -mediated transformation of plants and expression of the <i>LYK4</i> gDNA with a C-terminal mCitrine-tag under control of <i>pLYK4</i> .	Kan <sup>R</sup> , Basta <sup>®R</sup>	This work

<i>pGreenII-0229-JE-pLYM2::mCitrine-LYM2</i>	Binary vector for <i>A. tumefaciens</i> -mediated transformation of plants and expression of the <i>LYM2</i> gDNA with an N-terminal mCitrine-tag under control of <i>pLYM2</i> .	Kan <sup>R</sup> , Basta <sup>®R</sup>	This work
<i>pGEX4T1</i>	Vector for expression of proteins with an N-terminal GST-tag in <i>E.coli</i>	Amp <sup>R</sup>	GE Healthcare (Munich, Germany)
<i>pGEX4T1-LYK5 (ID)</i>	Vector for expression of <i>LYK5 (ID)</i> with an N-terminal GST-tag in <i>E.coli</i>	Amp <sup>R</sup>	Erwig, 2012
<i>pGEX4T1-LYK4 (ID)</i>	Vector for expression of <i>LYK4 (ID)</i> with an N-terminal GST-tag in <i>E.coli</i>	Amp <sup>R</sup>	Erwig, 2012
<i>pBAD-CERK1 (ID)</i>	Vector for expression of <i>CERK1 (ID)</i> with a C-terminal 6xHis-tag in <i>E.coli</i>	Amp <sup>R</sup>	Gimenez-Ibanez <i>et al.</i> , 2009a
<i>pBAD-CERK1-LOF (ID)</i>	Vector for expression of <i>CERK1-LOF (ID)</i> with a C-terminal 6xHis-tag in <i>E.coli</i>	Amp <sup>R</sup>	Gimenez-Ibanez <i>et al.</i> , 2009a

### 2.1.5 Oligonucleotides

The primers used in this study were ordered from Invitrogen (Darmstadt, Germany) or Sigma-Aldrich (Munich, Germany). The lyophilized oligonucleotides were diluted to a stock-concentration of 100 µM with ultrapure water. For standard usage, aliquots with a working concentration of 10 µM were prepared by dilution with ddH<sub>2</sub>O. Oligonucleotides were stored at -20°C. Table 4 lists all oligonucleotides used in this study.

Table 4: Primer used in this study.

Primer	sequence (5'-3')	Use
<b>Primers for genotyping</b>		
KP7	CCTGACTTACTTAGTCGCCATGGG	genotyping of <i>lyk5-2</i> , gene specific
UL220	TAATCTAACGCCTCTGCCACATCC	genotyping of <i>lyk5-2</i> , gene specific
EP64	ATTTTGCCGATTTTCGGAAC	genotyping of <i>lyk5-2</i> , LB T-DNA
KP11	AAACGTGACAGCCTGTTCTTC	genotyping of <i>lyk4-2</i> , gene specific
KP12	CGCTTTGGATATAGCAACAGG	genotyping of <i>lyk4-2</i> , gene specific
UU41	CCCATTTGGACGTGAATGTAGACAC	genotyping of <i>lyk4-2</i> , LB T-DNA
KP14	GATAGTGCCGTTGGCTATAC	genotyping of <i>lym1-1</i> , gene specific
KP15	TTACGGAGGCTTGGTCTCTG	genotyping of <i>lym1-1</i> , gene specific
UU41	CCCATTTGGACGTGAATGTAGACAC	genotyping of <i>lym1-1</i> , LB T-DNA
KP42	GCGTGAACCCGAATCAAGTC	genotyping of <i>lym2-1</i> , gene specific
KP45	CGTGATGCTTCAGGTGAAAC	genotyping of <i>lym2-1</i> , gene specific
CK31	GCTTCCTATTATATCTTCCCAAATTACCAATACA	genotyping of <i>lym2-1</i> , LB T-DNA
KP30	GTCGCGAATTCAGAGACTGACC	genotyping of <i>lym3-1</i> , gene specific
KP31	TCCGAGAACACAGCTGCATTG	genotyping of <i>lym3-1</i> , gene specific
EP64	ATTTTGCCGATTTTCGGAAC	genotyping of <i>lym3-1</i> , LB T-DNA
UL224	GAGCAAAGGTACATTCTCGATTTTC	genotyping of <i>cerk1-2</i> , gene specific
UL157	AGACAAAATATACGTGAGCATAACC	genotyping of <i>cerk1-2</i> , gene specific
UU41	CCCATTTGGACGTGAATGTAGACAC	genotyping of <i>cerk1-2</i> , LB T-DNA
<b>Primers for expression analysis</b>		
JE78	GCAGCTTGAGAGCAAGAATG	semi-quantitative RT-PCR of <i>WRKY30</i>
EP108	TCAAGAACCACCTTGTCAATCAAGA	semi-quantitative RT-PCR of <i>WRKY30</i>
MW418	ATGCCAGTTTGGATCATAATCG	semi-quantitative RT-PCR of <i>WRKY33</i>
MW419	TTTGTGGCGTAACCGCTACC	semi-quantitative RT-PCR of <i>WRKY33</i>
JE30	GAAGAGTTTGCCGATGGAGG	semi-quantitative RT-PCR of <i>WRKY53</i>
JE31	CGAGGCTAATGGTGGTGTTC	semi-quantitative RT-PCR of <i>WRKY53</i>
EP54	CCGGCCGGACATAAGACTGACTAA	semi-quantitative RT-PCR of <i>CERK1</i>
EP41	GCAATGGGTACATTTGGTTACATGGCAC	semi-quantitative RT-PCR of <i>CERK1</i>

UL211	ACCGAAGGTAACGAGCTTACATCAG	semi-quantitative RT-PCR of <i>LYK5</i>
UL212	ATAAATCTATTGACCATTGAGTCG	semi-quantitative RT-PCR of <i>LYK5</i>
EP70	GTACGACGATTCTTCCCAGTTC	semi-quantitative RT-PCR of <i>LYK4</i>
UL223	AACCATCTTAACATCATCCGTCTC	semi-quantitative RT-PCR of <i>LYK4</i>
ActinF	TGCGACAATGGAAGTGAATG	semi-quantitative RT-PCR of <i>ACTIN1</i>
ActinR	GGATAGCATGTGGAAGTGCATAC	semi-quantitative RT-PCR of <i>ACTIN1</i>
JE73	GGTCACAACAATCCGGAAGA	real-time RT-PCR of <i>WRKY33</i> (Cao <i>et al.</i> 2014)
JE74	GGAGAGACAAGAGAAGGAGAGA	real-time RT-PCR of <i>WRKY33</i> (Cao <i>et al.</i> 2014)
JE77	AGCCAAATTTCCAAGAGGAT	real-time RT-PCR of <i>WRKY30</i> (Cao <i>et al.</i> 2014)
JE78	GCAGCTTGAGAGCAAGAATG	real-time RT-PCR of <i>WRKY30</i> (Cao <i>et al.</i> 2014)
JE79	TCACCGAGCGTACAACCTTATTCC	real-time RT-PCR of <i>WRKY53</i> (Cao <i>et al.</i> 2014)
JE80	CGTTTATCGATGCCGGAGATT	real-time RT-PCR of <i>WRKY53</i> (Cao <i>et al.</i> 2014)
EP223	GGTTTTCCCCAGTGTGTTG	real-time RT-PCR of <i>ACTIN8</i>
EP224	CTCCATGTCATCCCAGTTGC	real-time RT-PCR of <i>ACTIN8</i>
<b>Primers for cloning</b>		
JE61	GGGCGAATTGGGTACCGGCGCGCCCGG	Cloning the <i>pAM-MCS-35S</i> expression cassette into <i>pGreenII-0229</i>
JE62	GCGGTGGCGAGCTCGGCCGGCCCGGTCCTACTG	Cloning the <i>pAM-MCS-35S</i> expression cassette into <i>pGreenII-0229</i>
JE43	CTACGCAGAACTGGGAAGAATCGTCTACTACGCTG GAGCGATGGTGAGCAAGGGCGAGGAGCTGTTCCACC	cloning <i>pLYK4::LYK4-mCitrine</i>
EP70	GTACGACGATTCTTCCCAGTTC	cloning <i>pLYK4::LYK4-mCitrine</i>
JE44	GCGGATAACAATTTTACACAGGAAACAGCCCCG GGCTACTTGACAGCTCGTCCATGCCGAGAGTG	cloning <i>pLYK4::LYK4-mCitrine</i> and <i>pLYK5::LYK5-mCitrine</i>
JE37	GTAACGCCAGGGTTTTTCCCAGTCACGACGGGCG CGCCACCTCTGTTTTTTGTTGTGATTATAG	cloning <i>pLYK5::LYK5-mCitrine</i>
EP72	GTTGCCAAGAGAGCCGGAACGA	cloning <i>pLYK5::LYK5-mCitrine</i>

JE42	CCTTCTTCGTTCCGGCTCTCTTGGAACACTACGCTGG AGCGATGGTGAGCAAGGGCGAGGAGCTGTTCCACC	cloning <i>pLYK5::LYK5-mCitrine</i>
JE7	CTCTCGGCATGGACGAGCTGTACAAGA TGACCGGAAACTTCAACTGC	cloning <i>pLYM2::mCitrine-LYM2</i>
JE10	CTTCCTCACTCTCTCCGCCAAATGGTGA GCAAGGGCGAGGAGCTGTTCCACC	cloning <i>pLYM2::mCitrine-LYM2</i>
JE15	TTGGGCGGAGAGAGTGAGGAAGA	cloning <i>pLYM2::mCitrine-LYM2</i>
JE18	GCGGATAACAATTTTACACAGGAAACAGCCCCGGG CTAGAGAAGGCAGAGACAAA	cloning <i>pLYM2::mCitrine-LYM2</i>
JE24	CTTGACAGCTCGTCCATGC	cloning <i>pLYM2::mCitrine-LYM2</i>
JE25	CCAAAAACCTGAGAACACACCGGCGACCTGAAAATG GAAACTTCCTGTTTTACCCTTCTCGGT	cloning <i>pLYM2::mCitrine-LYM2</i>

### Primers for colony PCR and sequencing

35S GC359	CTATAAGAACCCTAATTCCTTATCTG	sequencing and colony PCR of <i>pGreenII</i> vector constructs
CM29	GTGCGGGCCTCTTCGCTATTAC	sequencing and colony PCR of <i>pGreenII</i> and <i>pRS426</i> vector constructs
EP69	CACCTGATCTCGTTTTTCATTTTATCTCC	sequencing and colony PCR of <i>LYK4-</i> <i>mCitrine</i>
EP70	GTACGACGATTCTTCCCAGTTC	sequencing and colony PCR of <i>LYK4-</i> <i>mCitrine</i>
EP71	CACCATGGCTGCGTGTACTCCACG	sequencing and colony PCR of <i>LYK5-</i> <i>mCitrine</i>
EP155	TGTTGTACGGTGGTTGAGAC	sequencing and colony PCR of <i>LYK5-</i> <i>mCitrine</i>
EP157	GTCGGAAACAGAGCAATCAG	sequencing and colony PCR of <i>LYK4-</i> <i>mCitrine</i>
EP164	GACTGGTGATTTTTGCGGACTC	sequencing and colony PCR of <i>LYK4-</i> <i>mCitrine</i>
JE2	TTCTGGTCTCAACCACCGTAC	sequencing and colony PCR of <i>LYK5-</i> <i>mCitrine</i>
JE23	ATGGTGAGCAAGGGCGAGGAGC	sequencing and colony PCR of <i>mCitrine-</i> <i>LYM2</i>
JE27	TTTCAGGTCGCCGGTGTGTTCTCAGGT	sequencing and colony PCR of <i>mCitrine-</i> <i>LYM2</i>

---

KP9	ACGGATACTCATTCCCTAGAGATGG	sequencing and colony PCR of <i>LYK5-mCitrine</i>
KP28	GAATATCATCAATCTGCCGC	sequencing and colony PCR of <i>mCitrine-LYM2</i>
KP43	AACCGGGACATCGAATACAC	sequencing and colony PCR of <i>mCitrine-LYM2</i>

---

## 2.1.6 Enzymes

### 2.1.6.1 Restriction endonucleases

Restriction endonucleases were obtained from Thermo Fisher Scientific (Waltham, USA) or New England BioLabs (Frankfurt (Main), Germany), respectively. They were used with the supplied 10x reaction buffers according to the manufacturer's recommendations.

### 2.1.6.2 Polymerases and nucleic acid modifying enzymes

Homemade *Taq* DNA polymerase was used for standard polymerase chain reactions (PCR, see 2.2.5.3.1). PCR products for cloning were amplified with the proofreading iProof™ High-Fidelity DNA polymerase according to the manufacturer's instructions (Bio-Rad, Munich, Germany). cDNA was synthesized from total RNA using the RevertAid™ H Minus Reverse Transcriptase (Thermo Fisher Scientific, Waltham, USA) according to the manufacturer's instructions.

## 2.1.7 Chemicals

All chemicals in this work were purchased from the following manufacturers: AppliChem (Darmstadt, Germany), abcam (Cambridge, UK), Becton Dickinson (Franklin Lakes, NJ, USA), BioRad (Munich, Germany), Duchefa (Haarlem, The Netherlands), Invitrogen (Karlsruhe, Germany), Merck (Darmstadt, Germany), Roth (Karlsruhe, Germany), Sigma-Aldrich (Munich, Germany), Serva (Heidelberg, Germany), Thermo Fisher Scientific (Waltham, USA) or VWR (Darmstadt, Germany).

### 2.1.7.1 Antibiotics

The antibiotics used in this work are summarized in the following table. Aqueous solutions were filter sterilized (pore size of 0.2 µm). Stock solutions were stored at -20°C.



Table 5: Antibiotics used in this study.

Antibiotic	Stock conc.	Final conc.	Solvent
Ampicillin (Amp)	100 mg/ml	100 µg/ml	ddH <sub>2</sub> O
Gentamycin (Gent)	50 mg/ml	50 µg/ml	ddH <sub>2</sub> O
Kanamycin (Kan)	50 mg/ml	50 µg/ml	ddH <sub>2</sub> O
Rifampicin (Rif)	20 mg/ml	20 µg/ml	methanol
Hygromycin (Hyg)	50 mg/ml	50 µg/ml	ddH <sub>2</sub> O
Tetracyclin (Tet)	5 mg/ml	5 µg/ml	ethanol
Phosphinotricin (PPT)	25 mg/ml	25 µg/ml	ddH <sub>2</sub> O

### 2.1.7.2 Media

The media, as listed in the following table, were prepared using ultrapure water and autoclaved after preparation at 121°C for 20 min. Antibiotics were added after cooling down to 60°C or lower. Liquid and solid media without antibiotics were stored at room temperature; liquid and solid media with antibiotics were stored at 4°C.

Table 6: Growth media used in this study.

Medium	Composition	
<b><i>Escherichia coli</i> growth medium</b>		
Lysogeny broth/ Luria-Bertani broth (LB)	Tryptone	10.0 g/l
	Yeast extract	5.0 g/l
	NaCl	10.0 g/l
	pH	7.0
	for solid medium 1.5% (w/v) agar (bacterial grade) was added to the broth.	

***Agrobacterium tumefaciens* growth medium**

Double yeast, tryptone (DYT) medium	Yeast extract	10.0 g/l
	Tryptone	16.0 g/l
	NaCl	10.0 g/l
	pH	7.0
	for DYT agar plates 1.5% (w/v) agar (bacterial grade) was added.	

***Saccharomyces cerevisiae* growth media**

Yeast Extract-Peptone-Dextrose (YPD) Broth	Yeast extract	10.0 g/l
	Peptone	20.0 g/l
	Dextrose (Glucose)	20.0 g/l
	pH	6.5
For YPD agar plates 1.5% (w/v) agar (bacterial grade) was added.		

Synthetic complete (SC) medium (-Ura +Glu)	Yeast nitrogen base (YNB)	6.7 g/l
	w/o amino acids	
	Drop-out base (-Ura)	2.0 g/l
	Agar	20.0 g/l
	Glucose	20.0 g/l
	pH	5.6
All solutions were prepared in double strength because the glucose was sterilized separately and later combined with the medium containing the other components. The glucose solution was filter sterilized whereas the other components were autoclaved.		

***Arabidopsis thaliana* growth medium**

½ Murashige and Skoog (MS) plant growth medium	MS powder	2.2 g/l
	Sucrose	5.0 g/l
	pH	5.7 (KOH)
	For ½ MS agar 4.5 g/l plant agar were added before autoclaving.	

### 2.1.7.3 Inhibitors

The inhibitors used for pharmacological studies in this work are summarized in the following table. Stock solutions were prepared and stored at -20°C.

**Table 7: Inhibitors used in this study.**

<b>Inhibitor</b>	<b>Stock conc.</b>	<b>Working conc.</b>	<b>Solvent</b>	<b>Source</b>
2,3-butanedione monoxime (BDM)	500 mM	50 mM	ddH <sub>2</sub> O	abcam
Brefeldin A (BFA)	20 mM	30 µM	DMSO	abcam
Concanamycin A (ConcA)	100 µM	1 µM	DMSO	abcam
K252a	1 mM	10 µM	DMSO	abcam
MG132	50 mM	50 µM	DMSO	abcam
Okadaic acid (OA)	100 µM	1 µM	DMSO	abcam
Oryzalin	20 mM	20 µM	DMSO	Riedel-de Haën
Wortmannin (Wm)	10 mM	30 µM	DMSO	abcam

### 2.1.7.4 Antibodies

Primary and secondary antibodies used for immunoblot detection are listed below. The antibodies used in this study were aliquoted and kept at -80°C for long term storage. Aliquots in use were kept at 4°C to avoid repeated freeze-thaw cycles.

**Table 8: Antibodies (primary and secondary) used in this study.**

<b>Primary antibody</b>	<b>Produced in (organism)</b>	<b>Company</b>
αCERK1 (used 1:3000)	Rabbit, polyclonal	Eurogentec (Cologne, Germany) [custom made]
αp-MAPKs (Phospho-p44/42 MAPK) (used 1:10000)	Rabbit, polyclonal	Cell Signaling Technology, Danvers, MA, USA

$\alpha$ GFP (used 1:3000)	Rat, monoclonal	ChromoTek GmbH, Planegg- Martinsried, Germany
$\alpha$ GST (used 1:3000)	Mouse polyclonal	Sigma-Aldrich (München, Germany)
$\alpha$ 6xHistidine (used 1:2000)	Mouse polyclonal	GeneTex (Irvine, USA)
<b>Secondary antibody</b>	<b>Produced in (organism)</b>	<b>Company</b>
$\alpha$ -mouse IgG AP conjugate (used 1:5000)	Goat, polyclonal	Sigma-Aldrich (München, Germany)
$\alpha$ -rat IgG AP conjugate (used 1:5000)	Rabbit, polyclonal	Sigma-Aldrich (München, Germany)
$\alpha$ -rabbit IgG AP conjugate (used 1:5000)	Goat, Polyclonal	Sigma-Aldrich (München, Germany)

### 2.1.7.5 Buffers and solutions

All buffers and solutions were prepared with ultrapure water. Buffers and solutions used in this work were sterilized by autoclaving for 20 min at 121°C. Solutions which were not autoclaved were sterilized using filters with a pore size of 0.2  $\mu$ m. Table 9 lists the buffers and solutions used in this work.

**Table 9: Buffers and solutions used in this study.**

<b>Buffer/ Solution</b>	<b>Composition</b>	
<b>Agarose gel electrophoresis and PCR</b>		
Agarose solution	Agarose	1 -2% (w/v)
	TAE-Buffer	1x
DNA loading dye (6x)	Sucrose	4 g
	EDTA [0.5 M]	2 ml
	Bromophenol blue	25 mg

PCR reaction buffer for <i>Taq</i> (10x)	Tris base	100 mM
	KCl	500 mM
	MgCl <sub>2</sub>	15 mM
	Triton X-100	1% (w/v)
	pH	9.0 KOH
TAE (50x)	Tris base	2 M
	Glacial acetic acid	57.1 ml/l
	EDTA (0.5 M, pH 8.0)	100 ml/l
<b>Bacterial infiltration</b>		
<i>Agrobacterium</i> infiltration medium	MgCl <sub>2</sub>	10 mM
	Acetosyringone	150 μM
<b>Extraction of genomic DNA from plants</b>		
Extraction buffer	Tris-HCl, pH 7.5	0.2 M
	NaCl	1.25 M
	EDTA	0.025 M
	SDS	0.5% (w/v)
<b>Histochemical staining for microscopy</b>		
FM4-64 staining solution	FM4-64 (SynaptoRed) in DMSO	10 mM
Aniline Blue staining solution	Aniline Blue in KH <sub>2</sub> PO <sub>4</sub> buffer, pH 9.5	0.01% (w/v)

***In vitro* phosphorylation assay**

<b>10x Kinase buffer</b>	Tris-HCl (pH 7.5)	200 mM
	Glycerol	10% (v/v)
	MgCl <sub>2</sub>	100 mM
	MnCl <sub>2</sub>	10 mM
	DTT	10 mM
	ATP	2 mM

**Plasmid preparation**

Buffer P1	Tris-HCl, pH 8.0	50 mM
	EDTA, pH 8.0	10 mM
	RNase A (DNase free)	100 µg/ml
Buffer P2	NaOH	200 mM
	SDS	1% (w/v)
Buffer P3	Potassium acetate	3 M
	Acetic acid	2 M

**Preparation and transformation of chemically competent *S. cerevisiae* cells**

Li-PEG buffer	Lithium acetate	100 mM
	Tris-HCl, pH 8.0	10 mM
	EDTA, pH 8.0	1 mM
	PEG4000	50% (w/v)
	Autoclave before use.	
SORB buffer	Lithium acetate	100 mM
	Tris-HCl, pH 8.0	10 mM
	EDTA, pH 8.0	1 mM
	Sorbitol	1 M
	Autoclave before use.	

---

**Preparation of chemically competent *E. coli* cells**


---

CaCl <sub>2</sub> -solution	CaCl <sub>2</sub>	60 mM
	Glycerol	15% (v/v)
	PIPES-KOH, pH 7.0	10 mM
	The pH was adjusted with 1 M KOH before adding the CaCl <sub>2</sub> and the glycerol	

---

**Protein extraction and purification from *E.coli***


---

GSH-elution buffer	Tris-HCl, pH 8.0	125 mM
	NaCl	150 mM
	Glutathione reduced (GSH)	5 mM
GSH-wash buffer	Tris-HCl pH 8.0	125 mM
	NaCl	150 mM
His-binding and wash buffer	Tris-HCl, pH 8.0	50 mM
	NaCl	300 mM
	EDTA	1 mM
	Glycerin	10% (v/v)
	Imidazol	5 mM
His-elution buffer	Tris-HCl, pH 8.0	50 mM
	NaCl	300 mM
	EDTA	1 mM
	Glycerin	10% (v/v)
	Imidazol	500 mM
PBS (phosphate buffered saline)	NaCl	150 mM
	KCl	2 mM
	Na <sub>2</sub> HPO <sub>4</sub>	10 mM
	NaH <sub>2</sub> PO <sub>4</sub>	2 mM
	pH	7.4

---

---

**Protein extraction from plants**


---

CERK1 extraction buffer	Sucrose	250 mM
	HEPES-KOH, pH 7.5	100 mM
	Glycerol	5% (v/v)
	Na <sub>2</sub> MoO <sub>4</sub>	1 mM
	Na <sub>4</sub> P <sub>2</sub> O <sub>7</sub>	50 mM
	NaF	25 mM
	EDTA	10 mM
	DTT	1 mM
	Triton X-100	0.5% (w/v)
	Protease inhibitor Cocktail	(1:100)
Mild washing buffer for GFP pull-downs	Sucrose	250 mM
	HEPES-KOH, pH 7.5	100 mM
	Glycerol	5% (v/v)
	Triton X-100	0.5% (v/v)
Protease inhibitor cocktail (PIC, 200 ml, 100x)	4-(2-aminoethyl) benzenesulfonyl fluoride hydrochloride (AEBSF)	1 g
	Bestatin hydrochloride	5 mg
	Pepstatin A	10 mg
	Leupeptin hemisulfate	100 mg
	E-64 (trans-epoxysuccinyl-L-leucylamido-(4-guanidino)butane)	10 mg
	Phenanthroline (1, 10-phenanthroline monohydrate)	10 g

All components were dissolved separately in a small amount of DMSO before being combined and filled up with DMSO to a total volume of 200 ml. Aliquot in 2 ml tubes and store at -20°C.

---



---

**SDS-PAGE and Immunoblot analysis**


---

4x SDS loading buffer	Tris-HCl, pH 6.8	200 mM
	DTT	400 mM
	SDS	8% (w/v)
	Glycerol	40% (v/v)
	Bromophenol blue (store at -20°C)	0.1% (w/v)
10x SDS running buffer	Glycine	2 M
	Tris	250 mM
	SDS	1% (w/v)
10x Transfer buffer	Tris	500 mM
	boric acid	500 mM
	pH	8.3
Alkaline Phosphatase (AP) Buffer	Tris-HCl, pH 9.5	100 mM
	NaCl	100 mM
	MgCl <sub>2</sub>	50 mM
Coomassie staining solution	Methanol	45% (v/v)
	Glacial acetic acid	10% (v/v)
	Coomassie R-250	0.05% (w/v)
Destaining solution		
	for polyacrylamide gels	
	Methanol	25% (v/v)
	Glacial acetic acid	7% (v/v)
	Add H <sub>2</sub> O	
	for PVDF membranes	
	Methanol	45% (v/v)
	Glacial acetic acid	10% (v/v)
	Add H <sub>2</sub> O	

---

---

TBS-T (Tris Buffered Saline Tween)	NaCl	150 mM
	Tris-HCl (pH 8)	10 mM
	Tween-20	0.05% (v/v)
TBS-T+MP	TBS-T	
	Skimmed milk powder	50 g/l

---

## **2.2 Methods**

Basic molecular biology techniques were performed as described in Ausubel (2003) if not stated otherwise. For all experiments, sterile pipette tips and tubes were used.

### **2.2.1 Methods for working with plants and plant material**

#### **2.2.1.1 Surface sterilization of *Arabidopsis* seeds**

##### **2.2.1.1.1 Sterilization using chlorine**

For seed sterilization using chlorine, the packed seeds were placed in a desiccator. Next 5 ml HCl (37%) were added to 100 ml 12% NaClO in a glass beaker placed in this desiccator. Since the resulting gas is harmful the whole procedure takes place under the fume hood overnight.

##### **2.2.1.1.2 Sterilization using ethanol**

Seeds were placed into a 2 ml reaction tube and were washed 3 times with 1 ml 70% ethanol. After that, 1 ml ethanol (96%) was added and seeds were transferred to a filter paper for drying. The sterilization procedure was performed in a sterile workbench.

##### **2.2.1.2 Plant growth conditions for tissue culture**

Surface sterilized seeds were placed on ½ MS agar plates. Seeds were then stored for 2 d at 4°C to break dormancy and then transferred to a growth cabinet conditions (CLF Plant Climatics, Wertingen, Germany) with short day condition (light for 10 h at 22°C and darkness for 14 h at 20°C). Two weeks after germination the plants were transferred to soil.

*Arabidopsis* plants used in expression analyses were grown *in vitro* in 24-well plates. For this, the wells were filled with 2 ml liquid ½ MS medium before adding 3-5 surface sterilized *Arabidopsis* seeds. The seeds were allowed to germinate and grow for 13 d in a plant growth chamber under short day conditions (see above). Then the medium was replaced with 1.5 ml new ½ MS medium. The next day (day 14) the seedlings were treated with polymeric chitin or medium as control. For this, 0.5 ml ½ MS medium with 4x the final concentration of chitin was added.

##### **2.2.1.3 Plant growth conditions for cultivation on soil**

The soil (Frühstorfer Erde, Type T25, Str1, Archut) for plant cultivation was steamed prior to use (80°C for 20 min) to remove of soil-borne pests and pathogens. Seeds were placed directly on

soil and then stored for 2 d at 4°C to break dormancy. After that, the pots were transferred into short-day climate chambers with 8 h of light per day, 22°C/20°C day/night, 65% relative humidity and 120  $\mu\text{mol}/\text{m}^2\text{s}$  light intensity. After 10 d, seedlings were pricked out. Alternatively, seedlings grown *in vitro* on MS agar plates were transferred to soil after approximately 2 weeks. About 4-6 week-old plants were then used for experiments. 6-8 week-old plants were transferred from short-day to long-day conditions for seed propagation for further 3-4 weeks. For faster propagation, plants were directly grown under long-day conditions (16 h light [ $\sim 150 \mu\text{mol}/\text{m}^2\text{s}$ ], 22°C, 8 h dark, 20°C, 65% rel. humidity). Climate chambers: JC-ESC 300 chamber system (Johnson Controls, Milwaukee, WI, USA)

#### **2.2.1.4 Crossing *Arabidopsis thaliana***

In order to generate crosses of different *Arabidopsis* mutant lines the plants were manually crossed. Therefore, closed flower buds were chosen. First, a shoot was selected and all side branches were removed to prevent confusions with non-crossed flowers. Second, sepals, petals and stamina of the maternal flower were removed until only the carpel was left. The stigma was then pollinated with single stamina from the paternal flower. Finally, the plant was allowed to develop a silique at long-day conditions.

#### **2.2.1.5 *Agrobacterium*-mediated stable transformation of *Arabidopsis***

The floral dipping method was used to transform *Arabidopsis thaliana*. The protocol used is based on the method described by Clough and Bent (1998). Plants were grown under short day conditions for 2-4 weeks and then transferred to long day to induce flowering. The first bolts were clipped to break apical dominance. 2-4 days after clipping the new bolts were ready to be transformed. A single colony of *A. tumefaciens* cells transformed with the construct of interest (2.2.2.5) was used to inoculate a 25 ml pre-culture of DYT mixed with the appropriate antibiotics. The bacteria were grown at 28°C and 180 rpm in the Certomat<sup>®</sup> BS-1 incubator (Sartorius-Stedim Biotech, Göttingen, Germany) for 2 d and the pre-culture was used to inoculate 250 ml DYT with appropriate antibiotics. The culture was grown overnight and then spun down at 4500 g for 30 min at RT. The supernatant was discarded and the remaining pellet was resuspended in 250 ml 5% sucrose solution. Silwet L-77 was added to a concentration of 0.005 – 0.02 % to reduce surface tension. Inflorescences were dipped briefly in the *Agrobacterium* solution and were then stored at low light conditions under a cover for 16 – 24 h to maintain high humidity. Then, plants were placed into a climate chamber with long-day conditions to set seeds.

### 2.2.1.6 Selection of stably transformed *Arabidopsis* plants

#### 2.2.1.6.1 Basta<sup>®</sup> selection on soil

Selection of stably transformed, Basta<sup>®</sup>-resistant *Arabidopsis* plants was performed using Basta<sup>®</sup> solution (200 g/l glufosinate [phosphinothricin ammonium], Bayer CropScience AG, Monheim, Germany). For this purpose, T1 seeds were sown on soil and allowed to germinate covered with a plastic lid. One week after germination, seedlings were sprayed with a 1:1000 diluted Basta<sup>®</sup> solution. This was repeated three times in two day intervals. Successfully transformed seedlings were resistant and thus survived the Basta<sup>®</sup> treatment. The transformants were picked and transplanted into fresh single pots.

#### 2.2.1.6.2 *In vitro* selection of *Arabidopsis* transformants

*In vitro* selection was carried out to analyze the segregation pattern of transgenic *Arabidopsis* T2/T3 plants. For this purpose, sterilized seeds were spread onto ½ MS agar plates containing either 25 µg/ml phosphinothricin (PPT), 50 µg/ml kanamycin (Kan) or 50 µg/ml hygromycin (Hyg) as selection markers. Seedlings were grown under short-day conditions until transformed seedlings clearly differed from non-resistant seedlings. Transformants were picked and transferred onto soil for further propagation (see 2.2.1.3).

#### 2.2.1.7 Treatment of *Arabidopsis thaliana* leaves with elicitors and inhibitors

For assaying phosphorylation of CERK1, LYK5, LYK4 or MAPKs, 100 µg/ml chitin was vacuum-infiltrated into detached leaves of 6-8 week-old plants using a plastic desiccator and incubated for 10 min. For phosphorylation time course experiments, the incubation times are indicated in the figures. For quantitative real-time PCR experiments, chitin was added to the liquid growth medium of 2 week-old *in vitro* grown seedlings. The final chitin concentrations and incubation times varied and are indicated in the respective figures and legends. Treated plant material was then blotted dry and transferred into a new tube before being frozen in liquid nitrogen. The samples were either directly used for protein extraction or stored at -80°C.

For confocal microscopy, chitin or flg22 (EZBiolab) were vacuum-infiltrated into leaf pieces of preferably 4-6 week-old plants using a syringe. Polymeric chitin was used at a concentration of 100 µg/ml and flg22 at 1 µM. If not otherwise indicated, the incubation time was 60 min. For pharmacological studies, leaf pieces were pre-incubated in inhibitor solution for 30 min and then the inhibitor solution with or without 100 µg/ml chitin was vacuum-infiltrated. For K252a the pre-incubation step was omitted. The endocytic tracer dye FM4-64 (SynaptoRed) was purchased

from Sigma-Aldrich and a 10 mM stock solution was prepared in DMSO. Leaf pieces were incubated in 5  $\mu$ M FM4-64 for 15 min prior to microscopy or additional treatments. For callose the leaf discs were incubated for 15 min in aniline blue staining solution after elicitor treatment.

## 2.2.2 Methods for working with bacteria

### 2.2.2.1 Cultivation of bacteria

*E. coli* cells were either cultivated on solid LB plates or in liquid LB medium. Appropriate antibiotics were added as selective markers. Antibiotics used in this study are summarized in Table 5.

Single colonies from LB plates were used to inoculate liquid medium. *E. coli* cells on plates were grown at 37°C in an IPP 500 incubator (Mettler, Schwabach, Germany), liquid cultures were grown at 37°C and 220 rpm for aeration in an Innova 4230 incubator (New Brunswick Scientific, Enfield, CT, USA). For protein expression *E. coli* cells were grown in liquid culture at 28°C with 180 rpm shaking in the Certomat<sup>®</sup> BS-1 incubator (Sartorius-Stedim Biotech, Göttingen, Germany).

*A. tumefaciens* GV3101 (pMP90RK or pSoup) cells used for transformation of plants were cultivated in liquid DYT medium supplied with the respective antibiotics for selection (Table 5) or on the corresponding DYT agar plates. *Agrobacterium* were grown for 2-3 days at 28 °C and liquid cultures were additionally shaken at 180 rpm.

### 2.2.2.2 Preparation of chemically competent *E. coli* cells

A single colony of *E. coli* cells was used to inoculate 50 ml of selective LB medium. The culture was grown overnight at 37°C while shaking. The next day, 1 ml of this culture was used to inoculate 150 ml of LB. Cells were grown at 37°C while shaking to OD<sub>600</sub>= 0.4. All following steps were carried out on ice. The culture was divided into pre-chilled 50 ml tubes and spun down in a swing out centrifuge (Heraeus Multifuge 3SR+, Thermo Fisher Scientific, Waltham, USA) at 3000 rpm and 4°C for 10 min. After that, the supernatant was discarded and the remaining pellet was re-suspended in 10 ml ice-cold CaCl<sub>2</sub>-solution and the cells were then again spun down at 2800 rpm and 4°C for 7 min. This step was repeated once. The supernatant was again removed and the pellet was re-suspended in 2 ml ice-cold CaCl<sub>2</sub>-solution. Finally, the cells were aliquoted (50  $\mu$ l) and frozen in liquid nitrogen before being stored at – 80°C.

### 2.2.2.3 Preparation of electro-competent *A. tumefaciens* cells

50 ml DYT medium supplemented with the appropriate antibiotics were inoculated with an *A. tumefaciens* colony from a DYT plate. The culture was incubated at 28°C at 180 rpm overnight.

The next day, 250 ml DYT containing the appropriate antibiotics were inoculated to an  $OD_{600} = 0.3$  and the cells were grown at 28°C and 180 rpm to an  $OD_{600} = 1.2$ . The cultures were spun down at 4°C and 4500 g for 30 min. The supernatant was removed and the pellet was resuspended in 30 ml ice-cold 1 mM HEPES, pH 7.0. These steps were repeated twice. After removal of the supernatant, the pellet was resuspended in 30 ml ice-cold 10% glycerol and centrifuged as before. The supernatant was removed and the pellet was resuspended in 2 ml ice-cold 10% glycerol. The cells were divided into 50 µl aliquots in 1.5 ml reaction tubes and frozen in liquid nitrogen before being stored at – 80°C.

### 2.2.2.4 Transformation of chemically competent *E.coli* cells

Transformation started with thawing the cells on ice. Then up to 1 µg DNA was added and the cells were stored on ice for 20 min. After that, a short heat shock for 30 s at 42°C was carried out. Then, 800 µl LB were added and the cells were incubated for 60 min at 37°C while shaking. After incubation the cells were spun down in a table top centrifuge (Heraeus Pico21, Thermo Fisher Scientific, Waltham, USA) for 1 min at 10000 rpm. Nearly all of the supernatant was discarded and the pellet was re-suspended in the remaining supernatant which was then plated on selective LB agar and grown overnight at 37°C.

### 2.2.2.5 Transformation of electro-competent *A. tumefaciens* cells

First, the cells were thawed on ice and 1 µl plasmid DNA was added. The mixture was then transferred into a precooled electroporation cuvette with 0.1 cm gap width. Transformation was carried out using a Micro Pulser™ (BioRad, München, Germany) electroporation apparatus (setting: 25 µF, 2.5 kV and 400 Ω). 800 µl liquid DYT were then added and the bacterial solution was transferred into a 1.5 ml reaction tube. The sample was incubated at 28°C and 180 rpm for 2-3 h. Then 50 µl of the mixture were plated onto a DYT agar plate with the appropriate antibiotics and the plate incubated at 28°C for 2-3 days.

### 2.2.2.6 Storage of bacterial cultures

Short-term storage of bacteria is possible by keeping the cells on solid medium sealed with parafilm®. The cells are viable for up to one month at 4°C. For long-term storage, glycerol stocks

of the respective cells were made by mixing 1 ml overnight culture with 154  $\mu$ l sterile 85% glycerol. The cells were frozen in liquid nitrogen and subsequently stored at  $-80^{\circ}\text{C}$ .

### **2.2.3 Methods for working with *Saccharomyces cerevisiae***

#### **2.2.3.1 Cultivation and storage of *S. cerevisiae***

*S. cerevisiae* cells used for cloning via homologous recombination were either grown in liquid YPD medium or on YPD agar plates. The cells were incubated at  $28^{\circ}\text{C}$  for 2-3 days. Liquid cultures were grown at  $28^{\circ}\text{C}$  and 120 rpm. For preparation of glycerol stocks see 2.2.2.6. However in contrast to bacterial cultures, *S. cerevisiae* cells were not frozen in liquid nitrogen but directly stored at  $-80^{\circ}\text{C}$ .

#### **2.2.3.2 Preparation of chemically competent *S. cerevisiae* cells**

A 2 ml overnight culture of the S288C-derived *S. cerevisiae* strain BY4741 (Brachmann *et al.*, 1998) was used to inoculate a 20 ml YPD culture to an  $\text{OD}_{600} = 0.1$ . The culture was incubated for 6 h at  $30^{\circ}\text{C}$  and 120 rpm and then spun down at 2300 g for 3 min. The cell pellet was washed with 10 ml water, followed by a wash step with 2 ml SORB buffer. The cells were then resuspended in 180  $\mu$ l SORB buffer. To this, 20  $\mu$ l single-stranded carrier-DNA (salmon sperm DNA, 2 mg/ml) were added and the cell suspension was mixed. 50  $\mu$ l aliquots of the cells were either frozen at  $-80^{\circ}\text{C}$  (no liquid nitrogen) or directly used for transformation.

#### **2.2.3.3 Transformation of chemically competent *S. cerevisiae* cells**

*S. cerevisiae* cells can be transformed with plasmids and/or DNA fragments. For this purpose, 1 -10  $\mu$ l of DNA was mixed with chemically competent *S. cerevisiae* cells. Then 300  $\mu$ l Li-PEG buffer and 20  $\mu$ l DMSO were added. The sample was incubated for 30 min on a wheel at 18 rpm and room temperature, before heat shocking the cells at  $42^{\circ}\text{C}$  for 15 min. The cells were then centrifuged for 3 min at 2300 g and the supernatant was discarded. The pellet was resuspended in the residual liquid and the cell suspension was plated onto an SC medium agar plate (- Ura + Gluc). Cells were allowed to grow for 2 d at  $28^{\circ}\text{C}$ .

### **2.2.4 Molecular biological methods**

#### **2.2.4.1 Isolation of genomic DNA (gDNA) from *Arabidopsis thaliana***

Fast and simple gDNA preparation for genotyping by PCR was carried out by using one small rosette leaf that was harvested into a 1.5 ml tube and subsequently ground with a plastic pestle in 300  $\mu$ l extraction buffer. The sample was then incubated for 5 min at RT followed by centrifugation for 5 min at 17000 g. After that, the supernatant was transferred into a new 1.5 ml



tube and 300 µl isopropanol were added and the sample was mixed. Next, the sample was spun down in a table top centrifuge for 10 min at 17000 g at room temperature. The supernatant was then discarded and the formed pellet was washed with 70% ethanol. The pellet was then air dried and re-suspended in 50 µl ddH<sub>2</sub>O. 1-2 µl of this DNA was then used for a 20 µl PCR reaction.

#### **2.2.4.2 Isolation of plasmid DNA from *E.coli***

*Small-scale plasmid preparation* (Birnboim and Doly, 1979)

1.5 ml of liquid bacterial overnight culture were transferred into a 1.5 ml reaction tube and spun down for 1 min at 17000 g in a table top centrifuge. If the pellet was very small, the process was repeated with another 1.5 ml of culture. After removal of the supernatant the remaining pellet was re-suspended in 200 µl buffer P1. Next, 200 µl buffer P2 were added and mixed gently by inverting the tube. The samples were incubated for 3-5 min at room temperature. The lysis reactions were then stopped by adding 200 µl buffer P3 and immediately mixed by inverting several times. After that, the samples were centrifuged for 12 minutes at 17000 g. Then, 500 µl of the clear supernatant were transferred into a new 1.5 ml reaction tube. Care was taken not to disturb the white precipitate. 1 ml 96% ethanol was added to precipitate the DNA. Then, the tubes were centrifuged for 5 min at 17000 g. The supernatant was removed and the formed pellet was washed with 70% ethanol and centrifuged for 1 min at 17000 g. After removing the supernatant and an additional centrifugation step for 2 min at 17000 g, the remaining ethanol was removed and the formed pellet was air-dried at room temperature. Finally, the pellet was re-suspended in 50 µl of water.

*Medium-scale plasmid preparation*

To reach a higher yield and purity of DNA, 50 ml overnight culture were spun down and used for DNA isolation with the Plasmid Plus Midi Kit 100 (QIAGEN, Hilden, Germany) according to the manufacturer's instructions.

#### **2.2.4.3 Polymerase chain reaction (PCR)**

##### **2.2.4.3.1 Standard PCR and colony PCR**

For standard applications such as genotyping, PCR was performed with homemade *Taq* polymerase.

PCR Mix for one reaction:

10x reaction buffer	2 $\mu$ l
Primer 1 (10 $\mu$ M)	1 $\mu$ l
Primer 2 (10 $\mu$ M)	1 $\mu$ l
dNTPs (10 mM)	0.4 $\mu$ l
<i>Taq</i> Polymerase	0.4 $\mu$ l
template DNA	1 $\mu$ l (or a single bacterial colony)

**Table 10: General temperature profile for PCR with *Taq* polymerase.  $T_m$  indicates the average melting temperature of primers used.**

Step	Temperature [°C]	Time [min]	Repeats
Initial denaturation	94	02:00	1x
Denaturation	94	00:30	
Annealing	$T_m - 5^\circ\text{C}$	00:30	32x
Elongation	72	01:00 /kb	
Final elongation	72	10:00	1x
End	4	05:00	1x

#### 2.2.4.3.2 PCR for generation of DNA fragments used for cloning

For DNA fragments used for cloning, an accurate dsDNA synthesis is necessary. Therefore, proofreading polymerases with a low error frequency are used. Here the iProof™ High Fidelity PCR kit (BioRad, Munich, Germany) was used according to the manufacturer's instructions.

#### 2.2.4.4 DNA agarose gel electrophoresis

In order to separate and visualize DNA fragments, samples were mixed with 6x DNA loading dye and separated in a 1% to 2% agarose gel by gel electrophoresis. For gel preparation the respective amount of agarose was mixed with 1x TAE buffer and heated in a microwave until all of the agarose was dissolved. Then the mix was allowed to cool down to about 50°C and one drop ethidium bromide (10 mg/ml) was added per 50 ml. The solid gel was then transferred into Sub-Cell GT tank (BioRad, Munich, Germany) and the tank filled with 1x TAE buffer. The

samples and GeneRuler™ 1 kB DNA ladder (Thermo Fisher Scientific, Waltham, USA) were loaded into the wells. The gel was run at a voltage of 90 – 120 V for about 30 min. The gel was then analyzed with a G:Box Genoplex Transilluminator (UV at 312 nm) gel documentation and analysis system (VWR, Lutterworth, UK).

#### 2.2.4.5 Purification of DNA fragments

PCR products and DNA fragments for cloning and sequencing were either cleaned-up directly or after gel electrophoresis. For the latter, gel slices were cut out under UV-light (365 nm) for visualization using a scalpel and stored in a 1.5 ml reaction tube. For gel-elution and PCR product purification the NucleoSpin® Gel and PCR Clean-up kit (Macherey-Nagel, Düren, Germany) was used according to the manufacturer's instructions.

#### 2.2.4.6 Photometric measurement of DNA and RNA concentration

For determination of DNA and RNA concentrations as well as for checking the purity of the nucleic acids the TECAN Infinite® 200 PRO NanoQuant plate reader (Tecan Trading AG, Männedorf, Switzerland) was used. 2 µl of the sample were pipetted onto the NanoQuant Plate™ and the absorption was measured at 260 nm and 280 nm. The ratio between the absorbance of 260 nm and 280 nm indicates the purity of the sample. The optimal ratio ( $OD_{260/280}$ ) for DNA is ~ 1.8 and for RNA ~ 2.0.

#### 2.2.4.7 Cloning via homologous recombination in *S. cerevisiae*

Homologous recombination cloning in yeast was based on the protocol by Gera *et al.* (2002). Recombination was carried out in the vector pRS426. An example is given below: The construction of *pRS426-pLYK5::LYK5-mCitrine* requires two DNA fragments. The first fragment (1) was amplified from genomic DNA with primers adding a 5' overhang matching the plasmid pRS426 followed by an *AscI* restriction site. Amplified mCitrine represented the second fragment that carried a 5' overhang to fragment 1 and a 3' overhang to the pRS426 vector including a *SmaI* restriction site. *S. cerevisiae* cells were transformed with the amplified gene fragments together with the *KpnI/BamHI* linearized vector pRS426 as described in 2.2.4.3. Cells carrying recombined vectors were selected via growth on uracil deficient YNB plates. The pRS426 vector construct was isolated (see 2.2.5.8.) and then transformed into *E.coli* TOP10 cells for amplification (see 2.2.2.4). Next, the plasmid was isolated and cut with *AscI* and *SmaI* for cloning into the expression vector *pGreenII-0229-JE*.

#### **2.2.4.8 Isolation of plasmid DNA from *S. cerevisiae***

To isolate recombinant plasmids from *S. cerevisiae*, all cells on the selective medium were washed from plate using 1 ml ultrapure water. The solution was spun down at 2300 g for 2 min and the supernatant was discarded. The plasmid was then extracted using the Plasmid Plus Midi Kit 100 (QIAGEN, Hilden, Germany) according to the manufacturer's instructions. To facilitate cell disruption, glass beads were added and the resuspended cells were vigorously shaken for 15 min on an IKA<sup>®</sup> VIBRAX VXR basic at 1500 rpm. The obtained DNA was used to transform chemically competent *E. coli* TOP10 cells.

#### **2.2.4.9 Restriction enzyme digestion of DNA**

The restriction enzymes used were standard or FastDigest<sup>®</sup> enzymes from Thermo Fisher Scientific (Waltham, USA) and were used according to the manufacturer's instructions. For normal restriction digestion reactions 2 µl 10x reaction buffer were mixed with 2-5 units of the respective restriction endonuclease and 1 µg DNA. This mix was then filled up with water to 20 µl. The reaction was incubated at the appropriate temperature for 30 min (FastDigest<sup>®</sup>) to 4 h or overnight (standard enzymes). Digestion products were analyzed by agarose gel electrophoresis. Restriction digestion was used for genotyping, cloning and analysis of plasmids.

#### **2.2.4.10 Dephosphorylation of plasmid DNA**

In case of non-directional cloning or if singly cut vector fragments could not be easily separated by size from doubly cut ones, the vector fragment was dephosphorylated using shrimp alkaline phosphatase (SAP, 1 u/µl) (Thermo Fisher Scientific, Waltham, USA) according to the manufacturer's instructions. Up to 5 µg DNA were used in a dephosphorylating reaction. SAP was then inactivated by incubating the sample at 72°C for 20 min.

#### **2.2.4.11 Ligation of DNA fragments**

Ligation was performed using the T4 DNA ligase (Thermo Fisher Scientific, Waltham, USA). Vector backbones and inserts were cut with matching restriction enzymes and mixed at a molar ratio of 1:3 to 1:10. Ideally, ≥100 µg of the vector fragment should be used. 2 µl 10x reaction buffer, 2 µl 50 % PEG4000 solution, 1 µl (5 u) T4 DNA ligase were added and the reaction was filled up with water to a total volume of 20 µl. PEG4000 solution was added only for blunt-end ligations. Ligation was performed at RT for 1 h or at 16°C overnight. Up to 5 µl ligation reaction were then used for transformation of *E. coli* cells.

#### **2.2.4.12 Sequencing of DNA**

Small scale plasmid DNA preparations or PCR products were sequenced by SeqLab (Göttingen, Germany). DNA was premixed with the sequencing primer according to SeqLab's instructions. The resulting sequence was analyzed with ChromasLite (Technelysium Pty Ltd, Brisbane QLD, Australia) or Genious Software version 7.1.5 (Kearse *et al.*, 2012). If no errors in the DNA sequence were found, the plasmid was used for further experiments.

#### **2.2.4.13 Preparation of RNA from plants**

RNA isolation was carried out using the innuPREP Plant RNA Kit (Analytik Jena, Jena, Germany) according to the manufacturer's instructions. About 1 µg of RNA was then run on a 1% agarose gel for quality control.

#### **2.2.4.14 Synthesis of cDNA (complementary DNA)**

The RevertAid H Minus First Strand cDNA Synthesis kit (Thermo Fisher Scientific, Waltham, USA) with oligo(dT) primers was used to convert 1 µg total RNA into cDNA according to the manufacturer's instructions. The obtained cDNA was diluted 1:5 – 1:15 and then used for semi-quantitative PCR.

#### **2.2.4.15 Semi-quantitative RT-PCR**

For semi-quantitative RT-PCR, the cDNA (2.2.5.14) was diluted 1:5. 1 µl of this was used in a standard PCR reaction (2.2.5.3.1). The primers for various target genes and the reference gene ACTIN can be found in Table 4. The cycle number was empirically adjusted for each target gene and sample type to make sure that the reaction was terminated in the log phase. Typically, cycle numbers ranged from 25 for highly expressed genes to 32 for less abundant transcripts. PCR products were visualized on agarose gels.

#### **2.2.4.16 Quantitative reverse transcription PCR (qRT-PCR)**

qRT-PCR, the amplification and simultaneous quantification of DNA, was performed with a CFX96 Real- Time PCR System (BioRad, Munich, Germany) equipped with the CFX Manager™ Software (BioRad, Hercules, CA, USA) using SsoFast EvaGreen Supermix (BioRad) and matching qRT-PCR-96-well plates (BioRad, Munich, Germany) as recommended by the manufacturer. qRT-PCR Amplification and quantification were carried out according to a previously published protocol (Petutschnig *et al.*, 2014). The primers for amplification of target and reference genes can be found in Table 4. One reaction contained the following components:

qRT-PCR Mix for one reaction:

Evagreen mix	5 $\mu$ l
Primer mix (2 $\mu$ M each)	2 $\mu$ l
cDNA	3 $\mu$ l

**Table 11: PCR protocol used for qRT-PCR.**

Step	Temperature [°C]	Time [min]	Repeats
Initial denaturation	95	00:30	1x
Denaturation	95	00:05	45x
Annealing	55	00:10	

Melting curves were recorded during a temperature increase from 60°C to 95°C in 0.5°C and 5s steps. The curves were inspected manually to ensure formation of single PCR products.

To test primer efficiency and determine the optimum cDNA concentration, a calibration curve was analyzed for each experiment and primer combination. For this, 3  $\mu$ l of each sample within an experiment were pooled and a 1:3 dilution series of the pooled cDNA was pipetted in a PCR 8-tube strip resulting in 8 dilution steps.

A calibration curve was prepared by plotting C<sub>q</sub> values against log(10) of the dilution factor. From this curve the primer efficiency (E) was calculated ( $E = 10^{(-1/\text{slope of calibration curve})}$ ). If the calibration curve was linear the primers were used. For each sample, three technical replicates obtained. For this three replicates the  $E^{C_q}$  was calculated and the mean was determined. The calculated mean of the reference gene against the target gene represents the relative gene expression (gene of interest/reference gene). Each experiment was repeated three times. The results from the individual experiments were normalized by division by the mean of the respective experiment. The standard deviation was calculated out of the normalized values.

## 2.2.5 Biochemical methods

If not stated otherwise, protein extracts were handled at 4°C or kept on ice wherever possible.

### 2.2.5.1 Protein extraction and purification from plants

#### 2.2.5.1.1 Total protein extraction

Chitin treated and non-treated *Arabidopsis thaliana* rosette leaves were shock-frozen in liquid nitrogen and stored at -80°C until use. Frozen leaves were ground with 200 µl CERK1 extraction buffer and a small spatula of quartz sand using the IKA® RW 20 digital drill (IKA-Werke, Staufen, Germany) equipped with a glass pistil fitting 1.5 ml tubes. The pistil was then rinsed with an additional 200 µl of CERK1 extraction buffer and the sample was filled up to 1 ml with buffer. Then, the samples were centrifuged at 17000 g at 4°C for 10 min in a tabletop centrifuge. The supernatant was transferred into a new 1.5 ml reaction tube and placed on ice. The protein content was determined via the Bradford assay (see 2.2.6.5) and concentrations were equalized to the lowest concentrated sample. 60 µl were then mixed with 4x SDS-loading dye and stored at -20°C until use.

#### 2.2.5.1.2 Protein pull-down from total protein extracts

Chitin magnetic beads (NEB, Frankfurt/Main, Germany) or GFP-binding protein magnetic beads (GFP-Trap®\_M, ChromoTek, Planegg-Martinsried, Germany) were prepared according to the manufacturer's instructions. 20 µl of the beads were then transferred to protein extract (containing 500-1000 µg protein in total). The samples were then incubated on a wheel at 20 rpm and 4°C for 1 h and afterwards pelleted using a magnet. The supernatant was discarded and the beads were washed three times with 1 ml cold TBS-T. Next, the TBS-T was removed and the beads were washed with cold water. After pelleting the beads using a magnet the water was removed and the beads were mixed with 20 µl 1.5x SDS-loading dye. The samples were stored at -20°C until use.

#### 2.2.5.2 Lambda Protein Phosphatase (λPPase) treatment

Total protein extracts were prepared as described in 2.2.6.1.1. Protein extracts from chitin-treated as well as control plants were divided into three aliquots. The protein of interest was pulled down using appropriate magnetic beads. To do so, the samples were incubated with the beads at 4°C on a wheel for 1 h. Then, the supernatant was removed and the beads were washed twice with 1 ml mild washing buffer. After removal of the buffer from the last wash step, a dephosphorylation reaction was performed with λPPase (New England Biolabs, Ipswich, MA,

USA). 4  $\mu$ l 10x  $\lambda$ PPase buffer and 4  $\mu$ l 10x  $\text{MnCl}_2$  (10 mM) were added to each aliquot of beads. All aliquots were supplemented with water to a total volume of 40  $\mu$ l. One aliquot was directly mixed with 4x SDS sample buffer and frozen at  $-20^\circ\text{C}$  (**dir**). To one of the remaining two aliquots, 1  $\mu$ l of  $\lambda$ PPase was added ( **$\lambda$** ), to the other one 1  $\mu$ l of water (**-**). These two samples were then incubated for 1 h at RT. After the incubation the samples were mixed with 4x SDS sample buffer and stored at  $-20^\circ\text{C}$ .

### 2.2.5.3 Expression of 6xHis- and GST-fusion proteins in *E. coli*

First, the respective construct was transformed into chemically competent *E. coli* ArcticExpress<sup>®</sup> cells. These cells allow expression of recombinant proteins at low temperatures to facilitate correct protein folding and increased solubility of the active recombinant protein. This is enabled by the presence and co-expression of the cold-adapted chaperonins Cpn10 and Cpn60 from the marine bacterium *Oleispira Antarctica* (Ferrer *et al.*, 2003). Furthermore, the ArcticExpress<sup>®</sup> cells lack both the Lon protease and the OmpT protease, which can degrade proteins during purification (Grodberg and Dunn, 1988). For protein purification, a 30 ml liquid culture with appropriate antibiotics was inoculated with 15 *E. coli* colonies carrying the construct of interest. The culture was shaken at  $28^\circ\text{C}$  overnight. The next morning, a 250-1000 ml liquid culture was inoculated to an  $\text{OD}_{600}=0.2$  with the overnight culture. The main culture was grown to an  $\text{OD}_{600}=0.6$ . 1 ml culture was taken as non-induced control. Then the inducer (arabinose or IPTG) was added to a final concentration of 0.2 mM and the cultures were grown for 6 h at  $28^\circ\text{C}$  while shaking. The liquid culture was then divided into 50 ml tubes and centrifuged for 20 min at 4500 g in a Hereaus Multifuge 3SR+ (Thermo Fisher Scientific, Waltham, USA). The supernatant was discarded and the pellets were frozen at  $-20^\circ\text{C}$ .

### 2.2.5.4 Extraction and purification of 6xHis- and GST-tagged proteins from *E. coli*

Purification started with re-suspending the cell pellet in ice-cold buffer (PBS for GST-fusion and His-binding buffer for 6xHis-fusion proteins) containing 2 mM PMSF, 1 mg/ml lysozyme and 0.5 % Triton-X 100. Cell lysis was further facilitated by sonication using a Bandelin Sonoplus sonicator equipped with a MS 73 sonotrode (Bandelin electronic, Berlin, Germany). Sonication was carried out three times with 50% power, 50% cycle for 30 s followed by a 30 s pause. The cell lysate was then centrifuged in a Sorvall RCG+ centrifuge with a SS-34 rotor for 5 min at 10000 rpm and  $4^\circ\text{C}$ . The supernatant was then transferred into a new 50 ml tube. The proteins were purified using GSH-magnetic beads (Pierce<sup>™</sup>, Thermo Fisher Scientific, Waltham, USA) or His Mag Sepharose Ni magnetic beads (GE Healthcare, Munich, Germany) from total cell extracts according to the manufacturer's instructions. Bound proteins were eluted by washing



the beads with the respective elution buffers containing either reduced GSH or imidazole. The eluted proteins were then aliquoted (20  $\mu$ l) in 0.2 ml reaction tubes and frozen at  $-80^{\circ}\text{C}$ . These eluted proteins were then used for auto- and transphosphorylation reaction using radioactively labeled  $\gamma$ -[ $^{32}\text{P}$ ]-ATP.

#### **2.2.5.5 Protein concentration measurement via the Bradford assay**

Protein concentration determination was carried out according to Bradford (1976). First, the Bradford reagent (Roti<sup>®</sup>-Quant, Roth, Karlsruhe, Germany) was diluted 1:5 in ddH<sub>2</sub>O. Second, a dilution series of 0, 3, 5, 7, 10 and 15  $\mu\text{g/ml}$  bovine serum albumin in Bradford reagent was prepared. Next, an appropriate volume 2  $\mu\text{l}$  of each sample was mixed with 1 ml Bradford reagent. After 10 min incubation at RT the absorbance was measured at 595 nm using a WPA Biowave II photometer (Biochrom AG, Berlin, Germany). By plotting  $A_{595}$  of the BSA standards against their concentration, a standard curve was generated, which was used to calculate the protein concentration of the samples. To equalize protein concentrations, the samples were adjusted to sample with the lowest protein concentration using extraction buffer.

#### **2.2.5.6 SDS-polyacrylamide gel electrophoresis (SDS-PAGE)**

Protein separation according to their molecular weight was carried out by denaturing SDS-PAGE. To generate polyacrylamide gel systems, resolving gel mixes were prepared (see below), poured between two glass plates with a spacing of either 1.5 mm or 0.75 mm set in a gel stand and overlaid with isopropanol. After polymerization at RT, the isopropanol was removed and the stacking gel was poured over the resolving gel. Immediately after pouring, a comb was inserted. The acrylamide concentration used depends on the expected protein size and the purpose of the experiment. For most immunoblot applications, 1.5 mm 10% acrylamide gels were suitable. For band shift assays, 1.5 mm 8% gels were used. In experiments involving smaller proteins such as free tags, 15% gels were used. Gels with a thickness of 0.75 mm were prepared if they were to be dried after the run. SDS-PAGE was carried out in the Mini-PROTEAN<sup>®</sup> 3 system (BioRad, Munich, Germany). Before loading, the samples were boiled for 3-5 min at  $95^{\circ}\text{C}$ . Meanwhile, the gels were placed in the gel apparatus and 1x SDS-running buffer was used to fill up the tank. Up to 20  $\mu\text{l}$  sample volume were loaded (depending on the pocket size). As a size marker, PageRuler<sup>™</sup> Prestained Plus protein Ladder or PageRuler<sup>™</sup> Unstained Protein Ladder (Thermo Fisher Scientific, Waltham, USA) were used. 1.5 mm gels were run at 30 mA/gel and 0.75 mm gels were run at 15 mA/gel using a PowerPac<sup>™</sup> HC power supply (BioRad, Munich, Germany) until the bromophenol blue front reached the end. The gel apparatus was then disassembled and the gel was either stained directly with Coomassie

brilliant blue (protein expression and *in vitro* kinase assay) or used for Western blot experiments.

**Table 12: Composition of mixtures used for resolving and stacking gel preparation in this study.**

<b>SDS-PAGE gel buffer (250 ml)</b>		
8% resolving gel buffer	1 M Tris-HCl, pH 8.8	130.9 ml
	SDS (10%)	3.46 ml
	ddH <sub>2</sub> O	115.64 ml
10% resolving gel buffer	1 M Tris-HCl, pH 8.8	143.6 ml
	SDS (10%)	3.79 ml
	ddH <sub>2</sub> O	102.53 ml
15% resolving gel buffer	1 M Tris-HCl, pH 8.8	189.07 ml
	SDS (10%)	5.1 ml
	ddH <sub>2</sub> O	55.83 ml
Stacking gel buffer	1 M Tris-HCl, pH 6.8	38.58 ml
	SDS (10%)	3.06 ml
	ddH <sub>2</sub> O	208.24 ml
<b>SDS-PAGE gel mixes (10 ml)</b>		
8% gel resolving gel	8% gel buffer	7.2 ml
	30% acrylamide/ 0.8% bisacrylamide	2.7 ml
	APS (10%)	0.1 ml
	TEMED	0.006 ml
10% gel resolving gel	10% gel buffer	6.6 ml
	30% acrylamide/ 0.8% bisacrylamide	3.3 ml
	APS (10%)	0.1 ml
	TEMED	0.004 ml

---

15% gel resolving gel	15% gel buffer	4.9 ml
	30% acrylamide/ 0.8% bisacrylamide	5 ml
	APS (10%)	0.1 ml
	TEMED	0.004 ml
Stacking gel	stacking gel buffer	8.16 ml
	30% acrylamide/ 0.8% bisacrylamide	1.66 ml
	APS (10%)	0.05 ml
	TEMED	0.005 ml

---

### 2.2.5.7 *In vitro* kinase assay

*In vitro* kinase assays were performed with kinase domains expressed in *E.coli* using radioactively labeled ATP. Proteins (see 2.2.6.4) were kept on ice at all times. One kinase reaction (20  $\mu$ l) was pipetted according to the following scheme:

Autophosphorylation reaction	X $\mu$ l kinase (approximately 1 $\mu$ g) 2 $\mu$ l 10x kinase buffer 0.2 $\mu$ l $\gamma$ -[ <sup>32</sup> P]-ATP Add H <sub>2</sub> O to 20 $\mu$ l
Transphosphorylation reaction	8 $\mu$ l kinase X $\mu$ l substrate (approximately 1 $\mu$ g) 2 $\mu$ l 10x kinase buffer 0.2 $\mu$ l $\gamma$ -[ <sup>32</sup> P]-ATP Add H <sub>2</sub> O to 20 $\mu$ l

The reaction was incubated for 30 min at RT and then stopped by adding 4x SDS-loading dye and boiling at 95°C for 1 min. The samples were then loaded on a 15% polyacrylamide gel and a SDS-PAGE (see 2.2.6.6) was performed. The gels were then stained with Coomassie brilliant blue (see 2.2.6.9) and dried (see 2.2.6.10) before exposure to an AGFA CRONEX5 film (Agfa-Gevaert, Mortsel, Belgium).

### 2.2.5.8 Immunoblot analysis (Western blot)

Extracted proteins (see 2.2.6.1.1 and 2.2.6.1.2) were separated via SDS-PAGE (see 2.2.6.6) prior to immunoblotting. Proteins were transferred onto a PVDF membrane with a pore size of 0.45  $\mu\text{m}$  (Roth, Karlsruhe, Germany) by electroblotting in the TRANS-BLOT<sup>®</sup> CELL (BioRad, Munich, Germany) apparatus. For this purpose, the membrane was briefly dipped in methanol before applying to the gel. The blotting apparatus was assembled as followed:

cathode  
-----  
black grid of clamp  
sponge  
Whatman paper  
gel (facing the cathode)  
PVDF membrane  
Whatman paper  
sponge  
transparent/red grid of clamp  
-----  
anode

The blotting was performed in 1x transfer buffer at 90 V for 2 h at 4°C. After disassembling the blotting apparatus, the PVDF membrane was blocked with 10 ml TBS-T + MP for 1 h at RT on a rotary shaker. After removing the blocking solution, the primary antibody was added and incubated over night at 4°C on a shaker. The primary antibody was then removed and prior addition of the secondary antibody, the membrane was washed at least 4 times with TBS-T + MP for 10 min. The membrane was incubated in secondary antibody for 2 h at RT on a rotary shaker. The antibodies used in this study are summarized in Table 8. After antibody incubation, the membrane was washed 4 times with TBS-T for 10 minutes. The last washing step was followed by 10 min of equilibration in AP buffer. 500  $\mu\text{L}$  Immun-Star<sup>™</sup> AP substrate (BioRad, Munich, Germany), were placed on each membrane. Then, the membranes were wrapped in a transparent plastic bag and exposed to a CEA RP NEW Medical x-ray film (CEA, Hamburg, Germany). The film was developed and in case of over/under-exposure the exposure time was adjusted.

To enhance the detected signal and reduce the background in immunoblots using  $\alpha$ GFP, the SuperSignal™ Western blot Enhancer (Thermo Fisher Scientific, Waltham, USA) was used according to the manufacturer's instructions.

#### **2.2.5.9 Coomassie staining of SDS-PAGE gels and PVDF membranes**

In order to visualize protein bands, polyacrylamide gels or PVDF membranes were stained with Coomassie brilliant blue. For this purpose, gels or PVDF membranes were covered with coomassie staining solution and incubated for 5-10 min while shaking at RT. The coomassie staining solution was then removed and the gels were rinsed with water. The background was removed by adding destaining solution and incubation until sufficiently destained. Depending on the staining intensity destaining solution had to be changed once or several times.

#### **2.2.5.10 Drying of Coomassie stained SDS-PAGE gels**

Gels used for *in vitro* kinase assay had to be dried prior to x-ray film exposure. Therefore, destained gels (see 2.2.6.9) were placed on Whatman paper, covered with cling film and dried in the PHERO-TEMP (BIOTEC-FISCHER GmbH, Reiskirchen, Germany) vacuum gel dryer at 80°C for 1- 2 h.

### **2.2.6 Confocal laser scanning microscopy (CLSM) and endosome quantification**

#### **2.2.6.1 Confocal laser scanning microscopy (CLSM)**

Confocal laser scanning microscopy was performed on a Leica TCS SP5 system (Leica Microsystems, Wetzlar, Germany) equipped with an argon laser and HyD hybrid detectors. Small and preferably even leaf discs were cut out and treated as described in 2.2.1.7. After the incubation, the leaf discs were placed onto an object slide wetted with water, before the cover glass was placed on top. The excitation and emission spectra of the fluorophores that were used in this study are listed in Table 13.

Table 13: Parameters used for the detection of the different fluorophores.

Fluorophore	Excitation	Emission
Aniline Blue	405 nm	430-470 nm
GFP	488 nm	500-540 nm
FM4-64	488 nm	600-650 nm
mCitrine	514 nm	525-560 nm
mKate2	561 nm	620-640 nm
Chlorophyll autofluorescence		740-770 nm

Two fluorophores with overlapping emission spectra were sequentially scanned. Single focus images as well as image series were obtained for the different treatments. Images for endosome quantification were scanned at 400 Hz with a resolution of 512 x 512 pixels. Other images were scanned with a resolution of 1024 x 1024 pixels at 200 Hz. Single focus images, Z-stacks (maximum projections) or t-series (movies) were processed using the Leica LAS AF (Version 2.7.2.) and Adobe Photoshop CS4 software packages.

### 2.2.6.2 Endosome quantification

Images for endosome quantification were taken automatically using the Mark And Find feature of the Leica LAS AF software. For each imaging site, 12 consecutive focal plane images with a distance of 1  $\mu\text{m}$  were recorded and converted into maximum projections. For time course experiments, images were taken in 5-min intervals for 100 min. For each experiment, images from at least three independent transgenic lines were pooled.

A script for image processing and vesicle quantification was generated (Hassan Ghareeb, unpublished) in Fiji (ImageJ 1.49m; Schindelin *et al.* (2012)). The script is divided into two main parts. The first part includes the detection of plasma membrane (PM) and guard cell associated fluorescence signals and their removal from the original image. The second part comprises the detection and quantification of vesicles (Figure S5A). As a first step the Unsharp Mask algorithm was applied to the maximum-projected images to enhance the contrast at the edges of the PM signals. The Gaussian Blur algorithm was then used to smooth the image and enhance the signal of the PM by increasing the radius. To avoid detection of vesicles at this point, punctate structures were removed using a Despeckle filter. Next, the image was converted using the Make Binary algorithm. The resulting binary image was used as a mask to subtract PM and guard cell signals from the maximum-projected image (Figure S5A). For the second part,

background noise was reduced and contrast was enhanced in order to increase the sensitivity of vesicle detection in the subtracted image. To label the vesicles, the image was segmented by Autothresholding using the MaxEntropy algorithm (Figure S5A). Features of the vesicles such as number, size, and signal intensity were analyzed by the Analyze Particles command. The results were exported in CSV format. Additionally, an output image that contains an overlay of the detected vesicles and the maximum-projected image was produced for quality control (Figure S5A). During the time-lapse experiment, we noticed fluorophore bleaching at later time points. To correct for the loss of fluorescence intensity, a linear contrast stretching algorithm was applied with the level of saturated pixels set to 4% (Figure S5B).

### **2.2.7 Statistical analysis**

Statistical significance was tested with unpaired, two tailed t-tests using GraphPad QuickCalcs.

### 3 Results

CERK1 is an *Arabidopsis* LysM-RLK involved in the perception of the fungal PAMP chitin (Miya *et al.*, 2007; Wan *et al.*, 2008a) and can bind to chitin without any interaction partners (Iizasa *et al.*, 2010; Petutschnig *et al.*, 2010; Liu *et al.*, 2012b; Wan *et al.*, 2012). In addition to CERK1, three other LysM-containing proteins with chitin binding capacity were found in a proteomics study namely LYK5, LYK4 and LYM2 (Petutschnig *et al.*, 2010). Loss of CERK1 renders the affected plants chitin-insensitive (Miya *et al.*, 2007; Wan *et al.*, 2008a), indicating that it is a crucial component of the *Arabidopsis* chitin receptor. An involvement of LYK5 and LYK4 in general chitin perception and interaction with CERK1 has been recently reported (Wan *et al.*, 2012; Cao *et al.*, 2014). Surprisingly, LYM2 seems not to be involved in the canonical chitin perception pathway (Shinya *et al.*, 2012; Wan *et al.*, 2012), but has been shown to reduce cell-to-cell connectivity via PD in response to chitin (Faulkner *et al.*, 2013). While many components of the chitin receptor complex have been identified in rice and *Arabidopsis*, very little is known about the dynamics of chitin perception. Consequently, this work focuses on the subcellular localization and behavior of CERK1, LYK4, LYK5, and LYM2. To do so, fluorescently-tagged protein constructs were generated and microscopically analyzed in stably transformed *Arabidopsis* plants. While knock-out of CERK1 results in a completely chitin-insensitive phenotype, the situation is less clear for LYK4, LYK5, and LYM2. Thus, T-DNA lines for these genes were isolated and characterized regarding their chitin perception capacity. Finally, the generation of a triple mutant plant line of the three chitin binding proteins LYK5, LYK4, and LYM2 is described.

#### 3.1 Analysis of the subcellular behavior of CERK1

##### 3.1.1 The CERK1-GFP fusion protein is functional

To investigate the subcellular localization of *Arabidopsis* CERK1, a C-terminally GFP-tagged version of CERK1 driven by its endogenous promoter (*pCERK1::CERK1-GFP*) was expressed in the *cerk1-2* knock-out mutant (Petutschnig *et al.*, 2014). Prior to cell biological analyses, plants expressing *pCERK1::CERK1-GFP* were tested to confirm functionality of the fusion protein. To do so, total protein extracts of chitin infiltrated and unchallenged leaves were prepared. Next, chitin binding proteins were pulled down from this total extract using chitin magnetic beads. The total extracts and chitin pull-down samples of Col-0, *cerk1-2* and two representative *pCERK1::CERK1-GFP* lines were then used in Western blot experiments and probed with an antibody that specifically detects CERK1 (Petutschnig *et al.*, 2010). In Col-0



endogenous CERK1 protein was found migrating at approximately 70 kDa in total extracts as well as chitin pull-downs. In contrast, no signals for CERK1 were visible in the knock-out mutant *cerk1-2*. In the transgenic lines, CERK1-GFP was detected at an apparent molecular mass of 107 kDa. No endogenous CERK1 was found in these *pCERK1::CERK1-GFP* expressing plants because of the *cerk1-2* background. Importantly, CERK1-GFP bound to chitin magnetic beads with an affinity comparable to endogenous CERK1 (Figure 6A). In both, total extracts and chitin pull-downs, the endogenous CERK1 protein as well as the CERK1-GFP fusion protein showed a mobility shift in Western blots after chitin treatment (Figure 6) which is indicative of receptor phosphorylation (Petutschnig *et al.*, 2010). CERK1 and CERK1-GFP from chitin treated plants showed less binding to chitin beads *in vitro*, presumably due to occupied chitin binding sites. Thus overall, the CERK1-GFP protein showed similar chitin binding and chitin-induced phosphorylation to native CERK1. To test if CERK1-GFP is able to activate downstream signaling, the phosphorylation of MAPKs was tested (Figure 6B). For this purpose, total protein extracts from chitin-treated and unchallenged plants were used in Western blot experiments with an antibody specifically recognizing phosphorylated and thus activated MAPKs. Figure 6B shows that upon chitin treatment, MAPK phosphorylation was induced in Col-0 plants but not in the *cerk1-2* mutant. The presence of CERK1-GFP restored chitin-induced activation of MAPKs in the *cerk1-2* background confirming that the fusion protein is functional.

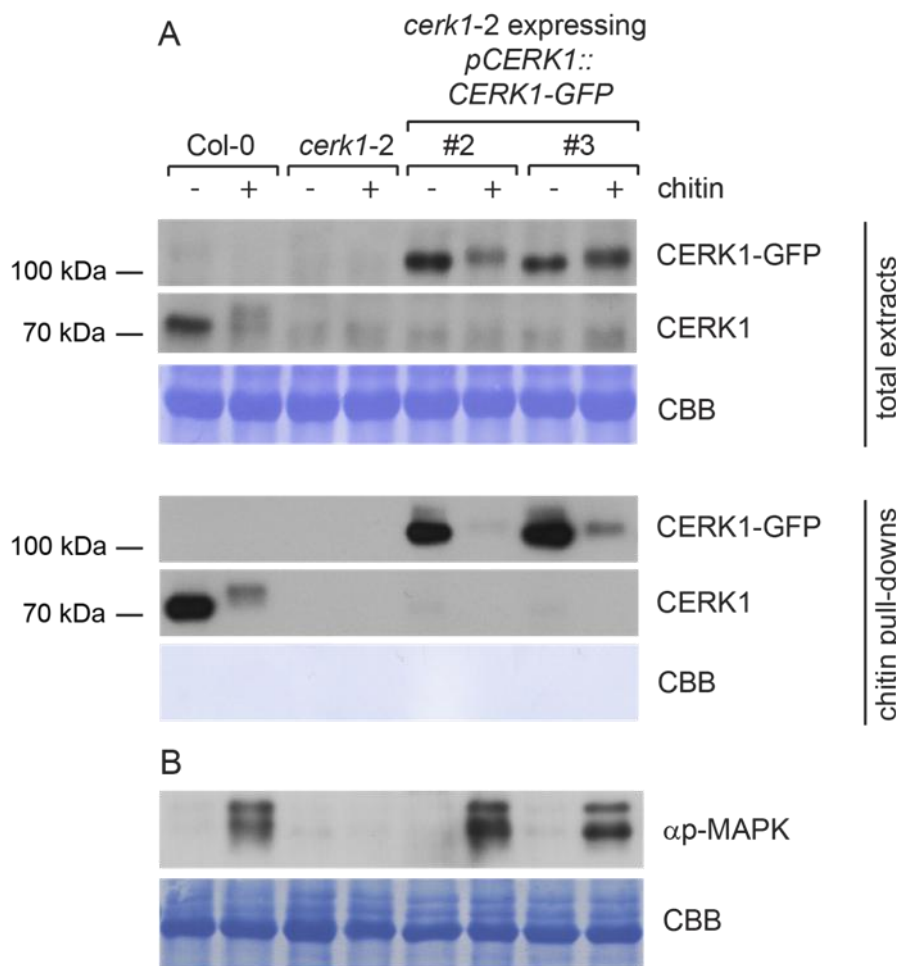


**Figure 6: Expression of *pCERK1::CERK1-GFP* rescues *cerk1-2* chitin insensitivity.**

Leaves of Col-0, *cerk1-2* and two independent transgenic lines expressing *pCERK1::CERK1-GFP* in the *cerk1-2* background were infiltrated with water or chitin (100  $\mu$ g/ml). **(A)** CERK1 protein analysis by Western blotting. Total protein extracts (upper panel) probed with a specific CERK1 antibody revealed band shifts that are caused by chitin-induced receptor phosphorylation. Chitin binding of CERK1-GFP was demonstrated by chitin pull-downs (lower panel). **(B)** Immunoblotting with an antibody recognizing phosphorylated MAPKs demonstrated that expression of CERK1-GFP restored chitin-induced activation of MAPKs in the *cerk1-2* background. Representative Western blots are depicted. All Experiments were performed at least three times with similar results. CBB: Coomassie Brilliant Blue-stained membranes.

### 3.1.2 Confocal microscopy suggests that chitin treatment does not alter the subcellular localization of CERK1-GFP

Plants producing CERK1-GFP were then examined regarding the subcellular dynamics of the fusion protein. It has previously been established that CERK1-GFP localizes to the PM (Petutschnig *et al.*, 2014). To investigate the subcellular behavior of CERK1-GFP upon chitin

treatment, leaves of transgenic plants were infiltrated with chitin or water as a control and then analyzed using confocal laser scanning microscopy (CLSM).

In leaves of water infiltrated plants, CERK1-GFP localized to the cell periphery (Figure 7). When plants were treated with chitin, the localization of CERK1-GFP was not altered. Figure 7 shows a representative sample 60 min after chitin infiltration, but observations at 15, 30 and 90 min time points yielded the same results (Figure S3). In summary, CLSM showed that functionally active CERK1-GFP localizes to the PM and suggested that chitin treatment does not induce dramatic changes in this subcellular localization pattern.

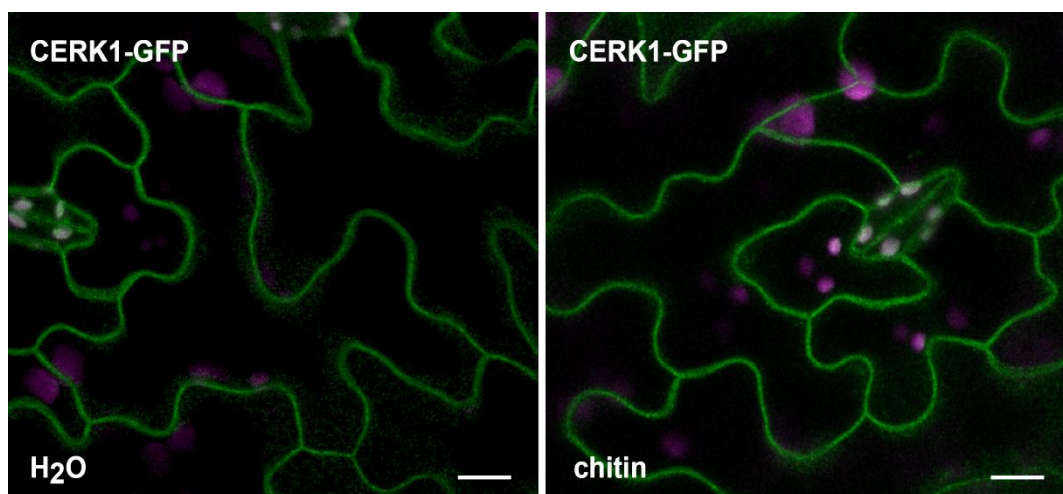


**Figure 7: CERK1-GFP localization is not responsive to chitin.**

*Arabidopsis* leaves stably expressing *pCERK::CERK1-GFP* in *cerk1-2* were infiltrated with 100 µg/ml chitin or water as a control and incubated for 60 min. CERK1-GFP subcellular localization did not change upon chitin infiltration. Representative maximum projections of 8 CLSM focal planes taken 1 µm apart 60 min after infiltration are shown. Experiment was performed with three independent transgenic lines. Images: Green, GFP; magenta, chloroplast autofluorescence. Scale bar = 10 µm

### 3.1.3 CERK1-GFP positive vesicles accumulate after co-treatment with ConcA and chitin

Ligand induced receptor endocytosis is known from the flagellin receptor FLS2, which is specifically internalized into vesicles upon flg22 treatment and targeted for degradation in the vacuole (Robatzek *et al.*, 2006; Beck *et al.*, 2012; Spallek *et al.*, 2013). However, no visible changes in CERK1-GFP localization after chitin treatment were observed in the previous experiments. This might be caused by slow turnover and low levels of receptor molecules undergoing endocytosis at any given time. In order to block transport of possibly existing endosomes to the vacuole and prevent degradation of CERK1-GFP, leaves of transgenic

*cerk1-2* plants expressing *CERK1-GFP* under control of endogenous 5' regulatory sequences (*pCERK1::CERK1-GFP*) were co-infiltrated with chitin and ConcA, an inhibitor of endosomal trafficking and vacuolar degradation (Irani and Russinova, 2009; Ben Khaled *et al.*, 2015) (Figure 8). As illustrated in figure 8, incubation with ConcA and subsequent infiltration with chitin led to the formation of GFP-tagged punctate structures within the cell. In contrast, infiltration with ConcA alone did not result in such vesicle formation. Also, no punctate structures could be observed upon infiltration of *CERK1-GFP* plants with DMSO alone or DMSO and chitin.

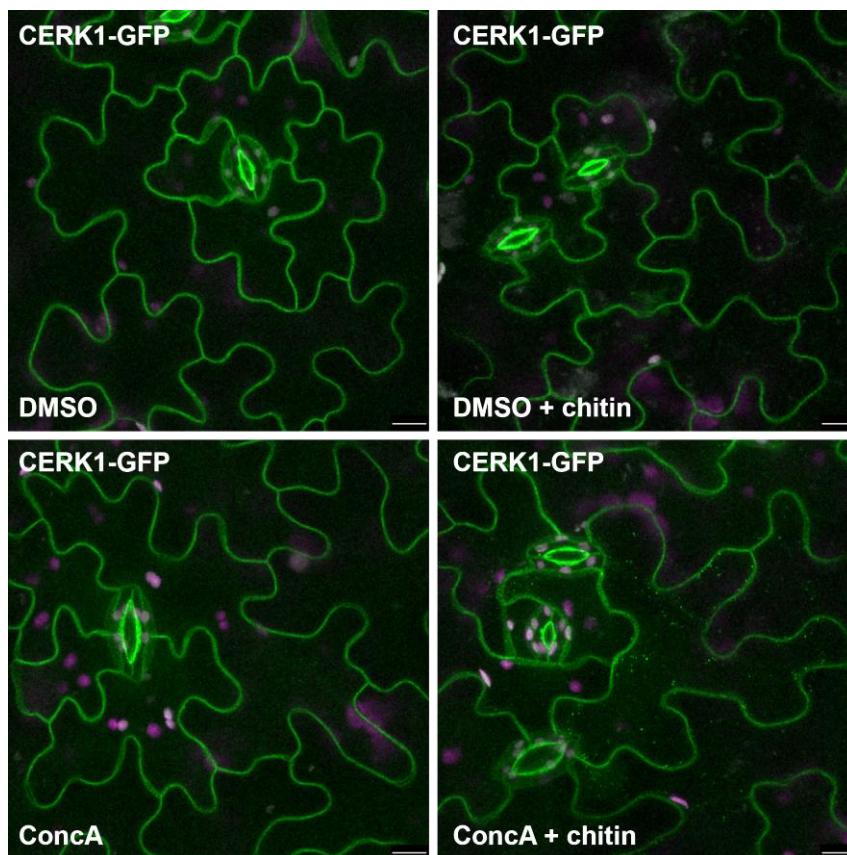


**Figure 8: Application of an endomembrane trafficking inhibitor identifies chitin-induced *CERK1-GFP* vesicles.**

Leaves of *cerk1-2* plants stably expressing *pCERK1::CERK1-GFP* were incubated in 1  $\mu$ M ConcA for 30 min, then infiltrated with or without 100  $\mu$ g/ml chitin and incubated for a further 90 min. Control samples were processed in the same way, but were incubated in the inhibitor solvent DMSO instead of ConcA. Representative maximum projections of 10 CLSM focal planes taken 1  $\mu$ m apart are shown. Experiment was performed with four independent transgenic lines. Green, GFP; magenta, chloroplast autofluorescence. Scale bar = 10  $\mu$ m

The fact that only the combination of ConcA and chitin triggered vesicle formation is in agreement with the postulated hypothesis that *CERK1* endocytosis without the use of inhibitors

is too low for detection by confocal microscopy. Even with the ConcA and chitin co-treatment, the resulting CERK1-GFP vesicles were weakly fluorescent suggesting low CERK-GFP cargo.

### 3.1.4 CERK1-GFP undergoes constitutive endomembrane trafficking

FLS2 has been reported to constitutively traffic to and from the PM in a ligand-independent manner (Beck *et al.*, 2012). To investigate if this also holds true for CERK1, *pCERK1::CERK1-GFP* expressing leaves were treated with BFA (Figure 9). BFA is an inhibitor of endomembrane trafficking and application leads to the formation of endomembrane aggregates. (Robinson *et al.*, 2008a). Figure 9 clearly shows that BFA treatment induces the formation of compartments that are positive for CERK1-GFP. Parallel FM4-64 staining indicated these compartments originate from the PM (Figure 9). FM4-64 is a lipophilic styryl dye that is nontoxic to the cell and inserts into the outer leaflet of the PM (Betz *et al.*, 1992; Bolte *et al.*, 2004; Jelinkova *et al.*, 2010). In agreement with previous reports (Petutschnig *et al.*, 2014) co-staining with FM4-64 showed overlapping signal with CERK1-GFP at the cell periphery, indicating that CERK1-GFP localizes to the PM (Figure 9) These compartments were observed regardless of chitin infiltration (Figure 9), suggesting that CERK1-GFP undergoes constitutive, ligand-independent endomembrane trafficking similar to FLS2.

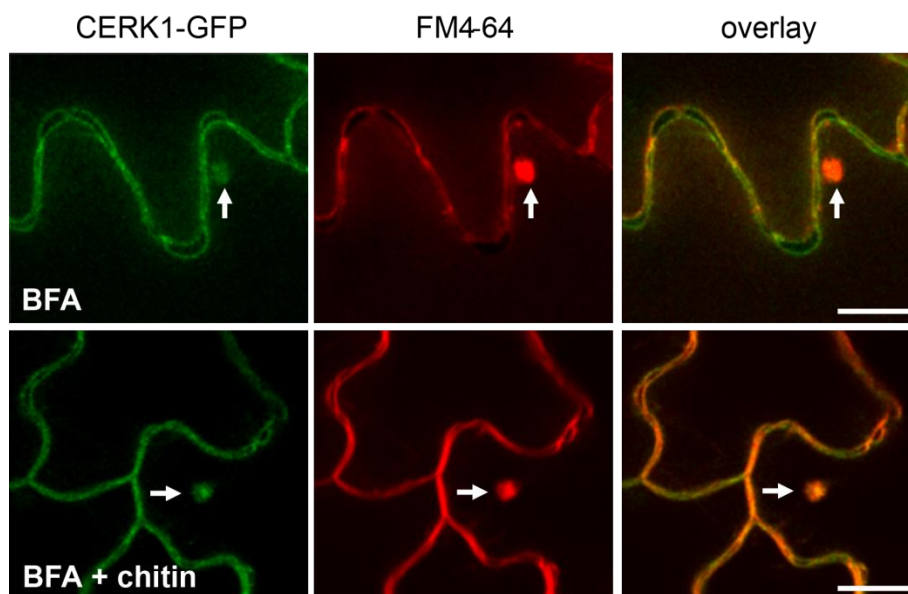


**Figure 9: CERK1-GFP localization is sensitive to BFA.**

*pCERK1::CERK1-GFP* expressing leaves were pre-treated with 30  $\mu$ M BFA for 30 min, stained with FM4-64 and then infiltrated with or without the addition of 100  $\mu$ g/ml chitin and further incubated for 60 min. Arrows indicate BFA-induced compartments. Representative single focus plane CLSM images are shown. Experiment was performed with three independent transgenic lines. Images: Green, GFP; Red, FM4-64. Scale bar = 10  $\mu$ m

## 3.2 Analysis of LYK5 and LYK4 T-DNA insertion lines

### 3.2.1 Isolation of *lyk5-2* and *lyk4-2* T-DNA insertion lines and *lyk5-2 lyk4-2* double mutants

Chitin pull-down experiments and subsequent mass spectrometry analysis identified the LysM-RLKs LYK5 and LYK4 as chitin binding proteins and putative CERK1 interaction partners (Petutschnig *et al.*, 2010). Recently, both LYK4 (Wan *et al.*, 2012) and LYK5 (Cao *et al.*, 2014) have been described as critical components of the *Arabidopsis* chitin receptor complex. Knock-out plants of both LysM-RLKs were reported to be less sensitive to chitin than the wild type, but neither matched the completely chitin insensitive phenotype of *cerk1-2* (Wan *et al.*, 2012; Cao *et al.*, 2014). To further investigate the contribution of LYK4 and LYK5 to chitin signaling, T-DNA insertion lines in the Col-0 ecotype background were obtained for both genes. For LYK5, a previously described line, *lyk5-2* (SALK\_131911C) (Cao *et al.*, 2014) was used, whereas for LYK4 a novel line, *lyk4-2* (GABI\_857A10), was characterized (Figure 10A). The position of the respective T-DNAs was determined by PCR and sequencing (Figure 10A and B). *lyk5-2* contains an insertion that disrupts the gene in the region encoding the transmembrane domain, while the position of the *lyk4-2* T-DNA insertion corresponds to the end of the kinase domain (Figure 10A). To circumvent potential functional redundancy (Wan *et al.*, 2012; Cao *et al.*, 2014) a *lyk5-2 lyk4-2* double mutant line was generated (Figure 10B). The single as well as the double mutants were then examined for effects on chitin signaling.

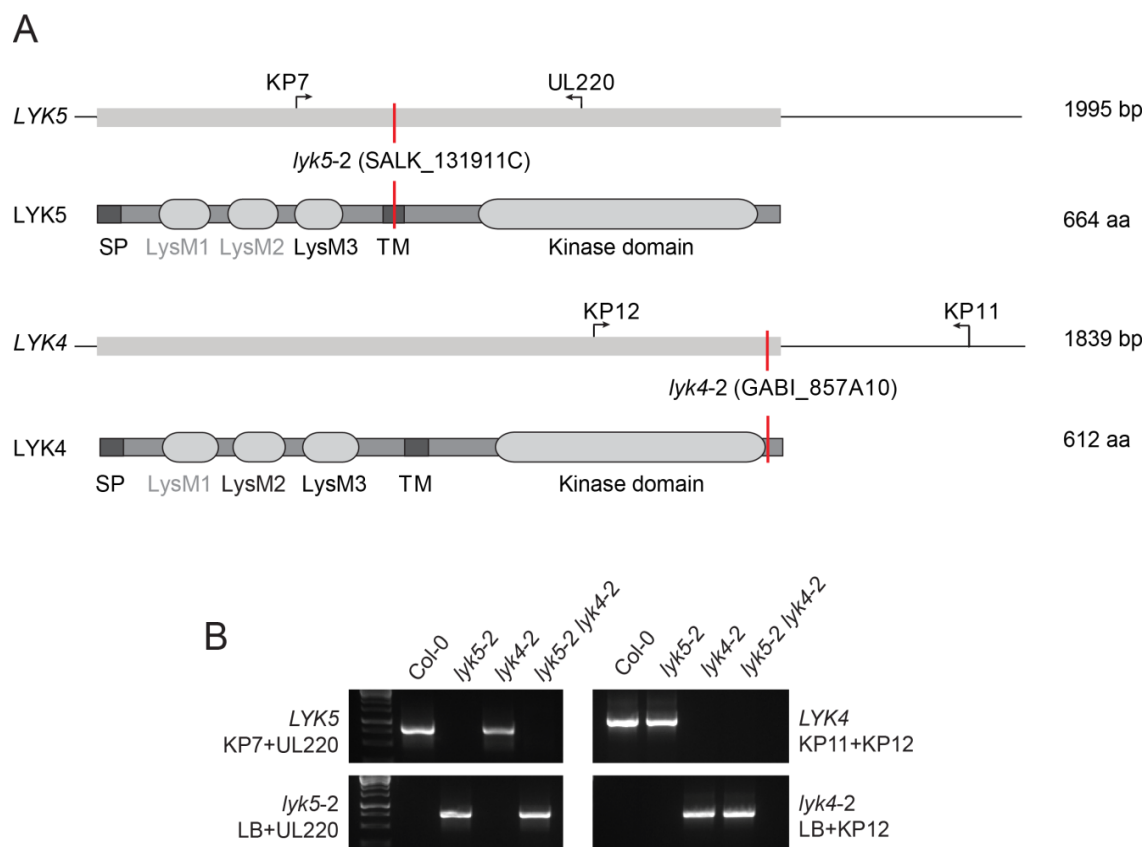


**Figure 10: *lyk5-2* and *lyk4-2* T-DNA insertion lines used in this study.**

**(A)** Schematic structures of *LYK* genes and *LYK* proteins. *lyk5-2* and *lyk4-2* T-DNA insertions are highlighted in red. Exons are depicted as grey boxes. Predicted protein features: signal peptide (SP), lysin motifs (LysM), transmembrane domain (TM), predicted using the TMHMM Server 2.0 (<http://www.cbs.dtu.dk/services/TMHMM/>, Krogh *et al.*, 2001), kinase domain. Protein domains were predicted using the TAIR integrated INTERPROSCAN and MyHits (<http://myhits.isb-sib.ch>, Pagni *et al.*, 2004). If detected by MyHits, LysMs are labelled black. LysM-domains labeled gray are predicted based on sequence similarity with other LysM-RLKs. Primers shown as black arrows were used for genotyping (B). **(B)** PCR-based genotyping of *lyk5-2*, *lyk4-2* and *lyk5-2 lyk4-2* double mutants. Homozygosity was verified using the primer pairs indicated in (A).

### 3.2.2 *lyk5-2* and *lyk5-2 lyk4-1* plants show reduced chitin-induced phosphorylation of CERK1 but MAPK activation is normal

MAMP recognition via the appropriate PRR leads to a number of signaling events that involve many phosphorylation reactions. Initially, the involved receptor proteins become phosphorylated. Consequently, MAPK cascades are activated by phosphorylation, which in turn, leads to phosphorylation and thus activation of transcription factors. Activated transcription factors then cause transcriptional re-programming and expression of defense genes (Boller and

Felix, 2009; Monaghan and Zipfel, 2012). To analyze if LYK5 and LYK4 are involved in defense signaling, the knock out mutants described above were tested for chitin-induced phosphorylation of CERK1 and MAPKs. CERK1 phosphorylation in response to chitin treatment can be visualized in Western blots with a specific CERK1 antibody as an upward mobility shift (Petutschnig *et al.*, 2010). The chitin-induced band shift of CERK1 was comparable to Col-0 in *lyk4-2*, but weaker in *lyk5-2*. In the *lyk5-2 lyk4-2* double mutant, CERK1 phosphorylation was reduced further but was not totally abolished (Figure 11A).

Chitin-induced activation of MAPKs was analyzed in the *lyk* mutants by Western blotting (Figure 11B) with an antibody detecting phosphorylated MAPKs ( $\alpha$ p-MAPK). Since MAPKs are activated by phosphorylation, such an assay can be used to monitor their activity. The antibody used detects activated MAPK3 and MAPK6 in *Arabidopsis* (Ye *et al.*, 2015).

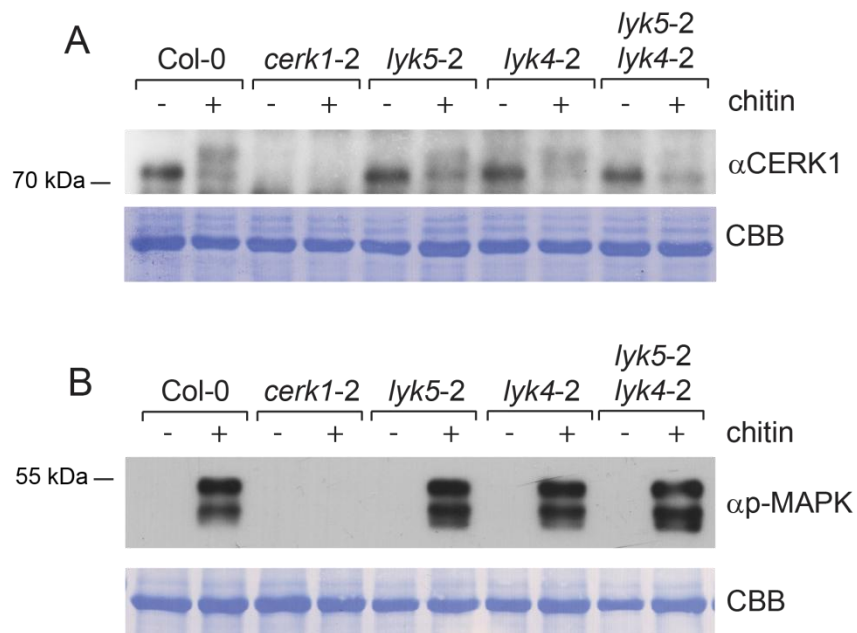


**Figure 11: Knock-out of *LYK5* causes moderately reduced CERK1 phosphorylation.**

*Arabidopsis lyk* mutant leaves were analyzed regarding CERK1 phosphorylation and activation of MAPKs. Leaves of the indicated genotypes were infiltrated either with water or 100  $\mu$ g/ml chitin and incubated for 10 min. **(A)** Western blot with  $\alpha$ CERK1 (upper panel) on total protein extracts showed reduced CERK1 phosphorylation in *lyk* mutants. **(B)** Phosphorylation of downstream MAPKs was not affected in *lyk* mutants. A Western blot was performed on Col-0, *cerk1-2* and *lyk* mutant leaves with an antibody specifically recognizing phosphorylated and thus active MAPKs ( $\alpha$ p-MAPK). Representative Western blots are depicted. All Experiments were performed at least three times with similar results. CBB: Coomassie Brilliant Blue-stained membranes.



As expected, MAPKs were clearly activated upon chitin treatment in Col-0, whereas no activation was observed in the negative control *cerk1-2* (Figure 11B). Chitin-induced MAPK activation was very similar to Col-0 in *lyk5-2 lyk4-2* and the respective single knockout lines. These results suggest that the remaining CERK1 phosphorylation observed in *lyk5-2 lyk4-2* mutants (Figure 11A) is sufficient to mediate full activation of MAPKs. In the CERK1 phosphorylation and MAPK activation assays, the same experimental conditions were used (100 µg/ml chitin, 10 min incubation). This indicates that disruption of LYK5 and LYK4 clearly reduces CERK1 phosphorylation, but the effect on downstream events must be subtle.

### 3.2.3 *lyk5-2* and *lyk5-2 lyk4-2* mutants show moderately decreased chitin-induced gene expression

As the activation of MAPKs was not affected in *lyk5-2*, *lyk4-1* and the double mutant, further effort was made to identify small differences in chitin response and to rule out saturation of the perception system. For this purpose, Col-0, *cerk1-2* and *lyk* mutant seedlings were grown in liquid culture and treated with a range of different chitin concentrations spanning five orders of magnitude. To quantify the effect of LYK5 and LYK4 disruption on transcription factor expression, qRT-PCR on the chitin-inducible genes *WRKY30*, *WRKY33* and *WRKY53* (Wan *et al.*, 2008a; Wan *et al.*, 2012; Cao *et al.*, 2014) was performed. In Col-0, all three tested genes were clearly induced upon chitin treatment in a dose-dependent manner, whereas no gene induction was observed in the knock-out mutant *cerk1-2* (Figure 12). *WRKY30*, *WRKY33* and *WRKY53* gene induction in *lyk4-2* was similar to Col-0. In contrast, the expression of chitin-inducible genes was moderately reduced in *lyk5-2* compared to Col-0, and reduced slightly further in the *lyk5-2 lyk4-2* double mutant. Interestingly, the reduction was clearest and most significant for *WRKY30*, with 1.5-fold less induced gene expression in *lyk5-2 lyk4-2* to Col-0 at the highest chitin concentration. For *WRKY33* and *WRKY53*, the reduction in expression was less significant (Figure 12).

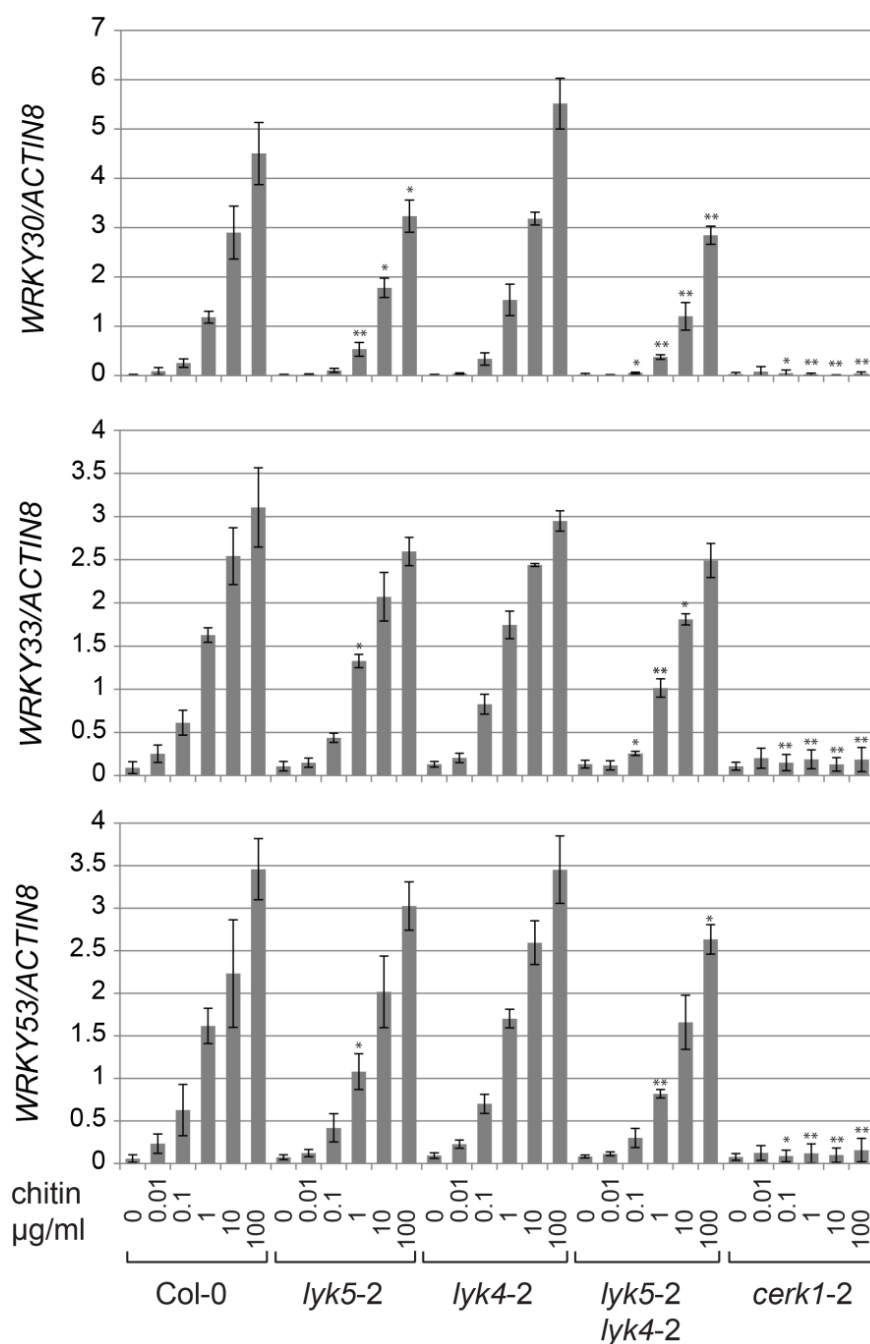


**Figure 12: *WRKY* transcription factor expression is moderately reduced in *lyk* mutants.**

Chitin-induced gene expression is slightly reduced in *lyk* mutants. The expression of *WRKY30*, *WRKY33* and *WRKY53* relative to *ACTIN8* was analyzed by quantitative RT-PCR. Seedlings were grown in liquid *in vitro* culture for 2 weeks. A chitin dilution series was prepared and added to the medium at final concentrations ranging from 10 ng/ml to 100 µg/ml. Seedlings were incubated in chitin for 30 min. The bars represent the mean  $\pm$  SD of three experiments and asterisks indicate statistically significant differences between Col-0 and mutant treated with the same chitin concentration. \* =  $p < 0.05$ , \*\* =  $p < 0.01$ .

In addition to dose-dependent induction of transcription factors, chitin-induced gene expression over time was monitored in the *lyk5-2 lyk4-2* double mutant, Col-0 and *cerk1-2* (Figure 13). To do so, *in vitro* grown seedlings were incubated in liquid growth medium containing 100 µg/ml chitin for different time periods ranging from 15 min to 1 d. As expected, no chitin-induced gene expression was observed in the *cerk1-2* mutant but *WRKY30*, *WRKY33* and *WRKY53* showed distinct induction peaks after 30 to 60 min in both Col-0 and *lyk5-2 lyk4-2* plants. There were no apparent differences in kinetics between *lyk5-2 lyk4-2* and Col-0. The same experimental setup was used to look at the expression of *CERK1*, *LYK5* and *LYK4*. For all three genes, primers spanning the respective T-DNA insertions were used to confirm disruption of transcripts. Thus, no gene induction of *LYK4* and *LYK5* was observed in the *lyk5-2 lyk4-2* mutant and no product for *CERK1* was amplified in *cerk1-2*. All three LysM-RLKs were induced by chitin. *CERK1* expression was induced slowly and remained elevated for several hours with a peak at 90 min in both Col-0 and *lyk5-2 lyk4-2* plants. *LYK4* and in particular *LYK5*, displayed a more rapid and transient induction compared to *CERK1* (Figure 13). *LYK5* expression showed the highest expression at 30 min of incubation and *LYK4* expression peaked after 60 min. Expression of both, *LYK4* and *LYK5* declined relatively quickly, returning to basal levels after approximately 2 h. Notably, the expression of *LYK5* and *LYK4* required *CERK1*, as chitin-triggered induction of these genes was not observed at any time point in *cerk1-2* (Figure 13).

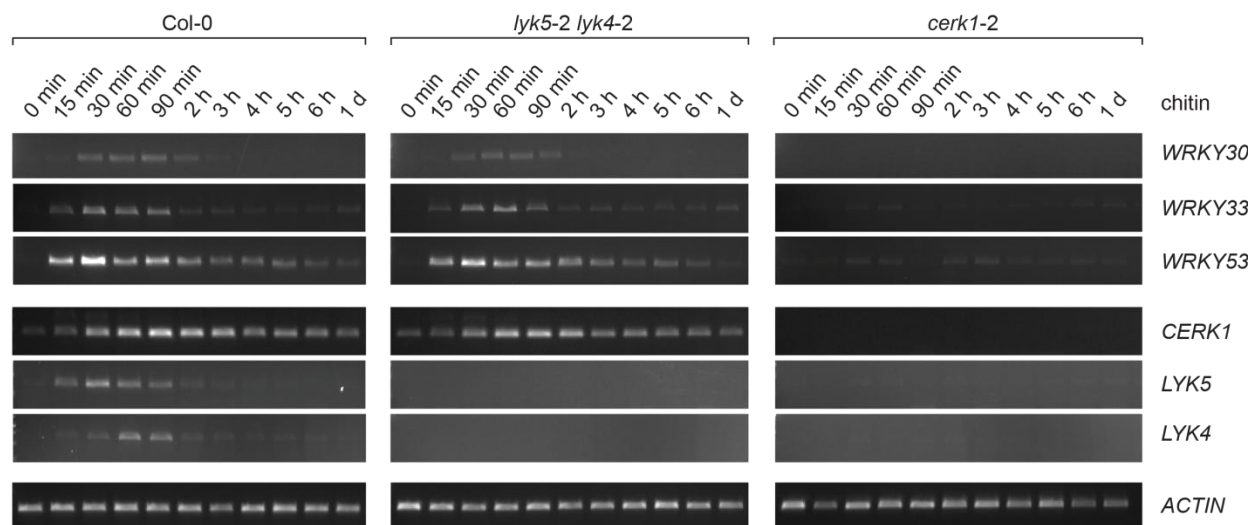


**Figure 13: Semi-quantitative expression analysis of *WRKY* and *LysM-RLK* genes.**

Expression analysis was performed on seedlings of Col-0, *lyk5-2 lyk4-2* and *cerk1-2* which were grown in liquid *in vitro* culture for 2 weeks. 100 µg/ml chitin were added to the medium and the seedlings were incubated for different time periods as indicated in the figure. Semi-quantitative RT-PCR was performed for *WRKY30*, *WRKY33*, *WRKY53*, *CERK1*, *LYK5* and *LYK4*. *ACTIN* served as a control. Experiments were performed three times and representative results are depicted here.

Taken together the data demonstrate that the loss of LYK5 subtly but significantly alters chitin related signaling events. This effect is enhanced by an additional mutation in *LYK4*, suggesting partial functional redundancy of LYK5 and LYK4. Furthermore, *LYK5* and *LYK4* gene expression requires CERK1. The data also show that chitin-induced *LYK5* and *LYK4* gene induction differs from that of *CERK1*.

### 3.3 Analysis of the subcellular behavior of LYK5 and LYK4

To investigate the subcellular localization and dynamics of LYK5 and LYK4, constructs were generated for expression of *LYK5-mCitrine* and *LYK4-mCitrine* fusion proteins from their endogenous promoters (*pGreenII-0229-JE-pLYK5::LYK5-mCitrine* and *pGreenII-0229-JE-pLYK4::LYK4-mCitrine*). These were transformed into wild type Col-0 as well as *cerk1-2* and *lyk5-2 lyk4-2* mutant plants. Transformants were screened for accumulation of LYK fusion proteins by confocal microscopy and Western blotting and lines with good signals were selected for further experiments.

Generally, the leaves of *pLYK4::LYK4-mCitrine* lines showed much lower accumulation of the transgenic protein than plants expressing *pLYK5::LYK5-mCitrine* (Figure 14). Only seven out of 50 screened plants expressing *LYK4-mCitrine* in the Col-0 background and eight out of 57 *cerk1-2* plants showed a detectable signal in microscopic images at all. This is in clear contrast to *LYK5-mCitrine*, plants where 43 out of 52 Col-0 and 14 out of 18 screened *cerk1-2* transformants showed good LYK5-mCitrine signals. Similar results were obtained for *lyk5-2 lyk4-2* double mutants transformed with *LYK5-mCitrine* or *LYK4-mCitrine*. In four out of 20 plants LYK4-mCitrine was detected and 18 out of 19 plants showed good results for LYK5-mCitrine. This difference is in agreement with publicly available microarray data, which show considerably lower expression values for LYK4 than for LYK5 in aerial tissues (Figure S4).

#### 3.3.1 LYK5-mCitrine and LYK4-mCitrine fusion proteins are functional

First, transgenic lines expressing *LYK5-mCitrine* and *LYK4-mCitrine* in *lyk5-2 lyk4-2* were tested for complementation of the *lyk5-2 lyk4-2* CERK1-phosphorylation phenotype. As described above, the *lyk5-2 lyk4-2* double mutant showed decreased chitin-induced CERK1 phosphorylation compared to the wild type. This can be observed as a reduced mobility shift of the CERK1 protein in Western blots (Figure 11A and Figure 14). Stable expression of *pLYK5::LYK5-mCitrine* could restore the chitin-induced CERK1 band shift in *lyk5-2 lyk4-2* to levels comparable to Col-0 whereas expression of *pLYK4::LYK4-mCitrine* partially restored CERK1 phosphorylation to *lyk5-2* levels (Figure 14). To confirm the presence of LYK-mCitrine fusion proteins a Western blot was probed with an antibody recognizing GFP and

GFP-derivatives such as mCitrine. While LYK5-mCitrine was readily detectable, the signals for LYK4-mCitrine were very weak, consistent with the lower activity of the LYK4 promoter (Figure 14).

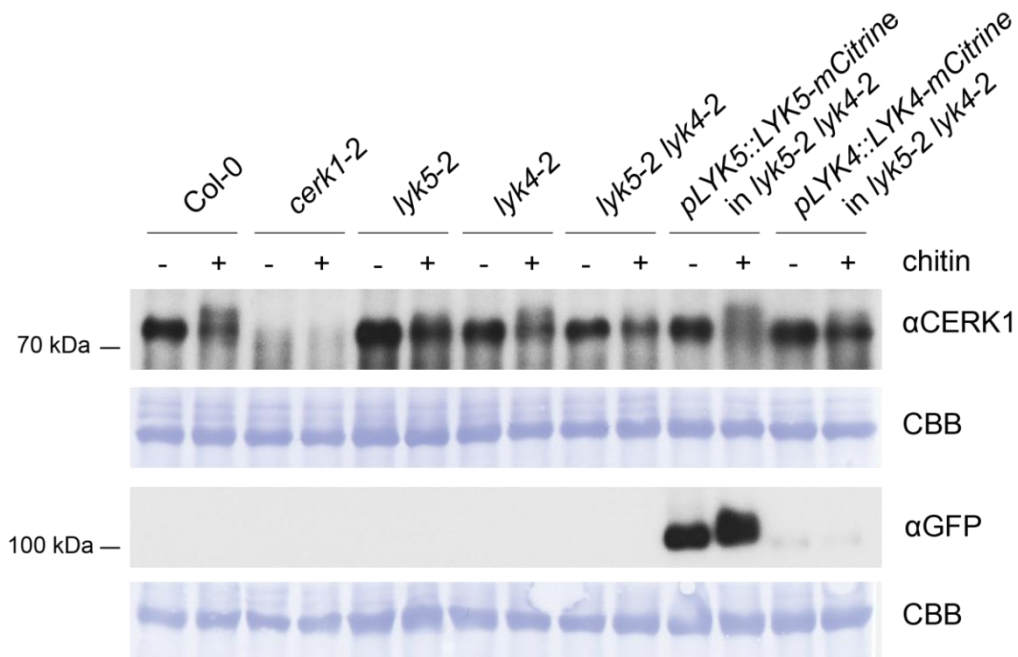


**Figure 14: Expression of *LYK5-mCitrine* and *LYK4-mCitrine* complement the reduced CERK1-phosphorylation in the *lyk5-2 lyk4-2* double mutant.**

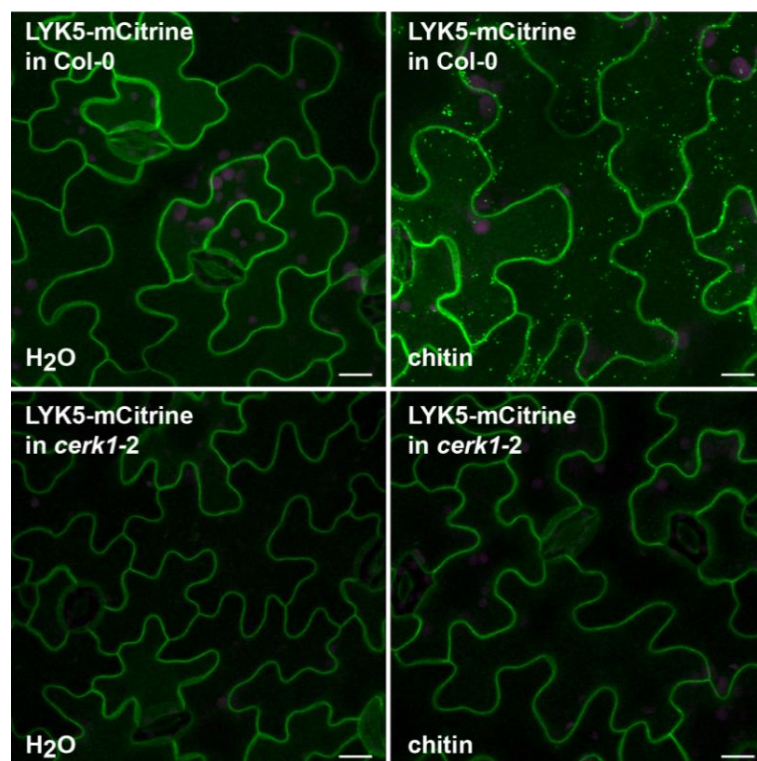
*Arabidopsis lyk* mutant leaves were analyzed regarding CERK1 phosphorylation and presence of LYK-mCitrine fusion proteins. Leaves of the indicated genotypes were infiltrated with water or 100 µg/ml chitin and incubated for 10 min. A Western blot with αCERK1 (upper panel) on total protein extracts showed reduced CERK1 phosphorylation in *lyk* mutants. This reduction was complemented by transgenic expression of *pLYK5::LYK5-mCitrine* and *pLYK4::LYK4-mCitrine*. Detection with αGFP (lower panel) was performed to visualize LYK5-mCitrine and LYK4-mCitrine. Representative Western blots are depicted. The experiment was performed at least three times with similar results. CBB: Coomassie Brilliant Blue-stained membranes.

The fact that expression of *pLYK5::LYK5-mCitrine* and *pLYK4::LYK4-mCitrine* could complement the reduced CERK1 phosphorylation phenotype in *lyk5-2 lyk4-2* demonstrates that LYK5-mCitrine and LYK4-mCitrine fusion proteins are functional and suitable for subcellular localization studies.

### 3.3.2 Chitin induces transient, CERK1-dependent formation of LYK5-mCitrine positive vesicles

To test the chitin-induced subcellular dynamics of LYK5, leaves expressing *LYK5-mCitrine* from the endogenous promoter in Col-0 or *cerk1-2* were vacuum-infiltrated with either water or chitin and incubated for 60 min. CLSM analysis showed that in water-infiltrated leaf epidermal cells of both backgrounds LYK5-mCitrine localized to the cell periphery. Upon chitin treatment, distinct LYK5-mCitrine-positive vesicles appeared in transgenic Col-0 plants (Figure 15A).

A



B

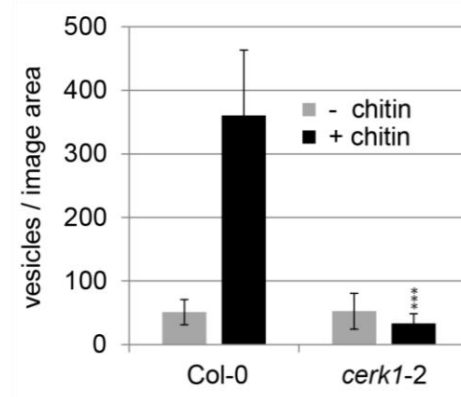


**Figure 15: Chitin-induced and CERK1-dependent formation of LYK5-mCitrine positive vesicles.**

**(A)** Leaves of plants expressing *pLYK5::LYK5-mCitrine* in the Col-0 or *cerk1-2* background were infiltrated with water or chitin and incubated for 60 min prior to analysis by CLSM. Images are representative maximum projections of 9 focal planes taken 1 μm apart. Similar results were obtained with four independent transgenic lines for the Col-0 background and three independent lines for *cerk1-2*. CLSM images: Green, mCitrine; magenta, chloroplast autofluorescence; Scale bar = 10 μm. **(B)** Quantification of LYK5-mCitrine positive vesicles in the absence and presence of chitin in Col-0 and *cerk1-2* plants. The data show the number of vesicles per image area and are averages of at least 65 imaging sites. Error bars: ± SD. In the *cerk1-2* background, the number of chitin-induced LYK5-mCitrine-containing vesicles was significantly reduced compared to Col-0. \*\*\*\*  $p \leq 0.0001$

In the *cerk1-2* mutant background however, chitin treatment did not lead to the formation of LYK5-mCitrine containing vesicles indicating that functional CERK1 is required for this process (Figure 15A). To support these findings, an ImageJ-based script was developed for quantification of LYK5-mCitrine-labeled vesicles in collaboration with Dr. Hassan Ghareeb. The computational method uses maximum projections of leaf epidermis images and comprises automated detection of PM and guard cell signals and their subsequent removal (Figure S5A). This is then followed by identification of fluorescent signals associated with punctate structures (Figure S5A). Quantitative analyses of *pLYK5::LYK5-mCitrine* leaves indicated that small numbers of LYK5-mCitrine-positive punctate structures are present already in unchallenged plants. The analysis also confirmed that chitin treatment triggered formation of LYK5-mCitrine containing vesicles in the Col-0 background, but not in *cerk1-2* (Figure 15B). The LYK5-mCitrine-containing vesicles were highly mobile (attached supplemental movie 1) and initial observations suggested that their appearance was transient. To characterize the dynamics of LYK5-mCitrine internalization, the number of chitin-induced endosomal compartments over time was quantified. The data in Figure 16 represent a detailed time course experiment where data were recorded in 5 min increments over 100 min to monitor the progression of LYK5-mCitrine vesicle formation. Prolonged laser exposure led to fluorophore bleaching over time, which was compensated for by introducing a signal normalization step into the quantification script (Figure S5B). At the lower fluorescence intensities typically observed at later time points, the normalization step to some extent also amplified unspecific background signals (Figure S5B). To allow correct interpretation of the data, punctate structures in water-infiltrated control samples were quantified for all time points (Figure 16, -chitin). Because of the normalization step, water treated samples showed a slight increase in detected punctae over time (Figure 16). LYK5-mCitrine positive vesicles started to appear after approximately 25 min of chitin exposure (Figure 16, +chitin). The peak vesicle density was reached at around 60 min and decreased at later time points (Figure 16, +chitin).

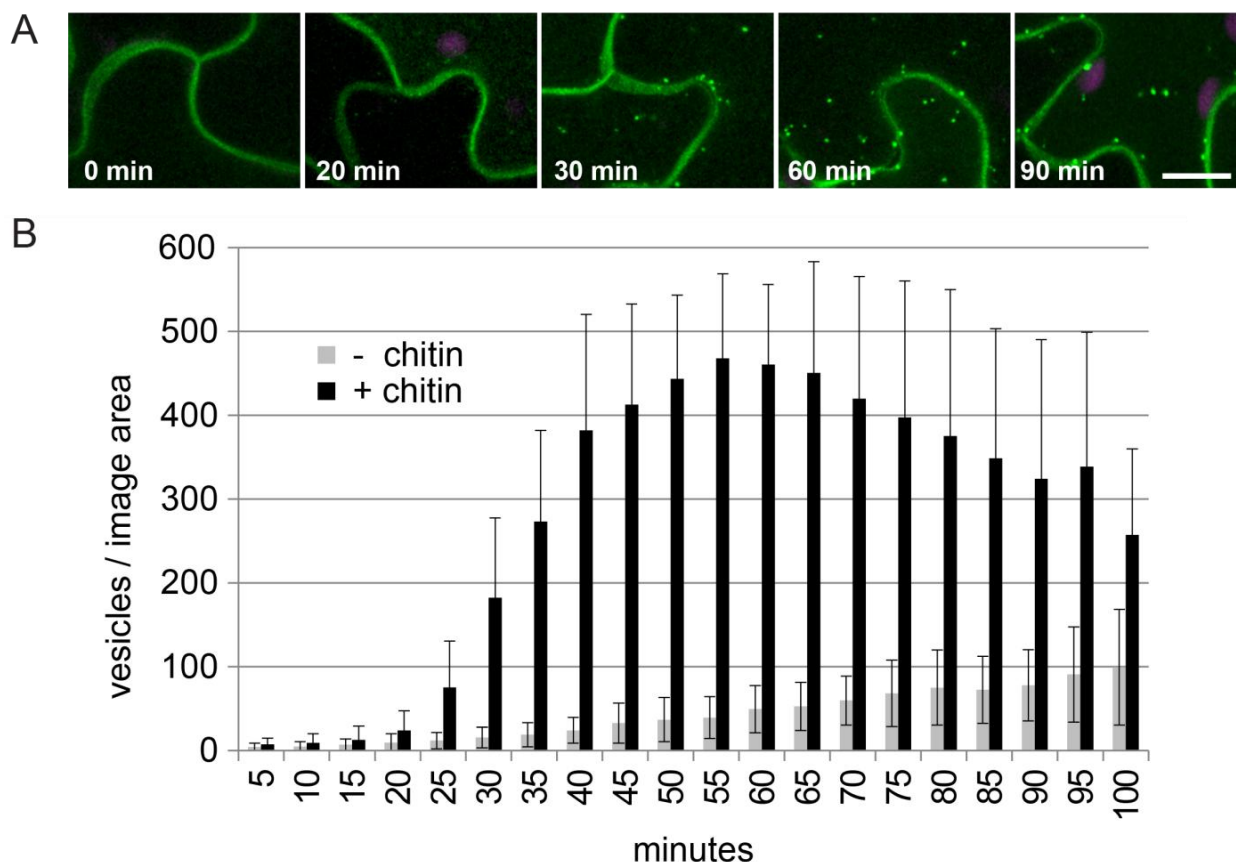


**Figure 16: Quantification of chitin-induced LYK5-mCitrine positive vesicles in Col-0 over time.**

*Arabidopsis* Col-0 leaves expressing *pLYK5::LYK5-mCitrine* were infiltrated with water or 100  $\mu\text{g}/\text{ml}$  chitin. **(A)** Representative images of LYK5-mCitrine vesicle formation at the indicated time points. CLSM images show a detail of the imaging area used in B. Green, mCitrine; magenta, chloroplast autofluorescence; Scale bar = 10  $\mu\text{m}$ . **(B)** Numbers of LYK5-mCitrine positive vesicles over time. Each time point represents an average  $\pm$  SD of 27 imaging sites. CLSM images are maximum projections of 10 focal planes taken 1  $\mu\text{m}$  apart.

### 3.3.3 LYK4-mCitrine is weakly expressed in leaves and may show chitin-induced vesicle formation

As mentioned above, fluorescence signal intensities were much lower in transgenic lines expressing *pLYK4::LYK4-mCitrine* compared to plants expressing *pLYK5::LYK5-mCitrine*. This is consistent with publicly available microarray data as summarized in figure S4. Only a few lines were obtained with robustly detectable *pLYK4::LYK4-mCitrine* signals. These lines were used to investigate the subcellular localization of LYK4-mCitrine in the Col-0 and *cerk1-2* background. For this purpose, *pLYK4::LYK4-mCitrine* expressing plants were vacuum infiltrated with either water or chitin and analyzed microscopically. The same chitin concentration and incubation time were used as for LYK5-mCitrine analysis, but higher laser power settings were



necessary to visualize LYK4-mCitrine. In figure 17 the resulting images of LYK4-mCitrine in water- or chitin-treated Col-0 and *cerk1-2* leaves are shown. In both backgrounds LYK4-mCitrine was detected at the cell periphery. Similar to LYK5-mCitrine, LYK4-mCitrine might also undergo chitin-induced and re-localization into vesicles in Col-0 plants. However, compared to LYK5-mCitrine, much fewer LYK4-mCitrine positive globular structures were identified. These structures were absent in chitin treated *cerk1-2* plants expressing *pLYK4::LYK4-mCitrine* (Figure 17), indicating that their formation is CERK1-dependent. Because the LYK4-mCitrine signals were close to the detection limit of the confocal system, further work was focused on LYK5-mCitrine.

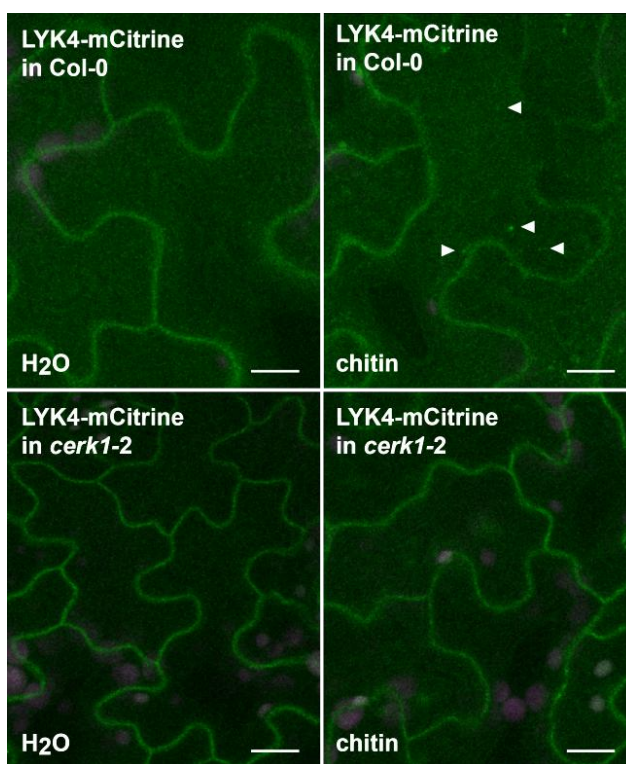


**Figure 17: LYK4-mCitrine may show chitin-induced, CERK1-dependent vesicle formation.**

*Arabidopsis* plants stably expressing *pLYK4::LYK4-mCitrine* showed weak fluorescence signals at the cell periphery. LYK4-mCitrine formed punctate structures (arrowheads) upon treatment with 100 µg/ml chitin when expressed in Col-0. These structures were absent when the same construct was expressed in the *cerk1-2* background. Images are representative maximum projections of 7 focal planes taken 1 µm apart. Similar results were obtained with three independent transgenic lines in each background. Green, mCitrine; magenta, chloroplast autofluorescence; Scale bar= 10 µm.

### 3.3.4 LYK5-mCitrine internalization is chitin specific

To test the specificity of LYK5-mCitrine vesicle formation, *pLYK5::LYK5-mCitrine* expressing Col-0 plants were treated with either chitin or flg22 (Figure 18). LYK5-mCitrine was not internalized after flg22 treatment. Only chitin induced the formation of LYK5-mCitrine-labelled endosomal compartments (Figure 18), demonstrating that this is a chitin-specific response. Plants expressing FLS2-GFP in Col-0 (Göhre *et al.*, 2008; Beck *et al.*, 2012) were included as a control. As expected, endocytosis of FLS2-GFP was triggered by flg22, but not by chitin (Figure 18).

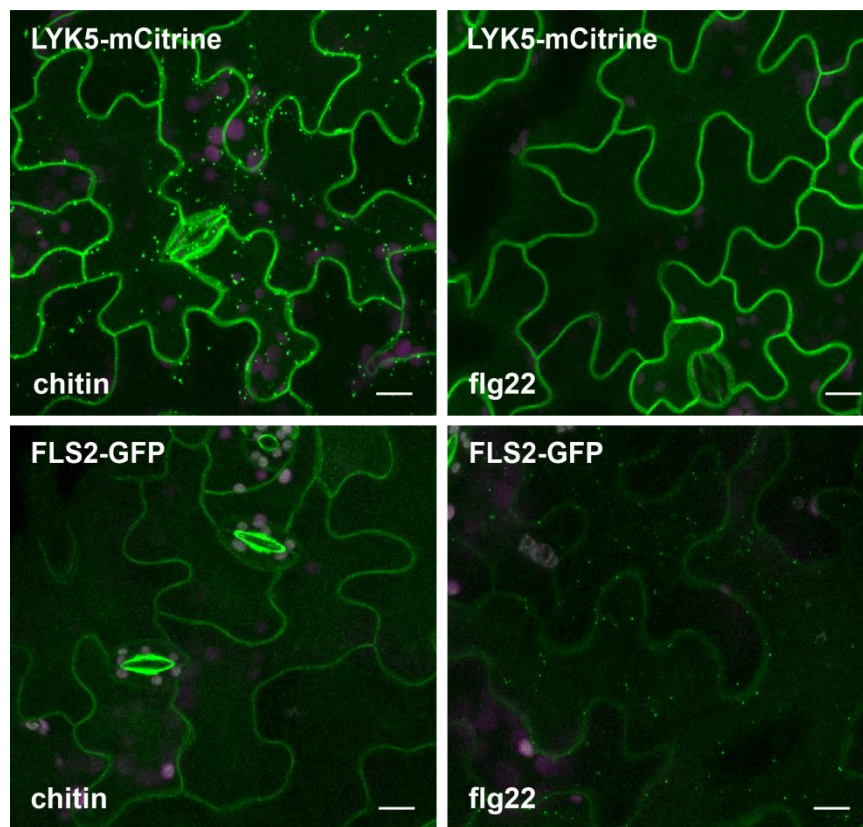


**Figure 18: LYK5-mCitrine vesicle formation is chitin specific.**

*Arabidopsis* leaves (Col-0) expressing either *pLYK5::LYK5-mCitrine* or *pFLS2::FLS2-GFP* were vacuum infiltrated with chitin (100 µg/ml) or flg22 (1 µM) solution. LYK5-mCitrine vesicle formation was only observed in chitin treated plants whereas FLS2-GFP was specifically endocytosed after flg22 treatment. CLSM images are representative maximum projections of 9 focal planes taken 1 µm apart. The experiment was repeated with four independent transgenic *pLYK5::LYK5-mCitrine* lines. *pFLS2::FLS2-GFP* plants were from a previously published line (Göhre *et al.*, 2008; Beck *et al.*, 2012). CLSM images: Green, mCitrine or GFP; magenta, chloroplast autofluorescence; Scale bar= 10 µm.

### 3.3.5 LYK5-mCitrine is specifically internalized from the plasma membrane

Next, the studies concentrated on the origin of LYK5-mCitrine vesicles. First, co-localization experiments with LYK5-mCitrine and the PM-marker protein LTI6b were performed. To generate *Arabidopsis* plants expressing both proteins, *pLYK5::LYK5-mCitrine* was transformed into a line expressing LTI6b (Cutler *et al.*, 2000) fused to the far red fluorescent protein mKate2 and driven by the ubiquitin promoter (*p35S::LTI6b-mKate2*, kindly provided by Dr. Hassan Ghareeb, unpublished) (Figure 19A). LYK5-mCitrine signal overlapped with the PM-marker in unchallenged plant lines confirming LYK5-mCitrine PM-localization. After chitin elicitation, LYK5-mCitrine positive vesicles appeared within the cell, whereas the LTI6b-mKate2 signal remained at the cell periphery (Figure 19A), suggesting that LYK5-mCitrine is specifically internalized and represents a selective cargo. To determine the identity of chitin-induced LYK5-mCitrine-tagged vesicles further, co-staining with FM4-64 was performed. As mentioned above (section 3.1.4.), FM4-64 stains the PM and PM-derived structures and thus can be used as endocytic tracer. After application, it successively stains the PM, endosomal compartments and the vacuole (Bolte *et al.*, 2004). Chitin-induced LYK5-mCitrine-labelled vesicles partially overlapped with FM4-64 stained compartments (Figure 19B). This indicates that LYK5-mCitrine is endocytosed from the PM and thus localizes to bona fide endosomes. In summary, LYK5-mCitrine is a PM-localized protein that undergoes chitin-induced endocytosis.

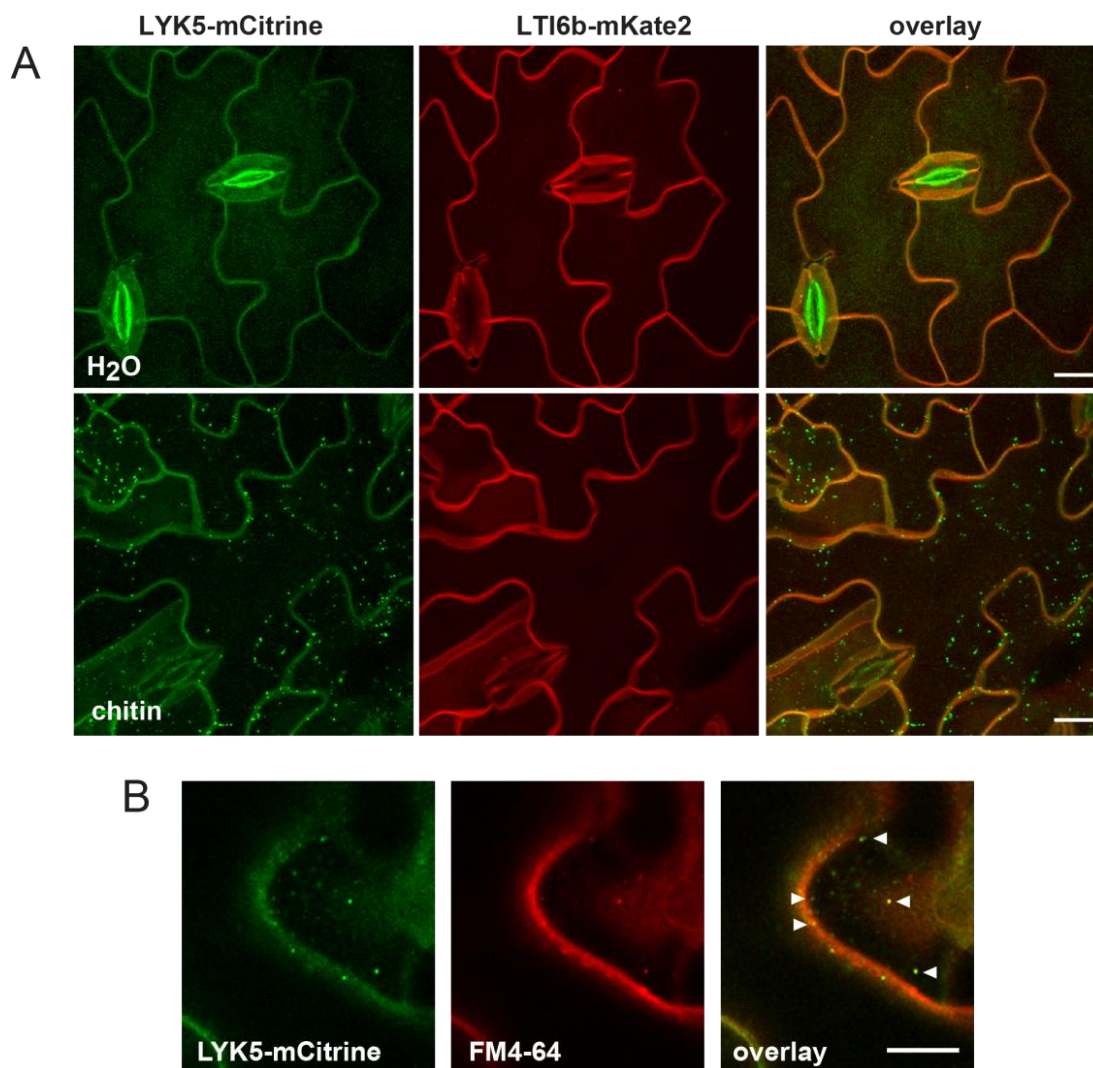


**Figure 19: Chitin-induced endocytosis of LYK5-mCitrine from the plasma membrane.**

Co-localization studies with the PM marker protein LTI6b and the lipophilic stain FM4-64 confirmed LYK5-mCitrine PM localization and revealed chitin-induced endocytosis. **(A)** *pLYK5::LYK5-mCitrine* was stably co-expressed with the PM marker protein LTI6b-mKate2 in *Arabidopsis* plants. Chitin treatment (100 µg/ml) for 60 min triggered the formation of intracellular LYK5-mCitrine positive compartments whereas the LTI6b-mKate2 signal remained at the PM. CLSM images are maximum projections of 10 focal planes taken 1 µm apart. Similar results were obtained with four independent transgenic lines. **(B)** FM4-64 stained intracellular compartments partially co-localized with chitin-induced LYK5-mCitrine vesicles. Leaves were incubated in FM4-64 solution for 15 min, then LYK5-mCitrine vesicle formation was triggered by infiltration with chitin (100 µg/ml) and subsequent incubation for 60 min. Arrow heads point to overlapping endosomes. Representative single plane CLSM images are shown. The staining was repeated with five independent transgenic lines yielding in similar results. CLSM images: Green, mCitrine; Red, mKate2 or FM4-64; Scale bar = 10 µm.

### 3.3.6 LYK5-mCitrine co-localizes with LE/MVB markers ARA6 and Rha1 but not with recycling endosomes

Ligand induced receptor endocytosis in plants is controlled, among other factors, by Rab GTPases (Beck *et al.*, 2012; Choi *et al.*, 2013; Spallek *et al.*, 2013). Plant Rab GTPases fall into a number of subfamilies that play different roles and thus localize differently within the endomembrane system (Rutherford and Moore, 2002; Vernoud *et al.*, 2003). Two subfamilies, Rab5/RabF and Rab11/RabA, are frequently used for co-localization studies to reveal distinct endosomal pathways (Ueda *et al.*, 2001; Lee *et al.*, 2004; Ganguly *et al.*, 2014; Lei *et al.*, 2014). Members of the Rab5/RabF family localize to prevacuolar compartments (PVCs), also known as MVBs or LEs and are involved in the traffic to the vacuole (Rutherford and Moore, 2002; Nielsen *et al.*, 2008). Rab11/RabA proteins are often associated with the TGN and play a role in traffic between the TGN and PM (Rutherford and Moore, 2002; Chow *et al.*, 2008; Nielsen *et al.*, 2008).

To investigate the endosomal trafficking pathway of LYK5-mCitrine, *pLYK5::LYK5-mCitrine* plants were crossed with marker lines expressing members of the Rab5/RabF family (ARA6/RabF1 and Rha1/RabF2a), or representatives of the Rab11/RabA family (RabA5d and RabA1g), fused to red fluorescent proteins RFP or mCherry. *Arabidopsis* Col-0 plants co-expressing *pLYK5::LYK5-mCitrine* with endosomal markers *p35S::ARA6-RFP* (kindly provided by Dr. U. Lipka) or *pUBQ10::mCherry-Rha1* (Geldner *et al.*, 2009) were vacuum infiltrated with water or chitin and analyzed microscopically (Figure 20). In water treated control plants, LYK5-mCitrine was detected at the cell periphery, while ARA6-RFP and mCherry-Rha1 both showed a punctate localization pattern (Figure 20). Upon chitin induction, LYK5-mCitrine was internalized into endosomes that co-localized with the endosomal compartments labeled by both ARA6-RFP and mCherry-Rha1 (Figure 20). Interestingly, LYK5-mCitrine signal totally overlaps with the mCherry-Rha1 marker but in LYK5-mCitrine and ARA6-RFP lines also ARA6-RFP-free vesicles were visible (Figure 20). Indeed, ARA6 and Rha1 partially overlap with their localization at LEs/MVBs (Ueda *et al.*, 2001; Lee *et al.*, 2004; Ueda *et al.*, 2004; Ebine *et al.*, 2011). Signal specificity for the respective fusion proteins was confirmed by imaging with the same settings in lines expressing either the RFP/mCherry-tagged endosomal markers or LYK5-mCitrine alone (Figure S6).

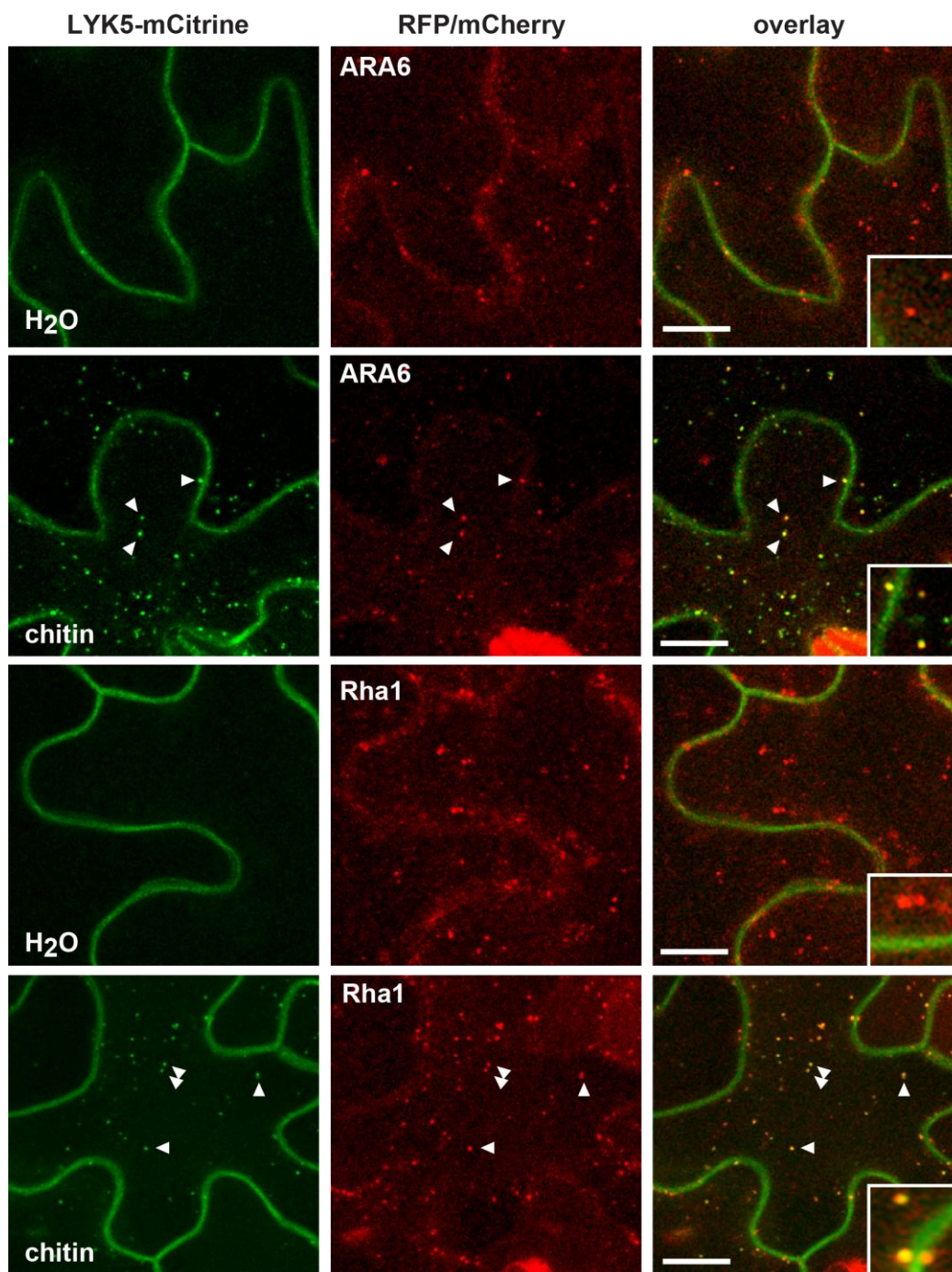


**Figure 20: Upon chitin treatment, LYK5-mCitrine co-localizes with LE/MVB markers ARA6 and Rha1.**

*Arabidopsis* Col-0 plants stably expressing *pLYK5::LYK5-mCitrine* and the LE/MVB markers *p35S::ARA6-RFP* or *pUBQ10::mCherry-Rha1* were infiltrated with water or chitin solution (100 µg/ml) and incubated for 60 min. Chitin-induced LYK5-mCitrine positive endosomes overlapped with ARA6-RFP and mCherry-Rha1-labelled endosomal compartments. Arrow heads point to overlapping endosomes. Inset pictures show details. All images are representative maximum projections of 10 focal planes taken 1 µm apart. Experiments were repeated with three independent transgenic lines. Green, mCitrine; red, RFP or mCherry; Scale bar = 10 µm.

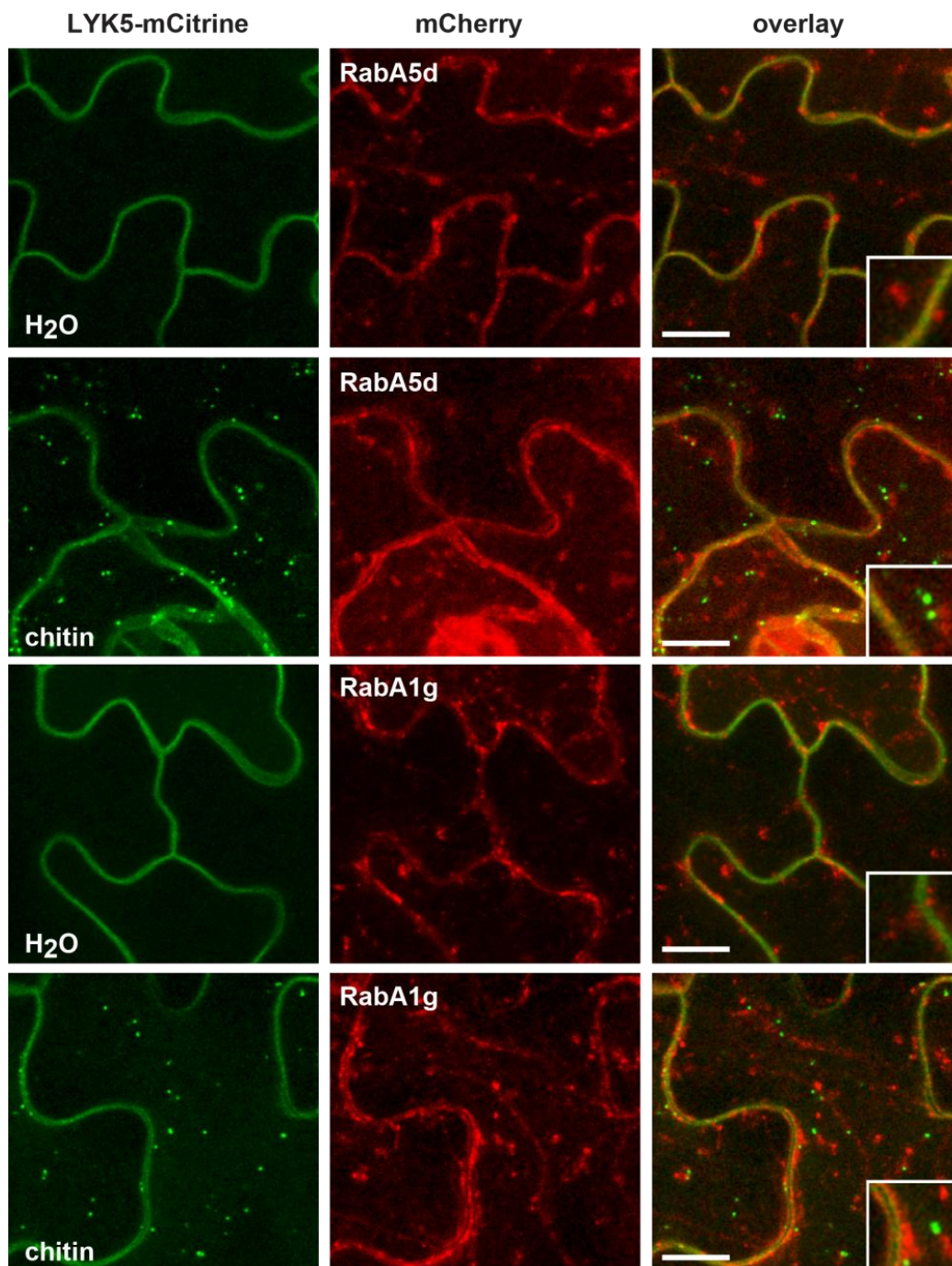


**Figure 21: LYK5-mCitrine does not co-localize with recycling endosomal markers RabA5d and RabA1g.**

*Arabidopsis* Col-0 plants stably expressing *pLYK5::LYK5-mCitrine* and the recycling endosomal markers *pUBQ10::mCherry-RabA5d* or *pUBQ10::mCherry-RabA1g* were infiltrated with water or chitin solution (100  $\mu\text{g/ml}$ ) and incubated for 60 min. Chitin-induced LYK5-mCitrine-positive endosomes did not overlap with mCherry-RabA5d and mCherry-RabA1g-labelled endosomal compartments. Inset pictures show details. All images are representative maximum projections of 10 focal planes taken 1  $\mu\text{m}$  apart. Experiments were repeated with three independent transgenic lines. Green, mCitrine; red, RFP or mCherry; Scale bar = 10  $\mu\text{m}$ .

Plants expressing the recycling endosomal and TGN marker *pUBQ10::mCherry-RabA5d* and *pUBQ10::mCherry-RabA1g* (Geldner *et al.*, 2009) together with *pLYK5::LYK5-mCitrine* were also infiltrated with water or chitin. In water infiltrated samples, mCherry-RabA5d and mCherry-RabA1g showed a patchy signal at the cell periphery and labeled globular endomembrane compartments. The LYK5-mCitrine endosomes that appeared after chitin treatment did not overlap with the mCherry-RabA5d or mCherry-RabA1g-positive intracellular structures. LYK5-mCitrine containing endosomes were frequently observed in close proximity to mCherry-RabA5d or mCherry-RabA1g-labeled compartments, suggesting that they are possibly associated in the cell (Figure 21).

Taken together, co-expression with marker proteins revealed that LYK5-mCitrine co-localizes with members of the Rab5/RabF family, namely ARA6 and Rha1, in LEs/MVBs after chitin elicitation. In contrast, no overlapping signals were observed for LYK5-mCitrine and mCherry-tagged RabA5d or RabA1g, which are both members of Rab11/RabA-family and localize to the TGN and TGN-derived structures.

### **3.3.7 Chitin-induced endocytosis of LYK5-mCitrine is BFA-insensitive.**

Since BFA treatment revealed constitutive endomembrane trafficking of CERK1-GFP (section 3.1.4) and FLS2 (Beck *et al.*, 2012), it was tested if this is also the case for LYK5. Indeed, BFA incubation of *pLYK5::LYK5-mCitrine* leaves led to the formation of LYK5-mCitrine-positive endomembrane compartments (Figure 22A and B), which were also labeled by FM4-64 (Figure 22A). To check if BFA treatment interferes with chitin-induced internalization of LYK5-mCitrine, Col-0 plants expressing *pLYK5::LYK5-mCitrine* were incubated with BFA and infiltrated with chitin. Interestingly, the BFA treatment did not block chitin-triggered endocytosis of LYK5-mCitrine (Figure 22B). As shown in Figure 22B, also the inhibitor solvent DMSO did not alter LYK5-mCitrine endocytosis. Next, quantification of LYK5-mCitrine labeled endosomes was performed in samples infiltrated with chitin in the presence or absence of BFA. The obtained results support the findings described above, as no significant differences between BFA and control treated samples were observed (Figure 22C). Vice versa, chitin did not suppress the formation of mCitrine-labeled BFA-induced compartments. In fact, chitin-induced LYK5-mCitrine endosomes were frequently found around BFA-induced bodies (Figure 22B), a localization pattern that has also been described for FLS2 (Beck *et al.*, 2012).



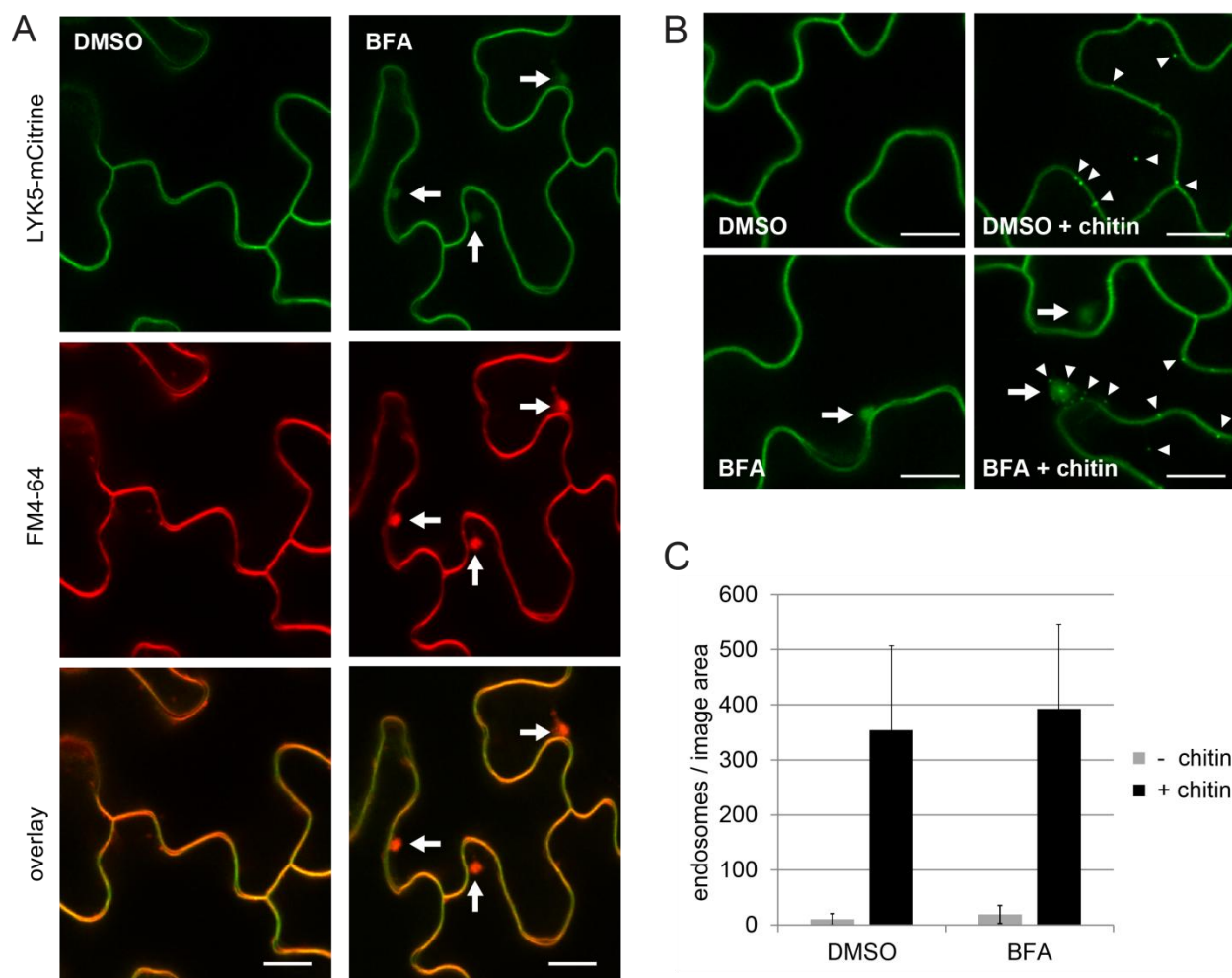


**Figure 22: BFA application affects constitutive endomembrane trafficking of LYK5-mCitrine, but not its chitin-induced endocytosis.**

**(A)** *Arabidopsis* Col-0 leaves expressing *pLYK5::LYK5-mCitrine* were incubated for 30 min with the solvent control DMSO or 30  $\mu$ M BFA and then stained with the lipophilic stain FM4-64. LYK5-mCitrine accumulated in BFA-induced compartments that co-localized with FM4-64 stained BFA-bodies. **(B)** LYK5-mCitrine accumulation in BFA-induced compartments is independent of chitin treatment. *pLYK5::LYK5-mCitrine* expressing leaves were treated with BFA and infiltrated with water or chitin (100  $\mu$ g/ml). (A) and (B) are representative single plane CLSM images. Similar results were obtained in experiments with three independent transgenic lines. Arrows point to BFA-induced compartments, arrow heads to chitin-induced LYK5-mCitrine-containing endosomes. Green, LYK5-mCitrine; Red, FM4-64; Scale bar = 10  $\mu$ m. **(C)** Quantification of LYK5-mCitrine positive endosomes per image area in leaves that were incubated with DMSO or BFA and infiltrated with or without chitin. The data are presented as average of 40 imaging sites. Error bars:  $\pm$  SD.

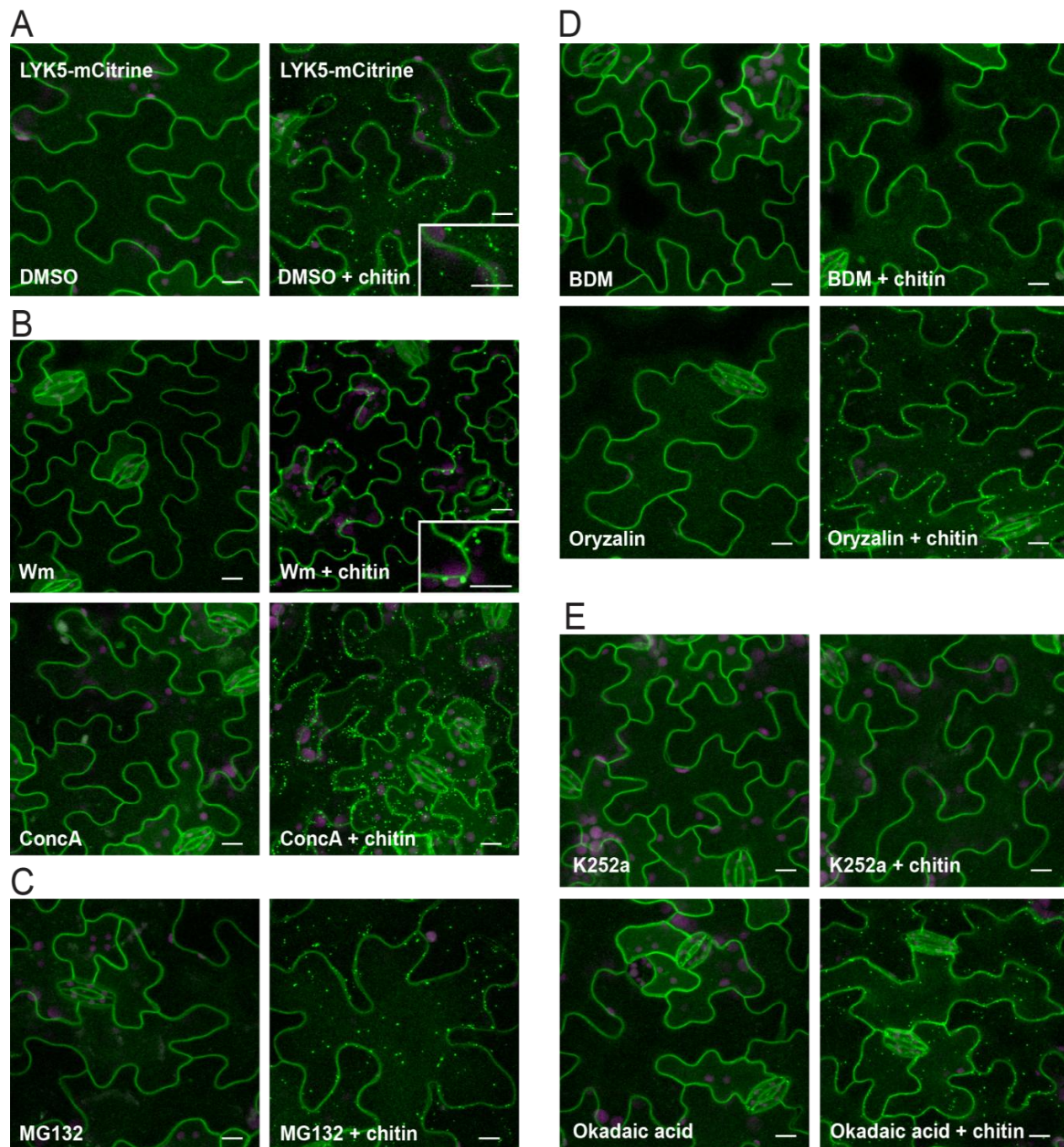
Additionally, double transgenic lines expressing LYK5-mCitrine and the recycling endosomal markers mCherry-RabA5d or mCherry-RabA1g (compare section 3.3.6) were tested for their response to BFA treatment. For this purpose, the respective plant lines were incubated with

BFA prior to chitin infiltration as described above. As a control, treatment with the inhibitor solvent DMSO was carried out. Upon chitin challenge LYK5-mCitrine containing endosomes were visible in both, DMSO and BFA treated leaves (Figure S7 and Figure S8). In samples incubated in BFA, the recycling endosomal markers mCherry-RabA5d or mCherry-RabA1g strongly accumulated in globular endomembrane compartments. LYK5-mCitrine also labeled these compartments, but the signal intensity was much lower compared to the mCherry-RabA fusions. Literature shows that recycling endosomal markers are highly sensitive to BFA treatment (Geldner *et al.*, 2009). In comparison to mCherry-RabA5d and mCherry-RabA1g, LYK5-mCitrine endocytic trafficking appeared less sensitive to BFA (Figure S7 and Figure S8).

### **3.3.8 LYK5-mCitrine endocytosis is affected by inhibitors of endomembrane trafficking, the cytoskeleton and protein phosphorylation.**

To further dissect the chitin-induced internalization of LYK5-mCitrine, chemical inhibitors were used either with or without chitin co-treatment in *pLYK5::LYK5-mCitrine* expressing Col-0 plants. Interference with endomembrane trafficking using pharmacological substances is a well-established approach for the investigation of trafficking routes and mechanisms. For this purpose, detached leaves were pre-incubated in the respective inhibitor solution and then infiltrated with or without chitin. The leaf samples were then microscopically analyzed regarding endosome formation. Furthermore, images were taken for quantification of LYK5-mCitrine vesicle abundance. First, the inhibitor solvent DMSO was tested and found not to interfere with chitin induced LYK5-mCitrine endosome formation. As can be seen in figure 23A and figure 23F, DMSO alone did not result in the formation of LYK5-mCitrine positive endosomes. Second, the endomembrane trafficking inhibitors Wm and ConCA were tested. Wm is a phosphatidylinositol 3-kinase inhibitor that covalently targets phosphoinositide 3 kinases (PI3Ks) at LE/MVB, thus affecting the formation of internal vesicles in MVBs and causing the MVBs to enlarge via homotypic fusion (Wang *et al.*, 2009). Additionally, Wm interferes with endocytosis at the PM (Emans *et al.*, 2002; Robinson *et al.*, 2008a). Leaves co-treated with chitin and Wm showed significantly reduced LYK5-mCitrine endosome numbers (Figure 23B and F) compared to control samples treated with DMSO and chitin (Figure 23and F). At the same time, larger-sized LYK5-mCitrine-tagged vesicles were observed that likely represent enlarged MVBs (Figure 23B). ConCA blocks trafficking at the TGN by inhibition of vacuolar type H<sup>+</sup>-ATPases (V-ATPases), thereby affecting transport of proteins to LEs/MVBs and the vacuole (Irani and Russinova, 2009; Ben Khaled *et al.*, 2015). Treatment with ConCA alone caused a slight, but significant increase in LYK5-mCitrine-positive endosomes (Figure 23B and F). This suggests

that there are low levels of LYK5-mCitrine transported to the vacuole even without ligand exposure. The number of LYK5-mCitrine positive endosomes was dramatically increased when samples were co-treated with ConcA and chitin (Figure 23B). Quantification revealed that in these samples the abundance of LYK5-mCitrine containing endosomes was nearly twice as high as in samples treated with DMSO and chitin (Figure 23F). These findings suggest that upon chitin challenge, LYK5-mCitrine molecules are transported to the vacuole via LEs/MVBs, where they are likely targeted for degradation. In contrast to ConcA, which is also a known inhibitor of protein degradation in the vacuole (Tamura *et al.*, 2003), blocking of proteasomal protein degradation with MG132 had no effect on chitin-induced LYK5-mCitrine endosomes as indicated by the microscopic images (Figure 23C) and endosome quantification (Figure 23F). Next, the inhibitors 2,3-butanedione monoxime (BDM) and oryzalin, were applied to investigate vesicle transport along the cytoskeleton. The non-competitive, reversible ATPase inhibitor BDM targets myosin motor proteins (Samaj *et al.*, 2000) whereas oryzalin, which belongs to the class of dinitroaniline class of herbicides, causes microtubule depolymerization (Baskin *et al.*, 1994). BDM almost completely blocked chitin-induced endocytosis (Figure 23D), resulting in a highly significant reduction of quantified LYK5-mCitrine positive vesicles (Figure 23F). In oryzalin-treated leaves, the number of chitin-induced LYK5-mCitrine endosomes was not affected compared to the control treatment with DMSO (Figure 23F). However, the observed LYK5-mCitrine containing endosomes were drastically reduced in their mobility (attached supplemental movie 2). The results from cytoskeleton-related inhibitor treatments suggest that LYK5-mCitrine labeled vesicle budding requires actin filaments in association with myosin motor proteins, while transport through the cell depends on microtubules. Finally, inhibitors were investigated that interfere with protein phosphorylation and de-phosphorylation. It has previously been shown that the broad specificity kinase inhibitor K252a reduces chitin-induced phosphorylation of CERK1, while the serine/threonine phosphatase inhibitor OA had a slightly enhancing effect on the CERK1 phosphorylation status (Petutschnig *et al.*, 2010). Indeed, K252a strongly inhibited the chitin induced formation of LYK5-mCitrine-positive vesicles (Figure 23E). As can be seen in Figure 23 F, the number of detected endosomes was significantly reduced in the K252a-treated samples. In contrast, OA caused no clear alteration of endosome density (Figure 23E and F). These data demonstrate that protein phosphorylation is an essential step in LYK5-mCitrine endocytosis, while the role of de-phosphorylation and the amino acids phosphorylated (serine/threonine or tyrosine) will need further research.



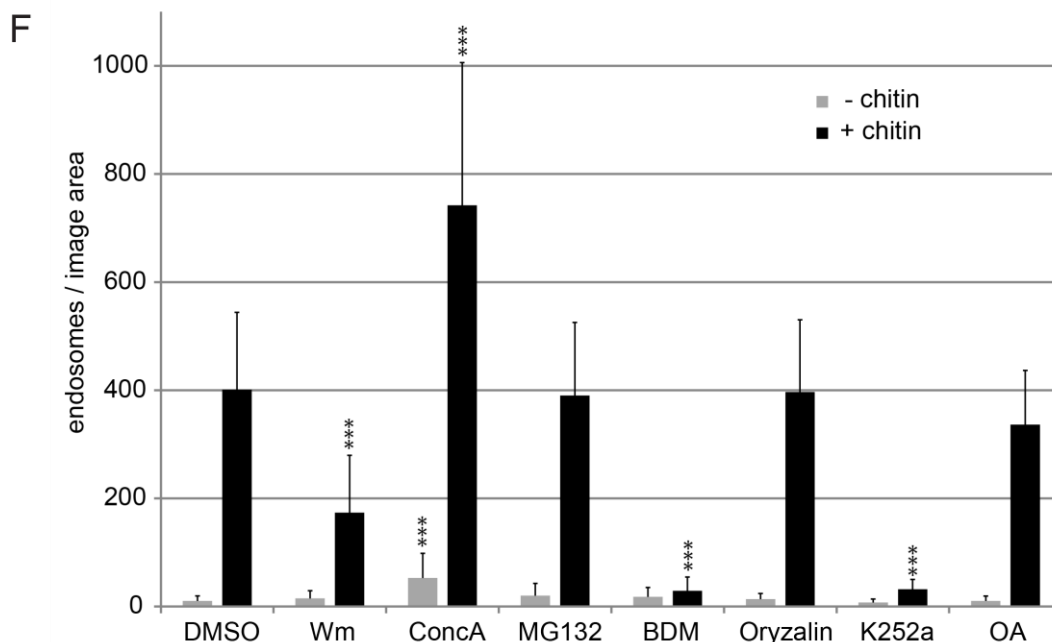


**Figure 23: Inhibitors of endomembrane trafficking, the cytoskeleton and protein phosphorylation affect LYK5-mCitrine endocytosis.**

*Arabidopsis* leaves stably expressing *pLYK::LYK5-mCitrine* in Col-0 were pre-incubated for 30 min in inhibitor solution and then infiltrated with or without chitin (100 µg/ml) and incubated for further 60 min in the presence of the indicated inhibitors. Images are shown for leaves treated with **(A)** DMSO (inhibitor solvent) as a control, **(B)** endomembrane trafficking inhibitors Wm (30 µM) and ConcA (1 µM), **(C)** the proteasome inhibitor MG132 (50 µM), **(D)** cytoskeleton inhibitors BDM (50 mM) and oryzalin (20 µM) and **(E)** K252a (10 µM), a kinase inhibitor as well as OA (1 µM), a phosphatase inhibitor. All images are representative maximum projections of 10 focal planes taken 1 µm apart. Each treatment was repeated at least 3 times with independent transgenic lines. Green, mCitrine; magenta, chloroplast autofluorescence; Scale bar = 10 µm. **(F)** Quantification of LYK5-mCitrine containing endosomes per image area. Leaves were treated as described above. The diagram presents data as average of ≥ 50 imaging sites. Error bars: ± SD. A student's t-test was performed to test for statistical significance. Inhibitor treatments were compared to DMSO, inhibitor + chitin treatments were compared to DMSO + chitin. \*\*\*  $p \leq 0.0001$ .

### 3.4 LYK5-mCitrine and CERK1 phosphorylation studies

#### 3.4.1 Chitin-induced and CERK1-dependent phosphorylation of LYK5-mCitrine

The chitin-induced formation of LYK5-mCitrine positive endosomes might require phosphorylation of LYK5 by CERK1 since the kinase inhibitor K252a blocked endocytosis of LYK5-mCitrine and chitin-induced LYK5-mCitrine endosomes are absent in the *cerk1-2* mutant. To investigate this hypothesis, transgenic lines expressing *pLYK5::LYK5-mCitrine* in the wild type Col-0 and *cerk1-2* background were assessed in Western blot experiments. Leaf samples

of two independent transgenic plants in each background were infiltrated with or without chitin. Col-0 and *cerk1-2* were included as controls and infiltrated the same way. CERK1 and LYK5-mCitrine were detected with  $\alpha$ CERK1 and  $\alpha$ GFP antibodies, respectively. In the Col-0 background, LYK5-mCitrine, displayed an upward mobility shift upon chitin treatment (Figure 24A), which was absent in lines expressing *pLYK5::LYK5-mCitrine* in the CERK1-deficient background *cerk1-2* (Figure 24A). This chitin-induced LYK5-mCitrine band shift is reminiscent of the chitin-induced mobility shift of CERK1 (Figure 24A), which was previously shown to be caused by phosphorylation (Petutschnig *et al.*, 2010).

To test whether the chitin-triggered mobility shift of LYK5-mCitrine is also caused by phosphorylation, the LYK5-mCitrine protein was pulled down from total extracts of chitin-treated and untreated plants with GFP-magnetic beads. The pulled down LYK5-mCitrine was subsequently incubated with Lambda phosphatase ( $\lambda$ -PPase).  $\lambda$ -PPase is a  $Mn^{2+}$ -dependent protein phosphatase with activity towards phosphorylated serine, threonine and tyrosine residues (Cohen and Cohen, 1989; Gordon, 1991; Zhuo *et al.*, 1993). Thus, treatment with  $\lambda$ -PPase releases phosphate groups from phosphorylated residues in proteins. Figure 24B clearly shows that the  $\lambda$ -PPase treatment reversed the chitin-induced band shift of LYK5-mCitrine. In contrast, the LYK5-mCitrine mobility shift remained present in control samples that were incubated without the enzyme (Figure 24B). Taken together, the data indicate that LYK5-mCitrine is phosphorylated *in planta* in a chitin- and CERK1-dependent manner.

To characterize the chitin-induced phosphorylation of LYK5-mCitrine further, time course experiments were performed (Figure 24C). Phosphorylation was analyzed in *pLYK5::LYK5-mCitrine* expressing Col-0 and *cerk1-2* plants that were infiltrated with chitin and incubated for 90 min. To monitor phosphorylation over time, samples were collected every 10 min. As illustrated in Figure 24C, the phosphorylation of both CERK1 and LYK5-mCitrine occurred within 10 minutes in the Col-0 background. Thus, receptor phosphorylation precedes visible LYK5-mCitrine endocytosis, which starts around 20 min after chitin elicitation. LYK5-mCitrine was not phosphorylated in the *cerk1-2* mutant at any time point, confirming the requirement of CERK1 for this process. LYK5-mCitrine phosphorylation significantly decreased after 20 min (Figure 24C), which correlates with the start of its endocytosis (compare Figure 16). The phosphorylation of CERK1, in contrast, was maintained for 60 min, after which time point the phosphorylation began to decline (Figure 24C). In fact, that is the time point when endocytosis of LYK5-mCitrine begins to decrease (Figure 16). These outcomes are consistent

with the observation that phosphorylation and subsequent endocytosis of LYK5 requires activated and phosphorylated CERK1.

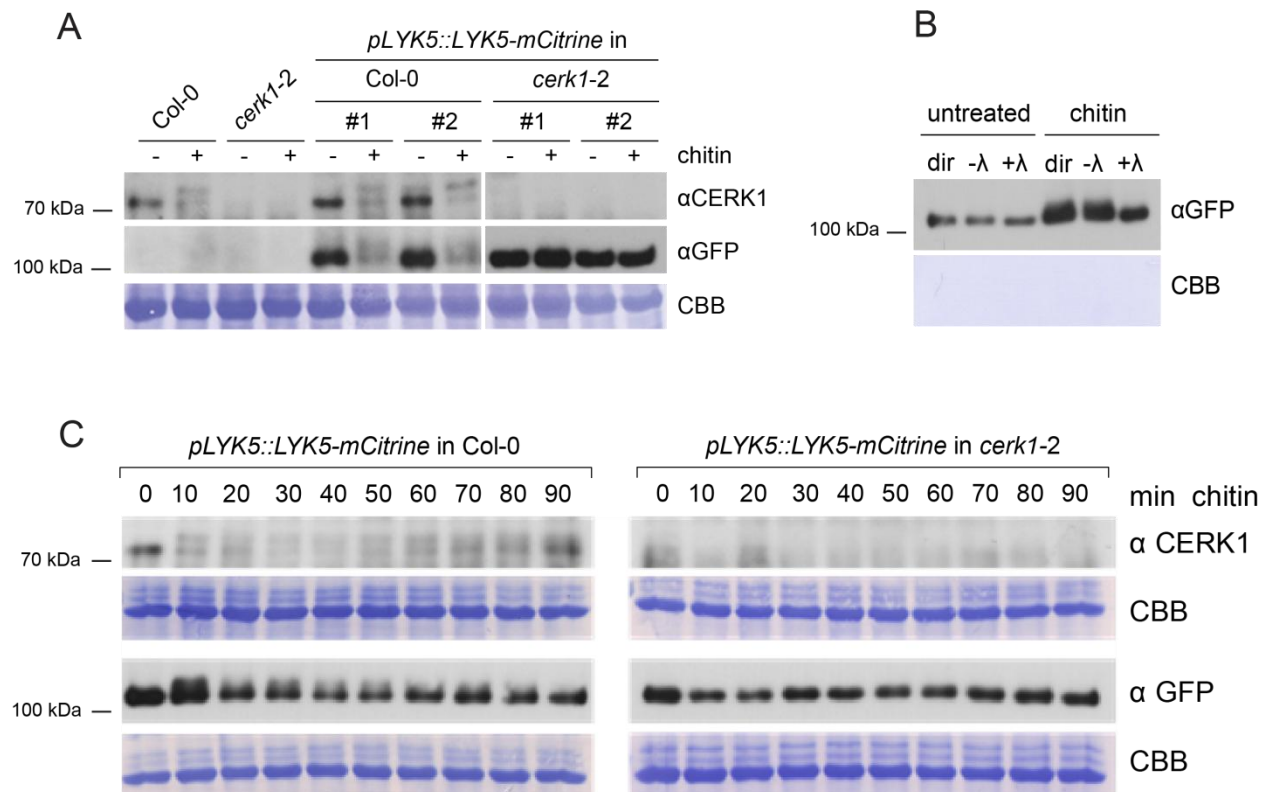


**Figure 24: Chitin-induced and CERK1-dependent phosphorylation of LYK5-mCitrine *in planta*.**

**(A)** CERK1 mediates chitin-induced LYK5-mCitrine phosphorylation *in planta*. Two independent transgenic lines of *Arabidopsis* Col-0 or *cerk1-2* plants stably expressing *pLYK5::LYK5-mCitrine* were infiltrated with water or 100 µg/ml chitin. Western blot analyses with αCERK1 and αGFP revealed a chitin-induced band shift of CERK1 and LYK5-mCitrine in Col-0 but not in *cerk1-2*. **(B)** The LYK5-mCitrine band shift is caused by phosphorylation. *pLYK5::LYK5-mCitrine* expressing Col-0 plants were infiltrated with water (untreated) or chitin (100 µg/ml). A λ-PPase assay was performed on LYK5-mCitrine pulled down using GBP-beads. LYK5-mCitrine was detected with αGFP in an Immunoblot experiment. dir: LYK5-mCitrine bound to GBP-beads directly mixed with loading dye. -λ and +λ: LYK5-mCitrine incubated in lambda phosphatase buffer for 30 min without (-) or with (+) the enzyme. **(C)** Kinetics of CERK1 and LYK5-mCitrine phosphorylation. *pLYK5::LYK5-mCitrine* expressing Col-0 and *cerk1-2* plants were infiltrated with 100 µg/ml chitin and incubated for the indicated time points. Representative αCERK1 and αGFP Western blots are shown. All experiments were repeated at least three times with similar results. All Western blots: CBB: Coomassie brilliant blue stained membrane.

### 3.4.2 LYK4-mCitrine may show chitin-induced and CERK1-dependent phosphorylation

LYK4-mCitrine was also tested for chitin-induced and CERK1-dependent phosphorylation, because cell biological analyses suggested it might undergo chitin-triggered endosome

formation similar to LYK5-mCitrine. In Western blot experiments with Col-0 plants stably expressing *pLYK4::LYK4-mCitrine*, only low amounts of the fusion protein were detected by the  $\alpha$ GFP antibody (Figure 25). This is consistent with the weak fluorescence signals seen in microscopic analyses and the low expression levels in microarray data (Figure 17 and Figure S4). Nevertheless, a slight mobility shift of LYK4-mCitrine was visible when comparing the chitin treated Col-0 samples to untreated ones, or to samples in the *cerk1-2* transgenic background. In comparison to LYK5-mCitrine or CERK1, the LYK4-mCitrine mobility shift was very small and thus more difficult to detect (Figure 25). Together, this suggests LYK4-mCitrine is probably post-translationally modified, most likely phosphorylated, after chitin treatment.

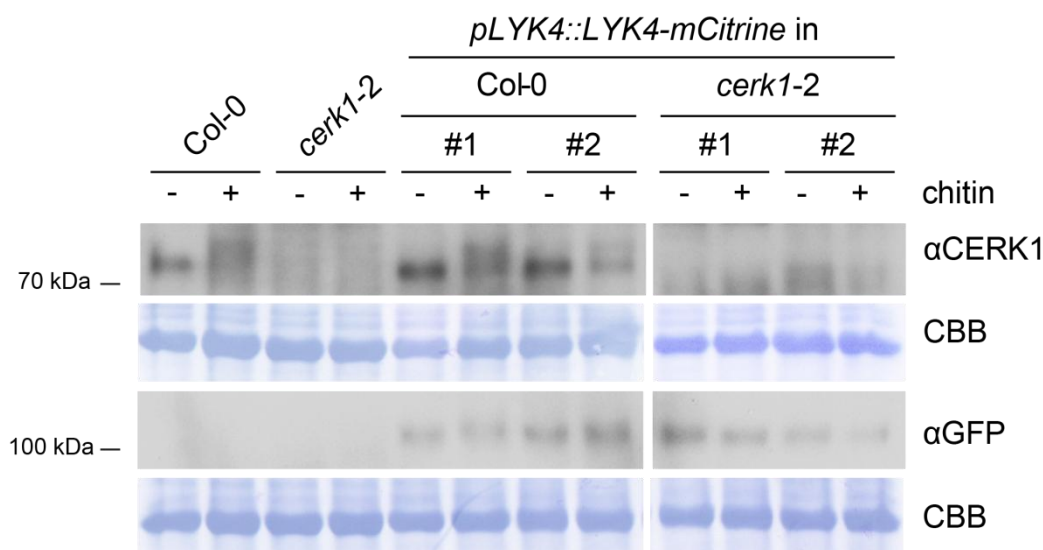


**Figure 25: LYK4-mCitrine may undergo chitin-induced and CERK1-dependent phosphorylation.**

*Arabidopsis* plants stably expressing *pLYK4::LYK4-mCitrine* show low amounts of the fusion protein and a weak chitin-induced, CERK1-dependent band shift in Western blot experiments. Two independent lines expressing *pLYK4::LYK4-mCitrine* in Col-0 or *cerk1-2* were infiltrated with water or chitin (100  $\mu$ g/ml). Western blots were performed with total protein extracts and developed with  $\alpha$ CERK1 or with  $\alpha$ GFP to detect LYK4-mCitrine. The experiment was repeated two times with similar results. CBB: Coomassie Brilliant Blue-stained membrane.

### 3.4.3 CERK1 directly phosphorylates LYK5 and LYK4 *in vitro*

CERK1 harbours an enzymatically active Ser/Thr kinase domain (Miya *et al.*, 2007; Wan *et al.*, 2008a; Petutschnig *et al.*, 2010). An alignment of the amino acid sequences of *Arabidopsis* LYKs shows that LYK5 and LYK4 lack conserved residues within the kinase subdomains and are therefore probably not catalytically active (Figure 3). Western blot experiments indicated that LYK5 and LYK4 are phosphorylated *in planta* after chitin treatment in a CERK1-dependent manner (compare Figure 24A and C). Since LYK5 and LYK4 probably do not function as



kinases themselves, the most likely explanation for this observation is that they are direct phosphorylation targets of CERK1. The question if LYK5 and LYK4 are kinase active and if they are phosphorylated by CERK1 was addressed in an *in vitro* phosphorylation assay using intracellular domains (IDs) of these proteins heterologously expressed in *E.coli* (Figure 26).

Constructs for wild type and catalytically inactive (loss of function, LOF) CERK1 intracellular domains were already available (Gimenez-Ibanez *et al.*, 2009a; Petutschnig *et al.*, 2010) in the pBAD vector that adds a C-terminal 6xhistidine tag to the proteins. LYK4 and LYK5 intracellular domains had previously been cloned into the pGEX4T1 vector (Erwig, 2012). The pGEX4T1 vector generates fusion proteins with an N-terminal glutathione-S-transferase (GST) tag. The CERK1, LYK5 and LYK4 ID-fusion proteins were produced in *E. coli* ArcticExpress® cells. After purification, the fusion-proteins were used for auto- and transphosphorylation assays using radioactively labeled  $\gamma$ -[<sup>32</sup>P]-ATP. GST alone was included as a negative control.

In figure 26 the upper panel shows the autoradiograph of the kinase assays. Reactions with single fusion proteins (lanes 1-5) were performed to investigate autophosphorylation activity and kinase reactions combining either wild type CERK1 (ID) or CERK1-LOF (ID) and a LYK (ID) were carried out to test transphosphorylation (lanes 6-11). The lower panel of figure 26 shows a Western blot of kinase reactions performed in parallel with non-radioactive ATP. The blot was probed with  $\alpha$ GST and  $\alpha$ 6xHis to visualize both types of fusion proteins. GST-LYK5 (ID) has a size of 67 kDa and GST-LYK4 (ID) one of 62 kDa. Both proteins are distinct from the GST tag control (26 kDa) and the 42 kDa large CERK1 (ID)-6xHis. Autophosphorylation activity could only be detected for CERK1 (ID), which has been reported previously (Miya *et al.*, 2007; Petutschnig *et al.*, 2010). As expected, CERK1-LOF (ID) showed no kinase activity (Petutschnig *et al.*, 2010). Reflecting enzymatic activity, wild type CERK1 (ID) was present as a double band in Western blots, where the upper band represents the phosphorylated form (Saka, 2010). In accordance, CERK1-LOF (ID) was only detected as a single, unphosphorylated band. LYK5 (ID) and LYK4 (ID) were enzymatically inactive (Figure 26), which was expected based on their amino acid sequence and is also in agreement with studies from other groups (Wan *et al.*, 2012; Cao *et al.*, 2014). Accordingly, no phosphorylated form of LYK5 (ID) and LYK4 (ID) could be detected in Western blots. However, the LYK4 (ID) protein preparation showed an additional weak band at 54 kDa, which likely represents a degradation product. Importantly, CERK1 (ID) transphosphorylated LYK5 (ID) and LYK4 (ID) (Figure 26), indicating that they are direct phosphorylation targets *in vitro*. In all three transphosphorylation reactions containing CERK1 (ID) another weak band was present that migrated at a similar molecular mass as free GST. However, GST could be excluded as the source of this signal, because it also occurred in

samples where no free GST was present i.e. CERK1 (ID)-6xHis alone and in combination with GST-LYK5 (ID) and GST-LYK4 (ID) (Figure 26). Negative control reactions containing CERK1-LOF (ID) in combination with GST-LYK5 (ID), GST-LYK4 (ID) or free GST showed no phosphorylation signals (Figure 26).

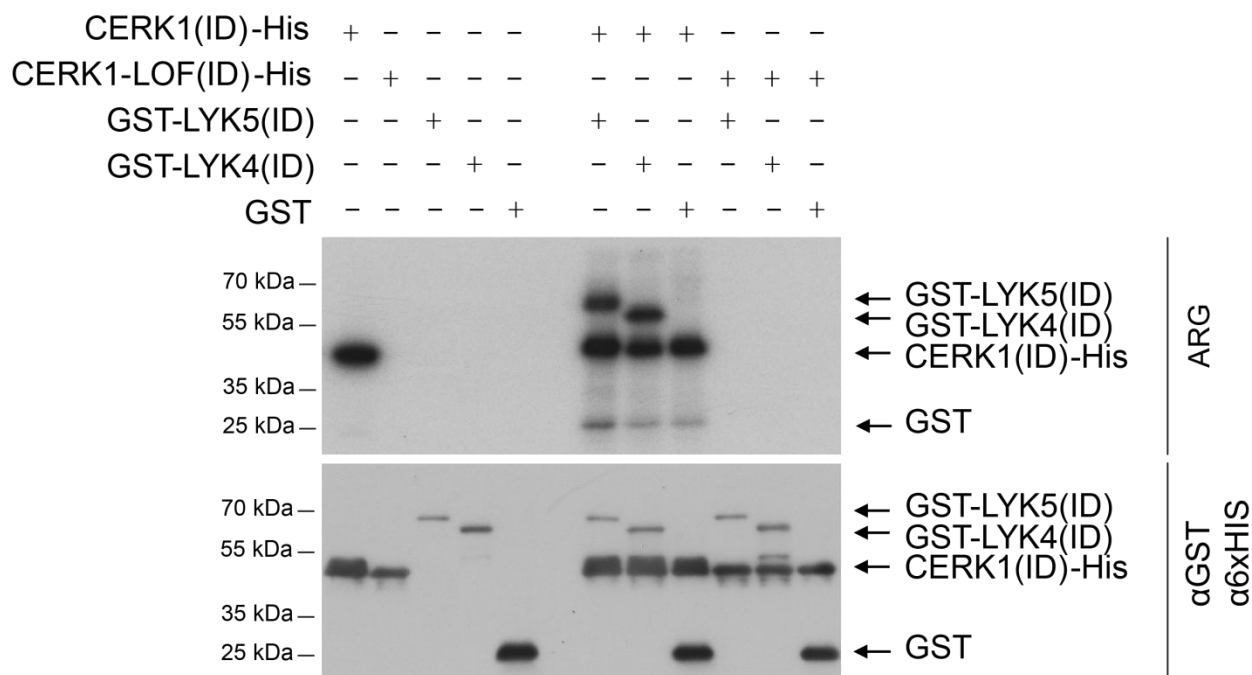


**Figure 26: The intracellular domain of CERK1 directly phosphorylates LYK5 and LYK4 endodomains *in vitro*.**

Auto- and transphosphorylation reactions with 6xHis- or GST-tagged intracellular domains (IDs) of CERK1, CERK1-LOF, LYK5 and LYK4. Free GST was included as a control. The fusion proteins were produced in *E.coli* and affinity purified for *in vitro* phosphorylation assay with radioactively labeled  $\gamma$ -[ $^{32}$ P]-ATP. The upper panel shows the autoradiograph (ARG) and indicates autophosphorylation activity for CERK1 but not for CERK1-LOF, LYK5 and LYK4, or GST. When incubated together with CERK1, LYK5 and LYK4 were phosphorylated. Kinase reactions containing CERK1-LOF (ID) showed no phosphorylation. The lower panel shows a Western blot probed with  $\alpha$ GST and  $\alpha$ 6xHis antibodies detecting the ID-fusion proteins as well as free GST and serves as loading control. The experiments were performed at least three times with similar results. A representative result is shown.

### 3.4.4 CERK1-dependent phosphorylation of LYK5-mCitrine is required for its endocytosis

So far, the results strongly suggest that CERK1 kinase activity is required for phosphorylation of LYK5 *in planta*. To investigate this hypothesis further and to study the role of CERK1 kinase activity in LYK5-mCitrine endocytosis, transgenic lines expressing *pCERK1::CERK1-WT* or *pCERK1::CERK1-LOF* in the *cerk1-2* knock-out background (Petutschnig *et al.*, 2010) were

transformed with *pGreenII-0229-JE-pLYK5::LYK5-mCitrine*. Transgenic expression of *pCERK1::CERK1-WT* was previously shown to complement the chitin-insensitive phenotype of *cerk1-2*. In contrast, *pCERK1::CERK1-LOF* expression in *cerk1-2* failed to mediate chitin signaling and CERK1-LOF was unable to autophosphorylate upon chitin stimulation (Petutschnig *et al.*, 2010). In three independent transgenic plant lines producing LYK5-mCitrine and CERK1, chitin treatment resulted in a pronounced mobility shift of both proteins in Western blots with total protein extracts (Figure 27A). Conversely, plant lines co-expressing *pCERK1::CERK1-LOF* and *pLYK5::LYK5-mCitrine* displayed no chitin-triggered band shift of either LYK5-mCitrine or CERK1-LOF (Figure 27A). These experiments clearly indicate that the kinase activity of CERK1 is required for chitin-induced phosphorylation of LYK5-mCitrine *in planta* and thus corroborate the idea that LYK5-mCitrine is phosphorylated by CERK1 upon chitin perception.

Subsequently, chitin-induced endocytosis of LYK5-mCitrine in the *pCERK1::CERK1-WT* and *pCERK1::CERK1-LOF* expressing lines was tested. LYK5-mCitrine-labeled endosomes were evident after chitin treatment in the *CERK1-WT* expressing lines, but not in the *CERK1-LOF* expressing background (Figure 27B). No endocytosis of LYK5-mCitrine could be observed in water treated samples of either line. Experiments confirmed the presence of chitin-induced LYK5-mCitrine-positive endosomes in *CERK1-WT* expressing plants. In contrast, in *CERK1-LOF* plants the number of LYK5-mCitrine containing vesicles was not significantly increased by chitin treatment over water treated control samples (Figure 27C). Surprisingly, chitin induced CERK1 and LYK5-mCitrine phosphorylation and LYK5-mCitrine endocytosis are enhanced in double transgenic lines compared to the controls but the cause of this effect is not known. Together, the data indicate that CERK1 kinase activity is a prerequisite for chitin-induced endocytosis of LYK5-mCitrine and suggest that phosphorylation by CERK1 triggers LYK5-mCitrine internalization.

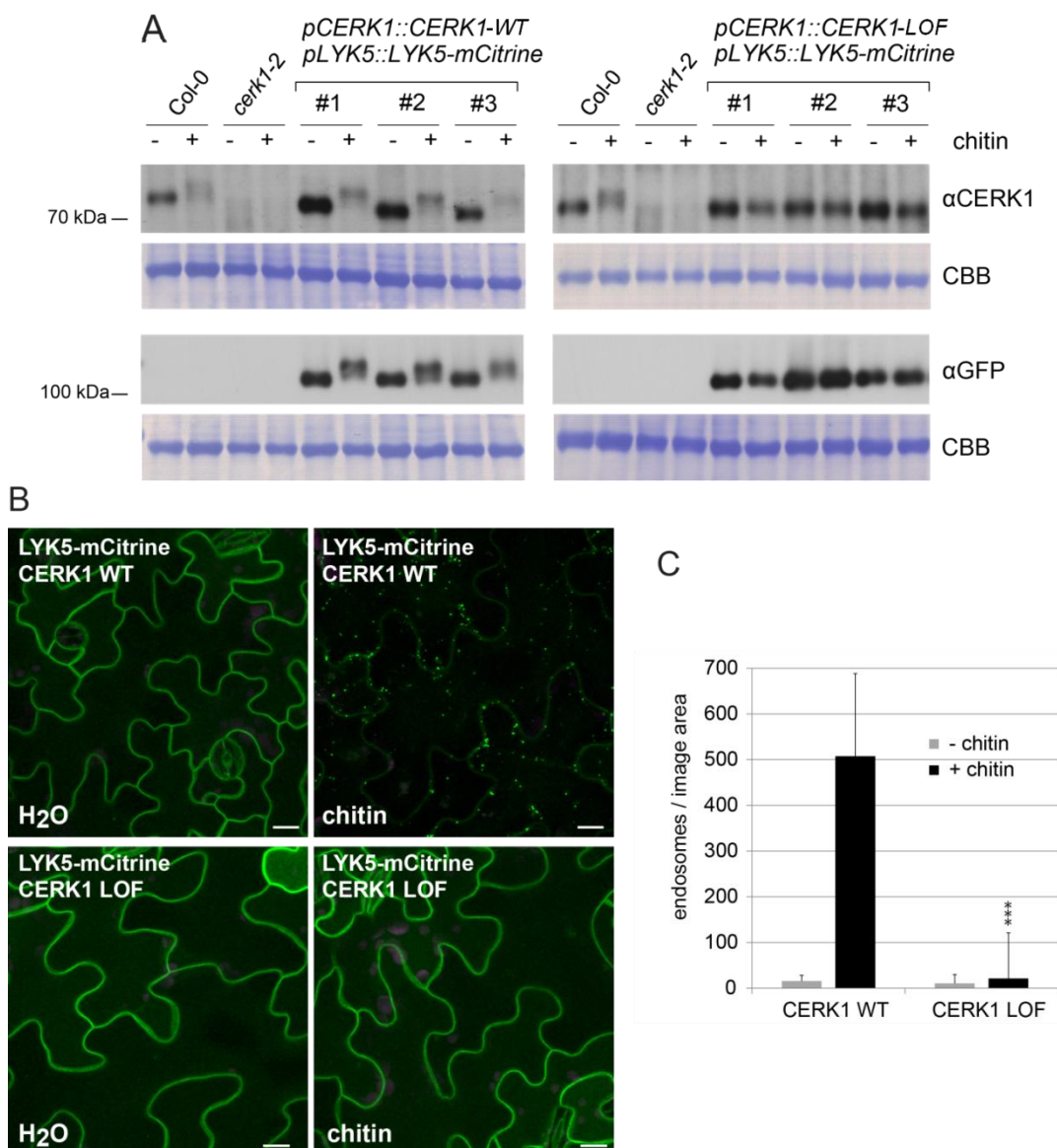


**Figure 27: CERK1 kinase activity is required for chitin-induced LYK5-mCitrine phosphorylation and endocytosis.**

*Arabidopsis* *cerk1-2* plants transgenically expressing *pCERK1::CERK1-WT* or *pCERK1::CERK1-LOF* were transformed to express *pLYK5::LYK5-mCitrine*. Three representative, independent plant lines in each background were infiltrated with water or 100 µg/ml chitin and analyzed by Western blotting and confocal microscopy. **(A)** Chitin-induced LYK5-mCitrine phosphorylation depends on CERK1 kinase activity. Western blots were probed with αCERK1 and αGFP. CERK1-WT and LYK5-mCitrine showed a prominent mobility shift after chitin treatment in the double transgenic lines, which was absent in the CERK1-LOF background. CBB: Coomassie brilliant blue stained membrane. **(B)** Transgenic expression of *CERK1-WT* restored chitin induced LYK5-mCitrine endocytosis in *cerk1-2* whereas *CERK1-LOF* did not. Representative images are shown (maximum projections of 12 focal planes recorded 1 µm apart). All experiments were repeated at least three times with similar results. Green, mCitrine; magenta, chloroplast autofluorescence; Scale bar = 10 µm. **(C)** Quantification of LYK5-mCitrine positive endosomes per image area for experiments described in (B). The data shown in the diagram are averages of 100 imaging sites. Error bars: + SD. \*\*\*  $p \leq 0.0001$ .

### 3.5 Analysis of LYM T-DNA insertion lines

#### 3.5.1 Isolation of *lym1-1*, *lym2-1* and *lym3-1* T-DNA insertion lines and *lym1-1 lym2-1 lym3-1* triple mutant

Like LYK5 and LYK4, LYM2 was identified in a chitin pull-down experiment together with CERK1 (Petutschnig *et al.*, 2010). LYM2 is the closest homolog to rice OsCEBiP. Since OsCEBiP is the main chitin receptor in rice and interacts with OsCERK1 in chitin signaling (Shimizu *et al.*, 2010; Shinya *et al.*, 2012), LYM2 is a likely candidate for an interaction partner of CERK1. However, *Arabidopsis* knock-out lines of LYM2 were reported to show normal general chitin signaling (Shinya *et al.*, 2012; Wan *et al.*, 2012; Faulkner *et al.*, 2013). Instead they displayed defects in chitin-induced regulation of PD connectivity (Faulkner *et al.*, 2013). A recent report identified two other OsCEBiP-like proteins in *Arabidopsis thaliana*, LYM1 and LYM3, acting together with CERK1 in perception of the bacterial MAMP PGN (Willmann *et al.*, 2011). *lym1* and *lym3* mutants showed reduced PGN responses, (Willmann *et al.*, 2011; Shinya *et al.*, 2012) but were not altered in chitin-specific downstream signaling (Shinya *et al.*, 2012). Triple mutants with T-DNA insertions in *LYM1*, *LYM2* and *LYM3* also showed normal chitin-induced ROS generation and defense gene activation (Shinya *et al.*, 2012; Wan *et al.*, 2012). To complement previously reported results and potentially investigate the role of LYM2 in chitin signaling further, a *lym2* T-DNA line was analyzed.

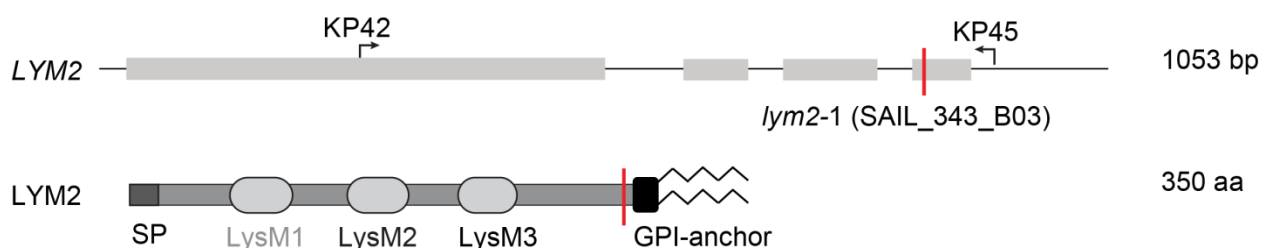


**Figure 28: The *lym2-1* T-DNA insertion line used in this study.**

Schematic structures of the *LYM2* gene and LYM2 protein. The *lym2-1* T-DNA insertion is highlighted in red. Exons are depicted as grey boxes. Predicted protein features: signal peptide (SP), lysin motifs (LysMs). If detected by MyHits (<http://myhits.isb-sib.ch>, Pagni *et al.*, 2004), LysMs are labeled black. The LysM-domain labeled gray is predicted based on sequence similarity with other LysM-Proteins; Presence of a GPI-anchor site was predicted by ([http://mendel.imp.ac.at/gpi/cgi-bin/gpi\\_pred.cgi](http://mendel.imp.ac.at/gpi/cgi-bin/gpi_pred.cgi)). Primers shown as black arrows were used for genotyping.

The *lym2-1* mutant line used in this study (SAIL\_343\_B03) (Shinya *et al.*, 2012; Faulkner *et al.*, 2013; Narusaka *et al.*, 2013) contains a T-DNA insertion in the fourth exon (Figure 28), upstream of a sequence encoding a predicted GPI anchor attachment site. As controls, the

T-DNA insertion lines *lym1-1* (GABI\_419G07) and *lym3-1* (SALK\_132566) (Willmann *et al.*, 2011; Shinya *et al.*, 2012) were obtained. All three *lym* mutants are in the Col-0 background. The position of the T-DNAs were determined by PCR and confirmed by sequencing (data not shown). To address the possibility of functional redundancy, a *lym1-1 lym2-1 lym3-1* triple mutant line (Shinya *et al.*, 2012) kindly provided by Prof. Naoto Shibuya was included in the analysis.

### 3.5.2 *LYM* single and triple mutants are not impaired in CERK1 chitin binding and phosphorylation

Chitin binding of CERK1 and its chitin-induced phosphorylation has previously been investigated for *lym2-1* (Faulkner *et al.*, 2013) but not for *lym1-1*, *lym3-1* or *lym* triple mutants. To address this open question, leaves of *lym* single mutants as well as the *lym* triple mutant were infiltrated with water or chitin. Western blots were prepared with total protein extracts and probed with the CERK1 antibody. The loss of none of the three individual *LYM* proteins affected CERK1 protein abundance and CERK1 chitin binding activity. The same was true for the *lym* triple mutant (Figure 29). Also, CERK1 displayed a mobility shift after chitin treatment in all of the *lym* mutant lines, indicating that chitin-induced phosphorylation of CERK1 is not impaired in these mutants (Figure 29).

*LYM2* has chitin binding affinity (Petutschnig *et al.*, 2010; Shinya *et al.*, 2012) but it apparently does not contribute to chitin binding of CERK1 and receptor phosphorylation. Similarly, *LYM1* and *LYM3* play no role in these processes, ruling out functional redundancy. This is in agreement with previous results on other chitin-triggered signaling and defense responses (Faulkner *et al.*, 2013; Narusaka *et al.*, 2013).

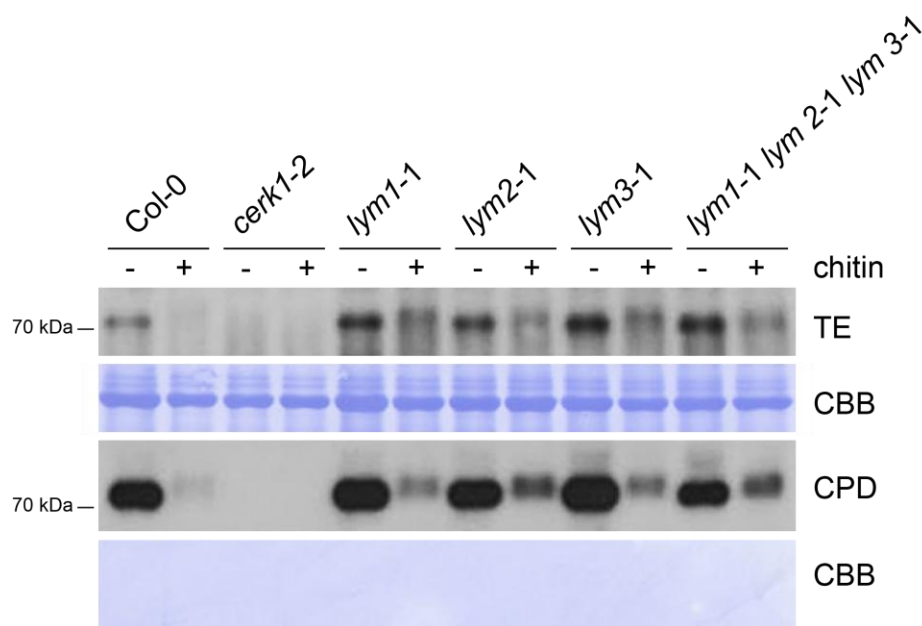


**Figure 29: The loss of LYM proteins does not affect chitin-induced CERK1 phosphorylation and chitin binding.**

Leaves of the indicated genotypes were vacuum infiltrated either with water or chitin (100  $\mu\text{g/ml}$ ). Col-0 and *cerk1-2* were included as controls. Samples were incubated for 10 min. Total protein extracts (TE) were prepared and pull-downs with chitin magnetic beads (CPD) were performed. Western blots of TE and CPD samples were developed with  $\alpha\text{CERK1}$ . The chitin-induced CERK1 mobility shift was present in all tested mutants. CERK1 was able to bind to chitin magnetic beads, even in its phosphorylated state, in all tested *lym* mutants. A representative blot is shown for the lines tested. The experiment was repeated two times yielding similar results. CBB: Coomassie brilliant blue stained membrane.

### 3.6 Analysis of LYM2 subcellular localization

#### 3.6.1 Chitin induces CERK1-independent mCitrine-LYM2 re-localization at the PM

LYM2 was recently found to specifically modulate PD connectivity in a chitin-dependent manner (Faulkner *et al.*, 2013). To investigate the subcellular localization and chitin-induced dynamics of LYM2, an endogenous promoter driven *mCitrine-LYM2* construct was generated (*pGreenII-0229-JE-pLYM2::mCitrine-LYM2*). The resulting fusion protein contains the fluorescent tag between the predicted signal peptide and the first LysM-domain. This construct was transformed into Col-0 and *cerk1-2* plants. The resulting transformants were screened by confocal microscopy and lines with good signals were chosen for further work. These initial microscopic studies revealed a localization of mCitrine-LYM2 at the cell periphery with spot-like areas of increased fluorescence intensity. To be able to compare the mCitrine-LYM2 signal to a PM marker, doubly transgenic lines were generated expressing both *pLYM2::mCitrine-LYM2*

and *p35S::LTI6b-mKate2* in Col-0. To do so, *Arabidopsis* Col-0 plants stably expressing *LTI6b-mKate2* were transformed with the native promoter driven *mCitrine-LYM2* construct. The resulting transformants were screened as mentioned above and lines with both signals were used for further studies.

Leaf pieces of plants expressing *pLYM2::mCitrine-LYM2* and *p35S::LTI6b-mKate2* were vacuum infiltrated with water or chitin and analyzed by confocal microscopy 60 min post infiltration. As can be seen in figure 30A, fluorescent signals of both mCitrine-LYM2 and LTI6b-mKate2 overlapped at the cell periphery. This suggests PM localization of mCitrine-LYM2, which would be expected for a GPI-anchored receptor-like protein. Consistent with initial findings, mCitrine-LYM2 was present in potential PM-subdomains that showed higher fluorescence in comparison to the surrounding PM. This accumulation was already visible in water-infiltrated leaves, but much more pronounced when the respective leaves were infiltrated with chitin solution (Figure 30A). Importantly, no areas of increased fluorescence intensity could be observed for LTI6b-mKate2 (Figure 30A). This indicates that the accumulations are a LYM2-specific phenomenon.

To test if the chitin-induced accumulation of mCitrine-LYM2 in subdomains requires CERK1, *pLYM2::mCitrine-LYM2* expressing Col-0 and *cerk1-2* lines were compared. In both backgrounds mCitrine-LYM2 was found at the cell periphery with some areas of increased fluorescence. Signal intensity at these subdomains increased upon chitin treatment in the *cerk1-2* background with no apparent differences to the wild type (Figure 30B). This demonstrates that the accumulation at these sites is CERK1-independent and supports the idea that LYM2 acts in a non-canonical chitin response.



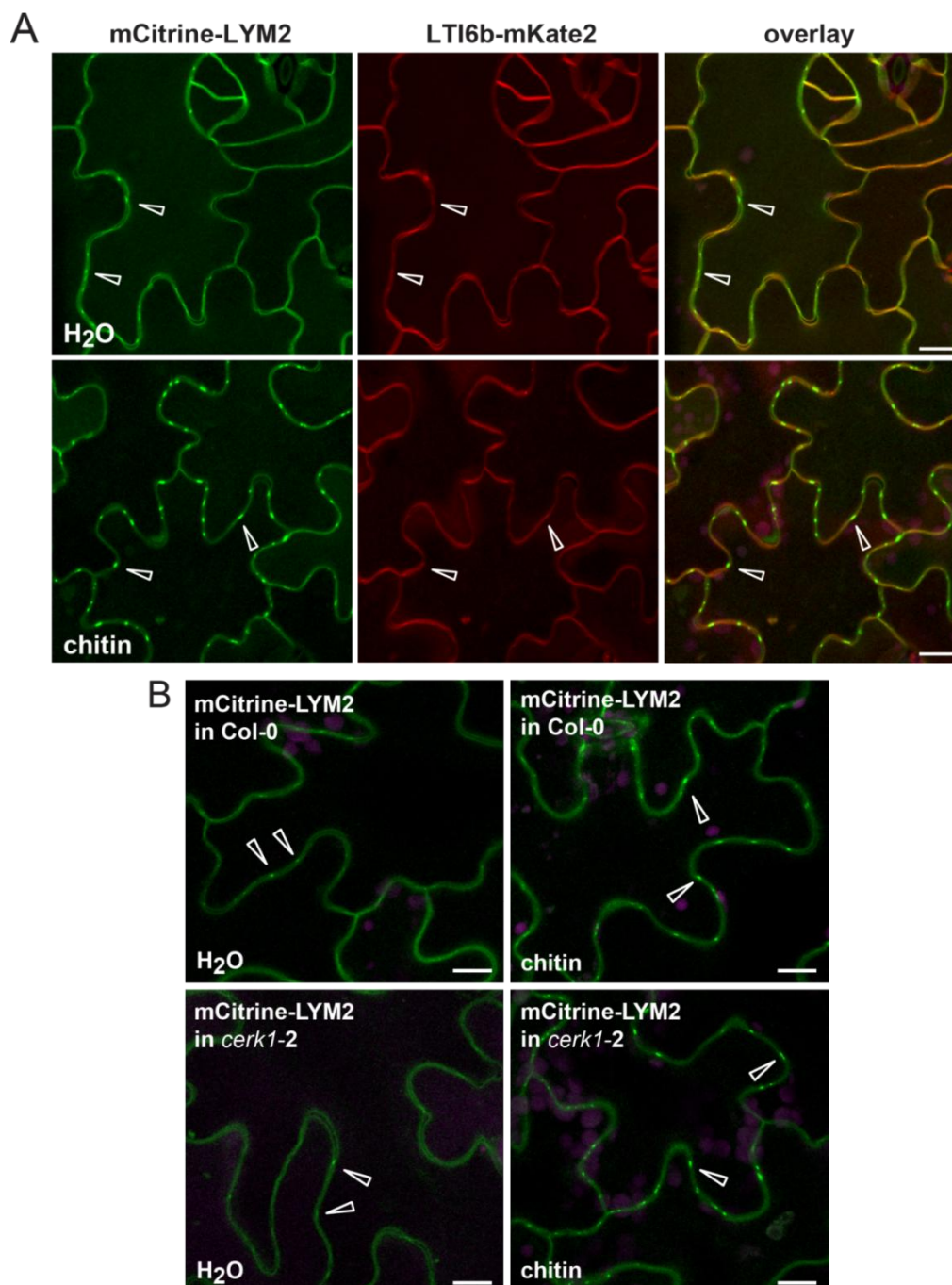


**Figure 30: Chitin-induced re-localization of mCitrine-LYM2 at the PM**

*Arabidopsis* leaves were treated with water or chitin solution (100 µg/ml) for 60 min to investigate the subcellular localization of mCitrine-LYM2. **(A)** Co-expression with the PM-marker protein LTI6b-mKate2 identified mCitrine-LYM2 at the PM. Vacuum infiltration with chitin led to re-localization of mCitrine-LYM2 to PM subdomains. **(B)** Chitin-triggered mCitrine-LYM2 accumulation in PM subdomains was observed in Col-0 and *cerk1-2* background. CLSM images are maximum projections of 10 focal planes taken 1 µm apart. Similar results were obtained in all experiments with three independent transgenic lines. Arrow heads point to accumulating mCitrine-LYM2 signal. CLSM images: Green, mCitrine; Red, mKate2; magenta: chloroplast autofluorescence; Scale bar = 10 µm.

### 3.6.2 Chitin triggers mCitrine-LYM2 accumulation at PD

LYM2 has previously been described to regulate PD-flux (Faulkner *et al.*, 2013) and the sites of mCitrine-LYM2 accumulation at the cell periphery resemble PD in size and shape. To test whether the subdomains with increased mCitrine-LYM2 signal are indeed PD, aniline blue staining was performed in Col-0 and *cerk1-2* plants stably expressing *pLYM2::mCitrine-LYM2* (Figure 31). Plants were treated with chitin and then stained with aniline blue solution (Stein *et al.*, 2006). This solution specifically stains callose, which plants deposit in the PD-neck regions to regulate the plasmodesmal flux (Guseman *et al.*, 2010; Zavaliev *et al.*, 2011). In both backgrounds the accumulating mCitrine-LYM2 signal mostly overlapped with aniline blue stained callose (Figure 31). Hence, mCitrine-LYM2 specifically accumulates at the sites of PD as a response to chitin application.

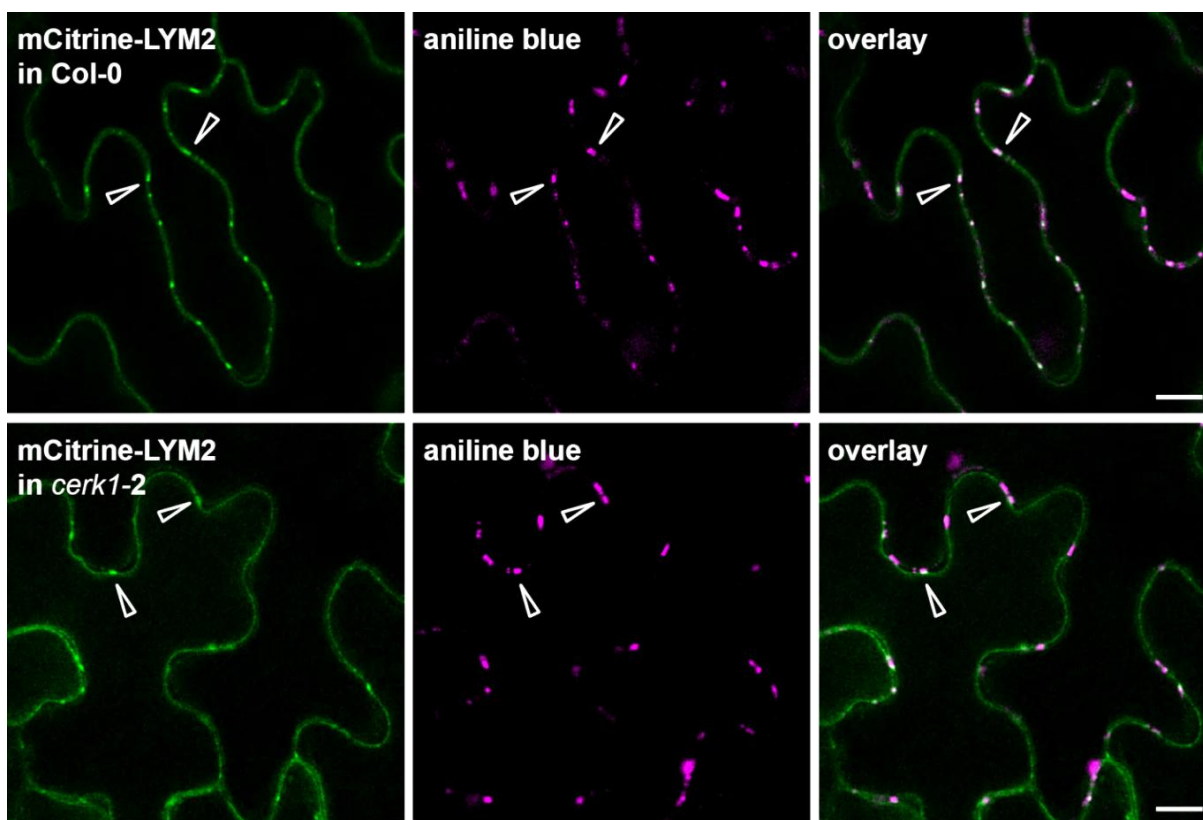


**Figure 31: PM and PD localization of mCitrine-LYM2 after chitin treatment.**

Leaves of Col-0 and *cerk1-2* plants transgenically expressing *pLYM2::mCitrine-LYM2* were infiltrated with chitin solution (100  $\mu\text{g/ml}$ ) and subsequently incubated for 60 min. Then they were incubated in 0.01% (w/v) aniline blue solution for 15 min. Co-staining with aniline blue revealed that mCitrine-LYM2 specifically accumulates at PD after chitin treatment. Images are single CLSM focus planes. Experiments were repeated with two independent transgenic lines for each background. Arrow heads point to overlapping mCitrine and aniline blue signal. CLSM images: Green, mCitrine; magenta, aniline blue stained callose; Scale bar = 10  $\mu\text{m}$ .

To test if LYM2 undergoes chitin-induced protein modifications or changes in protein abundance, plants expressing either *pLYK5::LYK5-mCitrine* or *pLYM2::mCitrine-LYM2* were treated with either water or chitin. Col-0 and *cerk1-2* were included as controls. A Western blot was performed with total protein extracts and probed with  $\alpha$ CERK1 and  $\alpha$ GFP (Figure 32). Compared to LYK5-mCitrine and CERK1 that both showed a mobility shift after chitin treatment no alterations in the apparent molecular mass of mCitrine-LYM2 were observed in this Blot (Figure 32). The abundance of mCitrine-LYM2 appeared slightly reduced after chitin treatment, which has been observed for other chitin binding LysM-containing proteins such as CERK1.

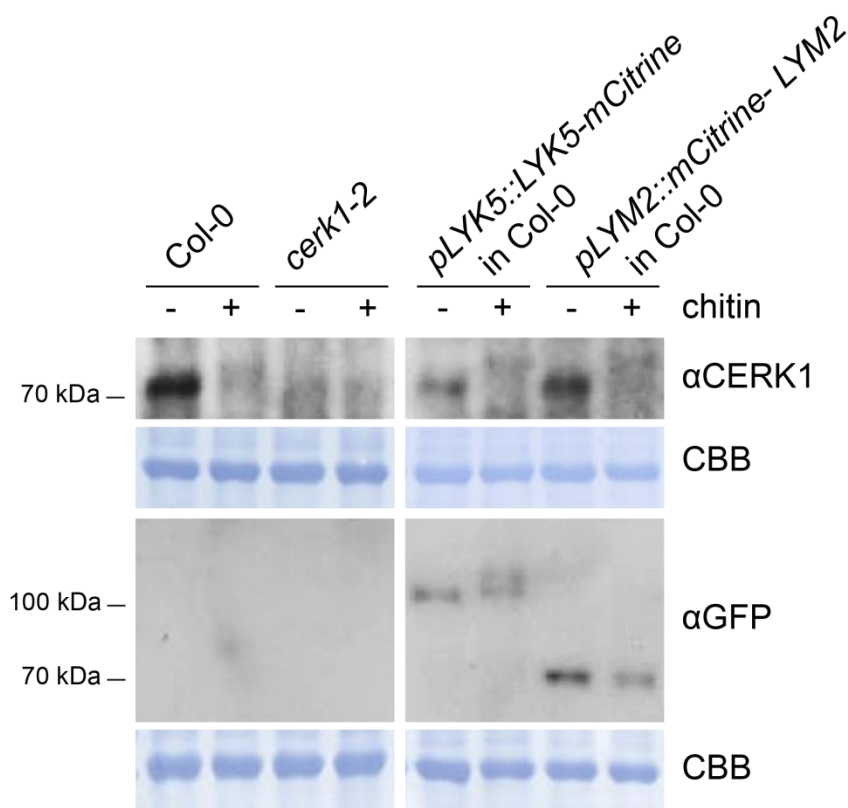


**Figure 32: mCitrine-LYM2 shows no chitin-induced changes in mobility in SDS-PAGE.**

*pLYM2::mCitrine-LYM2* was stably expressed in Col-0 and leaves were infiltrated with water or chitin (100  $\mu$ g/ml). Total protein extracts were analyzed by Western blotting with  $\alpha$ CERK1 and  $\alpha$ GFP antibodies. No mobility changes of the mCitrine-LYM2 protein after chitin infiltration could be detected. As controls, the chitin-induced CERK1 (upper panel) and the LYK5-mCitrine band shift (lower panel) are shown. The experiment was done with four independent *pLYM2::mCitrine-LYM2* expressing plant lines. A representative blot is shown. CBB: Coomassie brilliant blue stained membrane.

In summary, LYM proteins are likely not involved in the general CERK1-mediated chitin response. LYM2-mCitrine, localizes at the PM and shows a distinct accumulation at PD, which is strongly enhanced by chitin treatment. LYM2 re-localization to PD is CERK1-independent. In contrast to CERK1 and LYK5, LYM2 does not undergo chitin-induced phosphorylation or other modifications that would result in an altered migration pattern in Western blot experiments.


### 3.7 Generation and identification of *lyk5-2 lyk4-2 lym2-1* triple mutant plants

The *lym2-1* mutant is impaired in chitin-dependent regulation of PD connectivity and resistance to fungal pathogens (Faulkner *et al.*, 2013; Narusaka *et al.*, 2013). However, it shows normal canonical, CERK1-dependent chitin responses (section 3.5.2) (Faulkner *et al.*, 2013), which is in stark contrast to mutants of its rice homolog, OsCEBiP (Kaku *et al.*, 2006; Shimizu *et al.*, 2010; Hayafune *et al.*, 2014; Kouzai *et al.*, 2014a). Furthermore, experiments in this study showed that the single knockout line *lyk5-2* and the *lyk5-2 lyk4-2* double mutant only exhibit a very moderate reduction in chitin related defense responses. One explanation for this would be functional redundancy between LYM2 and LYKs in canonical chitin signaling. For example, LYM2 could interact with a receptor-like cytoplasmic kinase such as CLR1 (Ziegler, 2015) to take on the function of a LYK. To investigate this hypothesis, *lyk5-2 lyk4-2* plants were crossed with *lym2-1* (Hacke, 2013). Triply heterozygous F1 plants were propagated and the *lyk5-2 lyk4-2 lym2-1* F2 generation was tested regarding homozygosity for all three T-DNA insertions. In 230 tested plants no triply homozygous plants were found. This was not unexpected, because all three genes are on the lower arm of chromosome two (Figure S10). However, two plants were identified to be heterozygous for *lyk5-2* and *lyk4-2* and homozygous for the *lym2-1* mutation (further referred to as *lyk5-2 lyk4-2 lym2-1* (het/het/hom)). For the offspring of these plants, the probability of triply homozygous *lyk5-2 lyk4-2 lym2-1* individuals is 1/16, but none out of 275 genotyped F3 plants were triply homozygous, whereas 119 were *lyk5-2 lyk4-2 lym2-1* (het/het/hom). Also the *lyk5-2 lyk4-2 lym2-1* (het/het/hom) plants appeared smaller than the other genotypes. This raised the idea that harboring all three mutations may have a negative impact on plant fitness and triple homozygosity might be lethal. To investigate this, F3 *lyk5-2 lyk4-2 lym2-1* (het/het/hom) seeds were sown *in vitro* on solid ½ MS growth medium to possibly identify dead seeds or seedling lethality or observe differences in germination. To synchronize germination, seeds were vernalized for 48 h at 4°C. Two weeks after sowing, the germination status was determined and seeds were classified into four groups according to Boyes *et al.* (2001). Normally germinated seeds were represented by seedlings with fully opened cotyledons and/or 2 rosette leaves larger than 1 mm in length. Late germinated seeds

showed an emerging radicle or hypocotyl and cotyledons. Seeds were classified as abnormally germinated when neither a functional radicle was formed nor the seed was imbibed. Non-germinated seeds were imbibed but did not show an emerged radicle or hypocotyl and cotyledons. Table 14 summarizes the distribution of the mentioned classes in F3 seeds of the *lyk5-2 lyk4-2 lym2* (het/het/hom) line and the corresponding single and double mutant lines as well as Col-0 and *cerk1-2*. It is obvious that the number of normally germinated seeds was decreased (62.7%) while the number of late (16%) and non-germinated seeds (16.9%) was increased in the *lyk5-2 lyk4-2 lym2-1* (het/het/hom) line compared to the control lines. Half of the seeds that were not germinated *in vitro* within two weeks after sowing, germinated later after transfer to soil. Thus in the end, there were 52 seeds in total (24.5%) that showed delayed germination. Genotyping of all germinated plants demonstrated that all normally germinated seedlings were wild type for *lyk5-2* and *lyk4-2* and homozygous for the *lym2-1* mutation. All later germinated seedlings were found to be the parental genotype, *lyk5-2 lyk4-2 lym2-1* (het/het/hom), and no plants were found to be homozygous for all three T-DNA insertions.

**Table 14: Delayed germination of *lyk5-2 lyk4-2 lym2-1* (het/het/hom) seeds.**

The germination status of seeds of the indicated genotypes was classified according to Boyes *et al.* (2001) two weeks after sowing on solid ½ MS medium. Seeds of *lyk5-2 lyk4-2 lym2-1* (het/het/hom) mutants had increased numbers of seeds with delayed or no germination.

genotype					total
	germinated (normal)	germinated (late)	germinated (abnormal)	not germinated	
Col-0	166 (97.2%)	3 (2%)	1 (0.1%)	2 (0.7%)	172
<i>cerk1-2</i>	157 (97.1%)	3 (2%)	2 (0.1%)	1 (0.8%)	163
<i>lyk5-2</i>	180 (97.3%)	4 (2%)	1 (0.1%)	2 (0.6%)	187
<i>lyk4-2</i>	185 (98.7%)	2 (1%)	1 (0.1%)	2 (0.2%)	190
<i>lym2-1</i>	183 (91.7%)	10 (5%)	1 (0.3%)	7 (3%)	201
<i>lyk5-2 lyk4-2</i>	186 (95.3%)	6 (3%)	1 (0.1%)	5 (1.6%)	198
<i>lyk5-2 lyk4-2 lym2-1</i> F3 het /het/ hom	133 (62.7%)	34 (16%)	9 (4.2%)	36 (16.9%)	212

The fact that no triply homozygous plants were obtained supports the idea that harboring all three mutations homozygously might be lethal for the plant. To address this question further, plants were allowed to develop siliques and set seed. Four *lyk5-2 lyk4-2 lym2-1* (het/het/hom) F3 plants were chosen for analysis of seed production and were compared to the respective control plants. To visualize seeds, siliques were cleared with 200 mM NaOH and 1% SDS (Figure 33). Figure 33 clearly shows that the *lyk5-2 lyk4-2 lym2-1* (het/het/hom) plants had much smaller siliques containing fewer seeds, with many empty positions. Empty seed positions were randomly distributed within the silique.



**Figure 33: *lyk5-2 lyk4-2 lym2-1* (het/het/hom) mutants develop siliques with fewer seeds.**

Photographs of representative cleared siliques of the indicated genotypes. Mature siliques were harvested from each plant. Care was taken to collect siliques from comparable positions along the main inflorescence. They were cleared overnight in 200 mM NaOH and 1% SDS solution. Siliques from four independent *lyk5-2 lyk4-2 lym2-1* (het/het/hom) mutant plants (F3) were smaller and contained fewer mature seeds compared to WT and LysM-protein single and double mutants. Scale bar: 0.5 cm

To quantify the defects in seed production, at least 21 siliques per genotype were harvested and analyzed regarding the total number of seeds, aborted seeds and unfertilized ovules. Care was taken to collect the siliques from comparable positions along the main inflorescence. The results are summarized in Table 15 and depicted in Figure 34.

**Table 15: Fertility analyses of *lyk5-2 lyk4-2 lym2-1* (het/het/hom) mutants.** Total number of siliques, mature and aborted seeds, unfertilized ovules counted for the indicated genotypes.

genotype	siliques (N)	seeds (N)	aborted seeds (N)	unfertilized ovules (N)	seeds/silique	aborted seeds/silique	unfertilized ovules/silique
Col-0	30	1440	5	11	48.0	0.17	0.37
<i>cerk1-2</i>	25	1193	1	6	47.7	0.04	0.24
<i>lyk5-2</i>	27	1260	4	8	46.7	0.15	0.30
<i>lyk4-2</i>	30	1329	3	3	44.3	0.10	0.10
<i>lym2-1</i>	26	1103	5	33	42.4	0.19	1.27
<i>lyk5-2 lyk4-2</i>	25	972	3	16	38.9	0.12	0.64
<i>lyk5-2 lyk4-2 lym2-1</i> #1	27	497	27	262	18.4	1.00	9.70
<i>lyk5-2 lyk4-2 lym2-1</i> #2	21	71	9	186	3.4	0.43	8.86
<i>lyk5-2 lyk4-2 lym2-1</i> #3	28	767	29	301	27.4	1.04	10.75
<i>lyk5-2 lyk4-2 lym2-1</i> #4	24	312	23	318	13.0	0.96	13.25

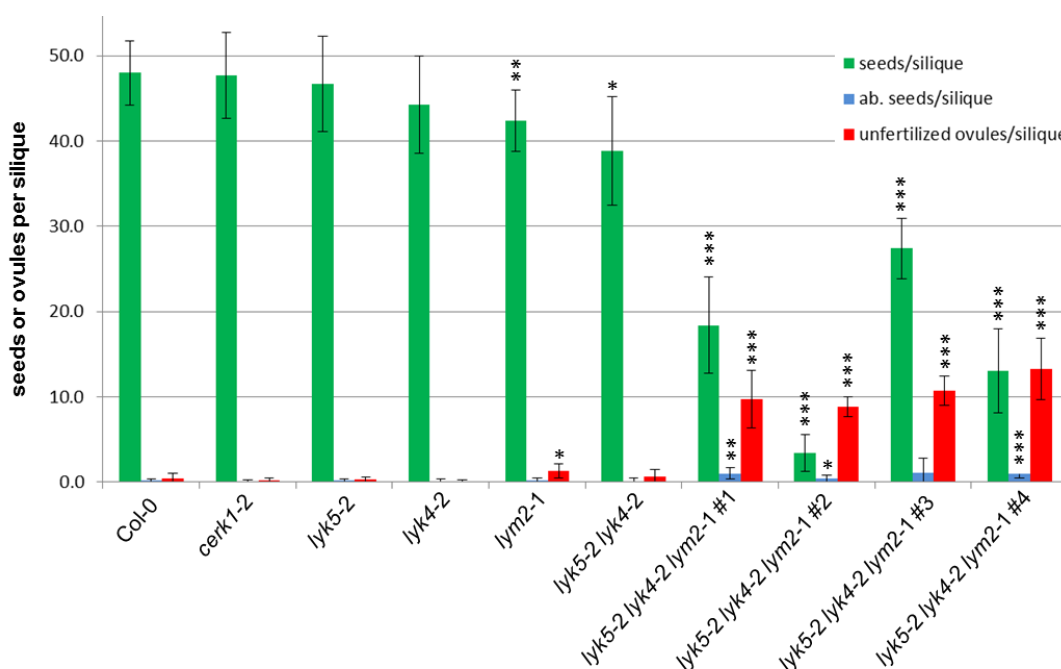


**Figure 34: *lyk5-2 lyk4-2 lym2-1* (het/het/hom) mutants show defects in fertility.**

Bar diagram generated out of the data presented in table 15. Mature seeds (green), aborted seeds (blue) and unfertilized ovules (red) per silique are shown. Siliques from four *lyk5-2 lyk4-2 lym2-1* (het/het/hom) F3 mutant plants contained significantly fewer matured seeds, but increased numbers of aborted seeds and unfertilized ovules compared to Col-0. The counted seeds or ovules in the mutant plants were compared to Col-0. \* =  $p < 0.05$ , \*\* =  $p < 0.01$ , \*\*\* =  $p < 0.001$

In siliques with normal seed development (all controls), typically about 40 seeds were counted and the number of aborted seeds or unfertilized ovules was less than 1 per silique (Table 15 and Figure 34). All four tested *lyk5-2 lyk4-2 lym2-1* (het/het/hom) plants showed a significant reduction in the number of mature seeds. Also, *lyk5-2 lyk4-2 lym2-1* (het/het/hom) plants had 10 times more aborted seeds per silique and a 30-fold increase in unfertilized ovules per silique compared to control lines. Interestingly, already the *lyk5-2 lyk4-2* double and the *lym2-1* single mutant showed a slight reduction in the number of seeds and an increase in unfertilized ovules per silique. These data indicate that *lyk5-2 lyk4-2 lym2* (het/het/hom) plants are defective in fertility. T-DNA insertions in all three genes may prevent correct chromosome recombination or the loss of all three chitin binding proteins might result in wrong or no fertilization of the ovule.



## 4 Discussion

In order to recognize pathogens and to mount active defense responses plants have evolved complex mechanisms for defense-related signaling. PRRs reside at the PM and monitor the environment for MAMPs released by potential pathogens. MAMP recognition is a crucial step for the initiation of further downstream responses (Jones and Dangl, 2006). It has become evident that plant PRRs act together with (co-) receptors to form complexes for efficient ligand binding and downstream signal transduction (Monaghan and Zipfel, 2012). Responses to different MAMPs are overlapping considerably, indicating that different MAMPs activate a conserved set of defense responses (Jones and Dangl, 2006). Once activated, signaling from PRRs has to be inactivated. One possibility to attenuate signaling is the removal of PRRs from the PM via endocytosis (Irani and Russinova, 2009; Sorkin and von Zastrow, 2009; Fan *et al.*, 2015). This study focuses on the function of the chitin binding LysM-RLKs CERK1, LYK5, LYK4, and the LysM-RLP LYM2. Their roles in activation of chitin-triggered defense responses were studied, as well as chitin-dependent transphosphorylation events between these components. A particular emphasis was placed on their subcellular localization and behavior in response to chitin.

### 4.1 The role of LYK5 and LYK4 in chitin perception and signaling

Plants perceive the fungal polysaccharide chitin through receptor complexes containing lysin motif receptor-like kinases (LysM-RLKs). CERK1 is an *Arabidopsis* LysM-RLK essential for chitin perception (Miya *et al.*, 2007; Wan *et al.*, 2008a), and the related LysM-RLKs LYK5 (Cao *et al.*, 2014) and LYK4 (Wan *et al.*, 2012) contribute to full chitin signaling. *cerk1* mutants are chitin insensitive and more susceptible to fungal and bacterial pathogens (Wan *et al.*, 2008a; Gimenez-Ibanez *et al.*, 2009a). Reports on the roles of LYK5 and LYK4 in chitin perception are not consistent throughout the literature (Miya *et al.*, 2007; Wan *et al.*, 2008a; Wan *et al.*, 2012; Cao *et al.*, 2014). Consequently, one goal of this work was to generate consistent and unequivocal results that allow a clear definition of the function of these proteins in chitin signaling. To do so, *lyk5-2* and *lyk4-2* T-DNA insertion lines were assessed for alterations in typical chitin-induced defense responses (see section 3.2). The earliest measurable response in chitin signaling is the phosphorylation of the receptor CERK1 (Petutschnig *et al.*, 2010). Thus, monitoring chitin-triggered CERK1 phosphorylation is a suitable method to assess the involvement of a protein in the earliest steps of chitin signal transduction. Assays that determine the phosphorylation status and thus the activity of MAPKs are well-established for investigation of further downstream chitin signaling events (Miya *et al.*, 2007; Petutschnig *et al.*, 2010; Cao *et*

*al.*, 2014; Petutschnig *et al.*, 2014). Analysis of CERK1 phosphorylation and activation of MAPKs provided evidence for LYK4 and LYK5 function in chitin signaling in a recent study (Cao *et al.*, 2014). In that report, chitin-triggered CERK1 phosphorylation and MAPK activation were drastically reduced in the *lyk5-2* single mutant (Cao *et al.*, 2014). Moreover, chitin-dependent MAPK phosphorylation and ROS production were totally abolished in the *lyk5-2 lyk4-1* double mutant (Cao *et al.*, 2014). In the work presented here, chitin-induced phosphorylation of CERK1 was visibly reduced in *lyk5-2*, but the effect was much less drastic than reported by Cao *et al.* (2014). In *lyk5-2 lyk4-2* double mutants, CERK1 phosphorylation was reduced further, but some phosphorylation was still visible (Figure 11). Nevertheless, *lyk5-2* and *lyk5-2 lyk4-1* plants were expected to display decreased chitin responses. Surprisingly, however, MAPK activation appeared to be normal in *lyk5-2* as well as *lyk5-2 lyk4-2* (Figure 11). To test if the reduced CERK1 phosphorylation in *lyk5-2* and *lyk5-2 lyk4-2* has an effect on chitin-induced gene expression, transcript levels of three *WRKY* transcription factors after treatment with a range of different chitin concentrations were tested by qRT-PCR (Figure 12). Cao *et al.* (2014) found highly reduced *WRKY30*, *WRKY33* and *WRKY53* expression in the *lyk5-2* mutant after chitooctaose treatment. In the current study however, the reduction in expression of *WRKY* genes in *lyk5-2* plants was very subtle (Figure 12). Out of the three *WRKY* genes tested, only *WRKY30* showed a statistically significant difference to Col-0 over several chitin concentrations. In *lyk5-2 lyk4-2* the expression of all tested *WRKY* genes was slightly more reduced and thus confirmed that the function of LYK4 and LYK5 is at least partially overlapping. However, even in *lyk5-2 lyk4-2* the decrease in chitin-triggered gene expression was very moderate (Figure 12). Taken together, the data indicate that the chitin-induced phosphorylation of CERK1, as indicated by the mobility shift in SDS-PAGE, does not correlate quantitatively with chitin-triggered MAPK activation and gene induction. The cause for this is currently not known, but might be explained by a number of different scenarios. Firstly, phosphorylation of CERK1 might be not the rate limiting step in chitin signaling. Other downstream components may cause either a signal transduction bottleneck or an additional checkpoint that modulates the intensity of the chitin response. In the *lyk5-2 lyk4-2* double mutant, some low level of chitin-induced CERK1 phosphorylation was still observed. Possibly, CERK1 can autophosphorylate in the absence of LYK5 and LYK4, albeit at a lower efficiency. Alternatively, the remnant CERK1 phosphorylation in *lyk5-2 lyk4-2* may be due to the fact that the *lyk4-2* mutant used in this study has a T-DNA insertion near the end of the gene and some functional LYK4 may still be present. If the bottleneck/additional modulator theory is true, low levels of CERK1 phosphorylation may be sufficient to trigger near-normal downstream responses. To definitively clarify this point, the

*lyk4-1* mutant, which harbors a T-DNA insertion more upstream than *lyk4-2* has been obtained and will be crossed with *lyk5-2*. Analyses of *lyk5-2 lyk4-1* double mutants should allow the unequivocal assessment of functional overlap between LYK5 and LYK4. The second possibility is that the information on CERK1 phosphorylation obtained by the SDS-PAGE mobility shift assay is not sufficiently detailed to fully understand the phosphorylation processes at the receptor. Several residues of the CERK1 intracellular domain were reported to be phosphorylated upon chitin elicitation (Petutschnig *et al.*, 2010) and not all phosphorylation events produce a visible band shift (Peck, 2006). Thus, it is possible that the loss of LYK5 and LYK4 affects CERK1 phosphorylation sites that cause the mobility shift detected in Western blots but are not the crucial residues for triggering downstream MAPK activation and gene expression. Therefore, LYK5 and LYK4 may not exert their primary function in the canonical chitin signal transduction pathway but rather have a more specialized role. Cao *et al.* reported drastically reduced chitin responses for *lyk5-2*. However, in the present study, the impairment of *lyk5-2* in chitin perception and signaling was very subtle (see section 3.2). This is in agreement with Miya *et al.* (2007), who found a normal chitin-induced ROS-burst for this line. It is also similar to *lyk5-1*, a mutant allele in the Ler background, which was reported in multiple studies to have either no (Wan *et al.*, 2008a; Wan *et al.*, 2012) or just a weak (Cao *et al.*, 2014) effect on chitin signaling. An aspect that may partially explain why there are contradictory findings for LYK4 and LYK5 in chitin signaling is the usage of different chitin preparations in different studies. In the work of Wan *et al.* (2012) and Cao *et al.* (2014) chitooctaose from Sigma with a purity of only 70% was used, whereas in this work colloidal polymeric chitin was used for analysis of LYK function. Chitin oligomers of the same degree of polymerization can yield different results, depending on the presence of short chitin oligomers, partially deacetylated chitooligosaccharides and other contaminants (Petutschnig, unpublished). Since chitin oligomers with a degree of polymerization of five and below can suppress CERK1-dependent signaling (Liu *et al.*, 2012b), this may substantially influence the biological activity of a chitin preparation. Since the chitooctaose preparation used by Wan *et al.* and Cao *et al.* is no longer available from Sigma, this question cannot be addressed experimentally.

According to Liu *et al.* (2012), two CERK1 molecules bind to one chitin oligomer, leading to CERK1 dimerization and subsequent activation of chitin signaling. Cao *et al.* suggest that CERK1 dimerizes also with LYK5 upon chitin binding and LYK5 forms constitutive homodimers. They also propose a binding model in which a binding site for chitooctaose is formed by all three LysMs of LYK5. Thus, it is not clear how LYK5 homodimerization, and in particular chitin-induced LYK5-CERK1 heterodimerization is achieved. To further examine the role of LYK5 and

LYK4 in chitin signaling and to dissect receptor complex formation, phosphorylation of CERK1, LYK5 and LYK4 will be studied in more detail and physical interaction of these RLKs will be analyzed by FRET and BiFC in stably transformed *Arabidopsis* plants. FRET analyses allow monitoring receptor interaction over time and having the potential to elucidate receptor complex dynamics. Cao *et al.* also report that LYK5 has a much higher chitin binding affinity than CERK1. They suggest that LYK5 is the main chitin receptor in *Arabidopsis* which uses CERK1 as a co-receptor, because it is not enzymatically active and requires a kinase active signaling partner. Chitin-dependent LYK5-CERK1 interaction (Cao *et al.*, 2014) indeed supports this hypothesis. However, the chitin binding affinity determined for CERK1 by Cao *et al.* ( $K_d = 455 \mu\text{M}$ ) does not match earlier measurements of Liu *et al.* ( $45 \mu\text{M}$ ) and a higher binding affinity of LYK5 to chitin magnetic beads in comparison to CERK1 could not be observed in the present study. Whether CERK1 or LYK5/LYK4 functions as the primary chitin receptor or high affinity binding is achieved by cooperative binding of more than one type of RLK remains an open question, as the exact structure of the receptor complex is not yet understood.

Tissue and organ specific expression of CERK1, LYK5 and LYK4 may also have a considerable impact on chitin receptor complex formation. Wan *et al.* (2012) generated plants expressing a *pLYK4::GUS* fusion and found a strong LYK4-promoter activity in leaves and roots suggesting that the LYK4 protein is active in both tissues. Indeed, expression studies of *WRKY53* and *MAPK3* conducted separately in roots and shoots revealed reduced chitin-triggered induction of these defense genes in both tissues of *lyk4-1* plants (Wan *et al.*, 2012).

Cao *et al.* (2014) analyzed the *LYK* expression using publicly available microarray data (Schmid *et al.*, 2005). They state that *LYK4*, *LYK5* and *CERK1* are equally expressed in all plant tissues. However, Cao and colleagues interpreted the expression values that had been normalized to the median for each gene across all samples (Schmid *et al.*, 2005). Interestingly, by using the same dataset but investigation of absolute values (Schmid *et al.*, 2005) in this study, the differences in the expression patterns of *CERK1*, *LYK5* and *LYK4* became obvious (Figure S4). While *CERK1* is well expressed in all organs, *LYK5* is expressed to similar levels as *CERK1* in all aerial tissues, but has low expression levels in the root. The expression pattern of *LYK4* is the reverse of *LYK5*, with low expression in aerial tissues and higher values in roots (Figure S4). These findings are in clear contrast to the data of Wan *et al.* (2012) and also Cao *et al.* (2014). The low *LYK4* expression levels in aerial tissues predicted from microarray data were confirmed in this study by the low signals obtained for LYK4-mCitrine in leaves by confocal microscopy as well as Western blotting (Figure 17 and Figure 25). Higher *LYK4* expression in roots and *LYK5*

expression in shoots suggests a tissue-specific function of these proteins and thus root tissue will be used in further experiments to analyze the subcellular behavior of LYK4. In comparison to shoots, the MAMP responses in roots are not very intensely studied. While elf18 is perceived only in shoots (Wyrsh *et al.*, 2015), flg22 (Millet *et al.*, 2010; Wyrsh *et al.*, 2015) and chitin (Millet *et al.*, 2010; Wan *et al.*, 2012) can also be sensed in roots. When *FLS2* was expressed in different specific tissue types of the root in a *FLS2*-deficient background, the intensity of the flg22 responses in the obtained plant lines did not correlate with *FLS2* expression levels (Wyrsh *et al.*, 2015). This suggests that different tissue types might contain factors other than *FLS2* that regulate the outcome of the flg22 response, which in turn supports the idea of tissue-specific function of PRR complexes.

## 4.2 The subcellular behavior of CERK1, LYK5, and LYK4

Despite extensive research in rice and *Arabidopsis*, no information on ligand-induced spatial dynamics of chitin receptor components is available to date. In this work, the subcellular behavior of *Arabidopsis* chitin binding LysM-RLKs CERK1, LYK5 and LYK4 was investigated. Transgenic lines expressing CERK1-GFP had been established previously (Petutschnig *et al.*, 2014). To analyze the localization of LYK5 and LYK4, mCitrine-fusions were generated and stably expressed in *Arabidopsis* plants. The described lines were analyzed by confocal laser scanning microscopy.

### 4.2.1 CERK1-GFP may show chitin-dependent endosomal localization

To visualize subcellular dynamics of CERK1 after chitin stimulus, transgenic plants expressing CERK1-GFP in the *cerk1-2* background were analyzed (see section 3.1). CERK1-GFP complemented the chitin insensitive phenotype of *cerk1-2* (Figure 6), indicating that the fusion protein is functional. Confirming previous results (Petutschnig *et al.*, 2014), CERK1-GFP localized to the PM in unchallenged plants (Figure 7 and Figure 8). Although CERK1 contains the tetrapeptide YXXΦ, a clathrin-dependent endocytosis motif (Geldner and Robatzek, 2008), chitin treatment did not discernibly change CERK1-GFP subcellular localization (Figure 7 and Figure 8). This is reminiscent of the fluorescence-tagged brassinosteroid receptor BRI1, whose subcellular localization is not visibly responsive to brassinosteroid levels in the cell (Geldner *et al.*, 2007). In contrast to CERK1, other PRRs have been found to readily become internalized after perception of their ligands, e.g. *FLS2* (Robatzek *et al.*, 2006) and the LRR-RLPs *LeEIX2* (Bar and Avni, 2009a) and *Cf4* (Postma *et al.*, 2015). It cannot be excluded that in the work conducted here chitin-induced CERK1-GFP endosomes were not observed due to technical limitations. *CERK1* gene expression is induced after chitin treatment (Figure 13) indicating that

the activated receptor might be replaced by newly produced CERK1 that has to be transported to the PM. In contrast to LYK5 and LYK4, CERK1 expression is induced slowly and remains elevated for several hours (Figure 13) which is in accordance with the relatively long presence of the shifted, phosphorylated form of CERK1 in chitin-treated leaves (Figure 24). CERK1 endocytosis might follow this slow pattern, and thus the number of CERK1-GFP molecules on endosomes and/or the number of CERK1-GFP carrying endosomes might never reach the threshold to be robustly detected by CLSM. Since endocytosis of LYK5 is dependent on CERK1, it makes sense that endocytosis of CERK1 occurs later and/or more slowly to ensure that all activated LYK5 molecules can be internalized.

Activated receptors are removed from the PM via endocytosis and may subsequently be degraded in the vacuole to attenuate signaling. The pharmacological inhibitor ConcA inhibits transport of endosomes carrying FLS2 (Beck *et al.*, 2012) or LYK5 from the TGN to the vacuole and thus leads to their accumulation. Therefore, ConcA was employed to potentially stabilize endosomes carrying CERK1-GFP and possibly prevent degradation of the internalized receptor. Indeed, upon interference with endocytosis using ConcA, accumulation of CERK1-GFP-positive vesicles occurred after about 90 min of chitin incubation (Figure 8). In samples treated with ConcA alone, no CERK1-GFP vesicles were observed. This suggests that upon chitin elicitation, CERK1-GFP is slowly internalized over a long period of time. However, since ConcA interferes with all trafficking pathways at the TGN, the enriched CERK1-GFP vesicles may also include secretory vesicles that carry newly synthesized CERK1-GFP from the TGN to the PM. To test this, cycloheximide (CHX) co-treatment could be performed. CHX blocks protein synthesis and would therefore show if the observed vesicles contain newly produced CERK1-GFP. Another valuable approach would be to stably express CERK1-GFP under a chitin-insensitive promoter such as pUbiquitin or p35S, and treat the resulting transgenic lines with ConcA and chitin.

#### 4.2.2 LYK5 undergoes chitin-induced endocytosis

To analyze the subcellular behavior of LYK5 and LYK4, stable transgenic lines expressing *pLYK5::LYK5-mCitrine* or *pLYK4::LYK4-mCitrine* were analyzed. Expression of *pLYK5::LYK5-mCitrine* and *pLYK4::LYK4-mCitrine* restored chitin-induced CERK1 phosphorylation in the *lyk5-2 lyk4-2* double mutant (Figure 14) and hence confirms that both fusion proteins are functional. Most tested LYK5-mCitrine expressing lines showed a good expression of the transgene in leaves. In contrast, LYK4-mCitrine showed very weak signals in all transgenic *Arabidopsis* lines tested. This is in keeping with data previously reported by Wan *et al.* (2012) as

well as microarray data that show low LYK4 expression in leaves (Figure S4). Since LYK5-mCitrine was well expressed in the transgenic lines and LYK4-mCitrine was close to the detection limit of the confocal microscopy system, further investigations focused mainly on the analysis of LYK5-mCitrine localization.

LYK5-mCitrine is a PM-localized protein as shown by co-expression with the PM-marker protein LTI6b and staining with FM4-64 (Figure 19). This is in accordance with recent studies that showed overlapping LYK5-GFP signal with FM4-64 (Cao *et al.*, 2014). Similar to LYK5-mCitrine, LYK4-mCitrine was also detected at the cell periphery (Figure 17). In contrast to CERK1, LYK5-mCitrine showed chitin-induced vesicle formation that became visible after 20 min. This might also be the case with LYK4-mCitrine, but the low expression in leaf tissue did not allow unequivocal results. Co-localization analysis using the endocytic tracer FM4-64 (Figure 19) and experiments with the pharmacological inhibitors ConcA and Wm (Figure 23) indicated that LYK5-mCitrine is internalized into endosomes and sorted into MVBs. The myosin inhibitor BDM blocked endocytosis of LYK5-mCitrine (Figure 23), whereas the mobility of LYK5-mCitrine endosomes was reduced by the tubulin depolymerizing agent oryzalin (attached supplemental movie 2). This implies that actin filaments and microtubules are required for LYK5-mCitrine internalization and intercellular trafficking, respectively. To characterize the dynamics of LYK5-mCitrine endocytosis, the number of chitin-induced endosomal compartments over time was quantified. These time lapse experiments showed that LYK5-mCitrine endocytosis is transient and peaks around one hour of chitin treatment (Figure 16) - a time point where early chitin-induced defense responses such as ROS generation or MAPK activation have already taken place. In that respect, the results on LYK5-mCitrine endocytosis are similar to those described for FLS2-GFP (Robatzek *et al.*, 2006; Beck *et al.*, 2012). FLS2 internalization becomes visible after early flg22-induced responses (Beck *et al.*, 2012) but is not required for early flg22-triggered events (Ben Khaled *et al.*, 2015). Thus, FLS2 may signal from the PM and not from endosomes. Signaling from the PM has been demonstrated for the brassinosteroid receptor BRI1 (Irani *et al.*, 2012). Based on the results of this work, a similar scenario may be true for LYK5. However, it has to be kept in mind that the bulk of the observed LYK5-mCitrine positive vesicles (and FLS2-positive vesicles (Beck *et al.*, 2012)) are probably LEs/MVBs and that endocytosis may start well before it can be detected by CLSM. A further piece of evidence for signaling from the PM is the fact that LYK5 is internalized upon chitin elicitation while the majority of CERK1 appears to stay at the PM.

The kinetics of chitin-induced LYK5 endocytosis is very similar to chitin-induced *LYK5* gene expression. Thus it is attractive to speculate that after successful induction of defense

responses, activated LYK5 is removed from the PM and at the same time newly synthesized LYK5 is delivered to the PM to refill the pool of signaling-competent receptors. The removal of activated receptors from the PM might contribute to desensitizing defense signaling from the PM (Luschnig and Vert, 2014; Smith *et al.*, 2014). Since LYK5 is necessary for full CERK1 phosphorylation, LYK5 endocytosis might lead to down-regulation of the CERK1 dependent signaling, and thus, inhibition of endocytosis may enhance or prolong chitin signaling. However, this theory does not fit the fact that *lyk5-2* mutant plants are only very mildly affected in chitin responses. Thus regulation by LYK5 endocytosis might only apply to non-canonical chitin signal transduction events that have not been identified so far.

It seems likely that many mechanistic aspects of endocytosis, similar to other typical MAMP responses, are conserved between LRR-RLK and LysM-RLK-type PRRs. The FLS2 endocytic pathway has been subject of several studies. It has been extensively characterized in co-localization studies with Rab GTPases and other endomembrane compartment markers (Beck *et al.*, 2012; Choi *et al.*, 2013; Spallek *et al.*, 2013) that are important determinants of membrane identity and membrane targeting (Woollard and Moore, 2008). It has been shown that ARA7/RabF2b is required for FLS2 endocytosis in *Arabidopsis* and that RabA members regulate different steps along its endocytic route in *N. benthamiana* (Beck *et al.*, 2012; Choi *et al.*, 2013). To complement inhibitor studies (see section 3.3.8) and to test if LYK5 follows the same endocytic route as FLS2, co-expression with endosomal marker lines were done. Upon chitin elicitation, LYK5-mCitrine clearly co-localized with ARA6/RabF1-RFP and the ARA7/RabF2b-homologue mCherry-Rha1/RabF2a (Figure 20) supporting its LE/MVB localization. Expectedly, the overlap between LYK5-mCitrine and GTPase-positive endosomes was not complete, since the internalized LYK5-mCitrine travels along endomembrane compartments with different identities. The overlap was quite extensive with mCherry-Rha1/RabF2a, which labels an early type of LE and less overlap was seen with ARA6/RabF1-RFP, which labels a later variant (Ueda *et al.*, 2004; Ebine *et al.*, 2011). These results are very similar to FLS2 co-localization with ARA6/RabF1-RFP and the RFP-ARA7/RabF2b (Beck *et al.*, 2012). In contrast, LYK5-mCitrine was not found to co-localize with recycling endosomal markers mCherry-RabA5d and mCherry-RabA1g (Figure 21), neither with nor without chitin treatment. Chitin-induced LYK5-mCitrine vesicles were often found near mCherry-RabA5d or mCherry-RabA1g-labeled endomembrane compartments, indicating that LYK5-mCitrine and mCherry-RabA5d or mCherry-RabA1g-positive compartments might associate.



An aspect that has not been addressed in the present study is the type of endocytic vesicles mediating LYK5 endocytosis. Clathrin-dependent as well as clathrin-independent mechanisms have been reported in plants (Li *et al.*, 2012; Fan *et al.*, 2015). Tyrphostin A23, is a tyrosine analog that inhibits clathrin-mediated endocytosis by interfering with the interaction of cargo proteins and the AP-2 adaptor complex (Robinson *et al.*, 2008a). Treatment with tyrphostin A23 reduced but did not abolish flg22-triggered endocytosis of FLS2 (Beck *et al.*, 2012), which suggests that FLS2 internalization involves both clathrin-dependent and independent mechanisms. *MtLYK3* is a LysM-RLK from *Medicago truncatula* that is similar to CERK1 and functions in rhizobial nod factor perception (Smit *et al.*, 2007). Interestingly, upon inoculation with symbiotic bacteria, *MtLYK3* is present in punctuate structures at the PM. These structures overlap with FLOT4 which has been shown to accumulate in membrane microdomains (Haney *et al.*, 2011). Remorins are also proteins that accumulate in membrane microdomains. In *Medicago*, the remorin *MtSYMREM1* was shown to be essential for establishment of symbiosis with rhizobia. *MtSYMREM1* interacted with *MtLYK3* and another LysM-RLK implicated in nod factor perception, *MtNFP*, in yeast and in transiently transformed *N. benthamiana* leaves (Lefebvre *et al.*, 2010). These data illustrate that membrane microdomains are important for LysM-RLK signal transduction. Since membrane microdomains are also the starting points for clathrin-independent endocytosis (Li *et al.*, 2012; Fan *et al.*, 2015), it is conceivable that they might also play a role in LysM-RLK internalization.

#### 4.2.3 CERK1 and LYK5 constitutively traffic in a BFA-sensitive manner

The fungal toxin Brefeldin A (BFA), a macrocyclic lactone, is commonly used to study vesicular trafficking pathways in yeast, mammalian, and plant cells. BFA inhibits ARF-type small GTPases by reversibly interacting with their associated guanine nucleotide exchange factors (GEFs) (Jackson and Casanova, 2000). *Arabidopsis* contains eight ARF-GEFs, five of which are sensitive to BFA (Geldner *et al.*, 2003). By inhibiting these, BFA blocks protein secretion (Nebenführ *et al.*, 2002) and endocytosis (Baluska *et al.*, 2002; Geldner *et al.*, 2003) in plants. One important BFA sensitive ARF-GEF is GNOM (Steinmann *et al.*, 1999) which localizes to TGN/EE/REs and mediates cycling of proteins between the PM and TGN (Geldner *et al.*, 2003; Richter *et al.*, 2007; Otegui and Spitzer, 2008). Thus, BFA sensitivity of subcellular localization is sometimes interpreted as evidence for constitutive TGN-PM recycling (Geldner *et al.*, 2003; Richter *et al.*, 2007; Teh and Moore, 2007). Results in this work show that the localization of CERK1-GFP, as well as LYK5-mCitrine, is BFA-sensitive (see sections 3.1.4 and 3.3.7). Upon BFA treatment of leaves, both RLKs accumulated in globular endomembrane compartments

that contained PM-derived material. Such BFA-inducible compartments have been reported in *Arabidopsis* leaves before (Nielsen *et al.*, 2012) and resemble BFA-induced TGN/EE-aggregates in *Arabidopsis* roots and cotyledons which are termed BFA-bodies or compartments (Geldner *et al.*, 2003; Beck *et al.*, 2012). These observed BFA-induced compartments in leaves likely contain CERK1 and LYK5 traveling to and/or from the PM. Since BFA likely affects multiple vesicle transport routes and displays different effects in different tissues (Robinson *et al.*, 2008b; Langhans *et al.*, 2011) the CERK1 and LYK5 molecules found in BFA-induced compartments may either be internalized from the PM or newly synthesized. BFA treatment did not block chitin-triggered endocytosis of LYK5-mCitrine and LYK5-mCitrine endosomes appear not to be part of the BFA-induced compartment (Figure 22), indicating that activated LYK5-mCitrine endocytosis is not facilitated by BFA-sensitive ARF-GEFs. Hence, ligand-induced LYK5-mCitrine endocytosis seems to be mechanistically distinct from constitutive transport, which was also reported for FLS2 (Robatzek *et al.*, 2006). A role for the BFA-insensitive ARF-GEF GNL1 (Richter *et al.*, 2007) in FLS2 endocytosis was suggested since flg22 sensitivity is reduced in *gnl1* mutants (Salomon, 2009). However, since BFA inhibits, at least, five ARF-GEFs simultaneously, it cannot be deduced which and how many ARF-GEFs might be involved in LYK5 and CERK1 trafficking.

### **4.3 Phosphorylation of LYK5 by CERK1 is a prerequisite for LYK5 endocytosis**

The recognition of a ligand via its cognate receptor activates different downstream signaling pathways which is typically facilitated by the transfer of phosphoryl groups (Battey *et al.*, 1999). Hence, protein phosphorylation is a crucial step in signal transduction including plant immune signaling. So far, the only known kinase active component of the chitin recognition complex is CERK1. CERK1 is a kinase with an intact RD motif in the catalytic loop and shows good kinase activity *in vitro*. This is a characteristic it shares with the brassinosteroid receptor BRI1, and its co-receptor BAK1. In contrast, the LRR-RLK immune receptors FLS2, EFR, and Xa21, belong to the category of non-RD kinases (Dardick *et al.*, 2012; Tanaka *et al.*, 2013). Consequently, FLS2 shows hardly detectable autophosphorylation activity *in vitro* (Schwessinger *et al.*, 2011). The physical interaction of FLS2 with its co-receptor BAK1 does not depend on kinase activity of either partner (Schwessinger *et al.*, 2011) and BAK1 phosphorylates FLS2 on several residues *in vitro* (Yan *et al.*, 2012). This leads to a model where the non-RD kinase FLS2 utilizes the enzymatically more active co-receptor BAK1 for transphosphorylation and subsequent signal transduction. An alignment of the full-length amino acid sequence of CERK1 and related LysM-

RLKs in *Arabidopsis* (Figure 3) shows that critical kinase subdomains are mutated or absent in LYK5 and LYK4 (Figure 3). The subdomain I, which contains the ATP-binding loop with the typical consensus sequence G-X-G-X-X-G is only rudimentary in both proteins (Figure 3). Nevertheless, the highly conserved lysine (K) residue in subdomain II, which is indispensable for the phosphotransfer reaction (Hanks *et al.*, 1988; Hanks and Hunter, 1995) is present in LYK5 and LYK4. The importance of this lysine is underlined by deleting or changing this residue results in kinase inactivation, which has been shown for RLKs like the LRR-RLK ERECTA (Shpak *et al.*, 2003), BAK1, BRI1 (Li *et al.*, 2002) and CERK1 (Petutschnig *et al.*, 2010). Moreover, LYK5 and LYK4 do not have the highly conserved DFG motif in subdomain VII, which is required for Mg<sup>2+</sup> (or Mn<sup>2+</sup>) binding. Both proteins lack the aspartic acid residue but harbor the conserved glycine. Since these essential kinase subdomains (Eyers and Murphy, 2013) are not conserved in LYK5 and LYK4, they were predicted to be enzymatically inactive. This is not unusual for plant RLKs. *Arabidopsis thaliana* contains approximately 600 RLKs and about 20% of them are putatively kinase dead (Castells and Casacuberta, 2007). Both LYK5 and LYK4 were recently tested regarding their autophosphorylation capacity and found to be enzymatically inactive (Wan *et al.*, 2012; Cao *et al.*, 2014). These results could be confirmed in the present study by *in vitro* phosphorylation assays with GST-tagged LYK intracellular domains (IDs) expressed in *E. coli* (Figure 26). Complementation assays with the *lyk5-2* mutant suggested that LYK5-mediated chitin signaling does not require LYK5 kinase activity, but the LYK5 kinase domain is essential for interaction with CERK1 and chitin signal transduction (Cao *et al.*, 2014). However, since the phenotype observed for *lyk5-2* in this study was very subtle, the results by Cao *et al.* have to be interpreted with caution.

So far, transphosphorylation assays with the CERK1 endodomain have not been reported in the literature. To investigate whether LYK5 and LYK4 are CERK1 substrates, *in vitro* transphosphorylation assays were performed with GST-LYK5 (ID), GST-LYK4 (ID) and CERK1 (ID)-6xHis (Figure 26). In these experiments, CERK1 could phosphorylate LYK5 and LYK4, but not a GST negative control, indicating that LYK5 and LYK4 are substrates of CERK1. To test, if LYK5 is also a substrate of CERK1 *in planta*, the phosphorylation status of LYK5-mCitrine in the presence or absence of CERK1 was analyzed. When *pLYK5::LYK5-mCitrine* was stably expressed in the Col-0 background, the LYK5-mCitrine fusion protein showed a chitin-induced band shift similar to CERK1 (Figure 24). Phosphatase assays confirmed that, like with CERK1, the LYK5-mCitrine mobility shift is caused by phosphorylation (Figure 24). When *pLYK5::LYK5-mCitrine* was expressed in *cerk1-2* plants, the chitin-induced mobility shift of LYK5-mCitrine did not take place (Figure 24). These results indicate that CERK1 is required for the chitin-induced

phosphorylation of LYK5-mCitrine in *Arabidopsis* plants. To investigate if chitin-triggered LYK5 phosphorylation specifically depends on the kinase activity of CERK1, stably transformed plants were generated that co-expressed LYK5-mCitrine with either a transgenic CERK1 wild type (CERK1-WT) protein or an enzymatically inactive CERK1 variant (CERK1-LOF) in *cerk1-2* (see section 3.4.4). CERK1-WT could mediate chitin-induced phosphorylation of LYK5-mCitrine, while CERK1-LOF did not (Figure 27) that directly links phosphorylation by an active CERK1 to LYK5-mCitrine endocytosis. In combination with the results of the *in vitro* phosphorylation assay, this suggests that LYK5-mCitrine is phosphorylated by CERK1 *in planta*. Western blots with LYK4-mCitrine expressed in Col-0 or *cerk1-2* gave very weak signals, but indicated a small CERK1-dependent band shift of LYK4-mCitrine. Together with the *in vitro* transphosphorylation assays this indicates that LYK4 might be phosphorylated *in planta* by CERK1, but this needs to be confirmed by further research.

Experiments in previous studies showed that the kinase activity of LYK5 is not important for immune signaling but the presence of the kinase domain seems to be important for proper signaling and the interaction of LYK5 with CERK1 (Cao *et al.*, 2014). Since LYK5 (and LYK4) is kinase inactive it needs a kinase active partner for downstream signaling. CERK1 represents such a kinase active partner resulting in a LYK5-CERK1 complex that resembles the interaction of FLS2 and BAK1 (Schwessinger *et al.*, 2011). Accordingly, a chitin triggered association of LYK5 (and LYK4) with CERK1 then leads to transphosphorylation events at the kinase domain of LYK5. Analysis of plants expressing LYK5-mCitrine in *cerk1-2* (Figure 15) revealed that not only LYK5-mCitrine phosphorylation, but also its chitin-induced endocytosis depends on CERK1. Similarly, LYK5-mCitrine was internalized upon chitin treatment when co-expressed with transgenic CERK1-WT but not when co-expressed with the enzymatically inactive variant CERK1-LOF (Figure 27). This indicates that LYK5-mCitrine endocytosis is initiated through phosphorylation by CERK1.

The fact that LYK5 endocytosis depends on the kinase activity of CERK1 is also reflected in the phosphorylation kinetics of the two proteins (Figure 24). LYK5-mCitrine phosphorylation occurs within 10 min which is comparable to the chitin-induced phosphorylation of CERK1. The abundance of phosphorylated LYK5-mCitrine declines after 20 min suggesting a relatively fast removal of the activated receptor and synthesis of new LYK5-mCitrine. Indeed, the reduction of phosphorylated LYK5-mCitrine correlates well with the onset of its endocytosis. In contrast, CERK1 phosphorylation remains elevated for 60 min which is the time point where LYK5-mCitrine endocytosis starts to decrease, suggesting the phosphorylation of CERK1 is required

for LYK5-mCitrine endocytosis. Observations from other studies show that the internalization of FLS2 requires its co-receptor BAK1 (Chinchilla *et al.*, 2007; Beck *et al.*, 2012). *In planta*, FLS2-BAK1 heteromerization occurs almost instantaneously after perception of the flg22 ligand (Chinchilla *et al.*, 2007; Heese *et al.*, 2007; Sun *et al.*, 2013b) and leads to very rapid phosphorylation of both RLKs (Schulze *et al.*, 2010). Hence, it is tempting to speculate that FLS2 phosphorylation by BAK1 is required for its endocytosis, but so far this has not been shown.

The analysis of doubly transgenic plants expressing *LYK5-mCitrine* together with *CERK1-WT* revealed a puzzling effect. In these plants, the chitin-induced phosphorylation of CERK1 and LYK5-mCitrine as well as LYK5-mCitrine endocytosis is enhanced compared to lines harboring the endogenous CERK1 allele (Figure 27). This was the case even though plants were chosen which produce CERK1-WT in comparable amounts to endogenous CERK1 in Col-0. Similarly, transgenic expression of *cerk1-4*, a CERK1 variant that causes cell death, leads to a stronger cell death phenotype than seen in the original *cerk1-4* mutant (Stolze and Petutschnig, unpublished). The CERK1 transgene construct contains the CERK1 CDS fused to 500 bp of the endogenous CERK1 promoter. It might be possible that the 500 bp promoter lacks some regulatory sequences or intron sequences that play a role in regulation of CERK1. Possibly, transgenic expression results in slightly elevated protein levels that lead to more CERK1 and LYK5-mCitrine phosphorylation and consequently increased endocytosis. However, the reason behind this effect remains unclear.

In animals, ligand-triggered receptor tyrosine phosphorylation serves as a signal for E3 ubiquitin ligases leading to receptor ubiquitination (Mosesson *et al.*, 2003; Mukherjee *et al.*, 2006; Goh and Sorkin, 2013). The recognition of ubiquitinated proteins can ultimately lead to recruitment of components of the CME-machinery (Jiang *et al.*, 2003). Thus, ubiquitination links protein phosphorylation at tyrosine residues to endocytosis and subsequent sorting into intraluminal vesicles for degradation (Sorkin and von Zastrow, 2009). It is now emerging that several plant RLKs have not only Ser/Thr but also Tyr kinase activity (Betz *et al.*, 1992; Macho *et al.*, 2015). For example, BRI1 and BAK1, which were initially classified as Ser/Thr protein kinases, showed autophosphorylation of tyrosine residues in the cytoplasmic domain (Oh *et al.*, 2009; Oh *et al.*, 2010). Tyrosine kinase activity was also described for EFR, the plasma membrane-localized protein BRI1-KINASE INHIBITOR 1 (BK11) (Macho *et al.*, 2015) and for SERK1, which is expressed during embryogenesis (Shah *et al.*, 2001). FLS2 is phosphorylated by BAK1 and BIK1 upon flg22 recognition (Lu *et al.*, 2010) and polyubiquitinated by E3 ubiquitin ligases PUB12 and PUB13 (which are themselves activated through phosphorylation by BAK1) (Lu *et*

*et al.*, 2011). Upon flg22 exposure, FLS2 undergoes endocytosis (Robatzek *et al.*, 2006; Beck *et al.*, 2012) and sorting into intraluminal vesicles at MVBs (Spallek *et al.*, 2013), a process which requires ubiquitination (Katzmann *et al.*, 2002; Raiborg and Stenmark, 2009; Shields and Piper, 2011; Cai *et al.*, 2014). Finally, flg22 treatment and subsequent endocytosis lead to transiently decreased FLS2 protein levels (Smith *et al.*, 2014), suggesting degradation in the vacuole. Although these findings from different studies have not yet been experimentally linked, they still raise the idea that ligand-induced endocytosis in plants might employ similar mechanisms to those observed in animal studies. Chitin-activated LYK5 seems to take a very similar endocytic route as flg22-activated FLS2. LYK5 is also found in MVBs and is probably sorted into intraluminal vesicles for degradation in the vacuole. Therefore, it is likely to be ubiquitinated upon chitin elicitation. Phosphorylation of LYK5 by CERK1 may drive ubiquitination of LYK5 by recruiting ubiquitin ligases. Alternatively, similar to BAK1 (Lu *et al.*, 2011) and the *Medicago* LysM-RLK LYK3 (Mbengue *et al.*, 2010), CERK1 could phosphorylate ubiquitin ligases to potentially activate them. Whether CERK1 has tyrosine kinase activity is currently not known. Also, whether receptor ubiquitination and endocytosis in plants relies on tyrosine phosphorylation or can (also) be mediated by serine/threonine phosphorylation remains an open question to be answered by future research.

#### **4.4 Chitin receptor complex formation in *Arabidopsis***

The experiments in this study very clearly demonstrated that chitin-activated CERK1 phosphorylates LYK5, which is required for its endocytosis. However, *lyk5-2* and *lyk5-2 lyk4-2* mutant plants also show a reduced chitin-triggered mobility shift of CERK1, which indicates that LYK5 (and possibly LYK4) are required for full phosphorylation of CERK1. This came as a surprise, because neither LYK5 nor LYK4 has kinase activity.

It has been shown that CERK1 homodimerizes upon chitin binding and this is a prerequisite for CERK1 phosphorylation and signaling (Liu *et al.*, 2012b). Thus one explanation would be that LYK5 (and/or LYK4) is required for CERK1 homodimer formation. Indeed it has been reported that LYK5 is necessary for homodimerization and phosphorylation of CERK1 (Cao *et al.*, 2014). However, how this is achieved has not been elucidated. Since LYK5 has chitin binding capacity (Petutschnig *et al.*, 2010; Wan *et al.*, 2012; Cao *et al.*, 2014) cooperative chitin binding with CERK1 is an attractive hypothesis. However, there are several reports in the literature that argue against this scenario but at the same time make it also rather challenging to find an alternative explanation: CERK1 binds chitin tetramers via its central LysM domain and two CERK1 molecules dimerize by binding to the same chitin octamer (Liu *et al.*, 2012b). A similar

mechanism has been discovered for the rice chitin receptor protein OsCEBiP (Hayafune *et al.*, 2014). According to these models, CERK1 would not need LYK5 for dimerization. Also, Cao *et al.* proposed that LYK5 binds chitin oligomers intramolecularly between two of its LysMs (Cao *et al.*, 2014). Their suggestion is based on the molecular structure of the *Cladosporium fulvum* LysM effector Ecp6, which binds chitin with very high affinity (Sanchez-Vallet *et al.*, 2013). Surprisingly, in contrast, to CERK1 (Liu *et al.*, 2012b) and the LysM-effector Ecp6 (Sanchez-Vallet *et al.*, 2013) LYK5 showed no affinity for chitin tetramers (Cao *et al.*, 2014). Thus, the proposed chitin induced LYK5-CERK1 dimerization (Cao *et al.*, 2014) cannot be brought about by both molecules simultaneously binding a chitin octamer. LYK5 has been reported to homodimerize constitutively (Cao *et al.*, 2014), which precludes the model that chitin-induced homodimerization of LYK5 and simultaneous LYK5-CERK1 interaction lead to CERK1 dimerization and activation of signaling.

Thus, there are many open questions in *Arabidopsis* chitin receptor formation. However, it seems likely that it involves the interaction of multiple LysM-RLKs, possibly via multiple LysM domains. Timing of the interactions may also play an important role and will be addressed in the future by FRET analyses.

Studies on legume LysM-RLKs and their interactions indicate that LysM-RLK-containing receptor systems may be even more complex. They may involve several different classes of LysM-RLKs as well as non-LysM-RLKs. In legumes, *LjNFR1-LjNFR5* (Madsen *et al.*, 2011) and *MtLYK3-MtNFP* (Smit *et al.*, 2007; Pietraszewska-Bogiel *et al.*, 2013; Rey *et al.*, 2013) complexes cooperatively recognize lipochitooligosaccharides from symbiotic rhizobia, which is essential to establish symbiosis (Oldroyd, 2013). CERK1 is the closest *Arabidopsis* homolog to *LjNFR1* and *MtLYK3*, while clear homologs of *LjNFR5* or *MtNFP* are not present in *Arabidopsis* (Figure S2) (Arrighi *et al.*, 2006). The closest *Medicago* homologs of *Arabidopsis* LYK5 and LYK4 are the enzymatically inactive LysM-RLKs *MtLYR4* and *MtLYR3* (Figure S2) (Arrighi *et al.*, 2006). Notably, *MtLYR3*, in contrast to its close homolog *MtLYR4*, has a high binding affinity to lipochitooligosaccharides (Fliegmann *et al.*, 2013), although no symbiosis phenotype has been reported for *lyr3* mutants so far. Thus, in legumes LysM-RLKs from three different clades (Figure S2) are implicated in lipochitooligosaccharide perception. Recent research shows that *LjNFR5* also physically interacts with SYMRK, a Malectin-LRR-RLK that is required for symbiosis with both rhizobia and mycorrhizal fungi (Antolin-Llovera *et al.*, 2014b). These findings give reason to speculate that chitin recognition complex(es) in *Arabidopsis* might be even more intricate than envisaged at present.

CERK1 phosphorylation is reduced in *lyk5-2 lyk4-1* lines, but not completely abolished (Figure 11). This might be due to the *lyk4-2* T-DNA insertion being at the end of the kinase domain, and the *lyk4-2* mutant still containing some functional LYK4 (compare above). However, the expression levels of *LYK4* and LYK4 protein abundance in leaves are very low. At the same time *lym2* mutants do not seem to be impaired in canonical chitin signaling (Shinya *et al.*, 2012; Wan *et al.*, 2012), even though LYM2 binds chitin and its rice homolog OsCEBiP plays an important role in chitin perception (Kaku *et al.*, 2006; Petutschnig *et al.*, 2010; Shinya *et al.*, 2012; Hayafune *et al.*, 2014; Kouzai *et al.*, 2014b). An explanation for both these phenomena would be functional redundancy between LYK5, LYK4 and LYM2. Recently it has been postulated that LRR-RLPs involved in immune signaling form an LRR-RLK equivalent by association with the adaptor RLK SOBIR1 (Gao *et al.*, 2009; Liebrand *et al.*, 2013; Zhang *et al.*, 2013; Gust and Felix, 2014). LYM2 could constitute a LysM-RLK equivalent by association with a not yet known adaptor RLK or possibly also with RLCKs involved in chitin signaling, such as PBL27 (Shinya *et al.*, 2014) or CLR1 (Ziegler, 2015). The kinase domain of CLR1 shows considerable similarities to LysM-RLKs (Ziegler, 2015) and like LYK5 and LYK4, PBL27 and CLR1 were shown to be phosphorylated by CERK1 *in vitro* (Shinya *et al.*, 2014; Ziegler, 2015). CERK1-dependent phosphorylation after chitin treatment has been shown also for CLR1 *in vivo* (Ziegler, 2015). In the case of LYM2 and RLCKs, the RLK equivalent could be stabilized by interaction with membrane-spanning proteins such as LYK5, LYK4 or CERK1 or unknown adaptor proteins.

#### 4.5 LYM proteins are not involved in CERK1-dependent chitin signaling

In rice, LysM-RLPs have been shown to play a significant role in the recognition of chitin (Kaku *et al.*, 2006; Liu *et al.*, 2012a; Hayafune *et al.*, 2014; Kouzai *et al.*, 2014b) and PGN (Willmann *et al.*, 2011; Liu *et al.*, 2012a; Ao *et al.*, 2014; Kouzai *et al.*, 2014a). OsCEBiP, a LysM-RLP with high affinity for chitin, is the key player in the rice chitin receptor (Kaku *et al.*, 2006; Hayafune *et al.*, 2014). OsCEBiP has been shown to interact with OsCERK1 for downstream signaling after chitin recognition (Shimizu *et al.*, 2010). Two additional LysM-RLPs, OsLYP4 and OsLYP6 mediate PGN as well as chitin recognition (Liu *et al.*, 2012a; Ao *et al.*, 2014; Kouzai *et al.*, 2014a). *Arabidopsis* contains three LysM-RLPs named LYM1-3. The closely related LYM1 and LYM3 are involved in PGN binding (Willmann *et al.*, 2011), but in contrast to their rice homologues OsLYP4 and OsLYP6 an additional role in chitin-induced defense could not be assigned (Willmann *et al.*, 2011). Similar to OsCEBiP, the *Arabidopsis* CEBiP homolog LYM2



has high chitin binding capacity (Petutschnig *et al.*, 2010; Shinya *et al.*, 2012). Because of this, it was seen as a potential CERK1 interaction partner in chitin perception (Petutschnig *et al.*, 2010). However, several studies showed that, in contrast to its rice homolog, LYM2 is not necessary for typical chitin responses (Shinya *et al.*, 2012; Wan *et al.*, 2012; Faulkner *et al.*, 2013). Since chitin/PGN recognition and downstream signaling in rice and *Arabidopsis* requires CERK1 for signal transduction, *Arabidopsis lym2* and *lym* triple mutants were tested regarding CERK1-phosphorylation and CERK1 chitin binding. This study shows that the loss of one or all three LYMs does not affect CERK1 chitin binding and chitin-induced phosphorylation (Figure 29) which confirms results from a previous study that tested CERK1 receptor phosphorylation in *lym2-1* (Faulkner *et al.*, 2013). Together, the data support the recent findings that CEBiP-like proteins have no impact on CERK1-dependent chitin signaling in *Arabidopsis*. Similar to *Arabidopsis* the rice genome encodes LYK4/LYK5-like proteins that may, together with LysM-RLPs, form receptor complexes for chitin and PGN perception. It is astonishing that the two systems differ between the two plant species although they are equipped with a similar set of proteins.

#### 4.5.1 LYM2 re-localizes at PD after chitin stimulus

LYM2 does not function in the canonical chitin response, but it was found to play a role in chitin-mediated regulation of PD-flux independently of CERK1 (Faulkner *et al.*, 2013). *lym2* mutants were also reported to be more susceptible to necrotrophic fungi (Faulkner *et al.*, 2013; Narusaka *et al.*, 2013). LYM2 was reported to localize to the PM with focal accumulation at PD (Faulkner *et al.*, 2013). To further investigate the localization of LYM2, a mCitrine-LYM2 fusion protein was stably expressed in *Arabidopsis* (see section 3.6). Co-expression of a PM-marker protein clearly demonstrated that mCitrine-LYM2 is localized at the PM (Figure 30). However, mCitrine-LYM2 focally accumulated in punctate structures within the PM, which was not seen with the PM marker protein. Aniline blue staining identified these structures as PD (Figure 31), confirming the observations of Faulkner and colleagues and a recent PD proteome study, which also identified LYM2 as a PD-associated protein (Fernandez-Calvino *et al.*, 2011). Interestingly, the mCitrine-LYM2 signal at PD became drastically intensified upon chitin treatment, suggesting that LYM2 migrates from the PM to PD after chitin binding. It is tempting to speculate that LYM2 translocates to the sites of PD in response to chitin by lateral movement through the PM, since the GPI-anchor confers high lateral mobility (Low and Saltiel, 1988; Paulick and Bertozzi, 2008). Both the basic level of PD localization as well as the increased mCitrine-LYM2 accumulation at PD after chitin treatment occurred also in the *cerk1-2* mutant (Figure 30). Thus, LYM2 targeting

to PD appears to be independent of CERK1. This is in keeping with the findings of Faulkner *et al.*, who also reported that regulation of the PD-flux by LYM2 is independent of CERK1. The mCitrine signal observed in this study becomes pronounced at PD after 60 min of chitin treatment. A recent report suggested that flg22-induced callose deposition starts as early as 60-90 minutes after induction (Ellinger and Voigt, 2014). Thus, the timing of LYM2 relocation might correlate with the onset of callose deposition and one could speculate that LYM2 might activate callose synthesis at PD to regulate the PD-flux. However, so far, no direct link between LYM2 accumulation at PD and callose deposition has been shown. A role for LysM-proteins in regulating the traffic through PD has been only observed for LYM2 in *Arabidopsis*. A PD-flux regulating function of its rice homolog OsCEBiP has not been observed so far. Rice has a close CEBiP homolog, Os09g0548200 that is even more similar to LYM2. Os09g0548200 shares an 36% sequence similarity with LYM2, whereas OsCEBiP/LYM2 similarity is 33%. Potentially, Os09g0548200 could perform the PD-specific function in rice.

While chitin-induced regulation of the PD-flux is independent of CERK1, flg22-induced PD-flux regulation requires FLS2 (Faulkner *et al.*, 2013). This suggests a role for FLS2 in callose deposition contributing to MAMP-induced restriction of bacterial proliferation. However, *bak1* mutants were still able to deposit callose in response to flg22 (Clay *et al.*, 2009). This implies that FLS2 mediates flg22-induced callose deposition without its canonical co-receptor BAK1, indicating that FLS2 could form response-specific receptor complexes with different partners. Unlike FLS2 or BAK1, LYM2 do not possess an intracellular part for signaling purposes. Thus, a PD-specific function of LYM2 requires an active signaling partner, for example an enzymatically active LYK, which then again resembles the OsCERK1/OsCEBiP complex in rice.

#### **4.6 Generation and identification of a *lyk5-2 lyk4-2 lym2-1* triple mutant**

LYK5 and LYK4 were identified in an *in vitro* pull-down experiment as chitin binding proteins (Petutschnig *et al.*, 2010). Thus, they represent good candidates for CERK1 complex partners. Since chitin-induced defense responses are not totally abolished in *lyk5-2 lyk4-2*, it is likely that other proteins are involved in regulating chitin signaling or that the *lyk4-1* mutant still containing some functional LYK4 (compare above). Moreover, it is likely that CERK1 dimerization does not primarily depend on the presence of a certain LysM-protein but any LysM-protein that enables correct chitin binding together with CERK1. This higher CERK1 plasticity regarding potential LysM-protein partners allows a rapid CERK1 homodimerization which might be the only important step for downstream signaling. LYM2 is a potential interaction partner with chitin binding capacity (Petutschnig *et al.*, 2010; Shinya *et al.*, 2012). As an RLP, LYM2 might be

required for correct stereochemical chitin binding or interaction with further proteins, such as a RLCK to form a protein complex that resembles a functional RLK-like protein. However, a role in the canonical chitin signaling was not assigned to LYM2 so far. To investigate a possible involvement of LYM2 in canonical chitin signaling and to address a putative redundant function between LYK5, LYK4 and LYM2, a *lyk5-2 lyk4-2 lym2-1* triple mutant should be generated and analyzed for chitin-induced defense.

#### 4.6.1 LYK5, LYK4, and LYM2 may play a role in embryogenesis and fertility

In a triple homozygous *lyk5-2 lyk4-2 lym2-1* knockout mutant all three LysM-proteins with chitin binding affinity, except CERK1 will be absent (or at least reduced). These plants might reveal putative redundancy and also expand the understanding of the chitin recognition system. By crossing the *lyk5-2 lyk4-2* double mutant with *lym2-1* a *lyk5-2 lyk4-2 lym2-1* triple homozygous mutant could not be generated (see section 3.7). Triply homozygous plants were identified neither in the F2 nor F3 generation. However, plants that were heterozygous for *lyk5-2* and *lyk4-2* and homozygous for the *lym2-1* mutation were found. The *lyk5-2 lyk4-2 lym2-1* (het/het/hom) plants had a smaller rosette size and altered leaf shape. Importantly, they had much smaller siliques that contained fewer seeds, with several empty positions. The empty seed positions were randomly distributed within the silique (Figure 33). This did not allow any conclusions concerning maternal or paternal effects causing the observed phenotype. To investigate this further, pollination of a wildtype plant with a *lyk5-2 lyk4-2 lym2-1* (het/het/hom) plant and vice versa has to be carried out. Since LYK5, LYK4, and LYM2 are not preferentially expressed in reproductive organs, as indicated by expression analysis using the BAR eFP browser (<http://bar.utoronto.ca>; (Winter *et al.*, 2007)), a possible function of these proteins in fertility seems relatively unlikely.

However, LysM-proteins might recognize endogenous signals that are structurally similar to chitin and play a role in fertilization or embryo development. Examples are fragments of GlcNAc-containing arabinogalactan proteins in carrot (van Hengel *et al.*, 2001) and Nod-factor-like lipochitooligosaccharides in norway spruce (Dyachok *et al.*, 2002) which were found to regulate somatic embryogenesis. A role for LysM-proteins in the recognition of endogenous signals has been proposed (Brotman *et al.*, 2012). In this study, fungal chitinases were overexpressed in *A. thaliana*, which increased the resistance to abiotic stress. The enhanced stress tolerance was dependent on CERK1. Thus, CERK1 might be able to perceive endogenous molecules released by chitinases (Brotman *et al.*, 2012). So far, LysM-proteins in *Arabidopsis* have only been implicated in the recognition of non-self-molecules. The presence of

putative endogenous ligands that are signals for plant development would explain the defects observed in mutant viability and extend the functions of LysM-proteins.

Another important factor might be the regulation of PD trafficking. Regulating the PD-flux and callose deposition plays an important role in plant development (Verma and Hong, 2001; Chen and Kim, 2009). Thus, altered regulation of the PD-flux might also affect embryogenesis or fertilization. GLUCAN SYNTHASE-LIKEs/CALLOSE SYNTHASEs (GSLs) are responsible for callose synthesis in diverse tissues and upon different environmental stresses (Verma and Hong, 2001; Chen and Kim, 2009). GSL members are directly involved in cytokinesis, cell patterning, and seedling maturation (Chen and Kim, 2009) as well as pollen development (Enns *et al.*, 2005) and male gametogenesis (Töller *et al.*, 2008; Huang *et al.*, 2009). Since LYM2 is important for mediating chitin-specific regulation of the PD-flux (Faulkner *et al.*, 2013) is tempting to speculate that LysM-proteins together with LysM-RLKs may also regulate callose deposition at PD in order to control fertilization and seed development.

However, a problem with chromosome integrity cannot be excluded as the reason why triply homozygous *lyk5-2 lyk4-2 lym2-1* mutants are not viable. One (or more) of the T-DNA insertions may have led to chromosomal rearrangements. In this case, homozygosity for the recombined allele could be lethal. Indeed it has been shown that recombination rates and gametophyte survival are affected by T-DNA induced inversions and translocations that pose a problem when crossing distinct T-DNA lines to create multiple mutants (Tax and Vernon, 2001; Curtis *et al.*, 2009). Thus, it is possible that the presence of three T-DNA inserts on the same chromosome (Figure S10) has an effect on *lyk5-2 lyk4-2 lym2-1* viability.

## 4.7 Conclusion

In this study, the role of LYK5, LYK4 and LYM2 in chitin signaling was investigated by characterization of the respective knock-out (or knock-down) mutants. Differently from previous reports, LYK5 (and LYK4) mutation reduced the chitin-induced phosphorylation of CERK1, but did not or only marginally affect canonical chitin-induced defense responses, such as MAPK activation or induction of defense genes. In agreement with previous reports, no function in canonical chitin signaling was found for LYM2. A non-canonical chitin-dependent function at PD is known for LYM2, but so far not for LYK5 and LYK4. Together, the data suggest a high complexity and possible plasticity of the chitin receptor system in *Arabidopsis* and a function of LysM-proteins beyond canonical chitin perception.

The subcellular behavior of CERK1, LYK5, LYK4, and LYM2 in response to chitin was analyzed in great detail by confocal microscopy in stably transformed *Arabidopsis* plants expressing fluorescence protein fusions of these receptors. For CERK1 and LYK4, some evidence for possible chitin-induced internalization was gained. With LYK5, chitin-induced and CERK1-phosphorylation dependent endocytosis was very clear and the LYK5 endocytic path was characterized by inhibitor and co-localization studies. However, the biological relevance of LYK5 endocytosis is still elusive. Ligand-induced endocytosis of LYK5 might contribute to transient desensitization of the chitin perception system and facilitate replenishment of newly synthesized signaling competent receptors at the PM. According to the literature, this work is the first study in plants that directly links auto- and transphosphorylation events within a receptor complex to ligand-mediated endocytosis. Based on this study and the work of others, a possible scenario for chitin-induced receptor signaling in *Arabidopsis* would start with chitin binding of CERK1, followed by its homodimerization and autophosphorylation (Liu *et al.*, 2012b). Subsequently, CERK1 could transiently heterodimerize with and phosphorylate LYK5. LYK5 is then activated for its role in canonical chitin signaling and/or more specialized functions. Ultimately, the phosphorylated LYK5 becomes internalized into endosomes while CERK1 stays at the PM.

## 4.8 Outlook

In contrast to a previous study (Cao *et al.*, 2014), *lyk5-2* mutants only showed a very moderate impairment in chitin signaling in this work. The difference in the observed *lyk5-2* phenotype is very clear, but the reasons behind the discrepancies remain unknown. In order to rule out differences in the *lyk4* mutant *lyk5-2 lyk4-1* double mutant as described by Cao *et al.* would be necessary. If the *lyk5-2 lyk4-1* double mutant indeed shows no chitin signaling, this would mean that the role of LYK4 in the process has been underestimated by Cao *et al.*. If *lyk5-2 lyk4-1* still shows chitin signal transduction, a considerable amount of research will have to be performed in the future to characterize the *Arabidopsis* chitin receptor formation and elucidate the interplay between CERK1, LYK5 and LYK4. In this study, it proved to be impossible to generate triply homozygous *lyk5-2 lyk4-2 lym2-1* mutants. To find out if simultaneous loss of these proteins is lethal, or if the problem is due to chromosome rearrangements, *lyk5-2 lyk4-2 lym2-1* (het/het/hom) plant lines could be transformed to express transgenic LYK5, LYK4 or LYM2. If this allows recovery of *lyk5-2 lyk4-2 lym2-1* (hom/hom/hom) plants, it would indicate that loss of the three proteins is lethal. If not, it would point to chromosome integrity issues. Alternatively, one could try to cross other alleles for *lyk5*, *lyk4* or *lym2* or to generate multiple mutants by CRISPR/Cas9.

LYK5 undergoes chitin-induced endocytosis, but the mechanisms mediating this are not known so far. To investigate whether LYK5 endocytosis relies on clathrin-coated vesicles, specific inhibitors such as Tyrphostin A23 could be used. To address clathrin-independent endocytosis, mutants with impaired microdomain formation could be studied. Since membrane microdomains are enriched in sphingolipids and sterols, sphingolipid and sterol synthesis mutants could be suitable candidates. From animals it is known that ubiquitination of receptors drive their endocytosis. Data from different studies on FLS2 indicate that this could also be the case for plant receptor kinases (Lu *et al.*, 2011; Spallek *et al.*, 2013). LYK5 might also undergo ubiquitination that targets it for internalization. This has to be answered in pull-down and immunoblot experiments using ubiquitin antibodies. Possibly, it would be necessary to perform these experiments with samples taken from tissues where endocytosis and thus LYK5 degradation has been blocked. If indeed LYK5 is ubiquitinated, it is probably sorted into intraluminal vesicles at MVBs via the ESCRT complex similar to FLS2 (Spallek *et al.*, 2013). This could be clarified by high-resolution microscopy of labeled MVBs or co-expression of LYK5-mCitrine with components of the ESCRT complex like VPS28-1, VPS28-2, and VSP37-1. Furthermore, LYK5 subcellular behavior in the respective ESCRT knock-out mutants might be

interesting to test. CERK1 phosphorylates LYK5 upon chitin elicitation, which seems to be the driving signal behind LYK5 endocytosis. CERK1 itself is also phosphorylated in response to chitin and SDS-PAGE mobility shift assays indicated that this is reduced in *lyk5-2* mutants, while canonical downstream events are largely unaffected. A detailed analysis of chitin-induced phosphorylation of CERK1, LYK5 and LYK4 would probably further our understanding of chitin signaling. To do this, CERK1, LYK5 and LYK4 could be pulled down via protein tags or with chitin magnetic beads and chitin-induced phosphorylation sites could be identified via Immobilized Metal Affinity Chromatography (IMAC) followed by mass spectrometry. This way phosphorylation of CERK1 could also be analyzed in the *lyk5*, *lyk4* or double mutant background. This might reveal LYK5 and/or LYK4-dependent phosphorylation sites on CERK1 and should also be able to clarify if CERK1 has tyrosine kinase activity. The exact role of specific phosphorylation sites or clusters could then be investigated by mutating them to residues that cannot be phosphorylated or mimic phosphorylation.

CERK1 has been reported to homodimerize in response to chitin (Liu *et al.*, 2012b), while LYK5 appears to homodimerize constitutively and heterodimerize with CERK1 upon chitin recognition (Cao *et al.*, 2014). These findings are based on transient expression in protoplasts subsequent Co-IP experiments. To investigate constitutive and chitin-induced interaction between CERK1, LYK5 and LYK4 in more detail, BiFC and FRET analyses could be performed. A cloning system that allows expression of multiple genes from one T-DNA has been established in the lab (Ghareeb *et al.*, 2016). This could be utilized to perform BiFC and FRET analysis in stably transformed *Arabidopsis* plants. Since LYK5 and LYK4 are substrates of CERK1 phosphorylation, their interaction with other CERK1 phosphorylation substrates could be tested. Potential candidates are the RLCKs CLR1 (Ziegler, 2015) and PBL27 (Shinya *et al.*, 2014). Again, Co-IP, BiFC or FRET approaches could be taken. It would also be interesting to study CLR1 and/or PBL27 phosphorylation in a *lyk5* and/or *lyk4* knock-out background.

Last but not least, fluorescently-tagged LYK5 lines could be tested for interaction with fungal pathogens to analyze the subcellular behavior of the protein upon fungal penetration attempts. Overall, the proposed further analyses would generate novel insights into membrane trafficking in plants and its contribution to immune responses.

## 5 References

**Alfano JR, Collmer A (1997)** The type III (Hrp) secretion pathway of plant pathogenic bacteria: trafficking harpins, Avr proteins, and death. *J Bacteriol* **179**: 5655-5662

**Alonso JM, Stepanova AN, Leisse TJ, Kim CJ, Chen H, Shinn P, Stevenson DK, Zimmerman J, Barajas P, Cheuk R, Gadrinab C, Heller C, Jeske A, Koesema E, Meyers CC, Parker H, Prednis L, Ansari Y, Choy N, Deen H, Geralt M, Hazari N, Hom E, Karnes M, Mulholland C, Ndubaku R, Schmidt I, Guzman P, Aguilar-Henonin L, Schmid M, Weigel D, Carter DE, Marchand T, Risseuw E, Brogden D, Zeko A, Crosby WL, Berry CC, Ecker JR (2003)** Genome-wide insertional mutagenesis of *Arabidopsis thaliana*. *Science* **301**: 653-657

**Aniento F, Robinson DG (2005)** Testing for endocytosis in plants. *Protoplasma* **226**: 3-11

**Antolin-Llovera M, Petutsching EK, Ried MK, Lipka V, Nurnberger T, Robatzek S, Parniske M (2014a)** Knowing your friends and foes--plant receptor-like kinases as initiators of symbiosis or defence. *New Phytol* **204**: 791-802

**Antolin-Llovera M, Ried MK, Binder A, Parniske M (2012)** Receptor kinase signaling pathways in plant-microbe interactions. *Annu Rev Phytopathol* **50**: 451-473

**Antolin-Llovera M, Ried MK, Parniske M (2014b)** Cleavage of the SYMBIOSIS RECEPTOR-LIKE KINASE ectodomain promotes complex formation with Nod factor receptor 5. *Curr Biol* **24**: 422-427

**Ao Y, Li Z, Feng D, Xiong F, Liu J, Li JF, Wang M, Wang J, Liu B, Wang HB (2014)** OsCERK1 and OsRLCK176 play important roles in peptidoglycan and chitin signaling in rice innate immunity. *Plant J* **80**: 1072-1084

**Arrighi JF, Barre A, Ben Amor B, Bersoult A, Soriano LC, Mirabella R, de Carvalho-Niebel F, Journet EP, Gherardi M, Huguet T, Geurts R, Denarie J, Rouge P, Gough C (2006)** The *Medicago truncatula* lysin [corrected] motif-receptor-like kinase gene family includes NFP and new nodule-expressed genes. *Plant Physiol* **142**: 265-279

**Asaoka R, Uemura T, Ito J, Fujimoto M, Ito E, Ueda T, Nakano A (2013)** *Arabidopsis* RABA1 GTPases are involved in transport between the trans-Golgi network and the plasma membrane, and are required for salinity stress tolerance. *Plant J* **73**: 240-249

**Ausubel FM (2003)** *Current protocols in molecular biology*, Brooklyn, N. Y.: Greene Publishing Associates ; Media.

**Ausubel FM (2005)** Are innate immune signaling pathways in plants and animals conserved? *Nat Immunol* **6**: 973-979

**Badel JL, Nomura K, Bandyopadhyay S, Shimizu R, Collmer A, He SY (2003)** *Pseudomonas syringae* pv. tomato DC3000 HopPtoM (CEL ORF3) is important for lesion formation but not growth in tomato and is secreted and translocated by the Hrp type III secretion system in a chaperone-dependent manner. *Mol Microbiol* **49**: 1239-1251



- Baluska F, Hlavacka A, Samaj J, Palme K, Robinson DG, Match T, McCurdy DW, Menzel D, Volkmann D (2002)** F-actin-dependent endocytosis of cell wall pectins in meristematic root cells. Insights from brefeldin A-induced compartments. *Plant Physiol* **130**: 422-431
- Bar M, Avni A (2009a)** EHD2 inhibits ligand-induced endocytosis and signaling of the leucine-rich repeat receptor-like protein LeEix2. *Plant J* **59**: 600-611
- Bar M, Avni A (2009b)** EHD2 inhibits signaling of leucine rich repeat receptor-like proteins. *Plant Signaling & Behavior* **4**: 682-684
- Bar M, Sharfman M, Ron M, Avni A (2010)** BAK1 is required for the attenuation of ethylene-inducing xylanase (Eix)-induced defense responses by the decoy receptor LeEix1. *Plant J* **63**: 791-800
- Barberon M, Zelazny E, Robert S, Conejero G, Curie C, Friml J, Vert G (2011)** Monoubiquitin-dependent endocytosis of the iron-regulated transporter 1 (IRT1) transporter controls iron uptake in plants. *Proc Natl Acad Sci U S A* **108**: E450-458
- Bartels S, Boller T (2015)** Quo vadis, Pep? Plant elicitor peptides at the crossroads of immunity, stress, and development. *J Exp Bot* **66**: 5183-5193
- Barth M, Holstein SE (2004)** Identification and functional characterization of Arabidopsis AP180, a binding partner of plant alphaC-adaptin. *J Cell Sci* **117**: 2051-2062
- Barton DA, Cole L, Collings DA, Liu DY, Smith PM, Day DA, Overall RL (2011)** Cell-to-cell transport via the lumen of the endoplasmic reticulum. *Plant J* **66**: 806-817
- Baskin TI, Wilson JE, Cork A, Williamson RE (1994)** Morphology and microtubule organization in Arabidopsis roots exposed to oryzalin or taxol. *Plant Cell Physiol* **35**: 935-942
- Batley NH, James NC, Greenland AJ, Brownlee C (1999)** Exocytosis and endocytosis. *Plant Cell* **11**: 643-660
- Beck M, Zhou J, Faulkner C, MacLean D, Robatzek S (2012)** Spatio-temporal cellular dynamics of the Arabidopsis flagellin receptor reveal activation status-dependent endosomal sorting. *Plant Cell* **24**: 4205-4219
- Ben Khaled S, Postma J, Robatzek S (2015)** A moving view: subcellular trafficking processes in pattern recognition receptor-triggered plant immunity. *Annu Rev Phytopathol* **53**: 379-402
- Betz WJ, Mao F, Bewick GS (1992)** Activity-dependent fluorescent staining and destaining of living vertebrate motor nerve terminals. *J Neurosci* **12**: 363-375
- Birnboim HC, Doly J (1979)** A rapid alkaline extraction procedure for screening recombinant plasmid DNA. *Nucleic Acids Res* **7**: 1513-1523
- Bittel P, Robatzek S (2007)** Microbe-associated molecular patterns (MAMPs) probe plant immunity. *Curr Opin Plant Biol* **10**: 335-341

- Böhm H, Albert I, Fan L, Reinhard A, Nurnberger T (2014)** Immune receptor complexes at the plant cell surface. *Curr Opin Plant Biol* **20**: 47-54
- Boller T, Felix G (2009)** A renaissance of elicitors: perception of microbe-associated molecular patterns and danger signals by pattern-recognition receptors. *Annu Rev Plant Biol* **60**: 379-406
- Boller T, He SY (2009)** Innate immunity in plants: an arms race between pattern recognition receptors in plants and effectors in microbial pathogens. *Science* **324**: 742-744
- Bolte S, Talbot C, Boutte Y, Catrice O, Read ND, Satiat-Jeunemaitre B (2004)** FM-dyes as experimental probes for dissecting vesicle trafficking in living plant cells. *J Microsc* **214**: 159-173
- Borner GH, Lilley KS, Stevens TJ, Dupree P (2003)** Identification of glycosylphosphatidylinositol-anchored proteins in Arabidopsis. A proteomic and genomic analysis. *Plant Physiol* **132**: 568-577
- Boyes DC, Zayed AM, Ascenzi R, McCaskill AJ, Hoffman NE, Davis KR, Gortlach J (2001)** Growth stage-based phenotypic analysis of Arabidopsis: a model for high throughput functional genomics in plants. *Plant Cell* **13**: 1499-1510
- Brachmann CB, Davies A, Cost GJ, Caputo E, Li J, Hieter P, Boeke JD (1998)** Designer deletion strains derived from *Saccharomyces cerevisiae* S288C: a useful set of strains and plasmids for PCR-mediated gene disruption and other applications. *Yeast* **14**: 115-132
- Bradford MM (1976)** A rapid and sensitive method for the quantitation of microgram quantities of protein utilizing the principle of protein-dye binding. *Anal Biochem* **72**: 248-254
- Broghammer A, Krusell L, Blaise M, Sauer J, Sullivan JT, Maolanon N, Vinther M, Lorentzen A, Madsen EB, Jensen KJ, Roepstorff P, Thirup S, Ronson CW, Thygesen MB, Stougaard J (2012)** Legume receptors perceive the rhizobial lipochitin oligosaccharide signal molecules by direct binding. *Proc Natl Acad Sci U S A* **109**: 13859-13864
- Brotman Y, Landau U, Pnini S, Lisec J, Balazadeh S, Mueller-Roeber B, Zilberstein A, Willmitzer L, Chet I, Viterbo A (2012)** The LysM receptor-like kinase LysM RLK1 is required to activate defense and abiotic-stress responses induced by overexpression of fungal chitinases in Arabidopsis plants. *Mol Plant* **5**: 1113-1124
- Buist G, Steen A, Kok J, Kuipers OP (2008)** LysM, a widely distributed protein motif for binding to (peptido)glycans. *Mol Microbiol* **68**: 838-847
- Burch-Smith TM, Stonebloom S, Xu M, Zambryski PC (2011)** Plasmodesmata during development: re-examination of the importance of primary, secondary, and branched plasmodesmata structure versus function. *Protoplasma* **248**: 61-74
- Burch-Smith TM, Zambryski PC (2012)** Plasmodesmata paradigm shift: regulation from without versus within. *Annu Rev Plant Biol* **63**: 239-260
- Cai Y, Zhuang X, Gao C, Wang X, Jiang L (2014)** The Arabidopsis Endosomal Sorting Complex Required for Transport III Regulates Internal Vesicle Formation of the Prevacuolar Compartment and Is Required for Plant Development. *Plant Physiol* **165**: 1328-1343

- Cao Y, Liang Y, Tanaka K, Nguyen CT, Jedrzejczak RP, Joachimiak A, Stacey G (2014)** The kinase LYK5 is a major chitin receptor in Arabidopsis and forms a chitin-induced complex with related kinase CERK1. *Elife* **3**
- Carvalho Ade O, Gomes VM (2011)** Plant defensins and defensin-like peptides - biological activities and biotechnological applications. *Current Pharmaceutical Design* **17**: 4270-4293
- Castells E, Casacuberta JM (2007)** Signalling through kinase-defective domains: the prevalence of atypical receptor-like kinases in plants. *J Exp Bot* **58**: 3503-3511
- Chatterjee S, Chaudhury S, McShan AC, Kaur K, De Guzman RN (2013)** Structure and biophysics of type III secretion in bacteria. *Biochemistry* **52**: 2508-2517
- Chen C, Zhang Y, Zhu L, Yuan M (2010)** The actin cytoskeleton is involved in the regulation of the plasmodesmal size exclusion limit. *Plant Signal Behav* **5**: 1663-1665
- Chen X, Irani NG, Friml J (2011)** Clathrin-mediated endocytosis: the gateway into plant cells. *Curr Opin Plant Biol* **14**: 674-682
- Chen XY, Kim JY (2009)** Callose synthesis in higher plants. *Plant Signaling & Behavior* **4**: 489-492
- Chinchilla D, Bauer Z, Regenass M, Boller T, Felix G (2006)** The Arabidopsis receptor kinase FLS2 binds flg22 and determines the specificity of flagellin perception. *Plant Cell* **18**: 465-476
- Chinchilla D, Zipfel C, Robatzek S, Kemmerling B, Nurnberger T, Jones JD, Felix G, Boller T (2007)** A flagellin-induced complex of the receptor FLS2 and BAK1 initiates plant defence. *Nature* **448**: 497-500
- Chisholm ST, Coaker G, Day B, Staskawicz BJ (2006)** Host-microbe interactions: shaping the evolution of the plant immune response. *Cell* **124**: 803-814
- Choi SW, Tamaki T, Ebine K, Uemura T, Ueda T, Nakano A (2013)** RABA members act in distinct steps of subcellular trafficking of the FLAGELLIN SENSING2 receptor. *Plant Cell* **25**: 1174-1187
- Chow CM, Neto H, Foucart C, Moore I (2008)** Rab-A2 and Rab-A3 GTPases define a trans-golgi endosomal membrane domain in Arabidopsis that contributes substantially to the cell plate. *Plant Cell* **20**: 101-123
- Christensen NM, Faulkner C, Oparka K (2009)** Evidence for unidirectional flow through plasmodesmata. *Plant Physiol* **150**: 96-104
- Christianson TW, Sikorski RS, Dante M, Shero JH, Hieter P (1992)** Multifunctional yeast high-copy-number shuttle vectors. *Gene* **110**: 119-122
- Clay NK, Adio AM, Denoux C, Jander G, Ausubel FM (2009)** Glucosinolate metabolites required for an Arabidopsis innate immune response. *Science* **323**: 95-101
- Clough SJ, Bent AF (1998)** Floral dip: a simplified method for Agrobacterium-mediated transformation of Arabidopsis thaliana. *Plant J* **16**: 735-743

- Cohen PT, Cohen P (1989)** Discovery of a protein phosphatase activity encoded in the genome of bacteriophage lambda. Probable identity with open reading frame 221. *Biochem J* **260**: 931-934
- Contento AL, Bassham DC (2012)** Structure and function of endosomes in plant cells. *J Cell Sci* **125**: 3511-3518
- Curtis MJ, Belcram K, Bollmann SR, Tominey CM, Hoffman PD, Mercier R, Hays JB (2009)** Reciprocal chromosome translocation associated with TDNA-insertion mutation in Arabidopsis: genetic and cytological analyses of consequences for gametophyte development and for construction of doubly mutant lines. *Planta* **229**: 731-745
- Cutler SR, Ehrhardt DW, Griffitts JS, Somerville CR (2000)** Random GFP::cDNA fusions enable visualization of subcellular structures in cells of Arabidopsis at a high frequency. *Proc Natl Acad Sci U S A* **97**: 3718-3723
- Dangl JL, Horvath DM, Staskawicz BJ (2013)** Pivoting the plant immune system from dissection to deployment. *Science* **341**: 746-751
- Dangl JL, Jones JD (2001)** Plant pathogens and integrated defence responses to infection. *Nature* **411**: 826-833
- Dardick C, Schwessinger B, Ronald P (2012)** Non-arginine-aspartate (non-RD) kinases are associated with innate immune receptors that recognize conserved microbial signatures. *Curr Opin Plant Biol* **15**: 358-366
- de Jonge R, van Esse HP, Kombrink A, Shinya T, Desaki Y, Bours R, van der Krol S, Shibuya N, Joosten MH, Thomma BP (2010)** Conserved fungal LysM effector Ecp6 prevents chitin-triggered immunity in plants. *Science* **329**: 953-955
- de Wit PJ (2007)** How plants recognize pathogens and defend themselves. *Cell Mol Life Sci* **64**: 2726-2732
- De Wit PJ, Mehrabi R, Van den Burg HA, Stergiopoulos I (2009)** Fungal effector proteins: past, present and future. *Mol Plant Pathol* **10**: 735-747
- Dettmer J, Hong-Hermesdorf A, Stierhof YD, Schumacher K (2006)** Vacuolar H<sup>+</sup>-ATPase activity is required for endocytic and secretory trafficking in Arabidopsis. *Plant Cell* **18**: 715-730
- Dhonukshe P, Aniento F, Hwang I, Robinson DG, Mravec J, Stierhof YD, Friml J (2007)** Clathrin-mediated constitutive endocytosis of PIN auxin efflux carriers in Arabidopsis. *Curr Biol* **17**: 520-527
- Di Rubbo S, Irani NG, Kim SY, Xu ZY, Gadeyne A, Dejonghe W, Vanhoutte I, Persiau G, Eeckhout D, Simon S, Song K, Kleine-Vehn J, Friml J, De Jaeger G, Van Damme D, Hwang I, Russinova E (2013)** The clathrin adaptor complex AP-2 mediates endocytosis of brassinosteroid insensitive1 in Arabidopsis. *Plant Cell* **25**: 2986-2997
- Dodds PN, Rathjen JP (2010)** Plant immunity: towards an integrated view of plant-pathogen interactions. *Nat Rev Genet* **11**: 539-548

- Drakakaki G, van de Ven W, Pan S, Miao Y, Wang J, Keinath NF, Weatherly B, Jiang L, Schumacher K, Hicks G, Raikhel N (2012)** Isolation and proteomic analysis of the SYP61 compartment reveal its role in exocytic trafficking in Arabidopsis. *Cell Res* **22**: 413-424
- Drdova EJ, Synek L, Pecenkova T, Hala M, Kulich I, Fowler JE, Murphy AS, Zarsky V (2013)** The exocyst complex contributes to PIN auxin efflux carrier recycling and polar auxin transport in Arabidopsis. *Plant J* **73**: 709-719
- Dyachok JV, Wiweger M, Kenne L, von Arnold S (2002)** Endogenous Nod-factor-like signal molecules promote early somatic embryo development in Norway spruce. *Plant Physiol* **128**: 523-533
- Ebine K, Fujimoto M, Okatani Y, Nishiyama T, Goh T, Ito E, Dainobu T, Nishitani A, Uemura T, Sato MH, Thordal-Christensen H, Tsutsumi N, Nakano A, Ueda T (2011)** A membrane trafficking pathway regulated by the plant-specific RAB GTPase ARA6. *Nat Cell Biol* **13**: 853-859
- Eisenhaber B, Bork P, Eisenhaber F (1999)** Prediction of potential GPI-modification sites in proprotein sequences. *J Mol Biol* **292**: 741-758
- Ellinger D, Voigt CA (2014)** Callose biosynthesis in Arabidopsis with a focus on pathogen response: what we have learned within the last decade. *Ann Bot* **114**: 1349-1358
- Elmore JM, Lin ZJ, Coaker G (2011)** Plant NB-LRR signaling: upstreams and downstreams. *Curr Opin Plant Biol* **14**: 365-371
- Emans N, Zimmermann S, Fischer R (2002)** Uptake of a fluorescent marker in plant cells is sensitive to brefeldin A and wortmannin. *Plant Cell* **14**: 71-86
- Enns LC, Kanaoka MM, Torii KU, Comai L, Okada K, Cleland RE (2005)** Two callose synthases, GSL1 and GSL5, play an essential and redundant role in plant and pollen development and in fertility. *Plant Mol Biol* **58**: 333-349
- Erwig J (2012)** The Function of Arabidopsis LysM-RLK3, LysM-RLK4 and LYM2 in Chitin Signaling and other CERK1-mediated Processes.
- Eyers PA, Murphy JM (2013)** Dawn of the dead: protein pseudokinases signal new adventures in cell biology. *Biochem Soc Trans* **41**: 969-974
- Fan L, Li R, Pan J, Ding Z, Lin J (2015)** Endocytosis and its regulation in plants. *Trends Plant Sci* **20**: 388-397
- Faulkner C, Petutschnig E, Benitez-Alfonso Y, Beck M, Robatzek S, Lipka V, Maule AJ (2013)** LYM2-dependent chitin perception limits molecular flux via plasmodesmata. *Proc Natl Acad Sci U S A* **110**: 9166-9170
- Felix G, Baureithel K, Boller T (1998)** Desensitization of the perception system for chitin fragments in tomato cells. *Plant Physiol* **117**: 643-650

**Feraru E, Feraru MI, Asaoka R, Paciorek T, De Rycke R, Tanaka H, Nakano A, Friml J (2012)** BEX5/RabA1b regulates trans-Golgi network-to-plasma membrane protein trafficking in Arabidopsis. *Plant Cell* **24**: 3074-3086

**Fernandez-Calvino L, Faulkner C, Walshaw J, Saalbach G, Bayer E, Benitez-Alfonso Y, Maule A (2011)** Arabidopsis plasmodesmal proteome. *PLoS One* **6**: e18880

**Ferrer M, Chernikova TN, Yakimov MM, Golyshin PN, Timmis KN (2003)** Chaperonins govern growth of Escherichia coli at low temperatures. *Nat Biotechnol* **21**: 1266-1267

**Fliegmann J, Canova S, Lachaud C, Uhlenbroich S, Gascioli V, Pichereaux C, Rossignol M, Rosenberg C, Cumener M, Pitorre D, Lefebvre B, Gough C, Samain E, Fort S, Driguez H, Vauzeilles B, Beau JM, Nurisso A, Imberty A, Cullimore J, Bono JJ (2013)** Lipochitooligosaccharidic symbiotic signals are recognized by LysM receptor-like kinase LYR3 in the legume Medicago truncatula. *ACS Chem Biol* **8**: 1900-1906

**Gadeyne A, Sanchez-Rodriguez C, Vanneste S, Di Rubbo S, Zauber H, Vanneste K, Van Leene J, De Winne N, Eeckhout D, Persiau G, Van De Slijke E, Cannoot B, Vercruysse L, Mayers JR, Adamowski M, Kania U, Ehrlich M, Schweighofer A, Ketelaar T, Maere S, Bednarek SY, Friml J, Gevaert K, Witters E, Russinova E, Persson S, De Jaeger G, Van Damme D (2014)** The TPLATE adaptor complex drives clathrin-mediated endocytosis in plants. *Cell* **156**: 691-704

**Ganguly A, Park M, Kesawat MS, Cho HT (2014)** Functional Analysis of the Hydrophilic Loop in Intracellular Trafficking of Arabidopsis PIN-FORMED Proteins. *Plant Cell* **26**: 1570-1585

**Gao M, Wang X, Wang D, Xu F, Ding X, Zhang Z, Bi D, Cheng YT, Chen S, Li X, Zhang Y (2009)** Regulation of cell death and innate immunity by two receptor-like kinases in Arabidopsis. *Cell Host Microbe* **6**: 34-44

**Geldner N, Anders N, Wolters H, Keicher J, Kornberger W, Muller P, Delbarre A, Ueda T, Nakano A, Jurgens G (2003)** The Arabidopsis GNOM ARF-GEF mediates endosomal recycling, auxin transport, and auxin-dependent plant growth. *Cell* **112**: 219-230

**Geldner N, Denervaud-Tendon V, Hyman DL, Mayer U, Stierhof YD, Chory J (2009)** Rapid, combinatorial analysis of membrane compartments in intact plants with a multicolor marker set. *Plant J* **59**: 169-178

**Geldner N, Hyman DL, Wang X, Schumacher K, Chory J (2007)** Endosomal signaling of plant steroid receptor kinase BRI1. *Genes Dev* **21**: 1598-1602

**Geldner N, Robatzek S (2008)** Plant receptors go endosomal: a moving view on signal transduction. *Plant Physiol* **147**: 1565-1574

**Gera JF, Hazbun TR, Fields S (2002)** Array-based methods for identifying protein-protein and protein-nucleic acid interactions. *Methods Enzymol* **350**: 499-512

**Ghareeb H, Laukamm S, Lipka V (2016)** COLORFUL-Circuit: a platform for rapid multigene assembly, delivery and expression in plants. *Front Plant Sci*

- Gimenez-Ibanez S, Hann DR, Ntoukakis V, Petutschnig E, Lipka V, Rathjen JP (2009a)** AvrPtoB targets the LysM receptor kinase CERK1 to promote bacterial virulence on plants. *Curr Biol* **19**: 423-429
- Gimenez-Ibanez S, Ntoukakis V, Rathjen JP (2009b)** The LysM receptor kinase CERK1 mediates bacterial perception in Arabidopsis. *Plant Signaling & Behavior* **4**: 539-541
- Goh LK, Sorkin A (2013)** Endocytosis of receptor tyrosine kinases. *Cold Spring Harb Perspect Biol* **5**: a017459
- Goh T, Uchida W, Arakawa S, Ito E, Dainobu T, Ebine K, Takeuchi M, Sato K, Ueda T, Nakano A (2007)** VPS9a, the common activator for two distinct types of Rab5 GTPases, is essential for the development of Arabidopsis thaliana. *Plant Cell* **19**: 3504-3515
- Göhre V, Spallek T, Haweker H, Mersmann S, Mentzel T, Boller T, de Torres M, Mansfield JW, Robatzek S (2008)** Plant pattern-recognition receptor FLS2 is directed for degradation by the bacterial ubiquitin ligase AvrPtoB. *Curr Biol* **18**: 1824-1832
- Gomez-Gomez L, Boller T (2000)** FLS2: an LRR receptor-like kinase involved in the perception of the bacterial elicitor flagellin in Arabidopsis. *Mol Cell* **5**: 1003-1011
- Gordon JA (1991)** Use of vanadate as protein-phosphotyrosine phosphatase inhibitor. *Methods Enzymol* **201**: 477-482
- Grison MS, Brocard L, Fouillen L, Nicolas W, Wewer V, Dormann P, Nacir H, Benitez-Alfonso Y, Claverol S, Germain V, Boutte Y, Mongrand S, Bayer EM (2015)** Specific membrane lipid composition is important for plasmodesmata function in Arabidopsis. *Plant Cell* **27**: 1228-1250
- Grodberg J, Dunn JJ (1988)** ompT encodes the Escherichia coli outer membrane protease that cleaves T7 RNA polymerase during purification. *J Bacteriol* **170**: 1245-1253
- Guenoune-Gelbart D, Elbaum M, Sagi G, Levy A, Epel BL (2008)** Tobacco mosaic virus (TMV) replicase and movement protein function synergistically in facilitating TMV spread by lateral diffusion in the plasmodesmal desmotubule of Nicotiana benthamiana. *Mol Plant Microbe Interact* **21**: 335-345
- Guseman JM, Lee JS, Bogenschutz NL, Peterson KM, Virata RE, Xie B, Kanaoka MM, Hong Z, Torii KU (2010)** Dysregulation of cell-to-cell connectivity and stomatal patterning by loss-of-function mutation in Arabidopsis chorus (glucan synthase-like 8). *Development* **137**: 1731-1741
- Gust AA, Biswas R, Lenz HD, Rauhut T, Ranf S, Kemmerling B, Gotz F, Glawischnig E, Lee J, Felix G, Nurnberger T (2007)** Bacteria-derived peptidoglycans constitute pathogen-associated molecular patterns triggering innate immunity in Arabidopsis. *J Biol Chem* **282**: 32338-32348
- Gust AA, Felix G (2014)** Receptor like proteins associate with SOBIR1-type of adaptors to form bimolecular receptor kinases. *Curr Opin Plant Biol* **21**: 104-111

- Gust AA, Willmann R, Desaki Y, Grabherr HM, Nurnberger T (2012)** Plant LysM proteins: modules mediating symbiosis and immunity. *Trends Plant Sci* **17**: 495-502
- Haas TJ, Sliwinski MK, Martinez DE, Preuss M, Ebine K, Ueda T, Nielsen E, Odorizzi G, Otegui MS (2007)** The Arabidopsis AAA ATPase SKD1 is involved in multivesicular endosome function and interacts with its positive regulator LYST-INTERACTING PROTEIN5. *Plant Cell* **19**: 1295-1312
- Hacke R (2013)** LysM-Proteins and Kinases - Putative Interactors of CERK1.
- Haglund K, Dikic I (2012)** The role of ubiquitylation in receptor endocytosis and endosomal sorting. *J Cell Sci* **125**: 265-275
- Han X, Hyun TK, Zhang M, Kumar R, Koh EJ, Kang BH, Lucas WJ, Kim JY (2014)** Auxin-callose-mediated plasmodesmal gating is essential for tropic auxin gradient formation and signaling. *Dev Cell* **28**: 132-146
- Haney CH, Long SR (2010)** Plant flotillins are required for infection by nitrogen-fixing bacteria. *Proc Natl Acad Sci U S A* **107**: 478-483
- Haney CH, Riely BK, Tricoli DM, Cook DR, Ehrhardt DW, Long SR (2011)** Symbiotic rhizobia bacteria trigger a change in localization and dynamics of the Medicago truncatula receptor kinase LYK3. *Plant Cell* **23**: 2774-2787
- Hanks SK, Hunter T (1995)** Protein kinases 6. The eukaryotic protein kinase superfamily: kinase (catalytic) domain structure and classification. *FASEB J* **9**: 576-596
- Hanks SK, Quinn AM, Hunter T (1988)** The protein kinase family: conserved features and deduced phylogeny of the catalytic domains. *Science* **241**: 42-52
- Hann DR, Rathjen JP (2007)** Early events in the pathogenicity of *Pseudomonas syringae* on *Nicotiana benthamiana*. *Plant J* **49**: 607-618
- Hayafune M, Berisio R, Marchetti R, Silipo A, Kayama M, Desaki Y, Arima S, Squeglia F, Ruggiero A, Tokuyasu K, Molinaro A, Kaku H, Shibuya N (2014)** Chitin-induced activation of immune signaling by the rice receptor CEBiP relies on a unique sandwich-type dimerization. *Proc Natl Acad Sci U S A* **111**: E404-413
- Haywood V, Kragler F, Lucas WJ (2002)** Plasmodesmata: pathways for protein and ribonucleoprotein signaling. *Plant Cell* **14 Suppl**: S303-325
- Heath MC (2000)** Nonhost resistance and nonspecific plant defenses. *Curr Opin Plant Biol* **3**: 315-319
- Heese A, Hann DR, Gimenez-Ibanez S, Jones AM, He K, Li J, Schroeder JI, Peck SC, Rathjen JP (2007)** The receptor-like kinase SERK3/BAK1 is a central regulator of innate immunity in plants. *Proc Natl Acad Sci U S A* **104**: 12217-12222
- Hellens RP, Edwards EA, Leyland NR, Bean S, Mullineaux PM (2000)** pGreen: a versatile and flexible binary Ti vector for *Agrobacterium*-mediated plant transformation. *Plant Mol Biol* **42**: 819-832



- Huang L, Chen XY, Rim Y, Han X, Cho WK, Kim SW, Kim JY (2009)** Arabidopsis glucan synthase-like 10 functions in male gametogenesis. *J Plant Physiol* **166**: 344-352
- Huffaker A, Pearce G, Veyrat N, Erb M, Turlings TC, Sartor R, Shen Z, Briggs SP, Vaughan MM, Alborn HT, Teal PE, Schmelz EA (2013)** Plant elicitor peptides are conserved signals regulating direct and indirect antiherbivore defense. *Proc Natl Acad Sci U S A* **110**: 5707-5712
- Huffaker A, Ryan CA (2007)** Endogenous peptide defense signals in Arabidopsis differentially amplify signaling for the innate immune response. *Proc Natl Acad Sci U S A* **104**: 10732-10736
- Iizasa E, Mitsutomi M, Nagano Y (2010)** Direct binding of a plant LysM receptor-like kinase, LysM RLK1/CERK1, to chitin in vitro. *J Biol Chem* **285**: 2996-3004
- Irani NG, Di Rubbo S, Mylle E, Van den Begin J, Schneider-Pizon J, Hnilikova J, Sisa M, Buyst D, Vilarrasa-Blasi J, Szatmari AM, Van Damme D, Mishev K, Codreanu MC, Kohout L, Strnad M, Cano-Delgado AI, Friml J, Madder A, Russinova E (2012)** Fluorescent castasterone reveals BRI1 signaling from the plasma membrane. *Nat Chem Biol* **8**: 583-589
- Irani NG, Russinova E (2009)** Receptor endocytosis and signaling in plants. *Curr Opin Plant Biol* **12**: 653-659
- Jackson CL, Casanova JE (2000)** Turning on ARF: the Sec7 family of guanine-nucleotide-exchange factors. *Trends Cell Biol* **10**: 60-67
- Jacobson AD, Zhang NY, Xu P, Han KJ, Noone S, Peng J, Liu CW (2009)** The lysine 48 and lysine 63 ubiquitin conjugates are processed differently by the 26 S proteasome. *J Biol Chem* **284**: 35485-35494
- Jelinkova A, Malinska K, Simon S, Kleine-Vehn J, Parezova M, Pejchar P, Kubes M, Martinec J, Friml J, Zazimalova E, Petrasek J (2010)** Probing plant membranes with FM dyes: tracking, dragging or blocking? *Plant J* **61**: 883-892
- Jiang X, Huang F, Marusyk A, Sorkin A (2003)** Grb2 regulates internalization of EGF receptors through clathrin-coated pits. *Mol Biol Cell* **14**: 858-870
- Jin Q, Thilmony R, Zwiesler-Vollick J, He SY (2003)** Type III protein secretion in *Pseudomonas syringae*. *Microbes Infect* **5**: 301-310
- Jones JD, Dangl JL (2006)** The plant immune system. *Nature* **444**: 323-329
- Kaksonen M, Toret CP, Drubin DG (2005)** A modular design for the clathrin- and actin-mediated endocytosis machinery. *Cell* **123**: 305-320
- Kaku H, Nishizawa Y, Ishii-Minami N, Akimoto-Tomiya C, Dohmae N, Takio K, Minami E, Shibuya N (2006)** Plant cells recognize chitin fragments for defense signaling through a plasma membrane receptor. *Proc Natl Acad Sci U S A* **103**: 11086-11091
- Kang Y, Jelenska J, Cecchini NM, Li Y, Lee MW, Kovar DR, Greenberg JT (2014)** HopW1 from *Pseudomonas syringae* disrupts the actin cytoskeleton to promote virulence in Arabidopsis. *PLoS Pathog* **10**: e1004232

- Kankanala P, Czymmek K, Valent B (2007)** Roles for rice membrane dynamics and plasmodesmata during biotrophic invasion by the blast fungus. *Plant Cell* **19**: 706-724
- Karlova R, Boeren S, van Dongen W, Kwaaitaal M, Aker J, Vervoort J, de Vries S (2009)** Identification of in vitro phosphorylation sites in the Arabidopsis thaliana somatic embryogenesis receptor-like kinases. *Proteomics* **9**: 368-379
- Katzmann DJ, Odorizzi G, Emr SD (2002)** Receptor downregulation and multivesicular-body sorting. *Nat Rev Mol Cell Biol* **3**: 893-905
- Kawaharada Y, Kelly S, Nielsen MW, Hjuler CT, Gysel K, Muszynski A, Carlson RW, Thygesen MB, Sandal N, Asmussen MH, Vinther M, Andersen SU, Krusell L, Thirup S, Jensen KJ, Ronson CW, Blaise M, Radutoiu S, Stougaard J (2015)** Receptor-mediated exopolysaccharide perception controls bacterial infection. *Nature* **523**: 308-312
- Kazacic M, Bertelsen V, Pedersen KW, Vuong TT, Grandal MV, Rodland MS, Traub LM, Stang E, Madshus IH (2009)** Epsin 1 is involved in recruitment of ubiquitinated EGF receptors into clathrin-coated pits. *Traffic* **10**: 235-245
- Kearse M, Moir R, Wilson A, Stones-Havas S, Cheung M, Sturrock S, Buxton S, Cooper A, Markowitz S, Duran C, Thierer T, Ashton B, Meintjes P, Drummond A (2012)** Geneious Basic: an integrated and extendable desktop software platform for the organization and analysis of sequence data. *Bioinformatics* **28**: 1647-1649
- Kelly BT, Graham SC, Liska N, Dannhauser PN, Honing S, Ungewickell EJ, Owen DJ (2014)** Clathrin adaptors. AP2 controls clathrin polymerization with a membrane-activated switch. *Science* **345**: 459-463
- Kirchhausen T (2000)** Three ways to make a vesicle. *Nat Rev Mol Cell Biol* **1**: 187-198
- Kirchhausen T (2009)** Imaging endocytic clathrin structures in living cells. *Trends Cell Biol* **19**: 596-605
- Kishimoto K, Kouzai Y, Kaku H, Shibuya N, Minami E, Nishizawa Y (2010)** Perception of the chitin oligosaccharides contributes to disease resistance to blast fungus *Magnaporthe oryzae* in rice. *Plant J* **64**: 343-354
- Kleinboelting N, Huet G, Kloetgen A, Viehoveer P, Weisshaar B (2012)** GABI-Kat SimpleSearch: new features of the Arabidopsis thaliana T-DNA mutant database. *Nucleic Acids Res* **40**: D1211-1215
- Koncz C, Schell J. 1986.** The promoter of TL-DNA gene 5 controls the tissue-specific expression of chimaeric genes carried by a novel type of Agrobacterium binary vector: Molecular and General Genetics MGG. *Molec Gen Genet* **204**: 383-396.
- Kotzer AM, Brandizzi F, Neumann U, Paris N, Moore I, Hawes C (2004)** AtRabF2b (Ara7) acts on the vacuolar trafficking pathway in tobacco leaf epidermal cells. *J Cell Sci* **117**: 6377-6389

- Kouzai Y, Mochizuki S, Nakajima K, Desaki Y, Hayafune M, Miyazaki H, Yokotani N, Ozawa K, Minami E, Kaku H, Shibuya N, Nishizawa Y (2014a)** Targeted gene disruption of OsCERK1 reveals its indispensable role in chitin perception and involvement in the peptidoglycan response and immunity in rice. *Mol Plant Microbe Interact* **27**: 975-982
- Kouzai Y, Nakajima K, Hayafune M, Ozawa K, Kaku H, Shibuya N, Minami E, Nishizawa Y (2014b)** CEBiP is the major chitin oligomer-binding protein in rice and plays a main role in the perception of chitin oligomers. *Plant Mol Biol* **84**: 519-528
- Krogh A, Larsson B, von Heijne G, Sonnhammer EL (2001)** Predicting transmembrane protein topology with a hidden Markov model: application to complete genomes. *J Mol Biol* **305**: 567-580
- Krol E, Mentzel T, Chinchilla D, Boller T, Felix G, Kemmerling B, Postel S, Arents M, Jeworutzki E, Al-Rasheid KA, Becker D, Hedrich R (2010)** Perception of the Arabidopsis danger signal peptide 1 involves the pattern recognition receptor AtPEPR1 and its close homologue AtPEPR2. *J Biol Chem* **285**: 13471-13479
- Lamesch P, Berardini TZ, Li D, Swarbreck D, Wilks C, Sasidharan R, Muller R, Dreher K, Alexander DL, Garcia-Hernandez M, Karthikeyan AS, Lee CH, Nelson WD, Plötz L, Singh S, Wensel A, Huala E (2012)** The Arabidopsis Information Resource (TAIR): improved gene annotation and new tools. *Nucleic Acids Res* **40**: D1202-1210
- Langhans M, Forster S, Helmchen G, Robinson DG (2011)** Differential effects of the brefeldin A analogue (6R)-hydroxy-BFA in tobacco and Arabidopsis. *J Exp Bot* **62**: 2949-2957
- Lee GJ, Sohn EJ, Lee MH, Hwang I (2004)** The Arabidopsis rab5 homologs rha1 and ara7 localize to the prevacuolar compartment. *Plant Cell Physiol* **45**: 1211-1220
- Lee JY, Lu H (2011)** Plasmodesmata: the battleground against intruders. *Trends Plant Sci* **16**: 201-210
- Lee JY, Wang X, Cui W, Sager R, Modla S, Czymmek K, Zybaliov B, van Wijk K, Zhang C, Lu H, Lakshmanan V (2011)** A plasmodesmata-localized protein mediates crosstalk between cell-to-cell communication and innate immunity in Arabidopsis. *Plant Cell* **23**: 3353-3373
- Lefebvre B, Timmers T, Mbengue M, Moreau S, Herve C, Toth K, Bittencourt-Silvestre J, Klaus D, Deslandes L, Godiard L, Murray JD, Udvardi MK, Raffaele S, Mongrand S, Cullimore J, Gamas P, Niebel A, Ott T (2010)** A remorin protein interacts with symbiotic receptors and regulates bacterial infection. *Proc Natl Acad Sci U S A* **107**: 2343-2348
- Lei L, Zhang T, Strasser R, Lee CM, Gonneau M, Mach L, Vernhettes S, Kim SH, D JC, Li S, Gu Y (2014)** The jiaoyao1 Mutant Is an Allele of korrikan1 That Abolishes Endoglucanase Activity and Affects the Organization of Both Cellulose Microfibrils and Microtubules in Arabidopsis. *Plant Cell* **26**: 2601-2616
- Li J, Wen J, Lease KA, Doke JT, Tax FE, Walker JC (2002)** BAK1, an Arabidopsis LRR receptor-like protein kinase, interacts with BRI1 and modulates brassinosteroid signaling. *Cell* **110**: 213-222

- Li R, Liu P, Wan Y, Chen T, Wang Q, Mettbach U, Baluska F, Samaj J, Fang X, Lucas WJ, Lin J (2012)** A membrane microdomain-associated protein, Arabidopsis Flot1, is involved in a clathrin-independent endocytic pathway and is required for seedling development. *Plant Cell* **24**: 2105-2122
- Li X, Lin H, Zhang W, Zou Y, Zhang J, Tang X, Zhou JM (2005)** Flagellin induces innate immunity in nonhost interactions that is suppressed by *Pseudomonas syringae* effectors. *Proc Natl Acad Sci U S A* **102**: 12990-12995
- Liang Y, Cao Y, Tanaka K, Thibivilliers S, Wan J, Choi J, Kang C, Qiu J, Stacey G (2013)** Nonlegumes respond to rhizobial Nod factors by suppressing the innate immune response. *Science* **341**: 1384-1387
- Liebrand TW, van den Berg GC, Zhang Z, Smit P, Cordewener JH, America AH, Sklenar J, Jones AM, Tameling WI, Robatzek S, Thomma BP, Joosten MH (2013)** Receptor-like kinase SOBIR1/EVR interacts with receptor-like proteins in plant immunity against fungal infection. *Proc Natl Acad Sci U S A* **110**: 10010-10015
- Limpens E, Franken C, Smit P, Willemse J, Bisseling T, Geurts R (2003)** LysM domain receptor kinases regulating rhizobial Nod factor-induced infection. *Science* **302**: 630-633
- Lipka V, Dittgen J, Bednarek P, Bhat R, Wiermer M, Stein M, Landtag J, Brandt W, Rosahl S, Scheel D, Llorente F, Molina A, Parker J, Somerville S, Schulze-Lefert P (2005)** Pre- and postinvasion defenses both contribute to nonhost resistance in Arabidopsis. *Science* **310**: 1180-1183
- Liu B, Li JF, Ao Y, Qu J, Li Z, Su J, Zhang Y, Liu J, Feng D, Qi K, He Y, Wang J, Wang HB (2012a)** Lysin motif-containing proteins LYP4 and LYP6 play dual roles in peptidoglycan and chitin perception in rice innate immunity. *Plant Cell* **24**: 3406-3419
- Liu T, Liu Z, Song C, Hu Y, Han Z, She J, Fan F, Wang J, Jin C, Chang J, Zhou JM, Chai J (2012b)** Chitin-induced dimerization activates a plant immune receptor. *Science* **336**: 1160-1164
- Liu Z, Wu Y, Yang F, Zhang Y, Chen S, Xie Q, Tian X, Zhou JM (2013)** BIK1 interacts with PEPRs to mediate ethylene-induced immunity. *Proc Natl Acad Sci U S A* **110**: 6205-6210
- Lohmann GV, Shimoda Y, Nielsen MW, Jorgensen FG, Grossmann C, Sandal N, Sorensen K, Thirup S, Madsen LH, Tabata S, Sato S, Stougaard J, Radutoiu S (2010)** Evolution and regulation of the *Lotus japonicus* LysM receptor gene family. *Mol Plant Microbe Interact* **23**: 510-521
- Low MG, Saltiel AR (1988)** Structural and functional roles of glycosyl-phosphatidylinositol in membranes. *Science* **239**: 268-275
- Lu D, Lin W, Gao X, Wu S, Cheng C, Avila J, Heese A, Devarenne TP, He P, Shan L (2011)** Direct ubiquitination of pattern recognition receptor FLS2 attenuates plant innate immunity. *Science* **332**: 1439-1442

- Lu D, Wu S, Gao X, Zhang Y, Shan L, He P (2010)** A receptor-like cytoplasmic kinase, BIK1, associates with a flagellin receptor complex to initiate plant innate immunity. *Proc Natl Acad Sci U S A* **107**: 496-501
- Luschnig C, Vert G (2014)** The dynamics of plant plasma membrane proteins: PINs and beyond. *Development* **141**: 2924-2938
- MacGurn JA, Hsu PC, Emr SD (2012)** Ubiquitin and membrane protein turnover: from cradle to grave. *Annu Rev Biochem* **81**: 231-259
- Macho AP, Lozano-Duran R, Zipfel C (2015)** Importance of tyrosine phosphorylation in receptor kinase complexes. *Trends Plant Sci* **20**: 269-272
- Macho AP, Zipfel C (2014)** Plant PRRs and the activation of innate immune signaling. *Mol Cell* **54**: 263-272
- Madsen EB, Antolin-Llovera M, Grossmann C, Ye J, Vieweg S, Broghammer A, Krusell L, Radutoiu S, Jensen ON, Stougaard J, Parniske M (2011)** Autophosphorylation is essential for the in vivo function of the *Lotus japonicus* Nod factor receptor 1 and receptor-mediated signalling in cooperation with Nod factor receptor 5. *Plant J* **65**: 404-417
- Madsen EB, Madsen LH, Radutoiu S, Olbryt M, Rakwalska M, Szczyglowski K, Sato S, Kaneko T, Tabata S, Sandal N, Stougaard J (2003)** A receptor kinase gene of the LysM type is involved in legume perception of rhizobial signals. *Nature* **425**: 637-640
- Maillet F, Poinot V, Andre O, Puech-Pages V, Haouy A, Gueunier M, Cromer L, Giraudet D, Formey D, Niebel A, Martinez EA, Driguez H, Becard G, Denarie J (2011)** Fungal lipochitooligosaccharide symbiotic signals in arbuscular mycorrhiza. *Nature* **469**: 58-63
- Martins S, Dohmann EM, Cayrel A, Johnson A, Fischer W, Pojer F, Satiat-Jeunemaitre B, Jaillais Y, Chory J, Geldner N, Vert G (2015)** Internalization and vacuolar targeting of the brassinosteroid hormone receptor BRI1 are regulated by ubiquitination. *Nat Commun* **6**: 6151
- Matsumoto ML, Dong KC, Yu C, Phu L, Gao X, Hannoush RN, Hymowitz SG, Kirkpatrick DS, Dixit VM, Kelley RF (2012)** Engineering and structural characterization of a linear polyubiquitin-specific antibody. *J Mol Biol* **418**: 134-144
- Maule A, Faulkner C, Benitez-Alfonso Y (2012)** Plasmodesmata "in Comunicado". *Front Plant Sci* **3**: 30
- Maule AJ, Benitez-Alfonso Y, Faulkner C (2011)** Plasmodesmata - membrane tunnels with attitude. *Curr Opin Plant Biol* **14**: 683-690
- Mayor S, Pagano RE (2007)** Pathways of clathrin-independent endocytosis. *Nat Rev Mol Cell Biol* **8**: 603-612
- Mbengue M, Camut S, de Carvalho-Niebel F, Deslandes L, Froidure S, Klaus-Heisen D, Moreau S, Rivas S, Timmers T, Herve C, Cullimore J, Lefebvre B (2010)** The *Medicago truncatula* E3 ubiquitin ligase PUB1 interacts with the LYK3 symbiotic receptor and negatively regulates infection and nodulation. *Plant Cell* **22**: 3474-3488

- Mentlak TA, Kombrink A, Shinya T, Ryder LS, Otomo I, Saitoh H, Terauchi R, Nishizawa Y, Shibuya N, Thomma BP, Talbot NJ (2012)** Effector-mediated suppression of chitin-triggered immunity by *magnaporthe oryzae* is necessary for rice blast disease. *Plant Cell* **24**: 322-335
- Merrifield CJ, Perrais D, Zenisek D (2005)** Coupling between clathrin-coated-pit invagination, cortactin recruitment, and membrane scission observed in live cells. *Cell* **121**: 593-606
- Millet YA, Danna CH, Clay NK, Songnuan W, Simon MD, Werck-Reichhart D, Ausubel FM (2010)** Innate immune responses activated in Arabidopsis roots by microbe-associated molecular patterns. *Plant Cell* **22**: 973-990
- Miya A, Albert P, Shinya T, Desaki Y, Ichimura K, Shirasu K, Narusaka Y, Kawakami N, Kaku H, Shibuya N (2007)** CERK1, a LysM receptor kinase, is essential for chitin elicitor signaling in Arabidopsis. *Proc Natl Acad Sci U S A* **104**: 19613-19618
- Molendijk AJ, Ruperti B, Palme K (2004)** Small GTPases in vesicle trafficking. *Curr Opin Plant Biol* **7**: 694-700
- Monaghan J, Zipfel C (2012)** Plant pattern recognition receptor complexes at the plasma membrane. *Curr Opin Plant Biol* **15**: 349-357
- Mosesson Y, Shtiegman K, Katz M, Zwang Y, Vereb G, Szollosi J, Yarden Y (2003)** Endocytosis of receptor tyrosine kinases is driven by monoubiquitylation, not polyubiquitylation. *J Biol Chem* **278**: 21323-21326
- Mukherjee S, Tessema M, Wandinger-Ness A (2006)** Vesicular trafficking of tyrosine kinase receptors and associated proteins in the regulation of signaling and vascular function. *Circ Res* **98**: 743-756
- Mulder L, Lefebvre B, Cullimore J, Imberty A (2006)** LysM domains of *Medicago truncatula* NFP protein involved in Nod factor perception. Glycosylation state, molecular modeling and docking of chitooligosaccharides and Nod factors. *Glycobiology* **16**: 801-809
- Murphy AS, Bandyopadhyay A, Holstein SE, Peer WA (2005)** Endocytotic cycling of PM proteins. *Annu Rev Plant Biol* **56**: 221-251
- Muzzarelli RAA (1977)** *Chitin*, 1st ed. edn. Oxford ; New York: Pergamon Press.
- Nakagawa T, Kaku H, Shimoda Y, Sugiyama A, Shimamura M, Takanashi K, Yazaki K, Aoki T, Shibuya N, Kouchi H (2011)** From defense to symbiosis: limited alterations in the kinase domain of LysM receptor-like kinases are crucial for evolution of legume-Rhizobium symbiosis. *Plant J* **65**: 169-180
- Nam KH, Li J (2002)** BRI1/BAK1, a receptor kinase pair mediating brassinosteroid signaling. *Cell* **110**: 203-212
- Narusaka Y, Shinya T, Narusaka M, Motoyama N, Shimada H, Murakami K, Shibuya N (2013)** Presence of LYM2 dependent but CERK1 independent disease resistance in Arabidopsis. *Plant Signaling & Behavior* **8**

- Nebenführ A, Ritzenthaler C, Robinson DG (2002)** Brefeldin A: deciphering an enigmatic inhibitor of secretion. *Plant Physiol* **130**: 1102-1108
- Nielsen E, Cheung AY, Ueda T (2008)** The regulatory RAB and ARF GTPases for vesicular trafficking. *Plant Physiol* **147**: 1516-1526
- Nielsen H, Krogh A (1998)** Prediction of signal peptides and signal anchors by a hidden Markov model. *Proc Int Conf Intell Syst Mol Biol* **6**: 122-130
- Nielsen ME, Feechan A, Bohlenius H, Ueda T, Thordal-Christensen H (2012)** Arabidopsis ARF-GTP exchange factor, GNOM, mediates transport required for innate immunity and focal accumulation of syntaxin PEN1. *Proc Natl Acad Sci U S A* **109**: 11443-11448
- Nomura K, Debroy S, Lee YH, Pumpilin N, Jones J, He SY (2006)** A bacterial virulence protein suppresses host innate immunity to cause plant disease. *Science* **313**: 220-223
- Nürnberger T, Kemmerling B (2006)** Receptor protein kinases--pattern recognition receptors in plant immunity. *Trends Plant Sci* **11**: 519-522
- Nürnberger T, Lipka V (2005)** Non-host resistance in plants: new insights into an old phenomenon. *Mol Plant Pathol* **6**: 335-345
- O'Connell RJ, Panstruga R (2006)** Tete a tete inside a plant cell: establishing compatibility between plants and biotrophic fungi and oomycetes. *New Phytol* **171**: 699-718
- Oh MH, Wang X, Kota U, Goshe MB, Clouse SD, Huber SC (2009)** Tyrosine phosphorylation of the BRI1 receptor kinase emerges as a component of brassinosteroid signaling in Arabidopsis. *Proc Natl Acad Sci U S A* **106**: 658-663
- Oh MH, Wang X, Wu X, Zhao Y, Clouse SD, Huber SC (2010)** Autophosphorylation of Tyr-610 in the receptor kinase BAK1 plays a role in brassinosteroid signaling and basal defense gene expression. *Proc Natl Acad Sci U S A* **107**: 17827-17832
- Oldroyd GE (2013)** Speak, friend, and enter: signalling systems that promote beneficial symbiotic associations in plants. *Nat Rev Microbiol* **11**: 252-263
- Oldroyd GE, Downie JA (2008)** Coordinating nodule morphogenesis with rhizobial infection in legumes. *Annu Rev Plant Biol* **59**: 519-546
- Osborn A, Goss RJ, Field RA (2011)** The saponins: polar isoprenoids with important and diverse biological activities. *Nat Prod Rep* **28**: 1261-1268
- Otegui MS, Spitzer C (2008)** Endosomal functions in plants. *Traffic* **9**: 1589-1598
- Ovecka M, Berson T, Beck M, Derksen J, Samaj J, Baluska F, Lichtscheidl IK (2010)** Structural sterols are involved in both the initiation and tip growth of root hairs in Arabidopsis thaliana. *Plant Cell* **22**: 2999-3019
- Pagni M, Ioannidis V, Cerutti L, Zahn-Zabal M, Jongeneel CV, Falquet L (2004)** MyHits: a new interactive resource for protein annotation and domain identification. *Nucleic Acids Res* **32**: W332-335

- Paulick MG, Bertozzi CR (2008)** The glycosylphosphatidylinositol anchor: a complex membrane-anchoring structure for proteins. *Biochemistry* **47**: 6991-7000
- Peck SC (2006)** Analysis of protein phosphorylation: methods and strategies for studying kinases and substrates. *Plant J* **45**: 512-522
- Petersen TN, Brunak S, von Heijne G, Nielsen H (2011)** SignalP 4.0: discriminating signal peptides from transmembrane regions. *Nat Methods* **8**: 785-786
- Petutschnig EK, Jones AM, Serazetdinova L, Lipka U, Lipka V (2010)** The lysin motif receptor-like kinase (LysM-RLK) CERK1 is a major chitin-binding protein in *Arabidopsis thaliana* and subject to chitin-induced phosphorylation. *J Biol Chem* **285**: 28902-28911
- Petutschnig EK, Stolze M, Lipka U, Kopischke M, Horlacher J, Valerius O, Rozhon W, Gust AA, Kemmerling B, Poppenberger B, Braus GH, Nurnberger T, Lipka V (2014)** A novel *Arabidopsis* CHITIN ELICITOR RECEPTOR KINASE 1 (CERK1) mutant with enhanced pathogen-induced cell death and altered receptor processing. *New Phytol* **204**: 955-967
- Pietraszewska-Bogiel A, Lefebvre B, Koini MA, Klaus-Heisen D, Takken FL, Geurts R, Cullimore JV, Gadella TW (2013)** Interaction of *Medicago truncatula* lysin motif receptor-like kinases, NFP and LYK3, produced in *Nicotiana benthamiana* induces defence-like responses. *PLoS One* **8**: e65055
- Postel S, Kemmerling B (2009)** Plant systems for recognition of pathogen-associated molecular patterns. *Semin Cell Dev Biol* **20**: 1025-1031
- Postel S, Kufner I, Beuter C, Mazzotta S, Schwedt A, Borlotti A, Halter T, Kemmerling B, Nurnberger T (2010)** The multifunctional leucine-rich repeat receptor kinase BAK1 is implicated in *Arabidopsis* development and immunity. *Eur J Cell Biol* **89**: 169-174
- Postma J, Liebrand TW, Bi G, Evrard A, Bye RR, Mbengue M, Kuhn H, Joosten MH, Robatzek S (2016)** Avr4 promotes Cf-4 receptor-like protein association with the BAK1/SERK3 receptor-like kinase to initiate receptor endocytosis and plant immunity. *New Phytol*
- Postma J, Liebrand TWH, Bi G, Evrard A, Bye RR, Mbengue M, Joosten MHAJ, Robatzek S (2015)** The Cf-4 receptor-like protein associates with the BAK1 receptor-like kinase to initiate receptor endocytosis and plant immunity.
- Preuss ML, Serna J, Falbel TG, Bednarek SY, Nielsen E (2004)** The *Arabidopsis* Rab GTPase RabA4b localizes to the tips of growing root hair cells. *Plant Cell* **16**: 1589-1603
- Qi X, Zheng H (2013)** Rab-A1c GTPase defines a population of the trans-Golgi network that is sensitive to endosidin1 during cytokinesis in *Arabidopsis*. *Mol Plant* **6**: 847-859
- Qi Z, Verma R, Gehring C, Yamaguchi Y, Zhao Y, Ryan CA, Berkowitz GA (2010)** Ca<sup>2+</sup> signaling by plant *Arabidopsis thaliana* Pep peptides depends on AtPepR1, a receptor with guanylyl cyclase activity, and cGMP-activated Ca<sup>2+</sup> channels. *Proc Natl Acad Sci U S A* **107**: 21193-21198



- Radutoiu S, Madsen LH, Madsen EB, Felle HH, Umehara Y, Gronlund M, Sato S, Nakamura Y, Tabata S, Sandal N, Stougaard J (2003)** Plant recognition of symbiotic bacteria requires two LysM receptor-like kinases. *Nature* **425**: 585-592
- Raffaele S, Bayer E, Lafarge D, Cluzet S, German Retana S, Boubekour T, Leborgne-Castel N, Carde JP, Lherminier J, Noirot E, Satiat-Jeunemaitre B, Laroche-Traineau J, Moreau P, Ott T, Maule AJ, Reymond P, Simon-Plas F, Farmer EE, Bessoule JJ, Mongrand S (2009)** Remorin, a solanaceae protein resident in membrane rafts and plasmodesmata, impairs potato virus X movement. *Plant Cell* **21**: 1541-1555
- Raiborg C, Stenmark H (2009)** The ESCRT machinery in endosomal sorting of ubiquitylated membrane proteins. *Nature* **458**: 445-452
- Rey T, Nars A, Bonhomme M, Bottin A, Huguet S, Balzergue S, Jardinaud MF, Bono JJ, Cullimore J, Dumas B, Gough C, Jacquet C (2013)** NFP, a LysM protein controlling Nod factor perception, also intervenes in *Medicago truncatula* resistance to pathogens. *New Phytol* **198**: 875-886
- Reyes FC, Buono R, Otegui MS (2011)** Plant endosomal trafficking pathways. *Curr Opin Plant Biol* **14**: 666-673
- Richter S, Geldner N, Schrader J, Wolters H, Stierhof YD, Rios G, Koncz C, Robinson DG, Jurgens G (2007)** Functional diversification of closely related ARF-GEFs in protein secretion and recycling. *Nature* **448**: 488-492
- Richter S, Kientz M, Brumm S, Nielsen ME, Park M, Gavidia R, Krause C, Voss U, Beckmann H, Mayer U, Stierhof YD, Jurgens G (2014)** Delivery of endocytosed proteins to the cell-division plane requires change of pathway from recycling to secretion. *Elife* **3**: e02131
- Richter S, Muller LM, Stierhof YD, Mayer U, Takada N, Kost B, Vieten A, Geldner N, Koncz C, Jurgens G (2012)** Polarized cell growth in *Arabidopsis* requires endosomal recycling mediated by GBF1-related ARF exchange factors. *Nat Cell Biol* **14**: 80-86
- Robatzek S, Chinchilla D, Boller T (2006)** Ligand-induced endocytosis of the pattern recognition receptor FLS2 in *Arabidopsis*. *Genes Dev* **20**: 537-542
- Robinson DG, Jiang L, Schumacher K (2008a)** The endosomal system of plants: charting new and familiar territories. *Plant Physiol* **147**: 1482-1492
- Robinson DG, Langhans M, Saint-Jore-Dupas C, Hawes C (2008b)** BFA effects are tissue and not just plant specific. *Trends Plant Sci* **13**: 405-408
- Rojas AM, Fuentes G, Rausell A, Valencia A (2012)** The Ras protein superfamily: evolutionary tree and role of conserved amino acids. *J Cell Biol* **196**: 189-201
- Ron M, Avni A (2004)** The receptor for the fungal elicitor ethylene-inducing xylanase is a member of a resistance-like gene family in tomato. *Plant Cell* **16**: 1604-1615
- Roux M, Schwessinger B, Albrecht C, Chinchilla D, Jones A, Holton N, Malinovsky FG, Tor M, de Vries S, Zipfel C (2011)** The *Arabidopsis* leucine-rich repeat receptor-like kinases

BAK1/SERK3 and BKK1/SERK4 are required for innate immunity to hemibiotrophic and biotrophic pathogens. *Plant Cell* **23**: 2440-2455

**Russinova E, Borst JW, Kwaaitaal M, Cano-Delgado A, Yin Y, Chory J, de Vries SC (2004)** Heterodimerization and endocytosis of Arabidopsis brassinosteroid receptors BRI1 and AtSERK3 (BAK1). *Plant Cell* **16**: 3216-3229

**Rutherford S, Moore I (2002)** The Arabidopsis Rab GTPase family: another enigma variation. *Curr Opin Plant Biol* **5**: 518-528

**Ryan CA (1987)** Oligosaccharide signalling in plants. *Annu Rev Cell Biol* **3**: 295-317

**Saka S (2010)** Functional Characterization of the Arabidopsis LysM-RLK CERK1 and its Interactors.

**Salmon MS, Bayer EM (2012)** Dissecting plasmodesmata molecular composition by mass spectrometry-based proteomics. *Front Plant Sci* **3**: 307

**Salomon SA (2009)** LINKING ENDOSOMAL TRAFFIC AND PAMP-TRIGGERED IMMUNITY IN PLANTS. PhD Thesis, Molekulare Phytopathologie, Cologne, Cologne

**Samaj J, Peters M, Volkmann D, Baluska F (2000)** Effects of myosin ATPase inhibitor 2,3-butanedione 2-monoxime on distributions of myosins, F-actin, microtubules, and cortical endoplasmic reticulum in maize root apices. *Plant Cell Physiol* **41**: 571-582

**Sanchez-Vallet A, Saleem-Batcha R, Kombrink A, Hansen G, Valkenburg DJ, Thomma BP, Mesters JR (2013)** Fungal effector Ecp6 outcompetes host immune receptor for chitin binding through intrachain LysM dimerization. *Elife* **2**: e00790

**Scheuring D, Viotti C, Kruger F, Kunzl F, Sturm S, Bubeck J, Hillmer S, Frigerio L, Robinson DG, Pimpl P, Schumacher K (2011)** Multivesicular bodies mature from the trans-Golgi network/early endosome in Arabidopsis. *Plant Cell* **23**: 3463-3481

**Schindelin J, Arganda-Carreras I, Frise E, Kaynig V, Longair M, Pietzsch T, Preibisch S, Rueden C, Saalfeld S, Schmid B, Tinevez JY, White DJ, Hartenstein V, Eliceiri K, Tomancak P, Cardona A (2012)** Fiji: an open-source platform for biological-image analysis. *Nat Methods* **9**: 676-682

**Schleifer KH, Kandler O (1972)** Peptidoglycan types of bacterial cell walls and their taxonomic implications. *Bacteriol Rev* **36**: 407-477

**Schmid M, Davison TS, Henz SR, Pape UJ, Demar M, Vingron M, Scholkopf B, Weigel D, Lohmann JU (2005)** A gene expression map of Arabidopsis thaliana development. *Nat Genet* **37**: 501-506

**Scholl RL, May ST, Ware DH (2000)** Seed and molecular resources for Arabidopsis. *Plant Physiol* **124**: 1477-1480

**Schulze B, Mentzel T, Jehle AK, Mueller K, Beeler S, Boller T, Felix G, Chinchilla D (2010)** Rapid heteromerization and phosphorylation of ligand-activated plant transmembrane receptors and their associated kinase BAK1. *J Biol Chem* **285**: 9444-9451

- Schwessinger B, Roux M, Kadota Y, Ntoukakis V, Sklenar J, Jones A, Zipfel C (2011)** Phosphorylation-dependent differential regulation of plant growth, cell death, and innate immunity by the regulatory receptor-like kinase BAK1. *PLoS Genet* **7**: e1002046
- Serrano M, Robatzek S, Torres M, Kombrink E, Somssich IE, Robinson M, Schulze-Lefert P (2007)** Chemical interference of pathogen-associated molecular pattern-triggered immune responses in Arabidopsis reveals a potential role for fatty-acid synthase type II complex-derived lipid signals. *J Biol Chem* **282**: 6803-6811
- Sessions A, Burke E, Presting G, Aux G, McElver J, Patton D, Dietrich B, Ho P, Bacwaden J, Ko C, Clarke JD, Cotton D, Bullis D, Snell J, Miguel T, Hutchison D, Kimmerly B, Mitzel T, Katagiri F, Glazebrook J, Law M, Goff SA (2002)** A high-throughput Arabidopsis reverse genetics system. *Plant Cell* **14**: 2985-2994
- Shah K, Vervoort J, de Vries SC (2001)** Role of threonines in the Arabidopsis thaliana somatic embryogenesis receptor kinase 1 activation loop in phosphorylation. *J Biol Chem* **276**: 41263-41269
- Shan L, He P, Li J, Heese A, Peck SC, Nurnberger T, Martin GB, Sheen J (2008)** Bacterial effectors target the common signaling partner BAK1 to disrupt multiple MAMP receptor-signaling complexes and impede plant immunity. *Cell Host Microbe* **4**: 17-27
- Sharfman M, Bar M, Schuster S, Leibman M, Avni A (2014)** Sterol-dependent induction of plant defense responses by a microbe-associated molecular pattern from *Trichoderma viride*. *Plant Physiol* **164**: 819-827
- Shields SB, Piper RC (2011)** How ubiquitin functions with ESCRTs. *Traffic* **12**: 1306-1317
- Shimizu T, Nakano T, Takamizawa D, Desaki Y, Ishii-Minami N, Nishizawa Y, Minami E, Okada K, Yamane H, Kaku H, Shibuya N (2010)** Two LysM receptor molecules, CEBiP and OsCERK1, cooperatively regulate chitin elicitor signaling in rice. *Plant J* **64**: 204-214
- Shinya T, Motoyama N, Ikeda A, Wada M, Kamiya K, Hayafune M, Kaku H, Shibuya N (2012)** Functional characterization of CEBiP and CERK1 homologs in Arabidopsis and rice reveals the presence of different chitin receptor systems in plants. *Plant Cell Physiol* **53**: 1696-1706
- Shinya T, Nakagawa T, Kaku H, Shibuya N (2015)** Chitin-mediated plant-fungal interactions: catching, hiding and handshaking. *Curr Opin Plant Biol* **26**: 64-71
- Shinya T, Yamaguchi K, Desaki Y, Yamada K, Narisawa T, Kobayashi Y, Maeda K, Suzuki M, Tanimoto T, Takeda J, Nakashima M, Funama R, Narusaka M, Narusaka Y, Kaku H, Kawasaki T, Shibuya N (2014)** Selective regulation of the chitin-induced defense response by the Arabidopsis receptor-like cytoplasmic kinase PBL27. *Plant J* **79**: 56-66
- Shiu SH, Bleeker AB (2001)** Plant receptor-like kinase gene family: diversity, function, and signaling. *Sci STKE* **2001**: re22
- Shiu SH, Bleeker AB (2003)** Expansion of the receptor-like kinase/Pelle gene family and receptor-like proteins in Arabidopsis. *Plant Physiol* **132**: 530-543

- Shiu SH, Karlowski WM, Pan R, Tzeng YH, Mayer KF, Li WH (2004)** Comparative analysis of the receptor-like kinase family in Arabidopsis and rice. *Plant Cell* **16**: 1220-1234
- Shpak ED, Lakeman MB, Torii KU (2003)** Dominant-negative receptor uncovers redundancy in the Arabidopsis ERECTA Leucine-rich repeat receptor-like kinase signaling pathway that regulates organ shape. *Plant Cell* **15**: 1095-1110
- Sikorski RS, Hieter P (1989)** A system of shuttle vectors and yeast host strains designed for efficient manipulation of DNA in *Saccharomyces cerevisiae*. *Genetics* **122**: 19-27
- Simpson C, Thomas C, Findlay K, Bayer E, Maule AJ (2009)** An Arabidopsis GPI-anchor plasmodesmal neck protein with callose binding activity and potential to regulate cell-to-cell trafficking. *Plant Cell* **21**: 581-594
- Smit P, Limpens E, Geurts R, Fedorova E, Dolgikh E, Gough C, Bisseling T (2007)** Medicago LYK3, an entry receptor in rhizobial nodulation factor signaling. *Plant Physiol* **145**: 183-191
- Smith JM, Salamango DJ, Leslie ME, Collins CA, Heese A (2014)** Sensitivity to Flg22 is modulated by ligand-induced degradation and de novo synthesis of the endogenous flagellin-receptor FLAGELLIN-SENSING2. *Plant Physiol* **164**: 440-454
- Sohn EJ, Kim ES, Zhao M, Kim SJ, Kim H, Kim YW, Lee YJ, Hillmer S, Sohn U, Jiang L, Hwang I (2003)** Rha1, an Arabidopsis Rab5 homolog, plays a critical role in the vacuolar trafficking of soluble cargo proteins. *Plant Cell* **15**: 1057-1070
- Sorkin A, von Zastrow M (2009)** Endocytosis and signalling: intertwining molecular networks. *Nat Rev Mol Cell Biol* **10**: 609-622
- Spallek T, Beck M, Ben Khaled S, Salomon S, Bourdais G, Schellmann S, Robatzek S (2013)** ESCRT-I mediates FLS2 endosomal sorting and plant immunity. *PLoS Genet* **9**: e1004035
- Stein M, Dittgen J, Sanchez-Rodriguez C, Hou BH, Molina A, Schulze-Lefert P, Lipka V, Somerville S (2006)** Arabidopsis PEN3/PDR8, an ATP binding cassette transporter, contributes to nonhost resistance to inappropriate pathogens that enter by direct penetration. *Plant Cell* **18**: 731-746
- Steinmann T, Geldner N, Grebe M, Mangold S, Jackson CL, Paris S, Galweiler L, Palme K, Jurgens G (1999)** Coordinated polar localization of auxin efflux carrier PIN1 by GNOM ARF GEF. *Science* **286**: 316-318
- Sun Y, Han Z, Tang J, Hu Z, Chai C, Zhou B, Chai J (2013a)** Structure reveals that BAK1 as a co-receptor recognizes the BRI1-bound brassinolide. *Cell Res* **23**: 1326-1329
- Sun Y, Li L, Macho AP, Han Z, Hu Z, Zipfel C, Zhou JM, Chai J (2013b)** Structural basis for flg22-induced activation of the Arabidopsis FLS2-BAK1 immune complex. *Science* **342**: 624-628
- Szumliński AL, Nielsen E (2009)** The Rab GTPase RabA4d regulates pollen tube tip growth in Arabidopsis thaliana. *Plant Cell* **21**: 526-544

- Takai R, Isogai A, Takayama S, Che FS (2008)** Analysis of flagellin perception mediated by flg22 receptor OsFLS2 in rice. *Mol Plant Microbe Interact* **21**: 1635-1642
- Tamura K, Shimada T, Ono E, Tanaka Y, Nagatani A, Higashi SI, Watanabe M, Nishimura M, Hara-Nishimura I (2003)** Why green fluorescent fusion proteins have not been observed in the vacuoles of higher plants. *Plant J* **35**: 545-555
- Tanaka H, Kitakura S, De Rycke R, De Groot R, Friml J (2009)** Fluorescence imaging-based screen identifies ARF GEF component of early endosomal trafficking. *Curr Biol* **19**: 391-397
- Tanaka K, Nguyen CT, Liang Y, Cao Y, Stacey G (2013)** Role of LysM receptors in chitin-triggered plant innate immunity. *Plant Signaling & Behavior* **8**: e22598
- Tax FE, Vernon DM (2001)** T-DNA-associated duplication/translocations in Arabidopsis. Implications for mutant analysis and functional genomics. *Plant Physiol* **126**: 1527-1538
- Teh OK, Moore I (2007)** An ARF-GEF acting at the Golgi and in selective endocytosis in polarized plant cells. *Nature* **448**: 493-496
- Teis D, Wunderlich W, Huber LA (2002)** Localization of the MP1-MAPK scaffold complex to endosomes is mediated by p14 and required for signal transduction. *Dev Cell* **3**: 803-814
- Thomas CL, Bayer EM, Ritzenthaler C, Fernandez-Calvino L, Maule AJ (2008)** Specific targeting of a plasmodesmal protein affecting cell-to-cell communication. *PLoS Biol* **6**: e7
- Thomas CM, Jones DA, Parniske M, Harrison K, Balint-Kurti PJ, Hatzixanthis K, Jones JD (1997)** Characterization of the tomato Cf-4 gene for resistance to *Cladosporium fulvum* identifies sequences that determine recognitional specificity in Cf-4 and Cf-9. *Plant Cell* **9**: 2209-2224
- Thomma BP, Nurnberger T, Joosten MH (2011)** Of PAMPs and effectors: the blurred PTI-ETI dichotomy. *Plant Cell* **23**: 4-15
- Thordal-Christensen H (2003)** Fresh insights into processes of nonhost resistance. *Curr Opin Plant Biol* **6**: 351-357
- Tilsner J, Linnik O, Louveaux M, Roberts IM, Chapman SN, Oparka KJ (2013)** Replication and trafficking of a plant virus are coupled at the entrances of plasmodesmata. *J Cell Biol* **201**: 981-995
- Töller A, Brownfield L, Neu C, Twell D, Schulze-Lefert P (2008)** Dual function of Arabidopsis glucan synthase-like genes GSL8 and GSL10 in male gametophyte development and plant growth. *Plant J* **54**: 911-923
- Traub LM (2009)** Tickets to ride: selecting cargo for clathrin-regulated internalization. *Nat Rev Mol Cell Biol* **10**: 583-596
- Tyler BM, Kale SD, Wang Q, Tao K, Clark HR, Drews K, Antignani V, Rumore A, Hayes T, Plett JM, Fudal I, Gu B, Chen Q, Affeldt KJ, Berthier E, Fischer GJ, Dou D, Shan W, Keller NP, Martin F, Rouxel T, Lawrence CB (2013)** Microbe-independent entry of oomycete RxLR

effectors and fungal RxLR-like effectors into plant and animal cells is specific and reproducible. *Mol Plant Microbe Interact* **26**: 611-616

**Ueda T, Uemura T, Sato MH, Nakano A (2004)** Functional differentiation of endosomes in Arabidopsis cells. *Plant J* **40**: 783-789

**Ueda T, Yamaguchi M, Uchimiya H, Nakano A (2001)** Ara6, a plant-unique novel type Rab GTPase, functions in the endocytic pathway of Arabidopsis thaliana. *Embo J* **20**: 4730-4741

**Ueki S, Citovsky V (2011)** To gate, or not to gate: regulatory mechanisms for intercellular protein transport and virus movement in plants. *Mol Plant* **4**: 782-793

**van Hengel AJ, Tadesse Z, Immerzeel P, Schols H, van Kammen A, de Vries SC (2001)** N-acetylglucosamine and glucosamine-containing arabinogalactan proteins control somatic embryogenesis. *Plant Physiol* **125**: 1880-1890

**Vaten A, Dettmer J, Wu S, Stierhof YD, Miyashima S, Yadav SR, Roberts CJ, Campilho A, Bulone V, Lichtenberger R, Lehesranta S, Mahonen AP, Kim JY, Jokitalo E, Sauer N, Scheres B, Nakajima K, Carlsbecker A, Gallagher KL, Helariutta Y (2011)** Callose biosynthesis regulates symplastic trafficking during root development. *Dev Cell* **21**: 1144-1155

**Verma DP, Hong Z (2001)** Plant callose synthase complexes. *Plant Mol Biol* **47**: 693-701

**Vernoud V, Horton AC, Yang Z, Nielsen E (2003)** Analysis of the small GTPase gene superfamily of Arabidopsis. *Plant Physiol* **131**: 1191-1208

**Wan J, Tanaka K, Zhang XC, Son GH, Brechenmacher L, Nguyen TH, Stacey G (2012)** LYK4, a lysin motif receptor-like kinase, is important for chitin signaling and plant innate immunity in Arabidopsis. *Plant Physiol* **160**: 396-406

**Wan J, Zhang XC, Neece D, Ramonell KM, Clough S, Kim SY, Stacey MG, Stacey G (2008a)** A LysM receptor-like kinase plays a critical role in chitin signaling and fungal resistance in Arabidopsis. *Plant Cell* **20**: 471-481

**Wan J, Zhang XC, Stacey G (2008b)** Chitin signaling and plant disease resistance. *Plant Signal Behav* **3**: 831-833

**Wang J, Cai Y, Miao Y, Lam SK, Jiang L (2009)** Wortmannin induces homotypic fusion of plant prevacuolar compartments. *J Exp Bot* **60**: 3075-3083

**Wang L, Li H, Lv X, Chen T, Li R, Xue Y, Jiang J, Jin B, Baluska F, Samaj J, Wang X, Lin J (2015)** Spatiotemporal Dynamics of the BRI1 Receptor and its Regulation by Membrane Microdomains in Living Arabidopsis Cells. *Mol Plant* **8**: 1334-1349

**Wang Q, Villeneuve G, Wang Z (2005)** Control of epidermal growth factor receptor endocytosis by receptor dimerization, rather than receptor kinase activation. *EMBO Rep* **6**: 942-948

**Wang X, Kota U, He K, Blackburn K, Li J, Goshe MB, Huber SC, Clouse SD (2008)** Sequential transphosphorylation of the BRI1/BAK1 receptor kinase complex impacts early events in brassinosteroid signaling. *Dev Cell* **15**: 220-235

**Waterhouse AM, Procter JB, Martin DM, Clamp M, Barton GJ (2009)** Jalview Version 2--a multiple sequence alignment editor and analysis workbench. *Bioinformatics* **25**: 1189-1191

**Waterman H, Yarden Y (2001)** Molecular mechanisms underlying endocytosis and sorting of ErbB receptor tyrosine kinases. *FEBS Lett* **490**: 142-152

**Willmann R, Lajunen HM, Erbs G, Newman MA, Kolb D, Tsuda K, Katagiri F, Fliegmann J, Bono JJ, Cullimore JV, Jehle AK, Gotz F, Kulik A, Molinaro A, Lipka V, Gust AA, Nurnberger T (2011)** Arabidopsis lysin-motif proteins LYM1 LYM3 CERK1 mediate bacterial peptidoglycan sensing and immunity to bacterial infection. *Proc Natl Acad Sci U S A* **108**: 19824-19829

**Winter D, Vinegar B, Nahal H, Ammar R, Wilson GV, Provart NJ (2007)** An "Electronic Fluorescent Pictograph" browser for exploring and analyzing large-scale biological data sets. *PLoS One* **2**: e718

**Woollard AA, Moore I (2008)** The functions of Rab GTPases in plant membrane traffic. *Curr Opin Plant Biol* **11**: 610-619

**Wyrsh I, Dominguez-Ferreras A, Geldner N, Boller T (2015)** Tissue-specific FLAGELLIN-SENSING 2 (FLS2) expression in roots restores immune responses in Arabidopsis fls2 mutants. *New Phytol* **206**: 774-784

**Xu M, Cho E, Burch-Smith TM, Zambryski PC (2012)** Plasmodesmata formation and cell-to-cell transport are reduced in decreased size exclusion limit 1 during embryogenesis in Arabidopsis. *Proc Natl Acad Sci U S A* **109**: 5098-5103

**Xu XM, Jackson D (2010)** Lights at the end of the tunnel: new views of plasmodesmal structure and function. *Curr Opin Plant Biol* **13**: 684-692

**Yamaguchi K, Yamada K, Ishikawa K, Yoshimura S, Hayashi N, Uchihashi K, Ishihama N, Kishi-Kaboshi M, Takahashi A, Tsuge S, Ochiai H, Tada Y, Shimamoto K, Yoshioka H, Kawasaki T (2013)** A receptor-like cytoplasmic kinase targeted by a plant pathogen effector is directly phosphorylated by the chitin receptor and mediates rice immunity. *Cell Host Microbe* **13**: 347-357

**Yamaguchi Y, Huffaker A, Bryan AC, Tax FE, Ryan CA (2010)** PEPR2 is a second receptor for the Pep1 and Pep2 peptides and contributes to defense responses in Arabidopsis. *Plant Cell* **22**: 508-522

**Yamaguchi Y, Pearce G, Ryan CA (2006)** The cell surface leucine-rich repeat receptor for AtPep1, an endogenous peptide elicitor in Arabidopsis, is functional in transgenic tobacco cells. *Proc Natl Acad Sci U S A* **103**: 10104-10109

**Yan L, Ma Y, Liu D, Wei X, Sun Y, Chen X, Zhao H, Zhou J, Wang Z, Shui W, Lou Z (2012)** Structural basis for the impact of phosphorylation on the activation of plant receptor-like kinase BAK1. *Cell Res* **22**: 1304-1308

**Yarar D, Waterman-Storer CM, Schmid SL (2005)** A dynamic actin cytoskeleton functions at multiple stages of clathrin-mediated endocytosis. *Mol Biol Cell* **16**: 964-975

- Ye L, Li L, Wang L, Wang S, Li S, Du J, Zhang S, Shou H (2015)** MPK3/MPK6 are involved in iron deficiency-induced ethylene production in Arabidopsis. *Front Plant Sci* **6**: 953
- Zambryski P, Crawford K (2000)** Plasmodesmata: gatekeepers for cell-to-cell transport of developmental signals in plants. *Annu Rev Cell Dev Biol* **16**: 393-421
- Zavaliev R, Ueki S, Epel BL, Citovsky V (2011)** Biology of callose (beta-1,3-glucan) turnover at plasmodesmata. *Protoplasma* **248**: 117-130
- Zhang J, Li W, Xiang T, Liu Z, Laluk K, Ding X, Zou Y, Gao M, Zhang X, Chen S, Mengiste T, Zhang Y, Zhou JM (2010)** Receptor-like cytoplasmic kinases integrate signaling from multiple plant immune receptors and are targeted by a *Pseudomonas syringae* effector. *Cell Host Microbe* **7**: 290-301
- Zhang J, Shao F, Li Y, Cui H, Chen L, Li H, Zou Y, Long C, Lan L, Chai J, Chen S, Tang X, Zhou JM (2007)** A *Pseudomonas syringae* effector inactivates MAPKs to suppress PAMP-induced immunity in plants. *Cell Host Microbe* **1**: 175-185
- Zhang W, Fraiture M, Kolb D, Loffelhardt B, Desaki Y, Boutrot FF, Tor M, Zipfel C, Gust AA, Brunner F (2013)** Arabidopsis receptor-like protein30 and receptor-like kinase suppressor of BIR1-1/EVERSHED mediate innate immunity to necrotrophic fungi. *Plant Cell* **25**: 4227-4241
- Zhuo S, Clemens JC, Hakes DJ, Barford D, Dixon JE (1993)** Expression, purification, crystallization, and biochemical characterization of a recombinant protein phosphatase. *J Biol Chem* **268**: 17754-17761
- Ziegler Y (2015)** The Role Of The Putative Receptor-Like Cytoplasmic Kinase CLR1 In Chitin Signalling Dissertation. PhD Thesis, Georg-August University Göttingen,
- Zipfel C, Kunze G, Chinchilla D, Caniard A, Jones JD, Boller T, Felix G (2006)** Perception of the bacterial PAMP EF-Tu by the receptor EFR restricts *Agrobacterium*-mediated transformation. *Cell* **125**: 749-760
- Zipfel C, Robatzek S, Navarro L, Oakeley EJ, Jones JD, Felix G, Boller T (2004)** Bacterial disease resistance in Arabidopsis through flagellin perception. *Nature* **428**: 764-767



## 6 Supplemental material

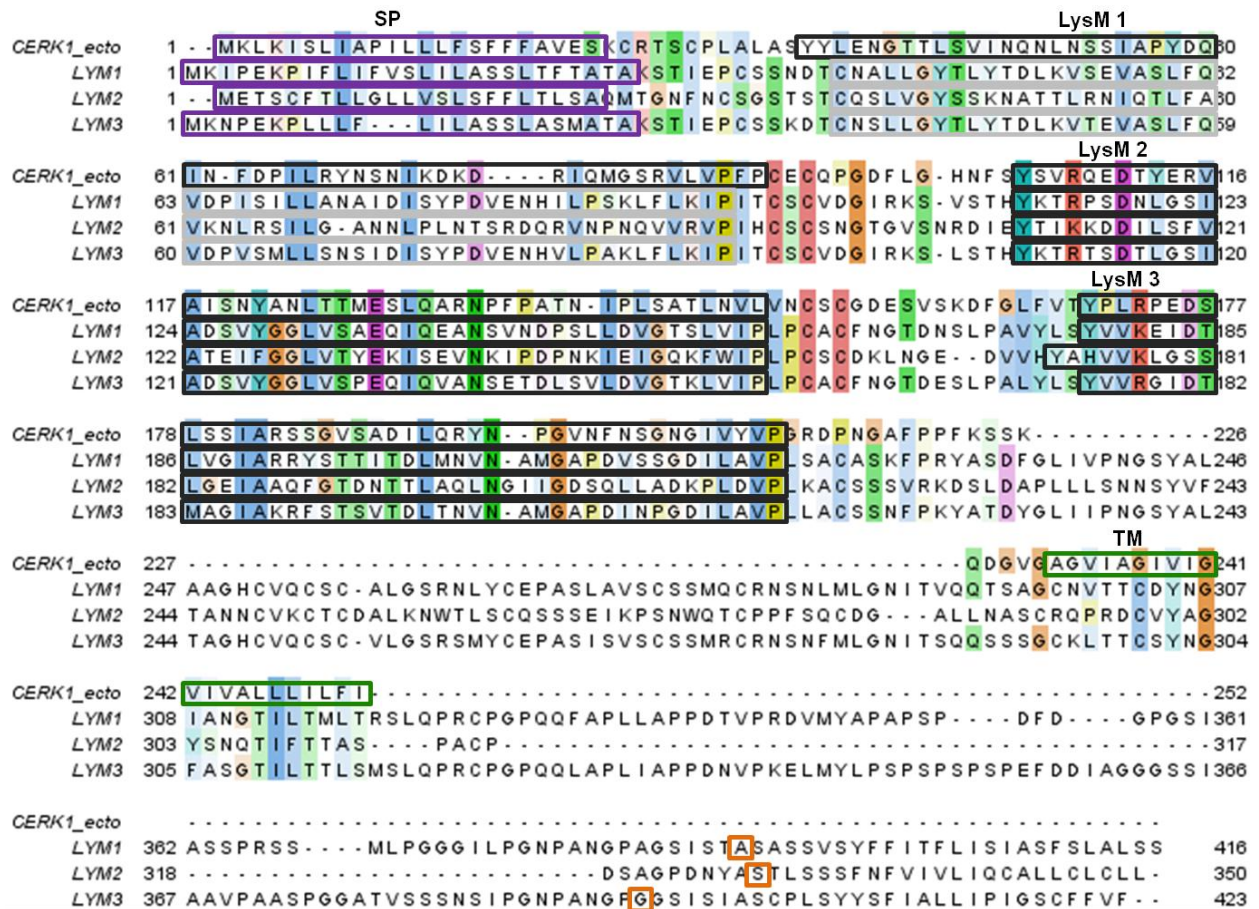


**Figure S1: Alignment of full length amino acid sequences of *Arabidopsis* CERK1 and LYM proteins.**

Protein features: SP: Signal peptide predicted by SignalP 4.1 (<http://www.cbs.dtu.dk/services/SignalP/>; Petersen *et al.* (2011)); LysM: lysin motif (black predicted by MyHits (<http://myhits.isb-sib.ch>, Pagni *et al.*, 2004), light grey predicted by sequence comparison); TM: Transmembrane domain predicted using the TMHMM Server 2.0 (<http://www.cbs.dtu.dk/services/TMHMM/>, Krogh *et al.*, 2001). Orange boxes indicate putative GPI-anchor attachment site (predicted by big PI Predictor ([http://mendel.imp.ac.at/sat/gpi/gpi\\_server.html](http://mendel.imp.ac.at/sat/gpi/gpi_server.html); Eisenhaber *et al.* (1999)) The alignment was generated with Genious 7.1.5 using the ClustalW algorithm Kearse *et al.* (2012) and colored in Jalview 2.9.0b2 (settings: ClustalX, conservation threshold of 30; Waterhouse *et al.* (2009)). Red: positive charged amino acids, purple: negative charged amino acids, blue: amino acids with hydrophobic side chains, green: neutral amino acids.

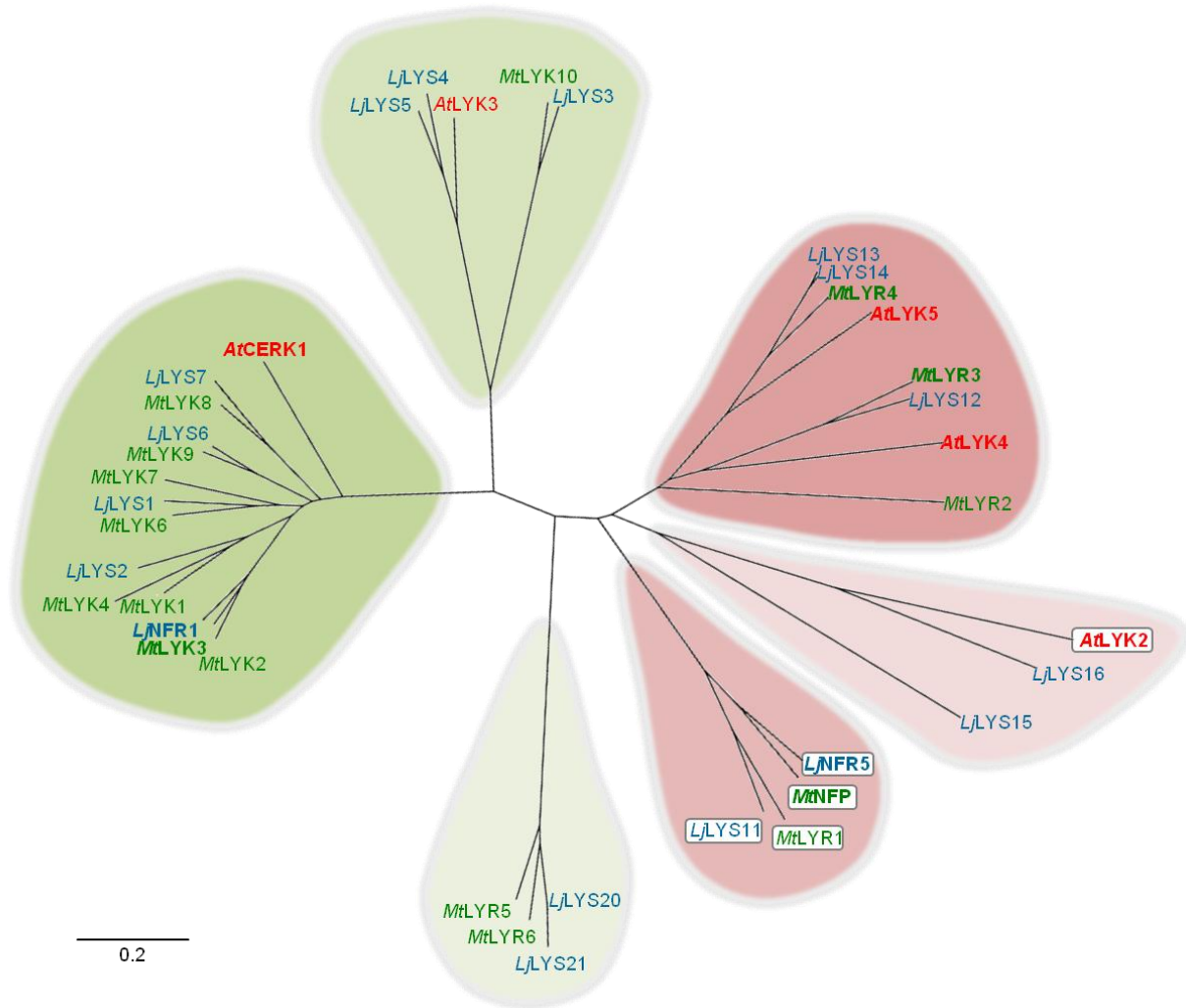


**Figure S2: Phylogenetic tree of *Arabidopsis thaliana*, *Medicago truncatula* and *Lotus japonicus* LysM-RLKs.**

*Medicago truncatula* sequences were published by Arrighi *et al.* (2006) and *Lotus japonicus* sequences by Lohmann *et al.* (2010). The *Arabidopsis* sequences were retrieved from TAIR (Lamesch *et al.*, 2012). A phylogenetic tree was constructed based on the amino acid sequences of full-length proteins using ClustalW (Kearse *et al.*, 2012). *Medicago* proteins are shown in green, *Lotus* in blue and *Arabidopsis* in red. LysM-RLKs on shaded green background are known or predicted to be active kinases. LysM-RLKs on shaded red background lack the ATP binding loop and Mg<sup>2+</sup>-binding motif and are (predicted to be) enzymatically inactive. Boxed LysM-RLKs have deletions in the activation loop. LysM-RLKs discussed in the main text are shown in bold.

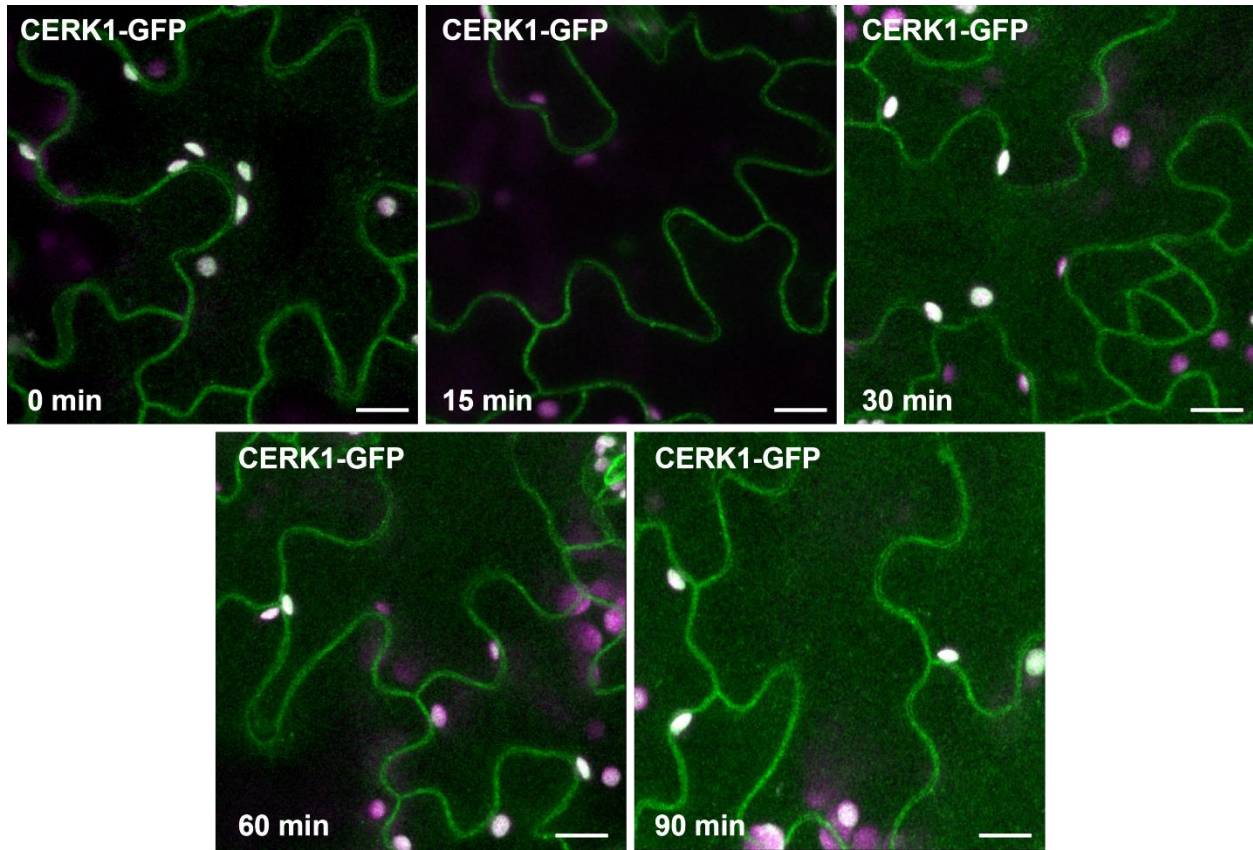
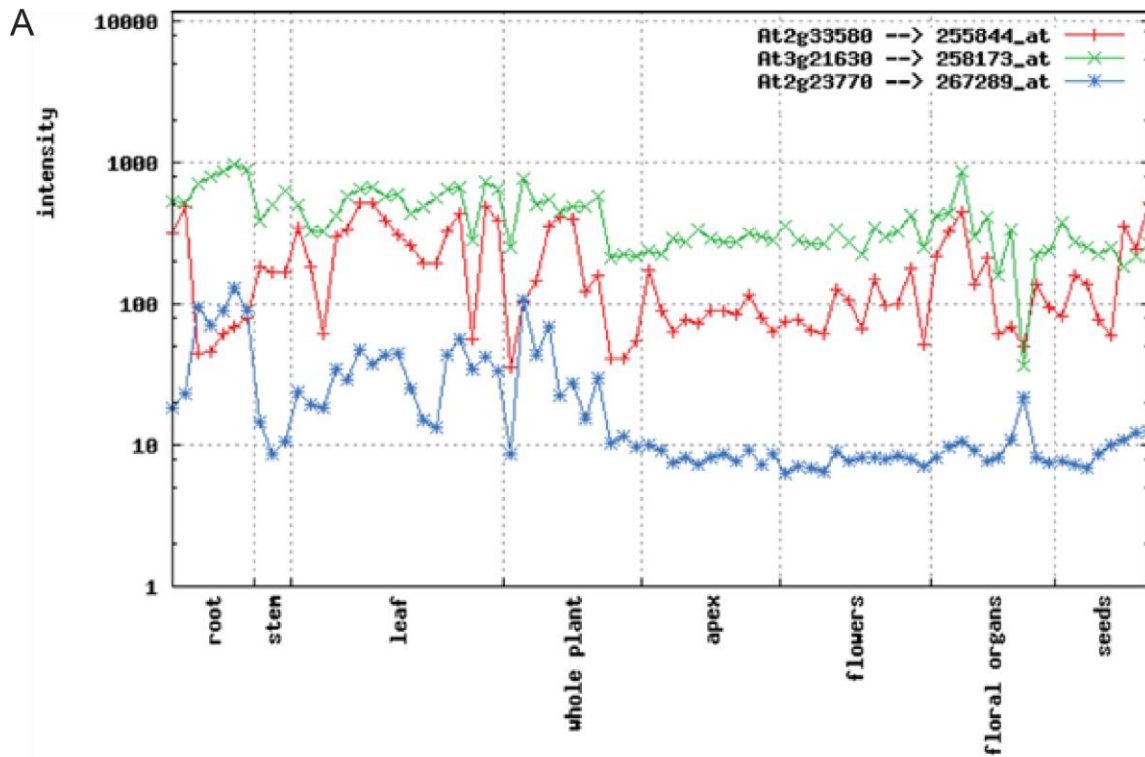


**Figure S3: CERK1-GFP localization is not responsive to chitin.**

*Arabidopsis* leaves stably expressing *pCERK::CERK1-GFP* in *cerk1-2* were infiltrated with 100  $\mu\text{g/ml}$  chitin and incubated for the indicated time points. CERK1-GFP subcellular localization did not change upon chitin infiltration. Representative maximum projections of 8 CLSM focal planes taken 1  $\mu\text{m}$  apart are shown. Experiment was performed with three independent transgenic lines. Images: Green, GFP; magenta, chloroplast autofluorescence. Scale bar = 10  $\mu\text{m}$



**B**

Expression values for

Tissue	Age	<i>CERK1</i> (At3g21630)	<i>LYK5</i> (At2g33580)	<i>LYK4</i> (At2g23770)
cotyledons	7 days	504.49	340.47	24.03
leaves 1 + 2	7 days	321.80	184.44	19.28
rosette leaf #4, 1 cm	10 days	326.43	61.77	18.17
rosette leaf #4, 1 cm	10 days	423.92	298.93	34.00
rosette leaf # 2	17 days	572.52	330.69	28.67
rosette leaf # 4	17 days	642.39	513.54	47.03
rosette leaf # 6	17 days	669.03	522.10	37.73
rosette leaf # 8	17 days	578.14	386.39	43.36
rosette leaf # 10	17 days	596.24	311.33	44.33
rosette leaf # 12	17 days	435.76	255.07	25.20
rosette leaf # 12	17 days	480.49	195.28	14.85
leaf 7, petiole	17 days	558.03	195.55	13.25
leaf 7, proximal half	17 days	654.31	323.26	42.93
leaf 7, distal half	17 days	668.66	433.41	56.72
leaf	15 days	278.63	57.01	34.48
senescing leaves	35 days	729.35	482.64	42.42
cauline leaves	21+ days	642.64	381.90	33.29

**Figure S4: *LYK4* is weakly expressed in leaves.**

**(A)** *LYK4* had lower expression levels in aerial tissues than *LYK5* and *CERK1*. Data were gathered from publicly available microarray experiments and the diagram was generated with the AtGenExpress visualisation tool (AVT) (<http://jsp.weigelworld.org/expviz/expviz.jsp>; Schmid *et al.* (2005)). Experiment set: AtGE Development, absolute expression values. **(B)** Detailed expression values in leaf experiments for *CERK1*, *LYK5* and *LYK4*.

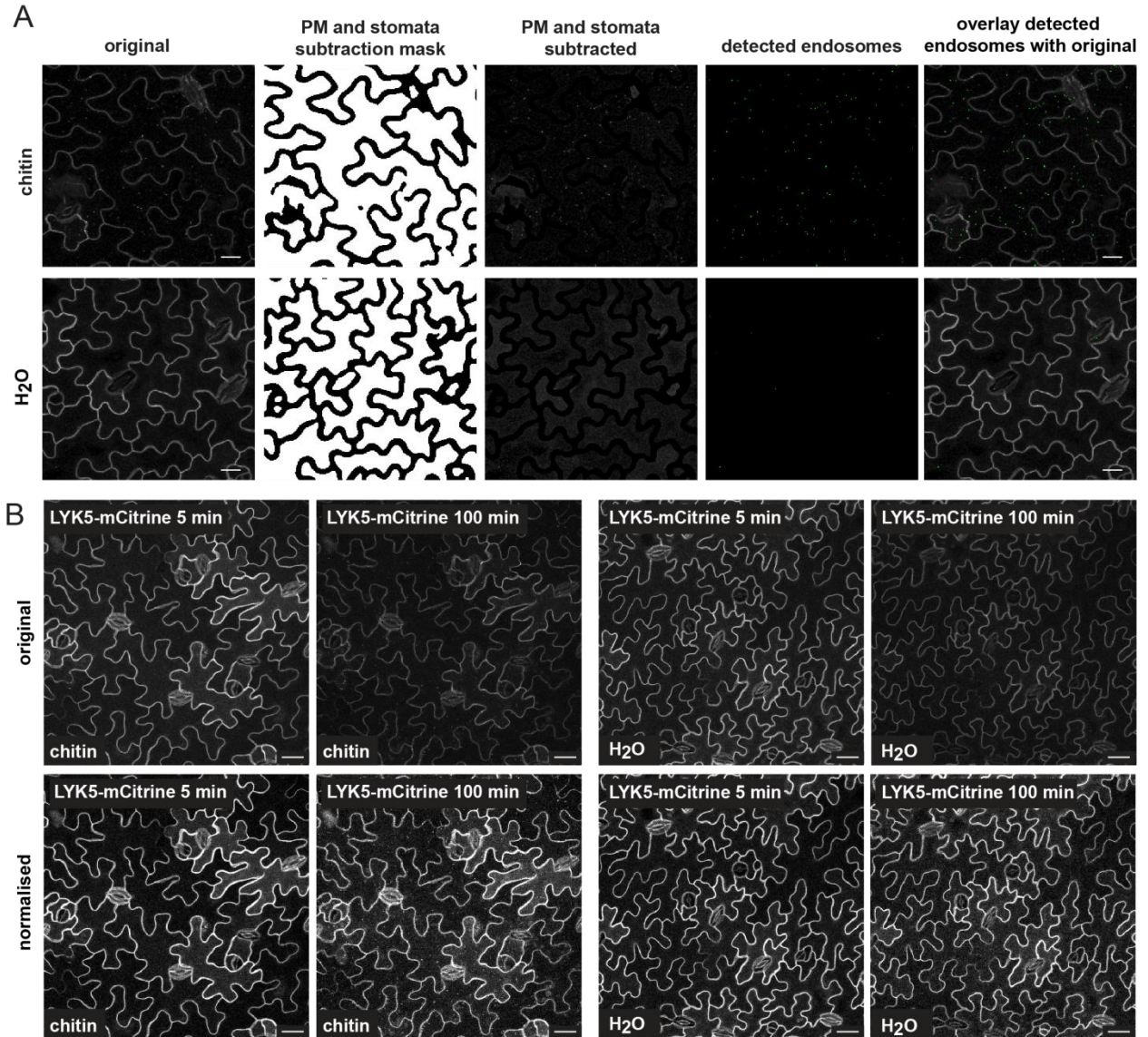


**Figure S5: Endosome quantification and image normalization.**

**(A)** Examples for single steps in endosome quantification from a chitin-treated and a control sample. Original images are maximum projections of 12 focal planes recorded 1  $\mu\text{m}$  apart. PM and guard cells were removed from the original image by first identification of the corresponding signal and subsequent subtraction of a so generated mask. Punctate structures were detected in the resulting image and highlighted in green. Scale bar = 10  $\mu\text{m}$ . **(B)** Normalization was performed to compensate for fluorophore bleaching in time course experiments. The upper panel shows original images of chitin- and water-infiltrated samples 5 min and 100 min after treatment. These images represent the first and last (20<sup>th</sup>) time points recorded. The lower panel shows the same images after the normalization process. Scale bar = 20  $\mu\text{m}$

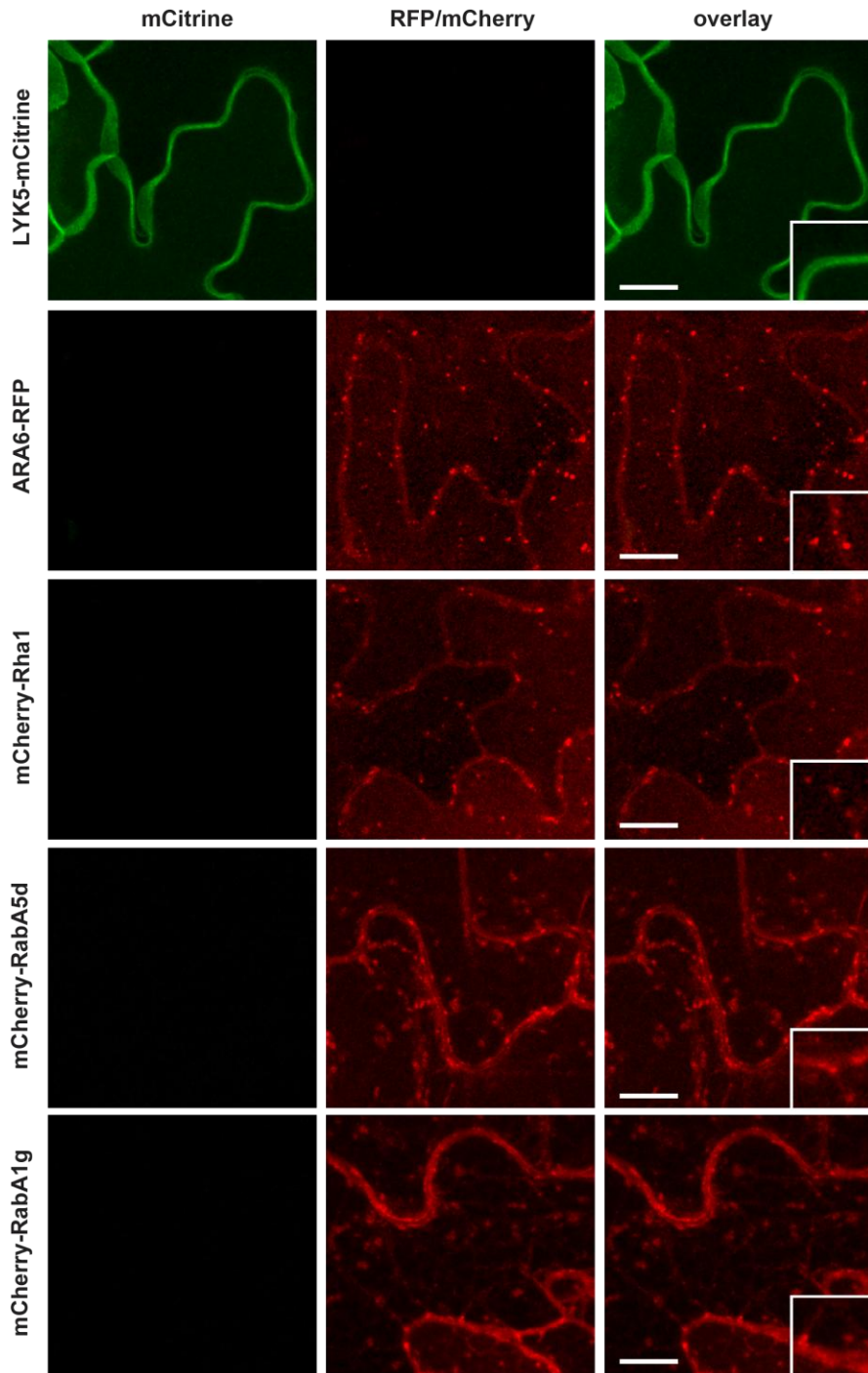


**Figure S6: The signal detected for LYK5-mCitrine and RFP/ mCherry- tagged endosomal markers is construct specific.**

*Arabidopsis* Col-0 plants stably expressing *pLYK5::LYK5-mCitrine* and the respective endosomal marker *p35S::ARA6-RFP*, *pUBQ10::mCherry-Rha1*, *pUBQ10::mCherry-RabA5d* or *pUBQ10::mCherry-RabA1g* (Geldner *et al.*, 2009) were infiltrated with water and incubated for 60 min. The signal for each fusion protein could be detected only in the respective channel for mCitrine or RFP/mCherry. Inset pictures show details. All images are maximum projections of 10 focal planes taken 1  $\mu$ m apart. Green, mCitrine; red, RFP or mCherry; Scale bar = 10  $\mu$ m.

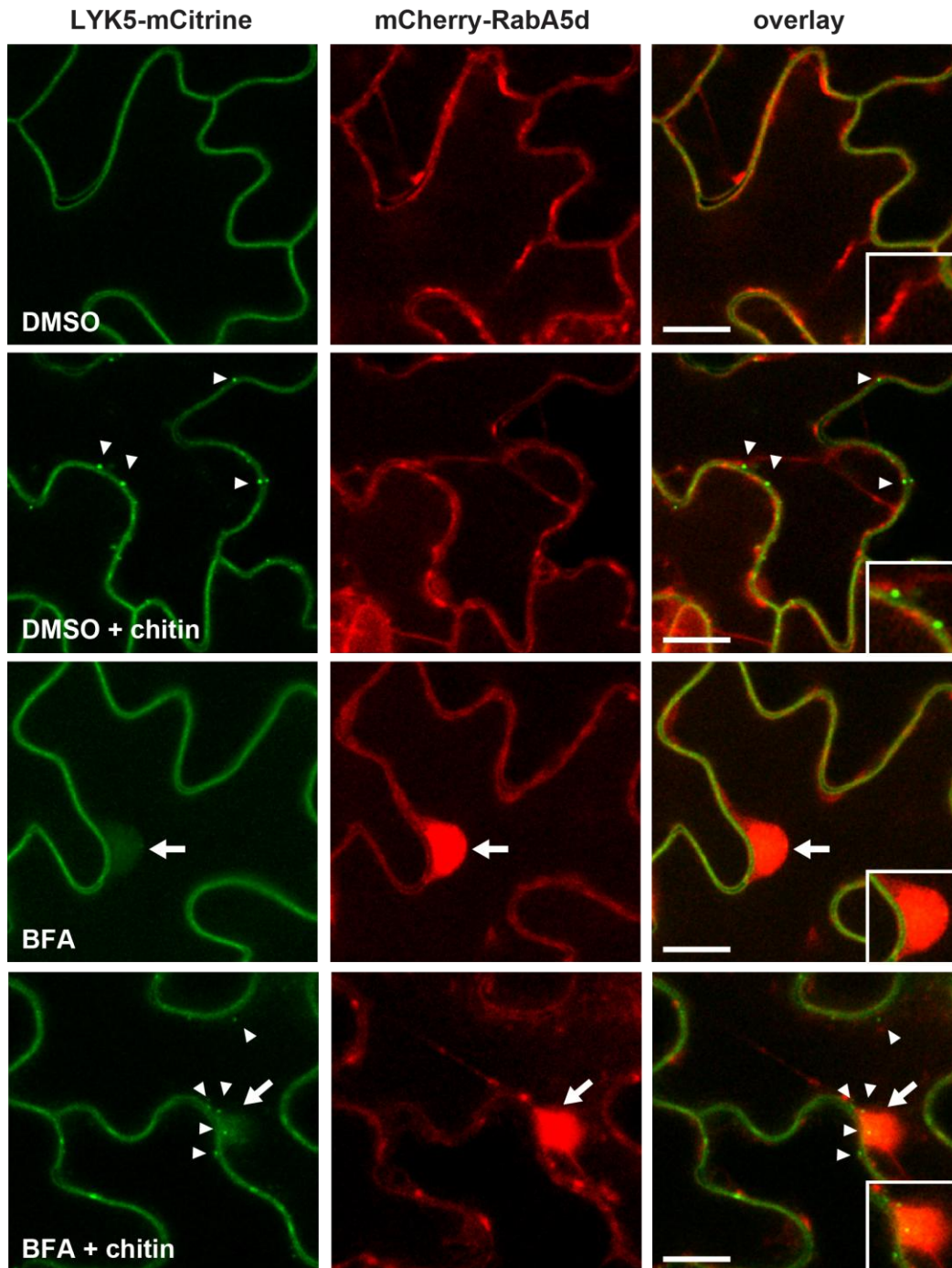


**Figure S7: LYK5-mCitrine together with mCherry-RabA5d accumulate in BFA induced compartments.**

*Arabidopsis* Col-0 plants stably expressing *pLYK5::LYK5-mCitrine* and the recycling endosomal marker *pUBQ10::mCherry-RabA5d* (Geldner *et al.*, 2009) were incubated with DMSO or BFA-solution prior to infiltration with or without 100  $\mu\text{g/ml}$  chitin. LYK5-mCitrine and mCherry-RabA5d form BFA-induced compartments. Additionally, LYK5-mCitrine endosome formation is not affected after BFA treatment. Inset pictures show details. All images are single plane CLSM images. Similar results were obtained in experiments with three independent transgenic lines. Arrows point to BFA-induced compartments, arrow heads to chitin-induced LYK5-mCitrine-containing endosomes. Green, LYK5-mCitrine; Red, mCherry- RabA5d; Scale bar = 10  $\mu\text{m}$ .

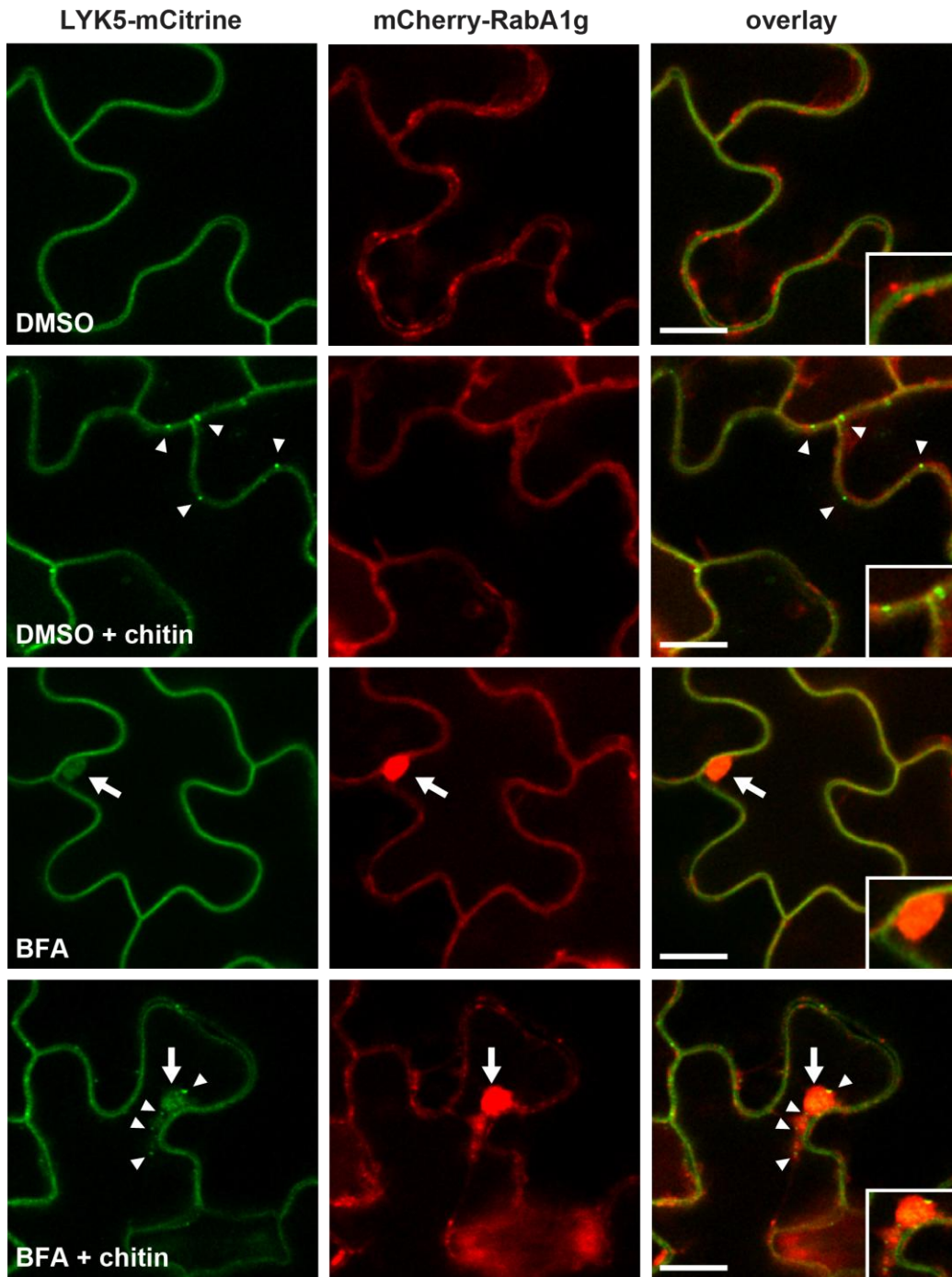


**Figure S8: LYK5-mCitrine together with mCherry-RabA1g accumulate in BFA induced compartments.**

*Arabidopsis* Col-0 plants stably expressing *pLYK5::LYK5-mCitrine* and the recycling endosomal marker *pUBQ10::mCherry-RabA1g* (Geldner *et al.*, 2009) were incubated with DMSO or BFA-solution prior to infiltration with or without 100  $\mu\text{g/ml}$  chitin. LYK5-mCitrine and mCherry-RabA1g form BFA-induced compartments. Additionally, LYK5-mCitrine endosome formation is not affected after BFA treatment. Inset pictures show details. All images are single plane CLSM images. Similar results were obtained in experiments with three independent transgenic lines. Arrows point to BFA-induced compartments, arrow heads to chitin-induced LYK5-mCitrine-containing endosomes. Green, LYK5-mCitrine; Red, mCherry-RabA1g; Scale bar = 10  $\mu\text{m}$ .



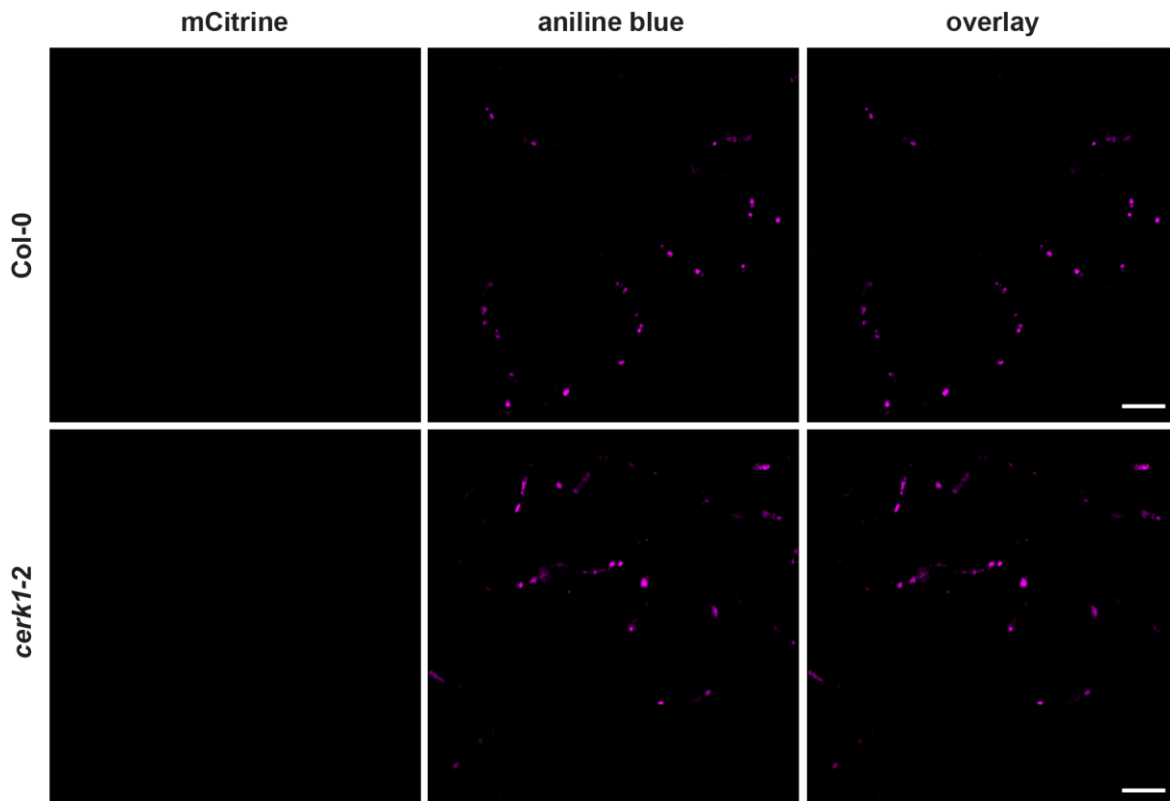


**Figure S9: Specific detection of aniline blue stained callose in Col-0 and *cerk1-2*.**

Leaves of Col-0 and *cerk1-2* plants were infiltrated and incubated with chitin solution (100  $\mu\text{g/ml}$ ) for 90 min. Then they were incubated in 0.01% (w/v) aniline blue solution for 15 min. Aniline blue staining results in punctate structures at the cell periphery. Images are single CLSM focus planes. No signal was observed in the mCitrine channel. Experiments were repeated with twice with similar results. magenta, aniline blue stained callose; Scale bar = 10  $\mu\text{m}$ .

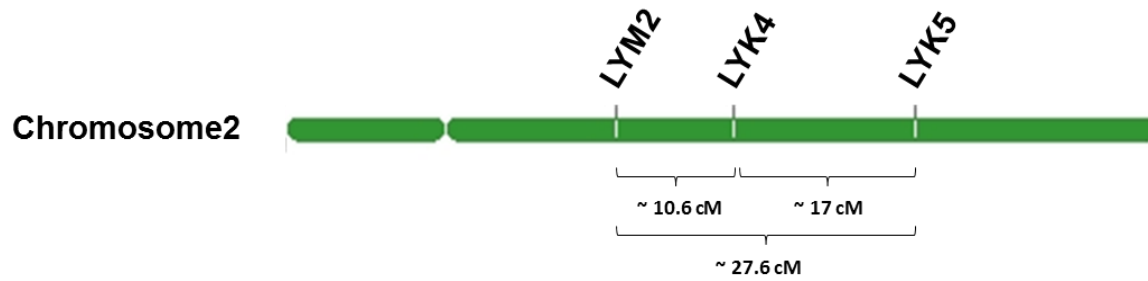


**Figure S10: *LYM2*, *LYK4* and *LYK5* are located on the same chromosome.**

Schematic representation of *LYM2*, *LYK4* and *LYK5* gene loci on chromosome 2. Scheme was generated using the TAIR integrated Chromosome Map Tool. Distances between the genes were determined using chromosomal markers. Distances are given in centi Morgan (cM).

## List of figures

Figure 1: Schematic representation of the plant immune system. ....	2
Figure 2: Model for LysM-RLK and LysM-RLP receptor complex formation upon perception of <i>N</i> -acetylglucosamine (GlcNAc)-containing ligands in <i>Arabidopsis</i> , rice and <i>Lotus japonicus</i> . ....	8
Figure 3: Alignment of full length amino acid sequences of <i>Arabidopsis</i> LysM-RLKs (LYKs).....	12
Figure 4: Schematic representation of the endocytic pathway in plants.....	16
Figure 5: Simplified model of a plasmodesma. ....	26
Figure 6: Expression of <i>pCERK1::CERK1-GFP</i> rescues <i>cerk1-2</i> chitin insensitivity. ....	73
Figure 7: CERK1-GFP localization is not responsive to chitin. ....	74
Figure 8: Application of an endomembrane trafficking inhibitor identifies chitin-induced CERK1-GFP vesicles.....	75
Figure 9: CERK1-GFP localization is sensitive to BFA. ....	76
Figure 10: <i>lyk5-2</i> and <i>lyk4-2</i> T-DNA insertion lines used in this study. ....	78
Figure 11: Knock-out of <i>LYK5</i> causes moderately reduced CERK1 phosphorylation. ....	79
Figure 12: <i>WRKY</i> transcription factor expression is moderately reduced in <i>lyk</i> mutants.....	81
Figure 13: Semi-quantitative expression analysis of <i>WRKY</i> and <i>LysM-RLK</i> genes. ....	82
Figure 14: Expression of <i>LYK5-mCitrine</i> and <i>LYK4-mCitrine</i> complement the reduced CERK1-phosphorylation in the <i>lyk5-2 lyk4-2</i> double mutant.....	84
Figure 15: Chitin-induced and CERK1-dependent formation of LYK5-mCitrine positive vesicles. ....	85
Figure 16: Quantification of chitin-induced LYK5-mCitrine positive vesicles in Col-0 over time. ....	87
Figure 17: LYK4-mCitrine may show chitin-induced, CERK1-dependent vesicle formation. ....	88
Figure 18: LYK5-mCitrine vesicle formation is chitin specific.....	89

---

Figure 19: Chitin-induced endocytosis of LYK5-mCitrine from the plasma membrane.....	91
Figure 20: Upon chitin treatment, LYK5-mCitrine co-localizes with LE/MVB markers ARA6 and Rha1.....	93
Figure 21: LYK5-mCitrine does not co-localize with recycling endosomal markers RabA5d and RabA1g.....	94
Figure 22: BFA application affects constitutive endomembrane trafficking of LYK5-mCitrine, but not its chitin-induced endocytosis.....	96
Figure 23: Inhibitors of endomembrane trafficking, the cytoskeleton and protein phosphorylation affect LYK5-mCitrine endocytosis. ....	100
Figure 24: Chitin-induced and CERK1-dependent phosphorylation of LYK5-mCitrine <i>in planta</i> . ....	102
Figure 25: LYK4-mCitrine may undergo chitin-induced and CERK1-dependent phosphorylation. ....	103
Figure 26: The intracellular domain of CERK1 directly phosphorylates LYK5 and LYK4 endodomains <i>in vitro</i> . ....	105
Figure 27: CERK1 kinase activity is required for chitin-induced LYK5-mCitrine phosphorylation and endocytosis.....	107
Figure 28: The <i>lym2-1</i> T-DNA insertion line used in this study. ....	108
Figure 29: The loss of LYM proteins does not affect chitin-induced CERK1 phosphorylation and chitin binding.....	110
Figure 30: Chitin-induced re-localization of mCitrine-LYM2 at the PM.....	112
Figure 31: PM and PD localization of mCitrine-LYM2 after chitin treatment.....	113
Figure 32: mCitrine-LYM2 shows no chitin-induced changes in mobility in SDS-PAGE.....	114
Figure 33: <i>lyk5-2 lyk4-2 lym2-1</i> (het/het/hom) mutants develop siliques with fewer seeds. ....	117

Figure 34: *lyk5-2 lyk4-2 lym2-1* (het/het/hom) mutants show defects in fertility. .... 118

## List of tables

Table 1: <i>Arabidopsis thaliana</i> T-DNA mutant lines used in this work. ....	30
Table 2: Transgenic <i>Arabidopsis thaliana</i> lines used in this work. ....	31
Table 3: Vectors used or generated in this study.....	34
Table 4: Primer used in this study. ....	36
Table 5: Antibiotics used in this study. ....	40
Table 6: Growth media used in this study.....	40
Table 7: Inhibitors used in this study. ....	42
Table 8: Antibodies (primary and secondary) used in this study.....	42
Table 9: Buffers and solutions used in this study.....	43
Table 10: General temperature profile for PCR with <i>Taq</i> polymerase. $T_m$ indicates the average melting temperature of primers used.....	57
Table 11: PCR protocol used for qRT-PCR.....	61
Table 12: Composition of mixtures used for resolving and stacking gel preparation in this study. .	65
Table 13: Parameters used for the detection of the different fluorophores.....	69
Table 14: Delayed germination of <i>lyk5-2 lyk4-2 lym2-1</i> (het/het/hom) seeds.....	116
Table 15: Fertility analyses of <i>lyk5-2 lyk4-2 lym2-1</i> (het/het/hom) mutants. Total number of siliques, mature and aborted seeds, unfertilized ovules counted for the indicated genotypes.....	118

## List of supplemental figures

Figure S1: Alignment of full length amino acid sequences of <i>Arabidopsis</i> CERK1 and LYM proteins.....	168
Figure S2: Phylogenetic tree of <i>Arabidopsis thaliana</i> , <i>Medicago truncatula</i> and <i>Lotus japonicus</i> LysM-RLKs. ....	169
Figure S3: CERK1-GFP localization is not responsive to chitin. ....	170
Figure S4: <i>LYK4</i> is weakly expressed in leaves. ....	171
Figure S5: Endosome quantification and image normalization. ....	172
Figure S6: The signal detected for LYK5-mCitrine and RFP/ mCherry- tagged endosomal markers is construct specific. ....	173
Figure S7: LYK5-mCitrine together with mCherry-RabA5d accumulate in BFA induced compartments. ....	174
Figure S8: LYK5-mCitrine together with mCherry-RabA1g accumulate in BFA induced compartments. ....	175
Figure S9: Specific detection of aniline blue stained callose in Col-0 and <i>cerk1-2</i> .....	176
Figure S10: <i>LYM2</i> , <i>LYK4</i> and <i>LYK5</i> are located on the same chromosome.....	177

## Danksagung

An dieser Stelle möchte ich mich bei allen Personen bedanken, die mich in den letzten Jahren bei der Arbeit an meiner Dissertation unterstützt haben.

Zuerst möchte ich mich bei Prof. Dr. Volker Lipka dafür bedanken, dass er mir dieses hochinteressante und spannende Thema für meine Promotion angeboten hat. Desweiteren möchte ich mich bei ihm dafür bedanken, dass er über die vielen Jahre meines Studiums mein Mentor war und mit seinem breiten Fachwissen immer konstruktive Kritik zum Thema eingebracht hat. Er hat mich gefordert und gefördert, mich belehrt und mich gelehrt ein guter Wissenschaftler zu werden. Sein Wissen und meine damit verbundene Ausbildung werden meinen weiteren Lebensweg intensiv beeinflussen. Auch für die Funktion als Erstprüfer und somit die Funktion als Doktorvater, sowie die Begutachtung der vorliegenden Arbeit spreche ich ihm meinen herzlichsten Dank aus.

Einen ebenso großen Anteil an dem Gelingen dieser Arbeit hat auch Dr. Elena Petutschnig. Danke Elena für die Betreuung meiner wissenschaftlichen Arbeiten, sowohl im Labor als auch am Schreibtisch. Deine kritischen Kommentare sind Gold wert, du bist eine ausgezeichnete Wissenschaftlerin und Lehrerin! (Fast) alles was ich zu dem Thema meiner Doktorarbeit weiß und was ich methodisch kann, hast du mir beigebracht. Neben der wissenschaftlichen Arbeit, deiner Geduld und den kritischen Bemerkungen hast du mir während meines Studiums und der anschließenden Promotion einiges beigebracht. Danke auch für das offene Ohr wenn es mal nicht so gut lief. Du hast für vieles Verständnis gezeigt. Ich hoffe ich kann dir davon mit meiner Arbeit etwas zurückgeben.

Ein weiterer Dank gilt Prof. Dr. Ivo Feussner. Ich möchte mich bei Ihnen für die Übernahme des Korreferats bedanken und dafür, dass Sie meiner Arbeit den nötig Hauch Biochemie gegeben haben. Ich danke Ihnen für die konstruktiven Vorschläge von Beginn meiner Promotion an, die auch zum Gelingen dieser Arbeit beigetragen haben.

Bei den weiteren Mitgliedern meiner Prüfungskommission möchte ich mich für die Bereitschaft zu der Begutachtung der vorliegenden Arbeit bedanken. Namentlich wären das Prof. Dr. Christiane Gatz, Prof. Dr. Andrea Polle, PD Dr. Thomas Teichmann und Dr. Martin Fulda.



Thomas, danke dass du bei allen Aktionen die wir Studenten uns für die Abteilung ausgedacht haben immer so begeistert dabei warst. Du hattest zudem immer ein offenes Ohr für uns und warst der Ansprechpartner wenn mal wieder alles nicht mehr so funktionierte wie es sollte.

Dr. Hassan Ghareeb, du bist so schnell ein so wichtiger Teil des Teams geworden. Da ist es für mich kein Zufall, dass deine Hilfe bei der Arbeit und damit auch bei der bevorstehenden Publikation einen hohen Stellenwert einnimmt. Du kannst mit deiner aufgeschlossenen Art Menschen inspirieren. Du gibst niemals auf und schaffst durch deinen unermüdlichen Einsatz ein Projekt in die richtige Richtung zu lenken. Danke dass ich dich kennengelernt haben durfte!

Ein riesen Dankeschön gebührt unseren technischen Assistenten Sabine Wohlfahrt, Ludmilla Heck-Hrarti und Katharina Dworak, Gaby und Melanie. Ihr habt mir nicht nur das Arbeiten sondern auch das Leben im Labor vereinfacht. Ich danke euch für die lockere Arbeitsatmosphäre, die Gespräche, das Lachen und das Ärgern. Ihr seid die guten Seelen des Labors, der Kleber der alles zusammenhält und ohne euch läuft einfach nichts. Danke dafür!

Danke auch an unsere Gärtner Feli, Susanne und Herrn Wedemeyer. Danke für die manchmal doch spontanen oder öfter sogar ziemlich großen Bestellungen die zügig erledigt wurden. Durch euch kann die Masse an Experimenten erst zustande kommen. Danke Feli und Susanne für die netten Gespräche und die Hilfe bei anderen Laborarbeiten. Ich wünsche euch von Herzen alles Gute!

Ein riesiges Dankeschön geht an meine „Leidensgenossen“ Charlotte, Yvonne, Karin, Sabine, Marnie, Johanna, Martin, Dimitri, Merlin und Christopher. Ich finde wir haben das doch in der Zeit ganz gut hinbekommen. Danke für die langen Tage/Abende im Labor aber vor allem für alles außerhalb der Arbeit. Zusätzlich möchte ich mich auch bei allen weiteren aktuellen und ehemaligen Mitgliedern der Abteilung bedanken!

Ich danke meinem Onkel Prof. Dr. Dr. Lars-Peter Erwig für die wertvollen Tipps, die Korrekturen und dass du mir aufgezeigt hast welche Wege ich einschlagen kann. Danke für deine Unterstützung die ich schon so lange erfahre.

Auch bei meinen Freunden außerhalb des Labors möchte ich mich für die lange Zeit der Freundschaft bedanken. Wir starteten gemeinsam und gehen auch zusammen durch das Ziel. Hier möchte ich meine Freunde Micha und Ulla, Karl, Stefan, Bernie und Christopher herausheben. Meinen Freunden denen auch die Entfernung zwischen uns nichts aus macht: Marc, Michel, Stefan, Wendy und Fred. Aber auch die Kerls vom SC Hainberg haben mich über die ganze Zeit immer wieder aufgebaut wenn es mal nicht so lief. Danke Jungs!

Meiner Familie habe ich alles zu verdanken. Ohne ihre Unterstützung wäre ich niemals so weit gekommen. Danke, dass ihr immer an mich geglaubt habt und mich in jeder Entscheidung bestärkt habt. Man kann das nicht einfach in Worte fassen was das für mich bedeutet...

Hierzu gehört auch Michelle, meine Freundin und meine Frau. Danke dass du diese, für mich wichtige Zeit, mit mir verbracht hast. Danke für dein offenes Ohr, dein Verständnis, deine Fürsorge und deine aufheiternden Worte. Danke dass es dich gibt und dass du den weiteren Weg mit mir gehen willst....

## Lebenslauf

Name: **Jan Erwig**  
 Anschrift: Schopenhauerweg 6, 37083 Göttingen  
 Geburtstag/-ort: 28. Mai 1988, Hildesheim

## Ausbildung

11/2012 - 04/2016 **Promotionsprogramm Biologie (Dr. rer. nat.)**  
 Georg-August Universität Göttingen, Abteilung: Zellbiologie der Pflanze

10/2010 – 11/2012 **M. Sc. “Microbiology and Biochemistry”**  
 Georg-August Universität Göttingen  
**Abschlussarbeit:** „The function of *Arabidopsis* LysM-RLK3, LysM-RLK4 and LYM2 in chitin signaling and other CERK1-mediated processes

10/2007 – 10/2010 **B. Sc. Biologie**  
**Schwerpunkt: Molekulare Biowissenschaften**  
 Georg-August Universität Göttingen  
**Abschlussarbeit:** „Functional characterization of *Arabidopsis* LysM-RLKs in defense signaling”

2000 - 2007 **Allgemeine Hochschulreife**  
 Gymnasium Groß Ilsede

## Weiterbildungen

2013 **Fernstudium „Patentrecht für Ingenieure und Naturwissenschaftler“**  
 Beuth Hochschule für Technik, Berlin

2011 **Zertifikat UNiCert III Scientific English**  
 Zentrale Einrichtung für Sprachen und Schlüsselkompetenzen, Göttingen

2010 **Zertifikat “Sozial- und Führungskompetenzen”**  
 Zentrale Einrichtung für Sprachen und Schlüsselkompetenzen, Göttingen

## Praktikum

10/2011 – 12/2011 **Laborpraktikum in der Abteilung Biochemie der Pflanze (Prof. Dr. Ivo Feussner)**  
 Thema: „The role of Long-Acetyl CoA Synthetases (LACS) in fatty acid metabolism“  
 Georg-August Universität Göttingen

08/2009- 09/2009 **Unternehmenspraktikum im Nationalpark Bayerischer Wald**  
 Grafenau

## Stipendium

9/2009 – 9/2012 | **Stipendiat der Friedrich-Ebert-Stiftung**

## Konferenzen

07/2015 | **International Conference on Arabidopsis Research (ICAR) 2015, Paris**  
**Posterpräsentation:** "Chitin-induced and CERK1-dependent endocytosis of the LysM-RLKs LYK4 and LYK5"

03/2013 | **Gemeinsame Jahrestagung der DPG-Arbeitskreise Mykologie und Wirt-Parasit Beziehungen, Göttingen**  
**Vortrag:** "Analyzing the function of putative CERK1 complex partners LysM-RLK3, LysM-RLK4 and LYM2 in plant immunity"

## Publikationen

**Erwig J. und Herbig E.** : Saubere Lösungen – Wasser zur Aufreinigung von Glutathion-S-transferase (GST) mittels Affinitätschromatographie, GIT 59.: S.48-51, (2015)

**Erwig J., Ghareeb H., Kopischke M., Hacke R., Matei A., Petutschnig E. and Lipka V.**, Chitin-induced and CERK1 phosphorylation-dependent endocytosis of *Arabidopsis* LYK5 (submitted)

## Weitere Kenntnisse

Sprachen | Deutsch (Muttersprache)  
 Englisch (C1, verhandlungssicher)  
 Französisch (Grundwissen)

EDV-Kenntnisse | MS Office (Word, Excel, PowerPoint, Outlook)  
 Adobe Creative Suite (Photoshop CS5, Illustrator CS5)  
 Literaturverwaltung (Endnote, Citavi, Zotero)

Göttingen, den 07. März 2016

---